DEVELOPMENT OF TWO ORGANOCATALYTIC PHOTOREDOX TRANSFORMATIONS: THE ENANTIOSELECTIVE CATION RADICAL DIELS-ALDER REACTION AND THE ANTI-MARKOVNIKOV HYDROAMINATION OF ALKENES

Tien M. Nguyen

A dissertation submitted to the faculty at the University of North Carolina at Chapel Hill in partial fulfillment of the requirements for the Degree of Philosophy in the Department of Chemistry.

Chapel Hill
2014

Approved by:

David A. Nicewicz

Wei You

Jillian L. Dempsey

Maurice S. Brookhart

David S. Lawrence

ABSTRACT

Tien M. Nguyen: Development of Two Organocatalytic Photoredox Transformations: The Enantioselective Cation Radical Diels-Alder Reaction and the Anti-Markovnikov Hydroamination of Alkenes
(Under the direction of David A. Nicewicz)

Herein we describe the development of two research projects within the field of organic photoredox catalysis. Both works involve the single electron oxidation of alkenes to generate cation radical intermediates which possess unique reactivity. The cation radical Diels-Alder reaction circumvents traditional electronic restraints on the substrates and allows for cycloaddition to occur between two electron-rich partners. We aimed to render this valuable reaction enantioselective by merging the fields of photoredox catalysis and chiral counteranion catalysis. The precedent for our research proposal and details of our findings are disclosed. We also employed cation radical intermediates for the development of an anti-Markovnikov hydroamination reaction catalyzed by an organic photoredox system. This transformation provides access to important pharmacological agents through the direct addition of amines to alkenes. The products are formed with complete anti-Markovnikov regioselectivity, a feature that is challenging to obtain without precious transition metals. We demonstrate 38 examples of the intra- and intermolecular anti-Markovnikov hydroamination reaction. Notably, the substrate scope includes trisubstituted aliphatic alkenes as well as heteroaromatic amines.

To my family for always supporting me and providing a loving and carefree safety net. To my advisor Dave Nicewicz for his kindness and support. To my amazing lab for being cheering me on and being the most pleasant and interesting group of people I have had the pleasure of seeing every day. To my friends who were quick to commiserate and made life in graduate school so enjoyable.

ACKNOWLEDGEMENTS

I'd like to acknowledge my advisor Dave Nicewicz for his guidance and assistance throughout my time in graduate school. I would also like to thank my labmates, past and present, for many discussions in lab, listening and providing feedback for presentations and for a lovely work atmosphere. Special thanks to the Crimmins, Alexanian, Johnson and Meek lab for their helpfulness in sharing equipment and chemicals.

PREFACE

The results and supporting information disclosed regarding the intramolecular anti-Markovnikov hydroamination reaction were published in the Journal of the American Chemical Society in 2013.

TABLE OF CONTENTS

LIST OF TABLES

Table

LIST OF FIGURES

LIST OF ABBREVIATIONS

ACDC	asymmetric counteranion-directed catalysis
Anethole	β-methyl-*p*-methoxystyrene
BDCN	1,1'-bis(2,4-dicyanonaphthalene)
BDE	bond dissociation energies
BINOL	1,1'-bi-2-napthyl
Boc	*tert*-butylcarbonyl
Cp	cyclopentadiene
DA	Diels-Alder
DCA	9,10-dicyanoanthracene
DCB	dicyanobenzene
DCE	dichloroethane
DCM	dichloromethane
DFT	density functional theory
DMAP	dimethyl amino pyridine
EDC	1-Ethyl-3-(3-dimethylaminopropyl)carbodiimide
ee	enantiomeric excess
GC	gas chromatography
HOMO	highest occupied molecular orbital
LED	light-emitting diode
LUMO	lowest occupied molecular orbital
MeCN	acetonitrile
NMR	nuclear magnetic resonance
Na_2SO_4	sodium sulfate
PET	photoinduced electron transfer
Photo-NOCAS	photochemical nucleophile-olefin combination aromatic substitution

PhSH	thiophenol
PMN	2-phenylmalononitrile
SCE	saturated calomel electrode
TEMPO	(2,2,6,6-tetramethylpiperidin-1-yl)oxidanyl
TFE	trifluoroethanol
THF	tetrahydrofurans
TMSCl	trimethylsilylchloride
TRIP	2,4,6-triisopropylphenyl phosphate BINOL
Ts	*p*-toluenesulfonyl
TPT	triaryloxopyrylium tetrafluoroborate
RBF	round bottom flask
UV	ultraviolet
Xylyl	3,5-dimethylphenyl

CHAPTER 1: BACKGROUND FOR THE DEVELOPMENT OF AN ENANTIOSELECTIVE CATION RADICAL DIELS-ALDER REACTION

Introduction

Synthetic organic chemists require an extensive array of transformations to construct complex molecules for drug discovery, industrial processes or new materials. We sought to develop a novel methodology that would also provide access to a relatively unexplored area of chemical space. As the platform on which to develop a new method, we looked to the Diels-Alder (DA) reaction, a well-established and powerful cycloaddition that forms two bonds and can set up to four stereocenters in a single step.[1] This transformation is strictly regulated by the electronic properties of the two coupling partners, generally limiting reaction between partners with mismatched electronic substitution. One strategy to circumvent this challenge is through the cation radical Diels-Alder, which relies on single electron oxidation to induce reactivity between two electronically matched starting materials.[2] The cation radical Diels-Alder has attracted the interest of many research groups and their findings will be discussed in turn.

Building on existing precedent we wanted to explore the possibility of rendering the cation radical Diels-Alder reaction enantioselective. We saw an opportunity to introduce chirality through a unique non-covalent interaction between the key cation radical intermediate and a chiral counteranion. Other research labs have reported asymmetric induction through ionic interaction, though most rely on a chiral cationic species, with limited examples in organic catalysis. We set out to construct a novel photo-oxidant with a chiral counteranion to catalyze a cation radical Diels-Alder reaction to furnish enantiomerically enriched cyclohexene products (**Figure 1.1**).

Figure 1.1 Proposal for an Enantioselective Cation Radical Diels-Alder Reaction

1.1 Normal and Inverse Demand Diels-Alder Reactions

In the classic Diels-Alder, reaction occurs between a diene and a dienophile in a concerted manner. Productive reactivity can be rationalized using frontier molecular orbitals.[3] In a normal demand Diels-Alder reaction, the orbitals of relevance are the highest occupied molecular orbital (HOMO) of the diene and the lowest occupied molecular orbital (LUMO) of the dienophile (**Figure 1.2**). The band gap between the two orbitals has to be sufficiently small in order for reaction to occur. Strategies to increase the likelihood of reaction involve adding electron density to the diene through substitution to raise its HOMO energy level or making the dienophile more electron-deficient to lower the LUMO energy level.

Conversely, the inverse demand Diels-Alder reaction relies on an electron deficient diene and an electron rich dienophile. This effectively allows for reaction to occur between the LUMO of the diene and the HOMO of the dienophile (**Figure 1.2**).[3] In both the normal and inverse demand Diels-Alder, partners of mismatched electronics are required. Over the years many research groups have taken advantage of substitutions on the reaction partners like imine or carbonyl groups on either starting material to coordinate to catalysts, chiral or racemic, to influence the rate of reactivity. Generally these interactions are covalent, as seen in Lewis[4] or Brønsted[5] acid and also amine catalysis[6] which involves the condensation of amines directly on to the substrate. This electronic requirement represents this transformation's greatest limitation.

Figure 1.2 Electronic Restrictions of the Normal and Inverse Demand Diels-Alder Reaction

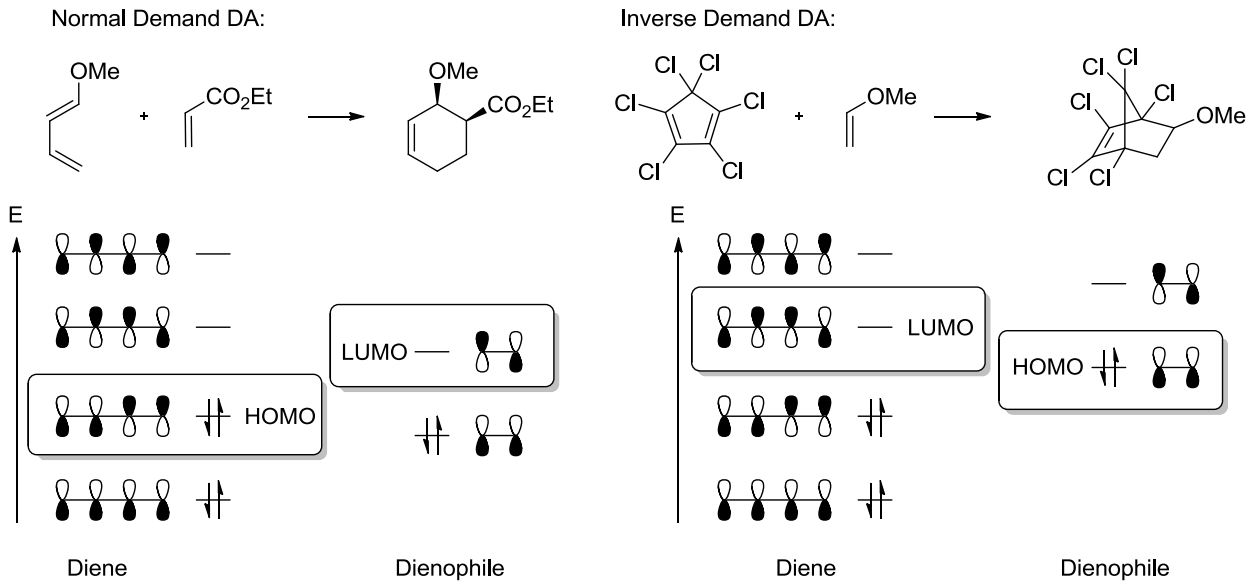

1.2 Cation Radical Diels-Alder Reactions

The cation radical Diels-Alder reaction offers a pathway into a new chemical space for the Diels-Alder. Research groups began exploring this transformation which occurs between two electron rich coupling partners with success in the 1980s. To the best of our knowledge, the first report came from the lab of Nathan Bauld in 1981, when they demonstrated the dimerization of cyclohexadiene with a radical cation catalyst, tris(*p*-bromophenyl)aminium hexachlorostibnate in 15 minutes at 0 °C in 70% yield (**Figure 1.3**).[2] This marked quite a breakthrough as the uncatalyzed thermal [4+2] of cyclohexadiene only occurs at 200 °C after 20h in a lower 30% yield.

Figure 1.3 First Report of Cation Radical Diels-Alder by Bauld in 1981

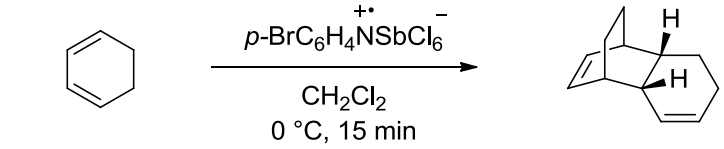

Bauld, *J. Am. Chem. Soc.* **1981**, *103,* 718

70%
5:1 endo:exo

The report also included the [4+2] cross-cycloaddition between cyclohexadiene and 2,4-dimethylhexadiene which proceeded in good yield and 5:1 diastereoselectivity, favoring the endo product.

They demonstrated that dienes which were not locked in the *cis* conformation were competent reaction partners as 1,1-dicyclopentenyl was dimerized in 50% yield by GC. With this initial finding, they offered a mechanistic proposal which began with single electon oxidation of the dienophile by the radical cation catalyst to produce a cation radical intermediate. This intermediate could then react with the diene forming a cyclic cation radical intermediate which could be reduced to give the desired cyclohexene (**Figure 1.4**). The following year the Bauld group disclosed the results of further investigation into the cation radical Diels-Alder to support their assertion that reaction occurs through formation of a dienophile cation radical and not a diene cation radical.[7] Using frontier molecular orbitar theory, they show that reaction between a neutral ethene and a diene radical cation in a [3+2] fashion is symmetry forbidden.

Figure 1.4 Proposed Mechanism for the Cation Radical DA by Bauld

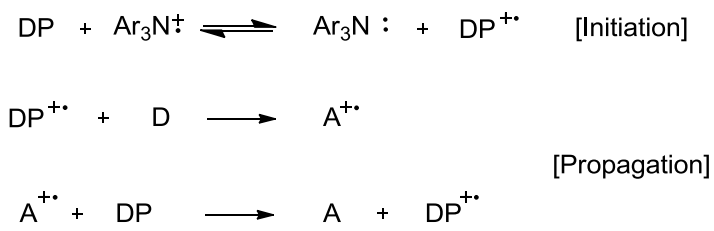

DP = Dienophile; A = Cycloadduct, D = Diene
Bauld, *J. Am. Chem. Soc.* **1981**, *103,* 718

In 1983, Bauld and co-workers expanded the scope of the cation radical Diels-Alder to include more electron-rich dienophiles (**Figure 1.5**).[8] They recognized the advantageous nature of the cation radical DA, in which electron-rich partners are essentially converted to electron-poor dienophiles through one-electron oxidation. Attempts to dimerize 1-methoxy-cyclohexadiene with their aminium radical cation catalyst proved unfruitful, hampered by polymerization. After switching to a photoinduced electron transfer sensitizer, 1,4-dicyanobenzene activated by UV-light, they were able to obtain the dimerized product in 70% yield. Light activated single electron oxidants have unique properties that will be discussed in-depth later in the chapter. Vinyl enol ether and phenyl vinyl sulfide both reacted with cyclohexadiene in the presence of the aminium salt in good yields, though an excess of the dienophile was

required. In this paper, they also show the first example of a styrene substrate, anethole, as a competent dienophile partner for cyclopentadiene in 74% yield and 3:1 dr.

Figure 1.5 Expanding Scope of Cation Radical Diels-Alder to Electron Rich Substrates

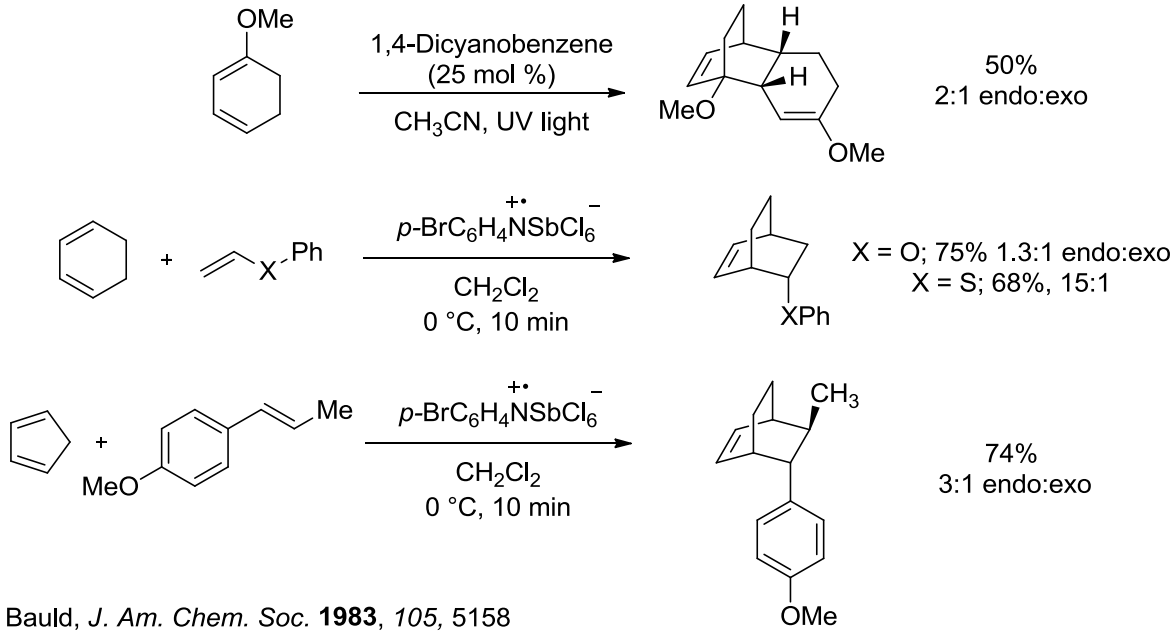

Bauld, *J. Am. Chem. Soc.* **1983**, *105,* 5158

The Bauld group performed extensive investigations of pericyclic cation radical reactions and also reported [2+2] cycloadditions,[9] though this class of reactions will not be discussed here. In their mechanistic investigations, they observed that in the case of 2,4-dimethyl-1,3-pentadiene, dimerization by the aminium salt or photoinduced electron transfer (PET) gave two different products (**Figure 1.6**).[9] It was only when the dimerization was promoted by the aminium salt in the presence of 2,6-di-*tert*-butyl lutidine did the products' identity match. The Bauld group suggests that for certain substrates, catalysis by the aminium salt may proceed through a Brønsted acid pathway, a pathway not seen in photoinduced electron transfer.

In 2000, Bauld and Gao investigated the mechanism specifically for the reaction between cyclopentadiene and *cis* and *trans* anethole.[10] They concluded that *cis*-anethole was most likely going through a step-wise mechanism after observing comparable amount of all four diastereomeric products in the reaction mixture. They proposed an intermediate in the step-wise mechanism that underwent bond rotation at a rate comparable to cyclization. This contrast with the reaction between Cp and *trans*-anethole

Figure 1.6 Mechanistic Investigation of Radical vs. Brønsted Acid Catalyzed Pathways

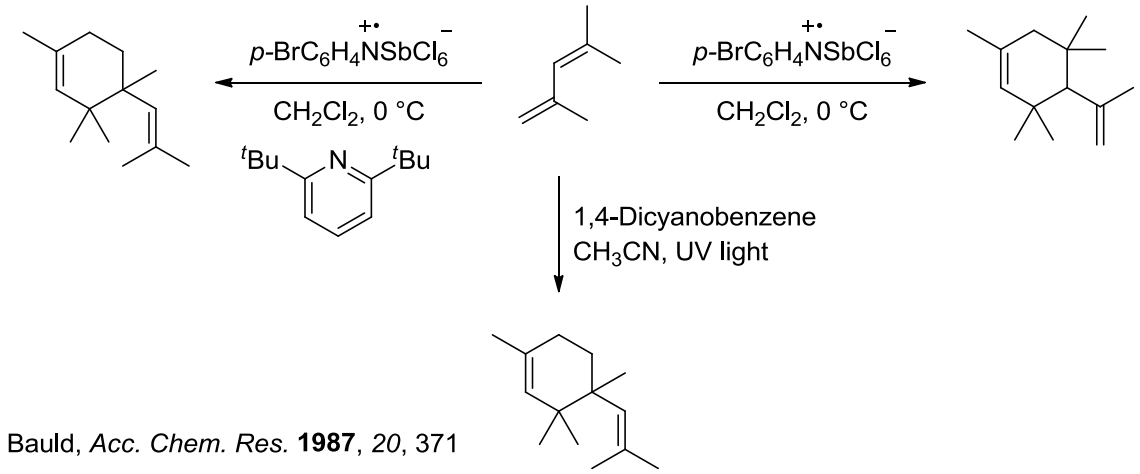

Bauld, *Acc. Chem. Res.* **1987**, *20*, 371

which did not produce any of the *cis* products. They also exposed the *cis* and *trans* products to the triarylaminium radical cation and observed isomerization to the trans product in the case of the *cis* product but no isomerization of the *trans* product (**Figure 1.7**). They assert that the *cis* product becomes oxidized and undergoes single bond rotation to relieve the unfavorable eclipsing interaction between the methyl and *p*-OMe phenyl groups. This finding supports the notion that the *cis* isomer of anethole is going through a stepwise mechanism and this leads them to suggest that it is likely that the *trans* isomer is operating under a similar mechanism. They noted that the same results are obtained when using photosensitized electron transfer conditions as well.

Figure 1.7 Cation Radical Diels-Alder Reaction Between *Cis* and *Trans*-Anethole and Cp

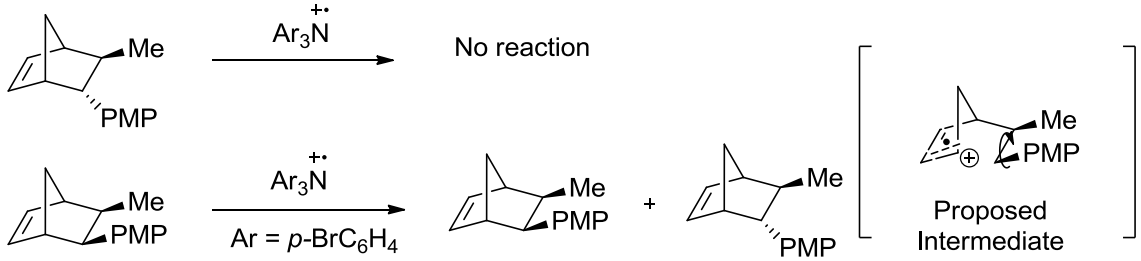

(1:1)

PMP = *p*-$OMeC_6H_4$
Bauld, *J. Chem. Soc. Perkin. Trans.* **2000**, *2*, 931

Other research labs have also contributed to the development of this transformation. In 1983, Jones and colleagues demonstrated the [4+2] dimerization of cyclohexadiene promoted by the UV-

activated 9,10-dicyanoanthracene (DCA) gave the desired cycloadducts in 60% yield in a 4:1 endo:exo dr (**Figure 1.8**).[11] In photoinduced electron transfer manifolds, the sensitizers are activated by light and act as strong electron acceptors in their excited state. In contrast to Bauld's aminium catalyzed cation radical DA, Jones suggests the formation of a exciplex in which free radical cations may not form but instead exist as a radical cation/anion pair. Extended irradiation in the presence DCA did result in the formation of very small amounts of adduct formation from the reaction between diene and sensitizer.

Figure 1.8 Photosenzitized Cation Radical Diels-Alder by Jones *et al.*

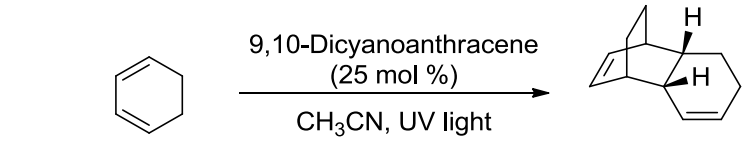

Jones, *J. Am. Chem. Soc.* **1983**, *105*, 652 — 60%, 4:1 endo:exo

In 1985, Mattay and colleagues introduced ketone-$LiClO_4$ salts as competent electron acceptors for the photolytic generation of radical cations. They evaluated these new electron acceptors against reported oxidants in photolytic cycloadditions (**Figure 1.9**).[12] The Mattay group found that each catalyst gave the desired cycloadducts in good yields but with varying endo to exo selectivities. The ketone-$LiClO_4$ mixtures showed no preference for either diastereomer while the aminium salt demonstrated a 4:1 (endo:exo) diastereoselectivity and triaryloxopyrylium tetrafluoroborate (TPT) gave 6:1 dr, also favoring the endo diastereomer.

Figure 1.9 Comparison of Electron Acceptors for the Cation Radical Diels-Alder Reaction

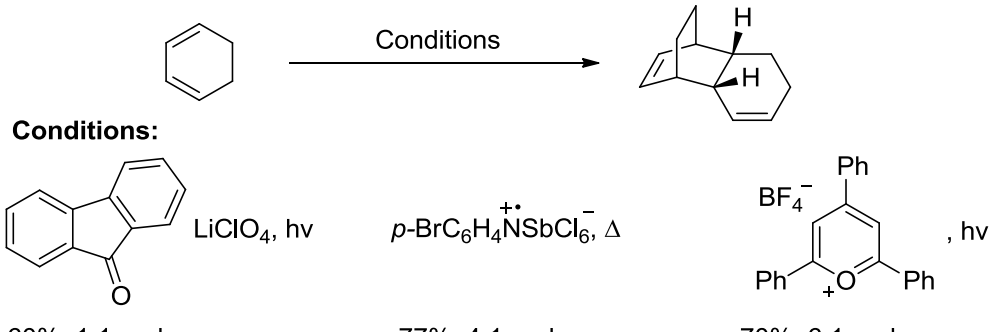

Mattay, *J. Chem. Soc., Chem. Commun.* **1985**, 1088

These results led the group to suggest that the mechanism of all cation radical reactions cannot simply be rationalized by a chain reaction mechanism. They present an alternative to Bauld's assertion on the role selectivity in the cation radical DA, in which cation radical intermediates arise from the dienophile. In the presence of excess diene, the Mattay group observed an increase in the formation of the exo isomer, leading them to suggest the formation of a diene radical cation intermediate. To support their claim, they drew on previous studies reported by Gross.[13] In the report by Gross, they investigated the gas phase cation radical DA with mass spectrometry methods and observed the acyclic octadienyl intermediate along with the cyclohexene radical cation. Gross and colleauges then proposed a step-wise mechanism for the DA reaction of 1,3-butadiene, with a radical cation diene intermediate instead of the concerted pericyclic mechanism in which a [3+2] cyclization would be symmetry forbidden.

In 1987, the Steckhan lab demontrated evidence for the presence of the cation radical of the diene.[14] They were able to electrochemically generate the radical cation of the diene in the presence of less oxidizable dienophiles and obtain the Diels-Alder cycloadducts, supporting a [3+2] mechanistic pathway. The role selectivity for the diene and dienophile in the cation radical Diels-Alder has been debated by many groups. Given that the Steckhan report contradicts Bauld's original assertion that the reaction went through a dienophile radical cation as a [4+1] cycloaddition, in 1990 Bauld and colleagues published another report that rigorously tested their understanding of the role selectivity in the cation radical Diels-Alder.[15] They evaluated the Diels-Alder reaction between two dienes with sufficiently different oxidation potentials, with the assumption that the more easily oxidizable partner would become the radical cation intermediate, even if it was the diene partner. The product distribution should reveal whether a diene or dienophile radical cation was formed.

The Bauld lab irradiated 1,3-cyclohexadiene (E_{ox} = 1.53 V) and 1,2-diethylidenecyclohexane (E_{ox} = 1.36 V) in the presence of a catalytic amount of *tris*(4-bromophenyl)aminium hexachlorostibnate and observes the [3+2] product along with the dimer of the 1,2-diethylidenecyclohexane (**Figure 1.10**).[15] They conclude that orbital symmetry allowedness/forbiddenness may not effect role selectivity in the

cation radical Diels-Alder. This suggests that the oxidation potential of the two reaction partners plays a very important role in determining the mechanistic pathway.

Figure 1.10 Testing Orbital Symmetry Control in the Cation Radical Diels-Alder

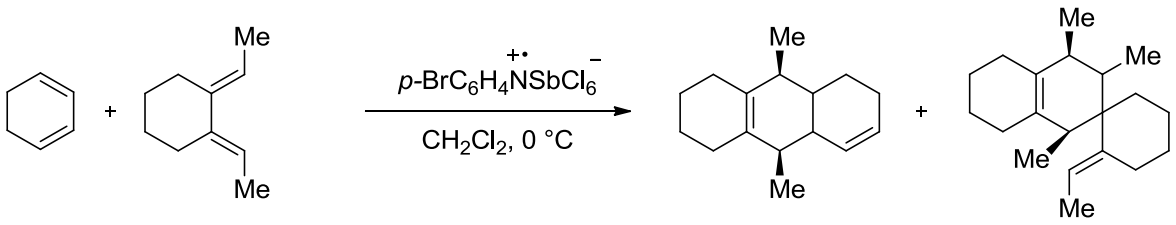

Bauld, *J. Am. Chem. Soc.* **1990,** *112,* 447 **Only products observed**

The Steckhan lab reported the cation radical DA reaction between indoles and electron-rich dienes in 1991, expanding the scope of competent dienophile partners for this transformation.[16] Initially, irradiation of indole, cyclohexadiene and TPT catalyst gave only very low yields of the DA cycloadducts. Their calculations showed that the expected product had a much lower oxidation potential than the starting indole (E_{ox} = 0.7 V vs. E_{ox} = 1.28 V vs NHE), and that the excited catalyst was being quenched by the product as it became present in higher concentrations. The Steckhan lab circumvented this challenge by including acetyl chloride and sodium bicarbonate into the reaction mixture and obtained the N-acylated cycloadduct product in 70% yield in 3.3:1 endo:exo diastereoselectivity. Other electron-rich dienes reacted with indoles in good yields, with the exception of dienes without rigid *s*-cis conformations of their double bonds, which gave slightly lower yields (**Figure 1.11**).

Substituted indoles did not react to give desired product, likely due to steric hindrance around the dienophile. A variety of nitrogen protecting groups were evaluated and methyl chloroformate and *p*-toluenesulfonyl chloride were also effective though gave slightly decreased yields (33% and 46%, respectively). Though the [2+2] reaction between enamides and cyclohexadiene has been reported, none of the [2+2] cycloadducts was detected by GC. Mechanistic investigations supported the accepted cation radical DA mechanism, starting with the oxidation of indole to give the cation radical indole intermediate. This intermediate can react with 1,3-cyclohexadiene to give the cyclic radical cation adduct, and then single electron reduction and protection by acetyl chloride furnishes the desired product.

Figure 1.11 Photolytic Cation Radical DA Reaction of Indole and Electron-Rich Dienes

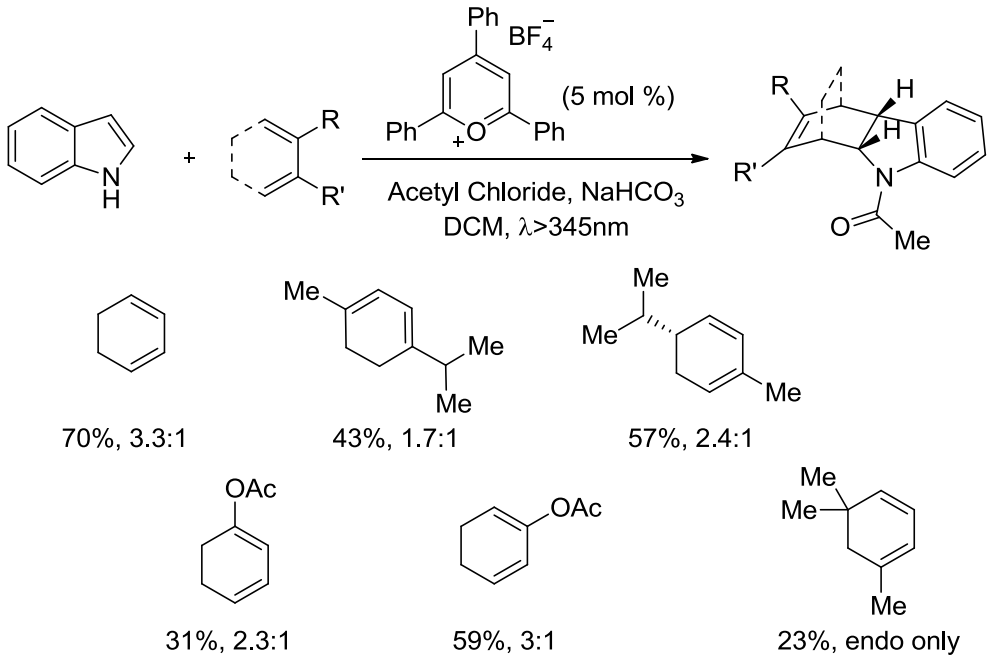

*All favor the endo isomer
Steckhan, *J. Org. Chem.* **1991,** *56,* 1405

In 1995, the Schmittel group reported the cation radical Diels-Alder reaction of electron-rich allenes (**Figure 1.12**).[17] Beyond expanding the scope of the dienophile partner, this transformation also provides access to valuable *exo*-alkylidine products, which can readily undergo further manipulation. They obtained the desired products in moderate to good yields. All reactions were run in the presence of 2,6-di-*tert*-butylpyridine as a base to suppress the acid catalyzed process which leads to rearrangement of the products. Electron withdrawing substituents were not tolerated at any position on the allene.

Figure 1.12 Cation Radical DA Reactions with Electron-Rich Allene Dienophiles

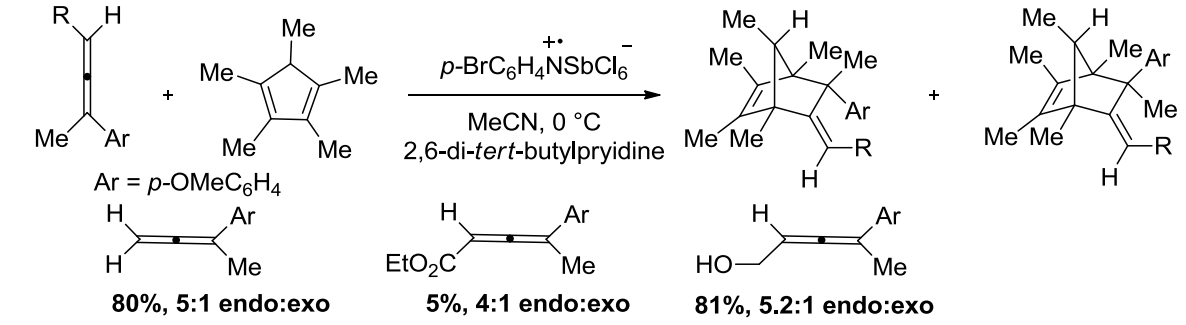

Schmittel, *J. Org. Chem.* **1995,** *60,* 8223

Recently, in 2011, the Yoon lab demonstrated the radical cation Diels-Alder reaction promoted by an inorganic ruthenium polypyridyl photocatalyst (**Figure 1.13**).[18] Using very low loadings of $Ru(bpz)_3(BArF)_2$ activated by visible light in the presence of air, they obtained the desired cycloadducts in good to excellent yields. Ruthenium complexes have been well-studied as single electron oxidants and in this case, benefit from its ability to be turned over by oxygen. Reactions with terminal styrenes, styrenes with unprotected alcohols, electron neutral styrenes and trisubstituted styrenes were unsuccessful in the reaction as well as electron deficient dienes and Danishefsky's electron rich diene.

Figure 1.13 Photocatalysis of the Cation Radical DA Reactions by $Ru(bpz)_3(BArF)_2$

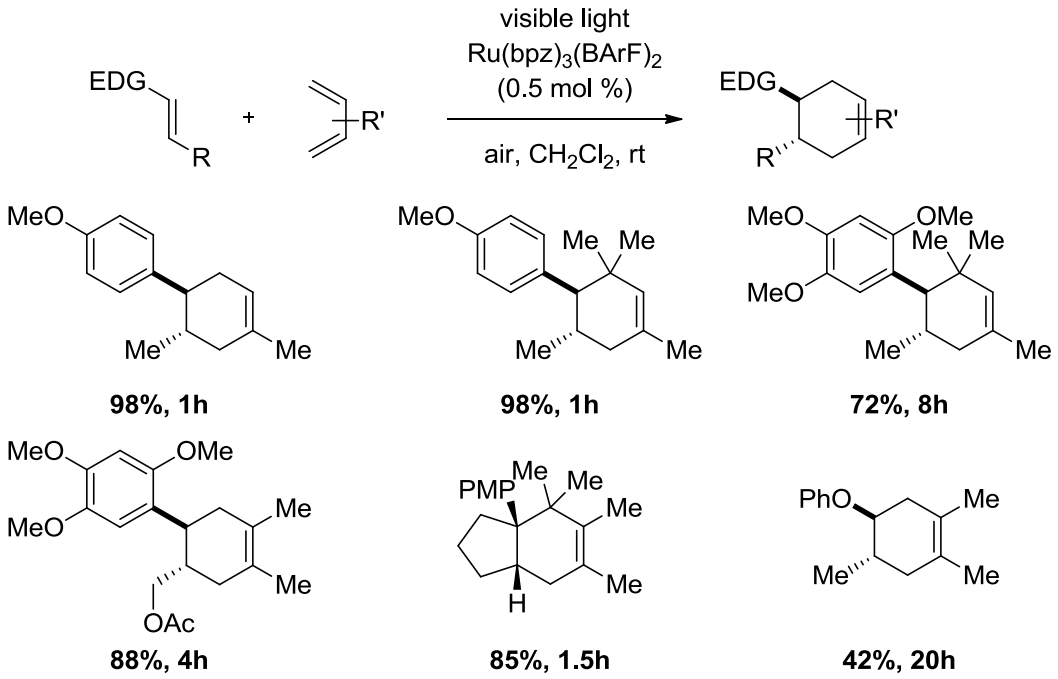

Yoon, *J. Am. Chem. Soc.* **2011,** *133,* 19350

The cation radical Diels-Alder reaction has been optimized by many groups to include a variety of electron-rich substrates and excellent reaction yields. To the best of our knowledge, there is only a single report of the enantioselective catalysis of the cation radical Diels-Alder reaction (**Figure 1.14**).[19] This example comes from Schuster and Kim in 1990, in which they report the reaction between β-methylstyrene and cyclohexadiene photocatalyzed by (-)-1,1'-bis(2,4-dicyanonaphthalene) [(-)BDCN] at -65 °C gave the cyclohexene adduct in 15% ee. The researchers found that raising the reaction temperature

to -30 °C or -5 °C gave essentially no enantioselectivity. They propose that enantioselectivity arises from the formation of diastereoselective exciplexes between the chiral catalyst and the prochiral styrene. It is possible that association between the radical cation intermediate and the reduced catalyst could direct reaction with cyclohexadiene with facial selectivity.

Figure 1.14 Enantioselective Cation Radical Diels-Alder reported by Schuster and Kim

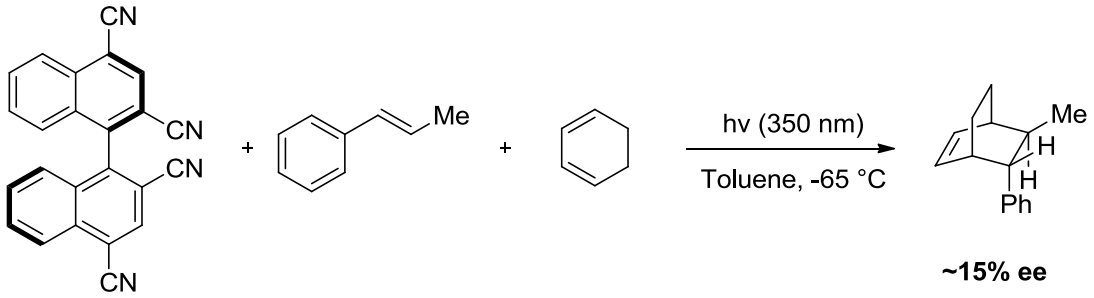

Schuster and Kim, *J. Am. Chem. Soc.* **1990**, *112*, 9635

An overview of existing cation radical methods has been discussed. All strategies rely on single electron oxidation to access the cation radical intermediates. Of interest to our group is photochemical oxidation for the catalysis of the cation radical Diels-Alder reaction. The next section will discuss basic tenets of photoinduced electron transfer and its advantages and limitations as it applies to the cation radical Diels-Alder reaction.

1.3 Photoinduced Electron Transfer

Photoinduced electron transfer is a fundamental process in chemical reactions. In general, it involves excitation of a compound to its excited state where is can easily gain a single electron from another molecule. One can predict the likelihood of such an event using the modified Rehm-Weller equation which states that the free energy of electron transfer is equal to the difference between the half-wave oxidation potential of a donor molecule and the half-wave excited state reduction potential of an acceptor molecule plus the coulombic constant [$\Delta G_{et} = E_{1/2(ox)} - E^*_{1/2(red)} + C$].[20] The coulombic term represents electrostatic energy and is determined by the charges of the ions, their distance apart and the dielectric constant of the solvent being used.

This equation allows researchers to judiciously select photo-oxidants as well as donor substrates. As discussed in the previous section, many groups believe that the role selectivity of the radical cation intermediate arises from the more easily oxizable reacting partner. Oxidation potentials of compounds can be measured by cyclic voltammetry against certain electrodes and are found in the literature (**Figure 1.15**).[21–23] Styrenes are popular substrates for the cation radical Diels-Alder reaction and generally more oxidizable than aliphatic di- or tri-substituted alkenes. Choosing an oxidant with an appropriate reduction potential to access alkenes is also critical in electron transfer reactions. These can be chemical oxidants which operate as oxidants in their ground state or photochemical oxidants, which generally have more oxidizing power. Our lab is particularly interested in the acridinium and triaryloxopyrylium salt photocatalysts as their oxidation potentials are around 2.0 V, which would provide access to substrates beyond styrenes like tri-substituted aliphatic alkenes.

Figure 1.15 Redox Potentials of Various Alkenes and Single Electron Oxidants

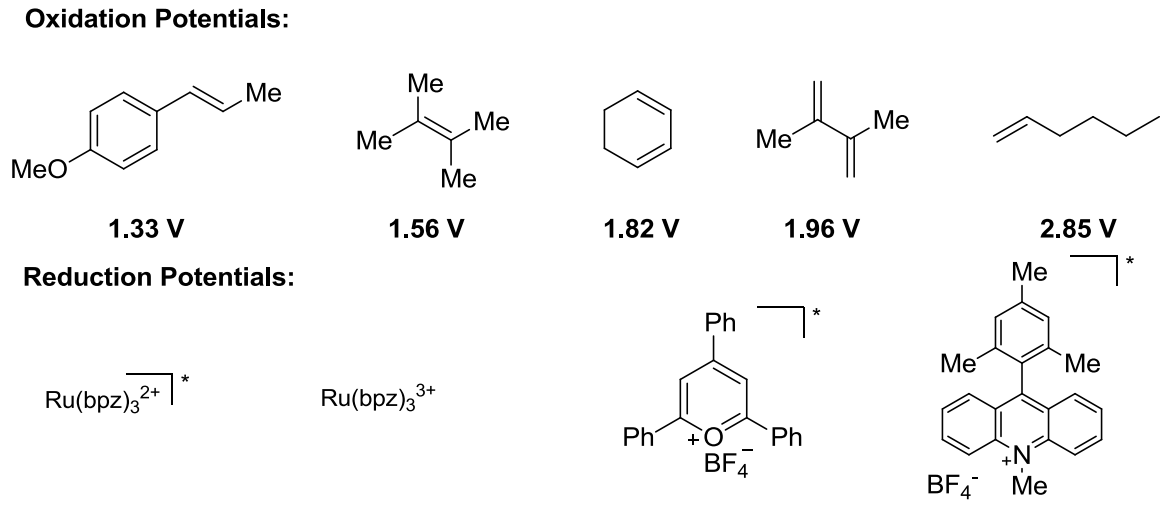

*Excited state potentials, All vs. SCE, [a]Measured
Schepp and Johnston, *J. Am Chem. Soc.* **1996,** *118,* 2872
MacMillan, *Chem. Rev.* **2013**, *113*, 5322
García, *Chem. Rev.* **1994**, 1063

Triaryloxopyrylium Salts as Photo-Oxidants

Of the photo-oxidants discussed, we were particularly interested in triaryloxopyrylium (TPT) salts. These photocatalysts have previously been evaluated in the cation radical Diels-Alder reaction and

have attracted interest for their unique properties. Variants of the salt are commercially available and readily accessible from simple starting materials. They also absorb light in the visible region which allows researchers to avoid using harmful UV-light. Simple substitution of various groups on the arene moiety allows for tunability of the absorbance, with wavelengths ranging from 412 nm for the parent triphenyloxopyrylium to 577 nm for the *p*-dimethylaminophenyl diphenyl substituted oxopyrylium. These salts are strong oxidants in their excited state and have been shown to act as an electron acceptor in their singlet or triplet state with an oxidation potential of ~2.0 V vs. SCE (**Figure 1.16**).[23]

Figure 1.16 Synthesis of Oxopyrylium Salts

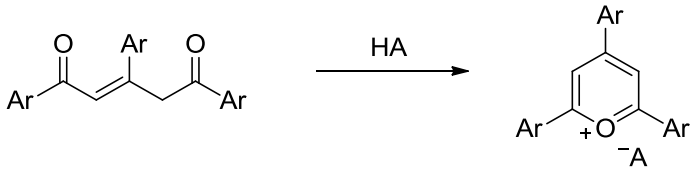

The organic oxopyrylium salts can be easily solubilized in dichloromethane or acetonitrile. They also benefit from their ionic nature. The lack of coulombic attraction between the radical cation and the oxopyrylium radical after electron transfer reduces the likelihood of non-productive back electron transfer, which is a major issue for other oxidants. This feature also suggests that the coulombic term in the Rehm-Weller equation would be essentially negligible for this electron transfer event as it lacks net charge separation. However, the oxopyrylium radical may be susceptible to dimerization with an identical species at low temperatures as observed by García and colleagues, which would sequester the active catalyst. They report that at room temperature this reaction is reversible.

García and coworkers also recognized the TPT salts unique lack of reactivity with oxygen. They found that TPT did not form singlet oxygen and reacted 100 times more rapidly with any donors in solution than with dissolved oxygen. They also reported that superoxide cannot be formed from electron transfer with TPT salts. This is rationalized by the Rehm-Weller equation which shows that the event is disfavored by ~11.3 kcal/mol. These properties make TPT salts attractive catalysts for studying organic reactions.

Lastly, we were interested in the TPT salts because we saw an opportunity to introduce a chiral organic anion to pair with the cationic oxopyrylium. The synthesis of these chiral salts will be discussed in the next chapter. We drew from the report by Schuster and Kim to hypothesize that the radical cation intermediate could potentially pair with the chiral anion as a means to induce asymmetry. In the next section, previous examples of chiral counteranion catalysis will be shown.

1.4 Chiral Counteranion Directed Catalysis

Chiral ionic catalysis has found extensive utility in phase transfer catalysis by cinchona alkaloid derivatives, in which the ionic pairing generally occurs between an oxygen enolate and a quaternary amine. This area of catalysis should be mentioned but because the chiral information is associated with the cationic partner it will not be discussed in depth. Within the last decade asymmetric counteranion-directed catalysis (ACDC) has emerged as an exciting new concept.

There has been some debate over which transformations can be classified as strictly ACDC. In a 2013 review,[24] List and Mahlau define ACDC as the "induction of enantioselectivity in a reaction proceeding through a cationic intermediate by means of ion pairing with a chiral, enantiomerically pure anion provided by the catalyst." However, it is possible that other stabilizing interactions exist in addition to the coulombic attraction within the ion pair. These interactions include hydrogen bonding, which suggests classic Brønsted acid catalysis,[25] transition metal catalysis,[26] where the anion is potentially acting as a chiral ligand, as well as anion binding catalysis which generally relies on the binding of an achiral anion to chiral thioureas.[27] Phosphoric acid derivatives have also been applied in asymmetric counteranion-directed Lewis acid catalysis for the opening of *meso*-aziridines[28] and in the Mukaiyama-aldol reaction.[29] These examples involve the simultaneous generation of the chiral counteranion and countercation after the transfer of a silyl group, and so will not be discussed. For the purposes of this project, only examples with presumably "pure" asymmetric counteranion directed catalysis will be presented.

In 2004, List and colleagues reported the enantioselective biomimetic transfer hydrogenation of enals with a slight excess of Hantzsch dihydropyridine and a catalytic amount of MacMillan's

imidazolidinone salt.[30] This transformation relies on chiral secondary amine catalysis but during their investigations, the List group was able to show a proof of concept for the catalytic asymmetric transformation hydrogenation with chiral phosphoramide salts. This result was unpublished at the time but appears in their 2013 review. Using an achiral morpholine, Hantzsch dihydropyridine and 20 mol % (*R*)-2,4,6-triisopropylphenyl phosphate BINOL [(*R*)-TRIP] anion, the authors obtain the hydrogenated product in 90% yield and 99:1 enantiomeric ratio (**Figure 1.17**).[24] They assert that there are no major stabilizing effects present as there are no nitrogen-hydrogen bonds present in the quaternary iminium intermediate. However, it is possible that there are weak hydrogen bonding interactions between the anion and CH. This result was impressive because it gave enantioselectivies even higher than obtained with chiral secondary amine catalysis.

Figure 1.17 Catalytic Asymmetric Transfer Hydrogenation through ACDC

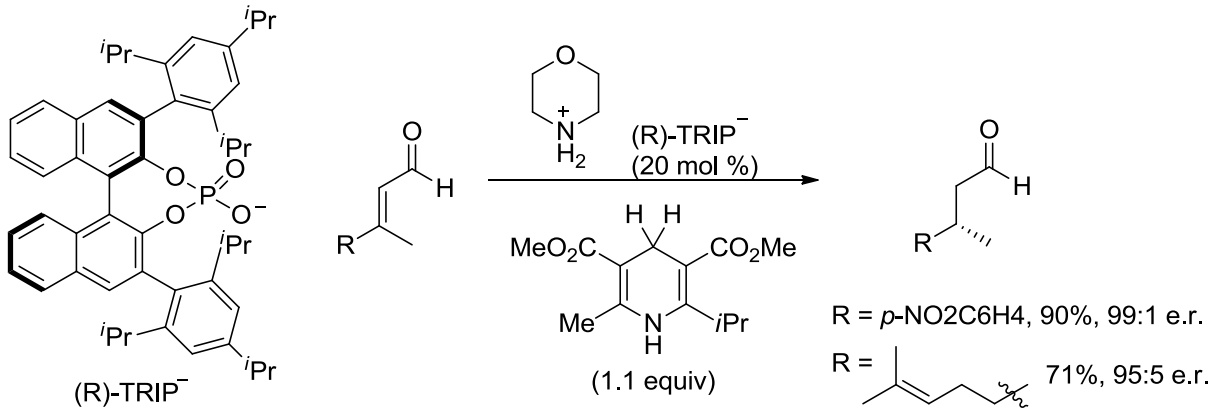

List, *Angew. Chem. Int. Ed.* **2013**, *52,* 518

In 2008, Toste and colleagues reported the enantioselective opening of meso-aziridines with alcohols using chiral counteranion catalysis (**Figure 1.18**).[31] This example of reverse polarity phase transfer catalyst represents the one of the clearest examples of using a chiral anion to induce asymmetry. By employing Ag_2CO_3 and a chiral phosphate silver salt, they abstract a chloride from the starting material to form the meso-aziridinium. They propose that the positively charged nitrogen of the aziridinium can pair with the chiral phosphate anion and block one face to selectively direct the nucleophilic opening by the alcohol. They demonstrate 11 examples of the transformation in good yields

and excellent ee's. Given that chiral phosphoric acids have been extensively reported in Brønsted acid catalysis, their use as chiral counteranions is quite appealing.

Figure 1.18 Asymmetric Opening of Meso-Aziridines Using Chiral Counteranion Catalysis

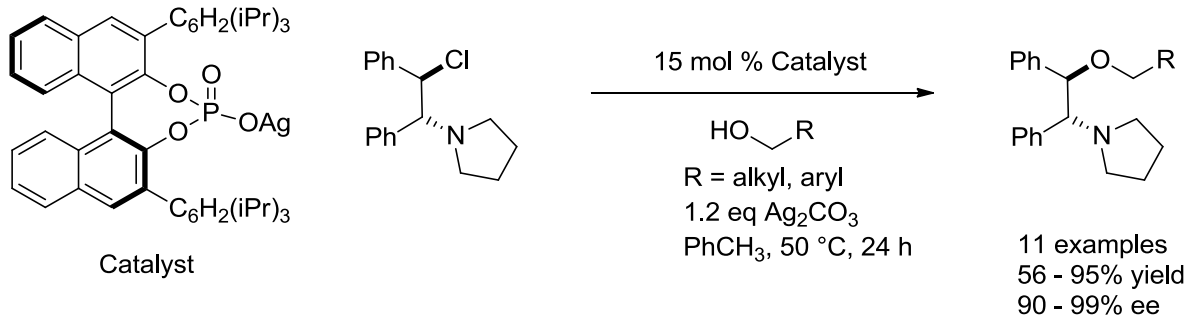

Toste, *J. Am. Chem. Soc.* **2008**, *130*, 14984

In the last year, Toste reported another example of ACDC with an asymmetric cross-dehydrogenative coupling catalyzed by chiral triazole-containing phosphoric acid (**Figure 1.19**).[32] Though this report appeared after we discontinued research on this project, it serves to represent the growth of this field. Notably, the Toste group is able to access a library of chiral triazole containing phosphoric acid catalysts through the well-established copper catalyzed azide/alkyl click reaction.

Figure 1.19 Asymmetry Cross-Dehydrogenative Coupling Using Chiral Counteranion Catalysis

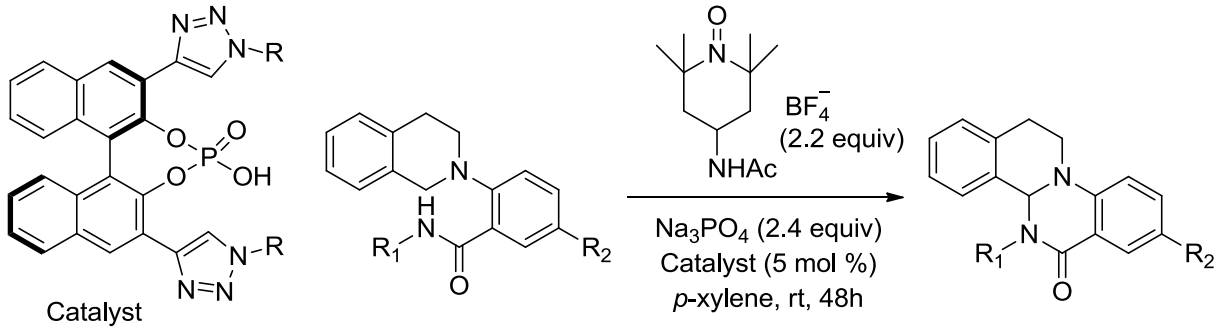

Toste, *J. Am. Chem. Soc.* **2013**, *135,* 14044

The mechanism is proposed to begin with initial substrate oxidation to form the cationic intermediate. The chiral phosphate could undergo anion exchange with the cationic oxidant, ultimately forming a close ion pair with the iminium substrate. Intermolecular nucleophilic addition is directed to one prochiral face to furnish the desired product and reprotonate the chiral phosphate. This method is

demonstrated in good to excellent yield and enantioselectivity. To investigate the role of the triazole in the selectivity of the reaction they synthesized three adamantane substituted isosteres and observed a significant loss in selectivity when the nitrogen atoms of the triazole were replaced with carbon atoms. This finding suggests that electronics of the substituents at the 3,3' positions play an important role in selectivity.

Summary

We saw an opportunity to develop a method for the enantioselective cation radical Diels-Alder reaction. As disclosed earlier, no previous reports have shown synthetically useful levels of enantioinduction in this transformation. We wanted to take advantage of an easily synthesized organic photo-oxidant like the triaryloxopyrylium and introduce chirality into the molecule through a chiral 1,1'-bi-2-napthyl (BINOL) derived counteranion. We hoped that a pairing between the radical cation intermediate and the chiral counteranion would induce asymmetry in the transformation. The next chapter will discuss the synthesis and evaluation of various chiral photo-oxidant salts and the optimization of the enantioselective cation radical Diels-Alder (**Figure 1.20**).

Figure 1.20 Proposal for an Asymmetric Cation Radical Diels-Alder Reaction

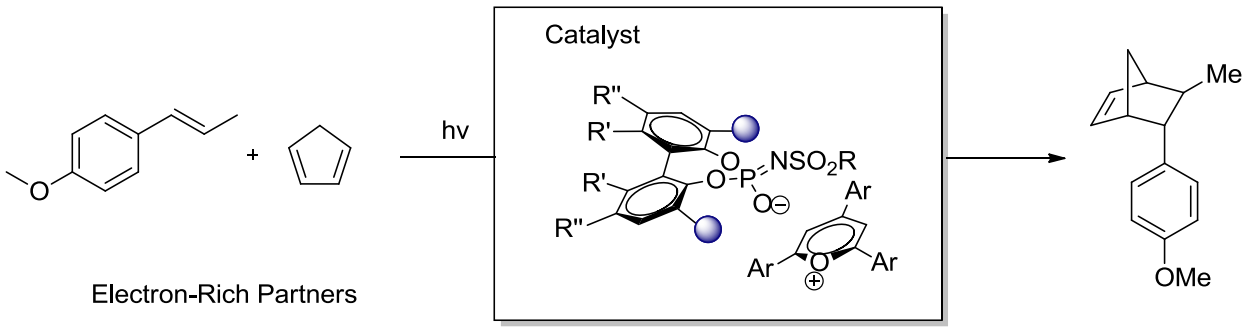

REFERENCES

(1) Norton, J. A. The Diels-Alder Diene Synthesis. *Chem. Rev.* **1942**, *31*, 319–523.

(2) Bellville, D. J.; Wirth, D. W.; Bauld, N. L. Cation-Radical Catalyzed Diels-Alder Reaction. *J. Am. Chem. Soc.* **1981**, *103*, 718–720.

(3) Houk, K. N. Generalized Frontier Orbitals of Alkenes and Dienes. Regioselectivity in Diels-Alder Reactions. *J. Am. Chem. Soc.* **1973**, *95*, 4092–4094.

(4) Evans, D. A.; Miller, S. J.; Lectka, T. Bis(oxazoline)copper(II) Complexes as Chiral Catalysts for the Enantioselective Diels-Alder Reaction. *J. Am. Chem. Soc.* **1993**, *115*, 6460–6461.

(5) Nakashima, D.; Yamamoto, H. Design of Chiral N-Triflyl Phosphoramide as a Strong Chiral Brønsted Acid and Its Application to Asymmetric Diels−Alder Reaction. *J. Am. Chem. Soc.* **2006**, *128*, 9626–9627.

(6) Ahrendt, K. A.; Borths, C. J.; MacMillan, D. W. C. New Strategies for Organic Catalysis: The First Highly Enantioselective Organocatalytic Diels−Alder Reaction. *J. Am. Chem. Soc.* **2000**, *122*, 4243–4244.

(7) Bellville, D. J.; Bauld, N. L. Selectivity Profile of the Cation Radical Diels-Alder Reaction. *J. Am. Chem. Soc.* **1982**, *104*, 2665–2667.

(8) Pabon, R. A.; Bellville, D. J.; Bauld, N. L. Cation Radical Diels-Alder Reactions of Electron-Rich Dienophiles. *J. Am. Chem. Soc.* **1983**, *105*, 5158–5159.

(9) Bauld, N. L.; Bellville, D. J.; Harirchian, B.; Lorenz, K. T.; Pabon, R. A.; Reynolds, D. W.; Wirth, D. D.; Chiou, H. S.; Marsh, B. K. Cation Radical Pericyclic Reactions. *Acc. Chem. Res.* **1987**, *20*, 371–378.

(10) Bauld, N. L.; Gao, D. Approaching a Possible Stepwise/concerted Mechanistic Crossover Point in the Cation Radical Cycloadditions of Cis- and Trans-Anethole. *J. Chem. Soc. Perkin Trans. 2* **2000**, 931–934.

(11) Jones, C. R.; Allman, B. J.; Mooring, A.; Spahic, B. Photosensitized [4 + 2] Cyclodimerization of 1,3-Cyclohexadiene. *J. Am. Chem. Soc.* **1983**, *105*, 652–654.

(12) Mattay, J.; Gersdorf, J.; Mertes, J. A New Type of Electron Acceptor for Diels–Alder Reactions via Radical Cations. *J. Chem. Soc. Chem. Commun.* **1985**, 1088–1090.

(13) Groenewold, G. S.; Gross, M. L. Cation Radical Diels-Alder Reaction of 1,3-Butadiene: A Two-Step Cycloaddition. *J. Am. Chem. Soc.* **1984**, *106*, 6569–6575.

(14) Mlcoch, J.; Steckhan, E. Electrochemically Induced [4+2]-Cycloadditions - a Mechanistic Interpretation of the Cation Radical Diels-Alder Reaction Based on Preparative Results. *Tetrahedron Lett.* **1987**, *28*, 1081–1084.

(15) Chockalingam, K.; Pinto, M.; Bauld, N. L. A Rigorous Test for Orbital Symmetry Control in Cation Radical/neutral Cycloadditions. *J. Am. Chem. Soc.* **1990**, *112*, 447–448.

(16) Gieseler, A.; Steckhan, E.; Wiest, O.; Knoch, F. Photochemically Induced Radical-Cation Diels-Alder Reaction of Indole and Electron-Rich Dienes. *J. Org. Chem.* **1991**, *56*, 1405–1411.

(17) Schmittel, M.; Woehrle, C. Cation Radical Catalyzed Diels-Alder Reaction of Electron-Rich Allenes. *J. Org. Chem.* **1995**, *60*, 8223–8230.

(18) Lin, S.; Ischay, M. A.; Fry, C. G.; Yoon, T. P. Radical Cation Diels–Alder Cycloadditions by Visible Light Photocatalysis. *J. Am. Chem. Soc.* **2011**, *133*, 19350–19353.

(19) Kim, J. I.; Schuster, G. B. Enantioselective Catalysis of the Triplex Diels-Alder Reaction: Addition of Trans-.beta.-Methylstyrene to 1,3-Cyclohexadiene Photosensitized with (-)-1,1'-bis(2,4-Dicyanonaphthalene). *J. Am. Chem. Soc.* **1990**, *112*, 9635–9637.

(20) Jayanthi, S. S.; Ramamurthy, P. Photoinduced Electron Transfer Reactions of 2,4,6-Triphenylpyrylium: Solvent Effect and Charge-Shift Type of Systems. *Phys. Chem. Chem. Phys.* **1999**, *1*, 4751–4757.

(21) Schepp, N. P.; Johnston, L. J. Reactivity of Radical Cations. Effect of Radical Cation and Alkene Structure on the Absolute Rate Constants of Radical Cation Mediated Cycloaddition Reactions1. *J. Am. Chem. Soc.* **1996**, *118*, 2872–2881.

(22) Prier, C. K.; Rankic, D. A.; MacMillan, D. W. C. Visible Light Photoredox Catalysis with Transition Metal Complexes: Applications in Organic Synthesis. *Chem. Rev.* **2013**, *113*, 5322–5363.

(23) Miranda, M. A.; Garcia, H. 2,4,6-Triphenylpyrylium Tetrafluoroborate as an Electron-Transfer Photosensitizer. *Chem. Rev.* **1994**, *94*, 1063–1089.

(24) Mahlau, M.; List, B. Asymmetric Counteranion-Directed Catalysis: Concept, Definition, and Applications. *Angew. Chem. Int. Ed.* **2013**, *52*, 518–533.

(25) Uraguchi, D.; Terada, M. Chiral Brønsted Acid-Catalyzed Direct Mannich Reactions via Electrophilic Activation. *J. Am. Chem. Soc.* **2004**, *126*, 5356–5357.

(26) Hamilton, G. L.; Kang, E. J.; Mba, M.; Toste, F. D. A Powerful Chiral Counterion Strategy for Asymmetric Transition Metal Catalysis. *Science* **2007**, *317*, 496–499.

(27) Taylor, M. S.; Jacobsen, E. N. Highly Enantioselective Catalytic Acyl-Pictet−Spengler Reactions. *J. Am. Chem. Soc.* **2004**, *126*, 10558–10559.

(28) Rowland, E. B.; Rowland, G. B.; Rivera-Otero, E.; Antilla, J. C. Brønsted Acid-Catalyzed Desymmetrization of Meso-Aziridines. *J. Am. Chem. Soc.* **2007**, *129*, 12084–12085.

(29) García-García, P.; Lay, F.; García-García, P.; Rabalakos, C.; List, B. A Powerful Chiral Counteranion Motif for Asymmetric Catalysis. *Angew. Chem. Int. Ed.* **2009**, *48*, 4363–4366.

(30) Yang, J. W.; Hechavarria Fonseca, M. T.; Vignola, N.; List, B. Metal-Free, Organocatalytic Asymmetric Transfer Hydrogenation of A,β-Unsaturated Aldehydes. *Angew. Chem. Int. Ed.* **2005**, *44*, 108–110.

(31) Hamilton, G. L.; Kanai, T.; Toste, F. D. Chiral Anion-Mediated Asymmetric Ring Opening of Meso-Aziridinium and Episulfonium Ions. *J. Am. Chem. Soc.* **2008**, *130*, 14984–14986.

(32) Neel, A. J.; Hehn, J. P.; Tripet, P. F.; Toste, F. D. Asymmetric Cross-Dehydrogenative Coupling Enabled by the Design and Application of Chiral Triazole-Containing Phosphoric Acids. *J. Am. Chem. Soc.* **2013**, *135*, 14044–14047.

CHAPTER 2: PROGRESS TOWARDS AN ASYMMETRIC PHOTOCATALYTIC DIELS-ALDER REACTION

Introduction

This chapter will detail our efforts to develop a photocatalytic enantioselective cation radical Diels-Alder reaction. We recognized the great utility of the cation radical Diels-Alder reaction, a powerful transformation that combines two electronically matched partners to form two bonds and up to four contiguous stereocenters. Rendering this reaction asymmetric would represent a significant advance for this area of organic synthesis. We chose to explore triaryloxopyrylium salts paired with various chiral anions as our chiral photoredox catalysts. Over the course of three years, we extensively evaluated numerous catalysts and reaction conditions but were unable to achieve synthetically practical levels of reactivity and enantioselectivity. We believe this transformation to be highly valuable and herein present our results as a contribution to the field of chiral counteranion directed catalysis.

2.1 Initial Investigation of Racemic Reaction

We began our investigations with the racemic reaction reported by Bauld[1] and colleagues between β-methyl-*p*-methoxystyrene (anethole) and cyclopentadiene (Cp) catalyzed by triphenyloxopyrylium tetrafluoroborate (TPT) in DCM under irradiation by four 60W fluorescent light bulbs. We used cyclopentadiene in excess (5 equivalents) as reported by Bauld, in hopes of increasing the likelihood of reaction between the anethole radical cation and cyclopentadiene. We assumed that anethole would occupy the role of the cation radical partner given its lower oxidation potential.[2] It was important to distill both starting materials before use. In the case of anethole, the radical inhibitor present as a stabilizer in its commercially available form had to be excluded from the reaction mixture. Cyclopentadiene dimerizes readily in a thermal [4+2]

reaction to form dicyclopentadiene at room temperature and must be heated to ~200 °C to obtain the retro-Diels-Alder product and distillate cyclopentadiene, which was kept at low temperatures to ensure its purity. The cation radical Diels-Alder reaction was run at -60 °C for 24 hours and the desired products were obtained in 88% GC yield in 10:1 dr. A chiral GC assay was developed for the isolated products (**Figure 2.1**).

Figure 2.1 Initial Racemic Cation Radical Diels-Alder Catalyzed by a TPT Salt

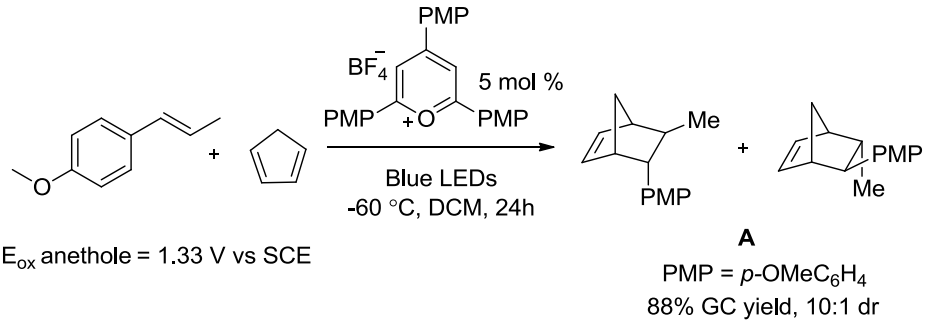

2.2 Optimization of the Cation Radical Diels-Alder Reaction

At the outset of the project we were very interested in C2-symmetric 1,1'-bi-2-naphthyl (BINOL) phosphate derivatives as counteranions to oxopyryliums to induce asymmetry in the reaction through the formation of a chiral ion pair. This class of compounds has been extensively used in enantioselective Brønsted acid catalysis[3] and allowed us to prepare our acid precursors following existing literature. We recognized that it would be crucial to find an adequately acidic partner to cyclize the ene dione precursor to form the oxopyrylium salt. The subsequently formed counteranion should be poorly nucleophilic to disfavor addition to the radical cation intermediate. While addition of the counteranion could be reversible, if the equilibrium favors addition it could result in a loss of reactivity. For that reason we chose to target *N*-trifluoromethanesulfonyl (*N*-trifyl) phosphoramides as opposed to the phosphoric acid analogs. The *N*-trifyl phosphoramide can delocalize the negative charge between five atoms as opposed to three atoms in the latter.

The aryl substituted BINOL chiral catalysts were synthesized starting from enantiopure BINOL. Methyl protection of the alcoholic groups followed by bromination at low temperature

proceeded in good yield to give intermediate **2.** This intermediate was treated with a nickel catalyst to install the aryl groups via a Kumada coupling then deprotection with boron tribromide revealed the pendant alcohols. The silyl-substituted BINOL catalysts also began from enantiopure BINOL. Hydrogenation of the back rings promoted by PtO_2 then selective bromination furnished intermediate **5** in quantitative yield. Silylation of intermediate **5** was followed by a retro-Brook rearrangement with *tert*-butyl lithium to furnish the substituted BINOL **6**. Treatment of intermediates **3** and **6** with phosphorous oxychloride, dimethylamino pyridine, triethylamine and trifluoromenthane sulfonamide produced the substituted *N*-trifyl phosphoramides **7** along with the phosphate side product, which can be separated via silica gel chromatography. With the phosphoramides in hand, we were pleased to find that upon heating with triaryl ene dione in ethanol by heat gun to ~80 °C the desired salt was precipitated upon cooling (**Figure 2.2**).

Figure 2.2 Synthesis of 3,3' Substituted BINOL and H8-BINOL Catalysts

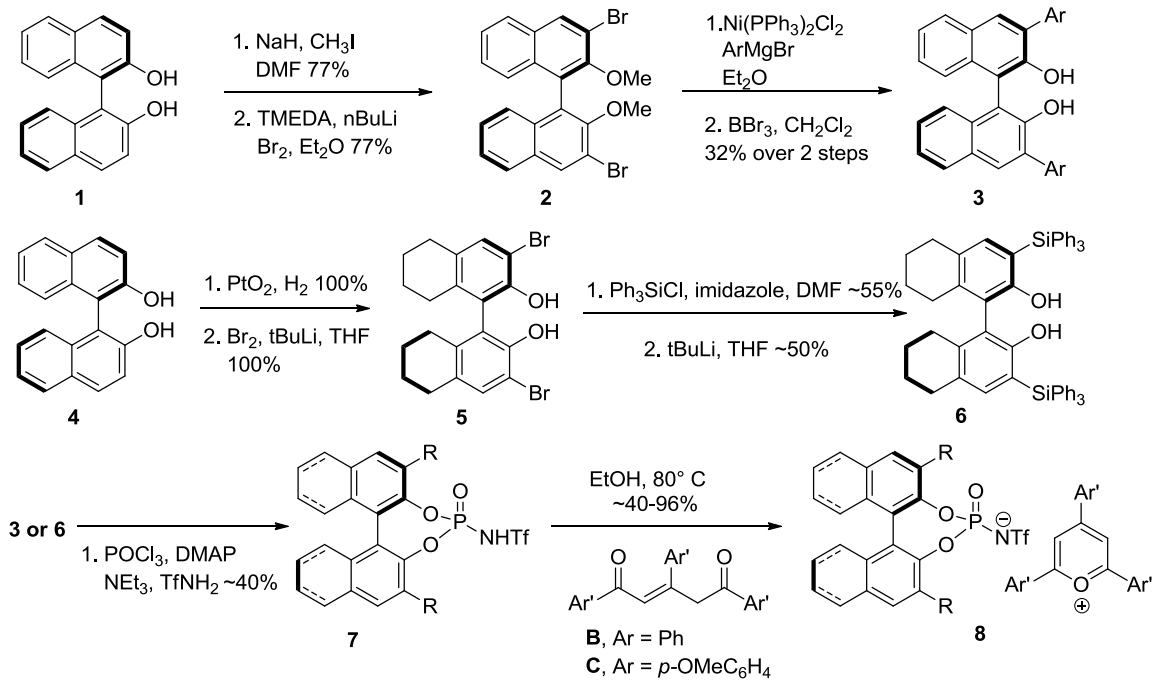

Impurities were removed after washing with hexanes or recrystallization with DCM/hexanes. We did experience some variation in our results with different batches of chiral

catalysts. We suspected that there may have been some inorganic counteranion contaminants present, which would lower the observed enantioselectivity. We tried to address this issue by careful recrystallization and drying the catalyst under vacuum at 60 °C overnight.

With the chiral catalysts in hand we tested their efficiency and selectivity in the cation radical Diels-Alder reaction (**Figure 2.3**). We found that bulky arenes at the 3 and 3' positions did not provide any useful levels of enantioselectivity. Interestingly, substitution with the bulky 3,3'-$SiPh_3$ gave a promising level of ee (enantiomeric excess) though very low yield was observed for the closely related tri-isopropyl substituted silane. We were interested in the H8-BINOL scaffold as the fully saturated back rings would increase the steric interaction between the binaphthyl framework. This modification increases the rigidity of the structure and also changes the bite angle close to the anionic center. By employing catalyst **8a,** we were pleased to observe an 18% yield with 18% ee and 4:1 dr, which is a similar level of diastereoselectivity obtained by Bauld with TPT.

Figure 2.3 Initial BINOL-Derived Catalyst Screen

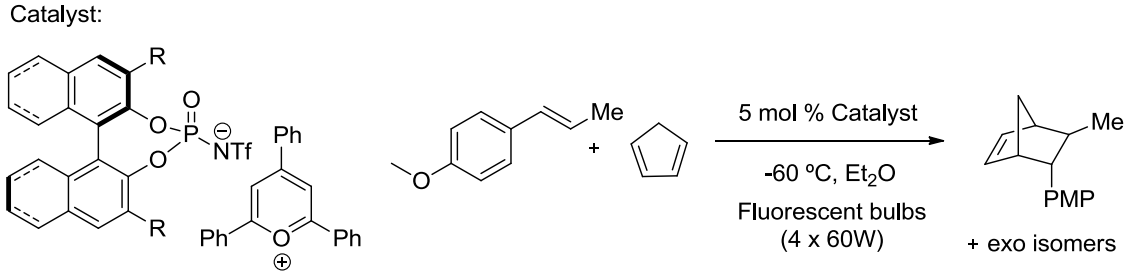

entry	R	% GC Yield	d.r. (endo/exo)	%ee
1	[a]2,4,6 (i-Pr)$_3$C$_6$H$_2$	**8a** 2%	4.1:1	5%
2	[a]2,4,6 (Me)$_3$C$_6$H$_2$	**8b** 37%	4.8:1	4%
3	[b]Anthracene	**8c** 100%	4.4:1	0%
4	[b]Si(i-Pr)$_3$	**8d** 2%	7:1	0%
5	[b]$SiPh_3$	**8e** 18%	4:1	18%

[a]BINOL backbone, [b]H8 BINOL backbone.

Given the promising initial results observed with the 3,3' $SiPh_3$-BINOL catalyst **8e**, we proceeded to optimize the reaction conditions with this catalyst. In evaluating the catalysts we

used 5.0 equivalents of cyclopentadiene in keeping with Bauld and co-workers' previous report. We did not observe any advantage in increasing or decreasing the equivalents of Cp used 5.0 equivalents of cyclopentadiene throughout for consistency. When we inverted the relationship between the starting materials, with anethole present in excess, we obtained many unidentifiable side products in the crude reaction mixture. These new products eluted close to the desired products by chiral gas chromatography (GC), making it difficult to accurately measure yield and selectivity, therefore, we decided to keep anethole as the limiting reagent.

We believed that solvent polarity would play a large role in enantioselectivity as we were relying on ionic interactions to control enantioinduction. We wanted to achieve tight ion pairing between the radical cation and chiral counteranion for good enantiocontrol through non-polar solvents. On the other hand, highly polar solvents would be more conducive for reactivity. The challenge would lie in finding a balance between selectivity and reactivity. When we evaluated our reaction in various solvents we observed inverse trends in yield and ee (**Figure 2.4**).

Figure 2.4 Comparing Dielectric Constant vs. Yield and Selectivity

Catalyst:

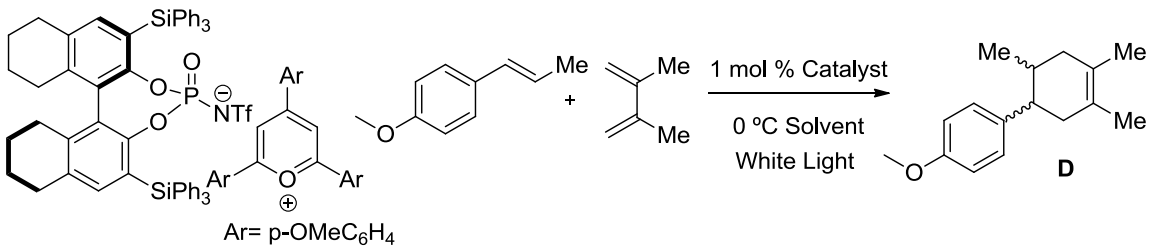

	DCM[a]	Chloroform[a]	Et_2O[b]	Toluene[b]	Xylenes[a]
Entry	1	2	3	4	5
Dielectric Constant	8.93	4.81	4.33	2.38	2.57
GC Yield (8h)	2.5%	0.1%	0.1%	0.5%	0.6%
% ee	1%	2.7%	4.0%	20.5%	22.0%

Irradiated with [a]Fluorescent lamp, [b]White LEDs

At this point we decided to switch from cyclopentadiene as the diene to 2,3-dimethyl butadiene because it would make the determination of enantioselectivity more facile because only

two isomers are formed as opposed to four diastereomers. Although all of the yields are low, the highest yield was obtained using the solvent DCM, which is the most polar. Polarity can be expressed through dielectric constants of the solvents and we saw that as the dielectric constant decreased, the enantioselectivities increased. The two least polar solvents, toluene and xylenes, gave a 20.5% ee and 22% ee, respectively.

We imagined addressing this delicate issue by evaluating the reaction in numerous different solvents as well as solvent mixtures (**Table 1**).

Table 1. General Solvent Screen

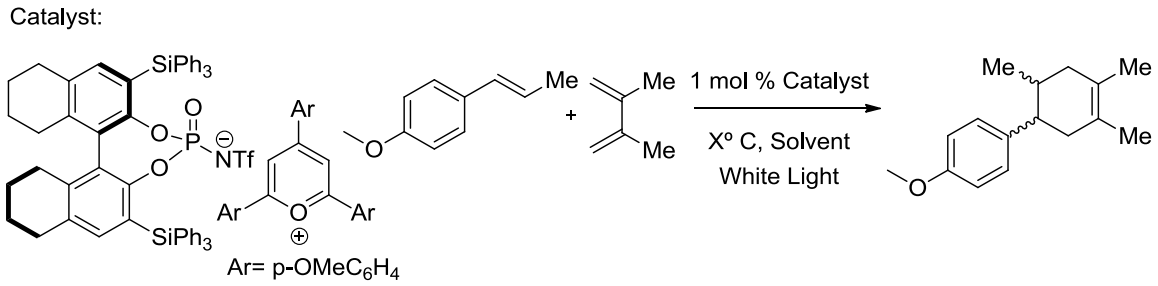

Entry	Solvent	Temperature	Time	GC Yield	% ee
1	Bromobenzene	-30 °C	24 h	9.3%	36%
2	Fluorobenzene	-30 °C	24 h	0.2%	22%
3	Acetone	-30 °C	24 h	0.1%	1%
4	Toluene	-30 °C	24 h	1.8%	23%
5	Toluene	0 °C	6 h	0.4%	12%
6	THF	0 °C	6 h	0.3%	12%
7	1%TFE/Toluene	0 °C	6 h	1.0%	1.2%
8	3% TFE/Toluene	0 °C	6 h	1.1%	0.6%
9	1% DCM/Toluene	0 °C	6 h	0.5%	16%
10	3% DCM/Toluene	0 °C	6 h	0.5%	13%
11	10% DCM/Toluene	0 °C	6 h	0.5%	14%
12	20% DCM/Toluene	0 °C	6 h	0.6%	10%
13	50% DCM/Toluene	0 °C	6 h	1.0%	11%
14	75% DCM/Toluene	0 °C	6 h	1.3%	5%
15	90% DCM/Toluene	0 °C	6 h	2.2%	0%

Using bromobenzene as a solvent gave interesting selectivity but was not pursued as a solvent because its melting point of -30 °C would potentially limit its optimization. Reactions run in other solvents such as dimethylformamide, ethyl acetate and 2-methyltetrahydrofuran

performed poorly. Ultimately, we did not identify any solvent or solvent mixture that provided results superior to 100% toluene.

We also conducted experiments evaluating various catalyst loadings (**Figure 2.5**). We found that lower catalyst loadings afforded higher enantioselectivities. The yields dropped from 9% to 5% when the catalyst loading was decreased from 5 to 1 mol %, however, moving from 1 mol % to 0.5 mol % did not have any effect on the yield. Moving forward we employed 0.5 mol % catalyst for our test reactions, not only in hopes of high selectivities but to conserve precious chiral catalyst.

Figure 2.5 Catalyst Loading Screen

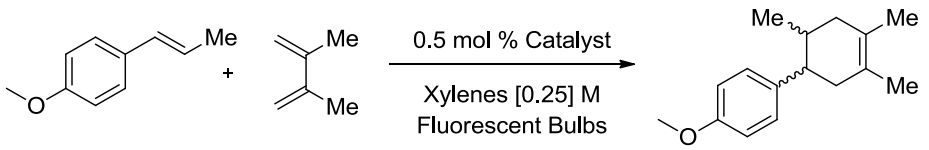

Catalyst:

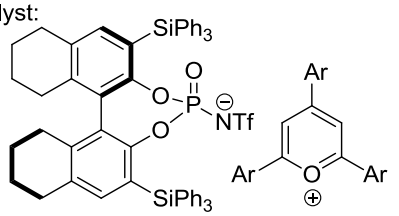

Ar= p-MeC_6H_4

Entry	Catalyst Loading	GC Yield	%ee
1	5 mol %	9%	15%
2	1 mol %	5%	19%
3	0.5 mol %	5%	24%

We then turned to investigate the effects of temperature on the reaction (**Figure 2.6**). We hypothesized that lowering the temperature would slow down the reaction and potentially lead to better selectivities. We assumed that if the reaction proceeded more slowly, that might allow more time for the chiral counteranion to coordinate to the cation radical intermediate before encountering the diene partner. Cooling the reaction vessel in a cryobath, we observed an increase in % ee as temperatures decreased though the yields were extremely poor. However, lowering the temperature beyond -60 °C did not lead to any gains in enantioselectivity, likely because it is close to toluene's freezing point of -95 °C and the yield was so low that it is difficult to be confident in the enantiomeric ratio via chiral GC.

Figure 2.6 Screening for Reaction Temperature

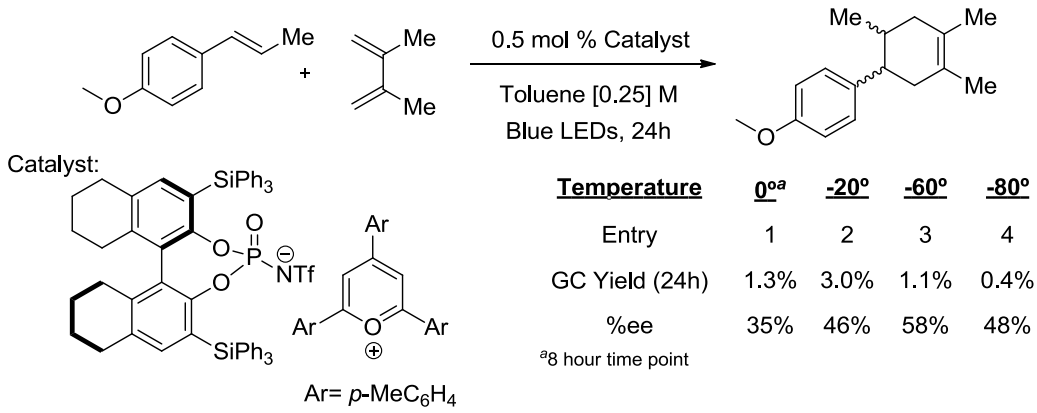

Temperature	0°[a]	-20°	-60°	-80°
Entry	1	2	3	4
GC Yield (24h)	1.3%	3.0%	1.1%	0.4%
%ee	35%	46%	58%	48%

[a] 8 hour time point

While we were quite pleased at the enantioselectivity observed at -60 °C, the yield was disappointingly low and needed to be addressed for this method to be viable. Moving away from our standard test reaction, we hoped that different substrates, specifically more reactive partners, would improve the observed product yields. There were a variety of substrates that did not participate even in the racemic cation radical Diels-Alder reaction (**Figure 2.7**). We attempted to react the electron rich *trans*-1-methoxy-3-trimethylsilyloxy-1,3-butadiene (Danishefsky's diene) with anethole but surprisingly was unable to detect any desired product. The trimethylsilyl protected analog of Danishefsky's diene also failed to react. It should be noted that this type of diene also did not react when promoted by ruthenium photoredox catalysts. Cyclohexadiene performed well as a reactive diene with anethole but was not pursued because the diastereomers could not be adequately separated by chiral GC. Reaction of substituted cyclohexadiene with anethole resulted in the formation of many side products. Furans have been reported as productive diene partners in normal demand Diels-Alder reactions but gave no desired product under our reaction conditions. We also saw no reaction between anethole and both 1,4-diphenyl butadiene and 7-methoxy-4-vinyl-1,2-dihydronaphthalene.

Figure 2.7 Failed Substrates for the Racemic Cation Radical Diels-Alder Reaction

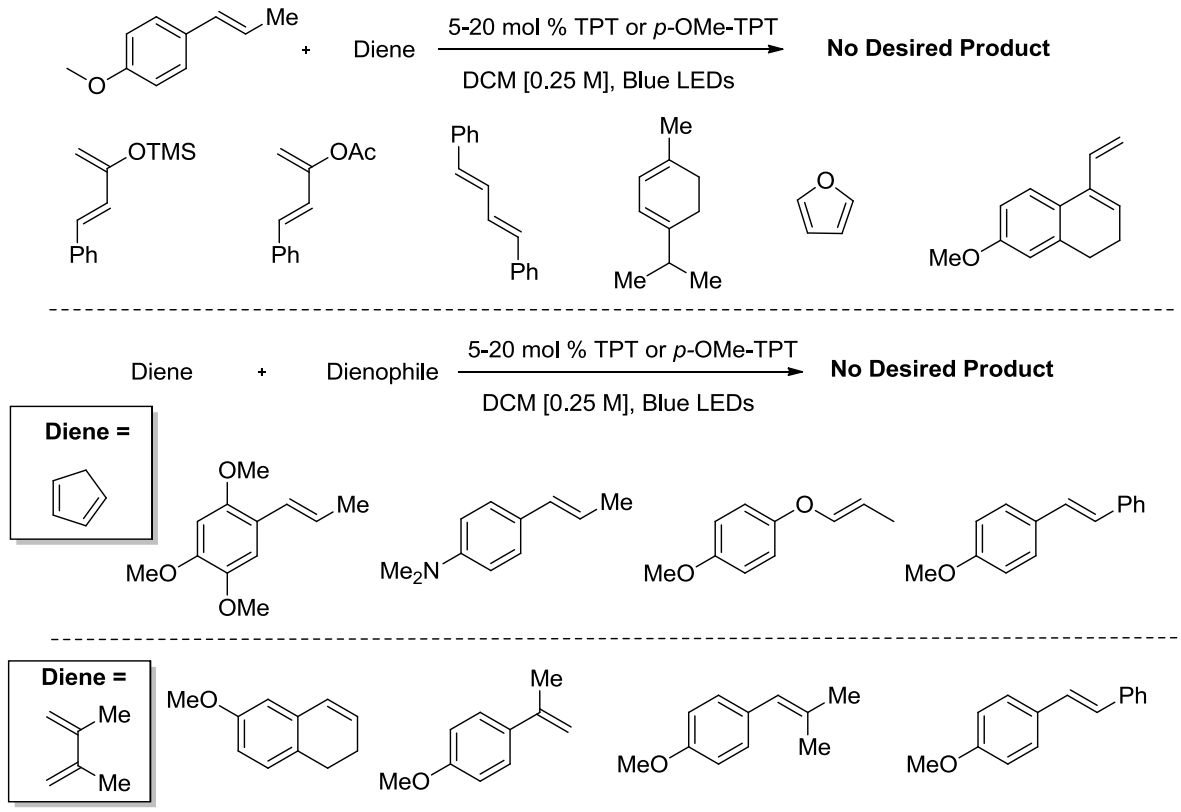

We also evaluated a number of dienophile partners that failed to react in the racemic reaction. Unsubstituted β-methylstyrene as well as α-methyl *p*-OMe styrene resulted in polymerization. The reaction did not tolerate tertiary amine or vinyl ether substitutions. We were quite interested in 6-methoxy-1,2-dihydronaphthalene as a dienophile that might allow us to explore the reactivity of a *cis* styrene, however we were unable to detect any desired product. Placing a phenyl ring at the β-position of the styrene resulted in no reaction, potentially because of unfavorable steric interactions or it may have deactivated the styrene towards oxidation.

We found a number of substrates that participated in the racemic cation radical Diels-Alder reaction yet did not produce synthetically useful levels of reactivity or enantioselectivity in the asymmetric transformation (**Figure 2.8**). We noticed that acyclic dienes generally resulted in lower reactivity. Substitution around the arene of the styrenyl

dienophiles was tolerated and in particular the triphenylsiloxy substituted styrene performed comparably to anethole. We investigated the effect of having the dienophile partner locked in the cis geometry, but observed no advantage in reactivity or selectivity.

Figure 2.8 Substrates that Resulted in Low Yields and Selectivity

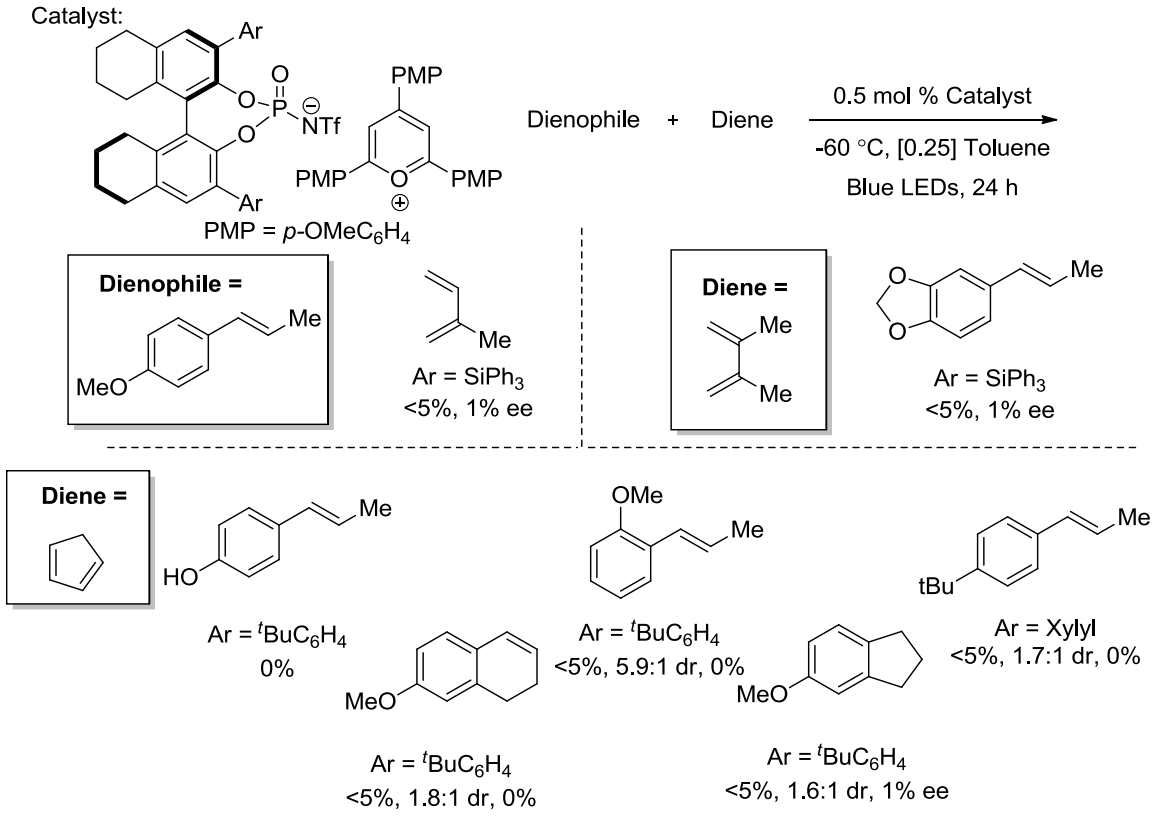

We realized that in order to move forward in the development of this method we had to address the low reactivity. While we were unsure of the cause, the lack of reactivity likely stems from the presence of the chiral anion as the oxopyrylium with the inorganic tetrafluoroborate counteranion catalyzes the racemic reaction quantitatively within a few hours. It was possible that the anion was binding to the cation radical intermediate and suppressing reactivity. We decided to focus on cyclopentadiene as the diene partner over 2,3-dimethyl butadiene because of its increased reactivity which it owes to its locked cis geometry. Encouragingly, a side by side

comparison of 2,3-dimethyl butadiene and cyclopentadiene did reveal an increase in yield from 1.1% to 29% with Cp; however we observed a loss in enantioselectivity (**Figure 2.9**).

Figure 2.9 Comparison of 2,3-Dimethyl Butadiene and Cyclopentadiene

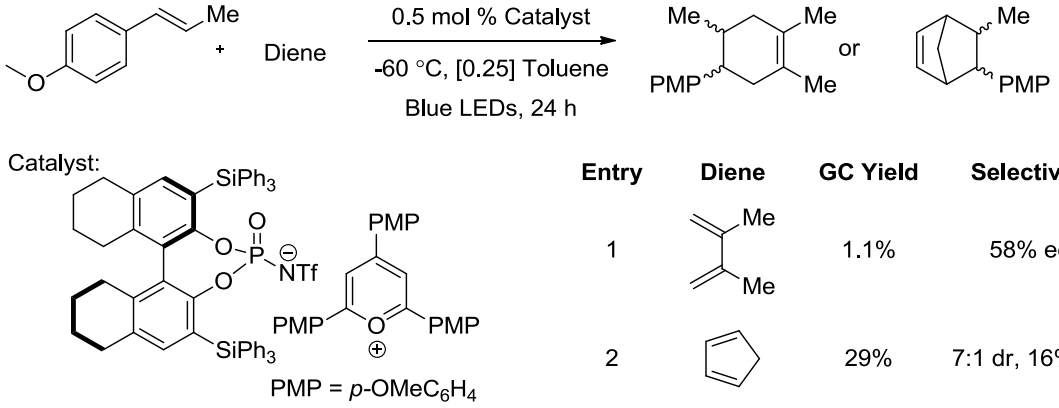

Entry	Diene	GC Yield	Selectivity
1		1.1%	58% ee
2		29%	7:1 dr, 16% ee

We were encouraged by the modest levels of both reactivity and enantioselectivity observed with the use of cyclopentadiene. We hoped to find a way to increase both through optimization of the reaction conditions. We evaluated a series of concentrations and found that more dilute solutions led to higher enantioselectivities (**Figure 2.10**). Using a concentration of [0.063 M] in toluene gave the most promising result with 38% yield, 10:1 dr and 45% ee after 24 hours. We repeated this result on a large scale for 72 hours and obtained the products in 63% yield, 9:1 dr and 36% ee.

Figure 2.10 Optimization for Concentration with Cyclopentadiene Reaction Partner

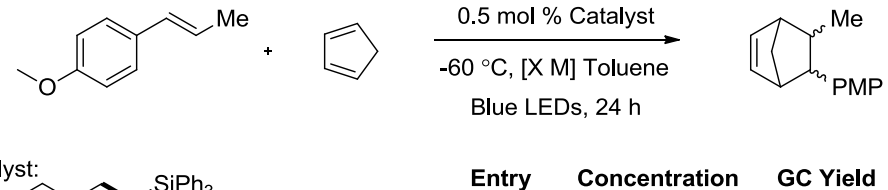

Entry	Concentration	GC Yield	Selectivity
1	[0.25 M]	28%	7:1 dr, 16% ee
2	[0.125 M]	35%	7:1 dr, 18% ee
3	[0.0625 M]	38%	10:1 dr, 45% ee
4	[0.0313 M]	11%	5:9 dr, 30% ee

We believed we were close to exhausting all remaining optimization strategies for this transformation, save catalyst design and other miscellaneous ideas which will be discussed in a separate section. We synthesized a small set of substrates bearing different aliphatic groups at the β-position of the styrene to probe the substrate scope of this reaction. We had difficulty obtaining reliable results for the β-cyclohexyl substrate as we were unable to purify the starting styrene. We also synthesized the β-adamantyl substrate and developed a chiral GC assay for its reaction with cyclopentadiene but were unable to confidently calculate the enantioselectivity as new side products eluted around the same GC retention time as our products. The only productive variation was synthesizing the β-ethyl para-methoxy styrene which reacted with Cp after four days to give the desired products in a good 85% yield and modest enantioselectivity.

Figure 2.11 Substrate Scope for the Enantioselective Cation Radical Diels-Alder

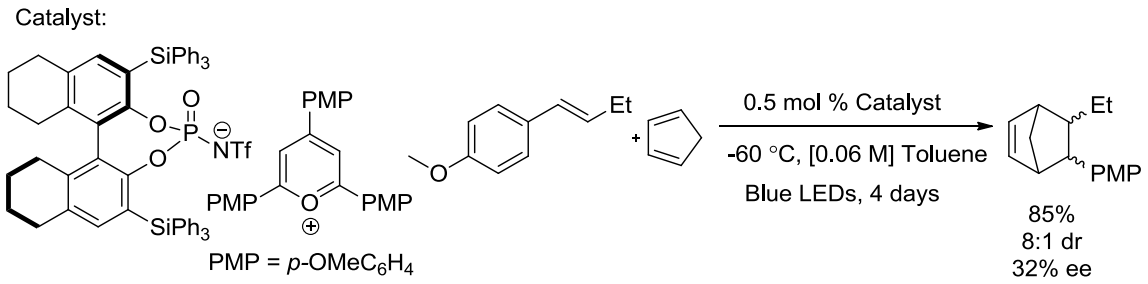

We then decided to pursue other avenues of exploration, including the intramolecular variant of this transformation with efforts led by fellow graduate student Peter Morse. The subsequent sections disclose the evaluation of various catalysts and strategies that failed to provide a breakthrough for the project, though these results should be of use if this project is revisited in the future.

2.3 Chiral Catalyst Screen for the Enantioselective Cation Radical DA

The catalysts evaluated in this transformation were developed by myself and fellow Nicewicz group members Jean-Marc Grandjean, Dr. Nicole Torres Knight and Peter Morse. Concurrent with this research, Jean-Marc Grandjean worked on the enantioselective cation radical cyclopropanation reaction, simultaneously testing this library of chiral catalysts.

Early on we recognized that the 3,3' $SiPh_3$ BINOL *N*-trifylphosphoramide triaryl oxopyrylium **8a** was a promising catalyst. We were interested in making minor modifications to this scaffold to hopes of gleaning information as to which moieties were critical to reactivity and/or selectivity (**Figure 2.12**). We evaluated the analogous phosphate catalyst **9** and found that moving away from nitrogen to oxygen resulted in a complete loss in reactivity and selectivity.

Figure 2.12 Effect of Modifications on the 3,3'-SiAr3-H8-BINOL Catalyst Scaffold

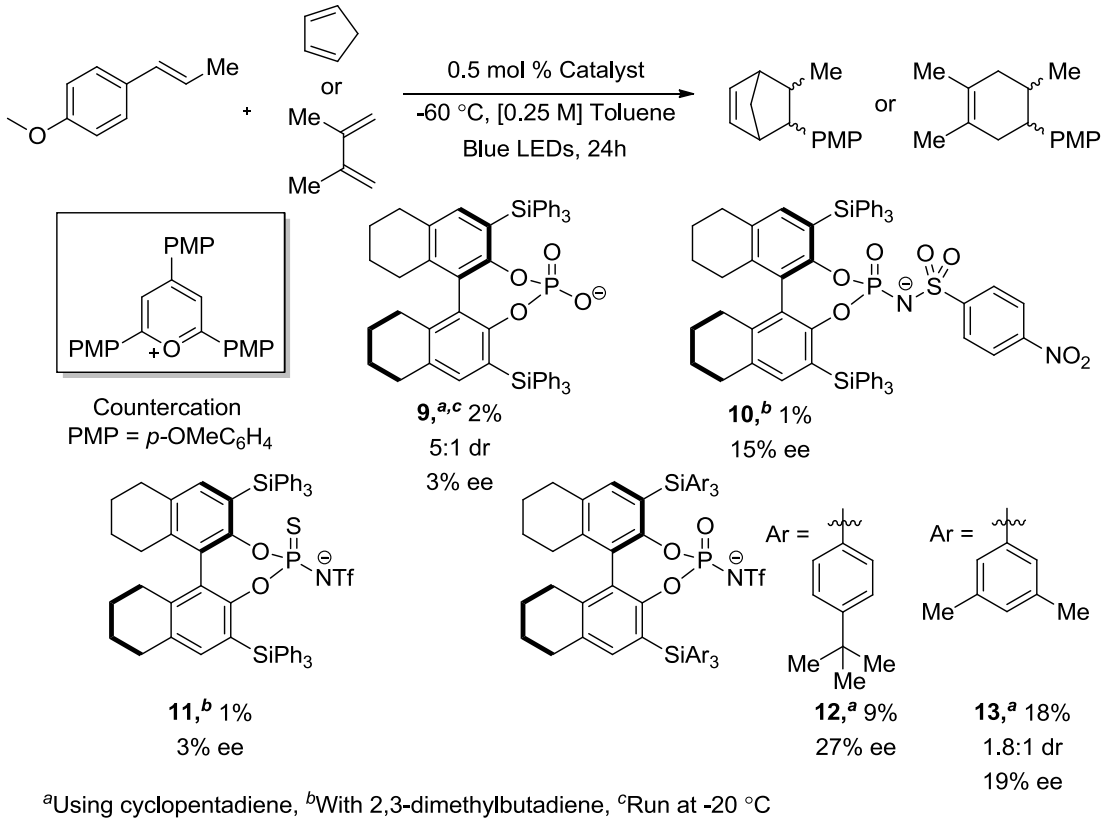

[a]Using cyclopentadiene, [b]With 2,3-dimethylbutadiene, [c]Run at -20 °C

We hypothesized that the phosphate was too nucleophilic towards to the radical cation intermediate, shutting down reactivity. We then modulated the electronic nature of the sulfonamide, replacing trifluoromethane sulfonamide with *p*-nitrobenzene sulfonamide in compound **10** and while a modest 15% ee was observed, hardly any product was formed. We synthesized and tested the thiophosphoramide **11** and also observed a disappointing lack of reactivity and enantioselectivity. These results demonstrated that any changes around the anionic center and its nucleophilicity, in terms of sterics or electronics, resulted in dramatic decreases in

yield and enantioselectivity. The *N*-trifluoromethane sulfonyl phosphoramide moiety appears to be essential for reactivity.

Dr. Nicole Torres Knight in our lab first synthesized the catalysts **12** and **13** which bear *p-tert*-butylphenyl and 3,5-dimethylphenyl (xylyl) trisubstituted silanes, respectively. We were intrigued by initial results from catalyst **12** but eventually abandoned further optimization after attempts to increase the yields were unfruitful. The trixylylsilyl substituted catalyst **13** provided similar but slightly decreased yield and selectivity to the triphenylsilyl catalyst **8a** at our optimized conditions. Upon catalyst loading optimization we observed that yields could be much improved though selectivity did suffer (**Figure 2.13).**

Figure 2.13 Optimization using the 3,3'-Si(xylyl)$_3$-H8-BINOL Catalyst 13

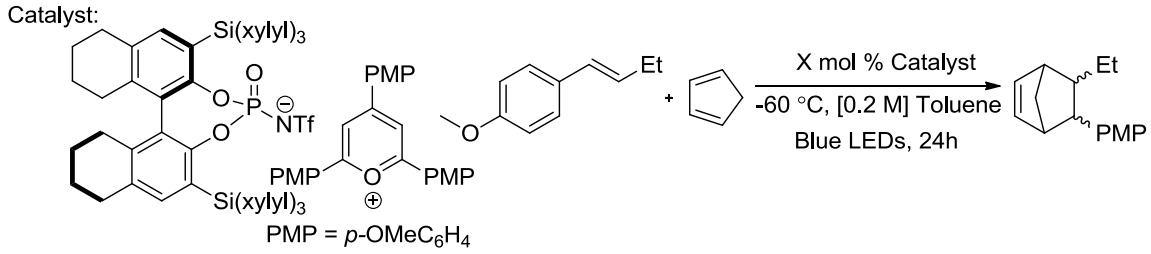

Entry	Concentration	Catalyst Loading	GC Yield	Selectivity
1	[0.2 M]	0.5 mol %	12%	1.6:1 dr 25% ee major, 68% ee minor
2	[0.2 M]	2.0 mol %	59%	2.3:1 dr 12% ee major, 62% ee minor
3	[0.2 M]	5 mol %	73%	2.1:1 dr 11% ee major, 64% ee minor
4	[1.0 M]	2.0 mol %	64%	3.2:1 dr 1% ee major, 46% ee minor
5	[0.0625 M]	2.0 mol %	18%	1.8:1 dr 19% ee major, 65% ee minor
6	[0.025 M] *after48h	2.0 mol %	30%	2.1:1 dr 20% ee major, 62% ee minor

Closer inspection of these chiral GC traces revealed that the %ee of the minor set of diastereomers was actually quite high and the diastereoselectivity was approximately 2:1. We wondered if we could exploit this low diastereoselectivity and reverse the preference to the minor diastereomers. After running the reaction in a series of concentrations we saw that going to more

dilute concentrations decreased yields and the diastereoselectivity while increasing the enantioselectivity for both sets of diastereomers. However, after a certain point the diastereomeric ratio does not decrease to 1:1 or reverse as we had hoped. Ultimately, we were unable to strike a balance between yield and selectivity to give a synthetically useful result.

In 2011, Toste and colleagues reported the use of BINOL catalysts bearing biaryl moieties on the 3 and 3' positions as Brønsted acids for the enantioselective intramolecular addition of sulfonamides to dienes.[4] Following their literature procedure we synthesized the oxopyrylium *N*-trifylphosphoramide with 10-(2,4,6-$(CH_3)_3$-C_6H_2)-9-anthracenyl groups at the 3, 3' positions (**14)**. We hoped that the biaryl groups would project further towards the radical cation intermediate to induce selectivity. We found however, that while a decent 41% yield was obtained, the enantioselectivity did not exceed 9% (**Figure 2.14**).

Figure 2.14 Screening of Various Catalyst Scaffolds

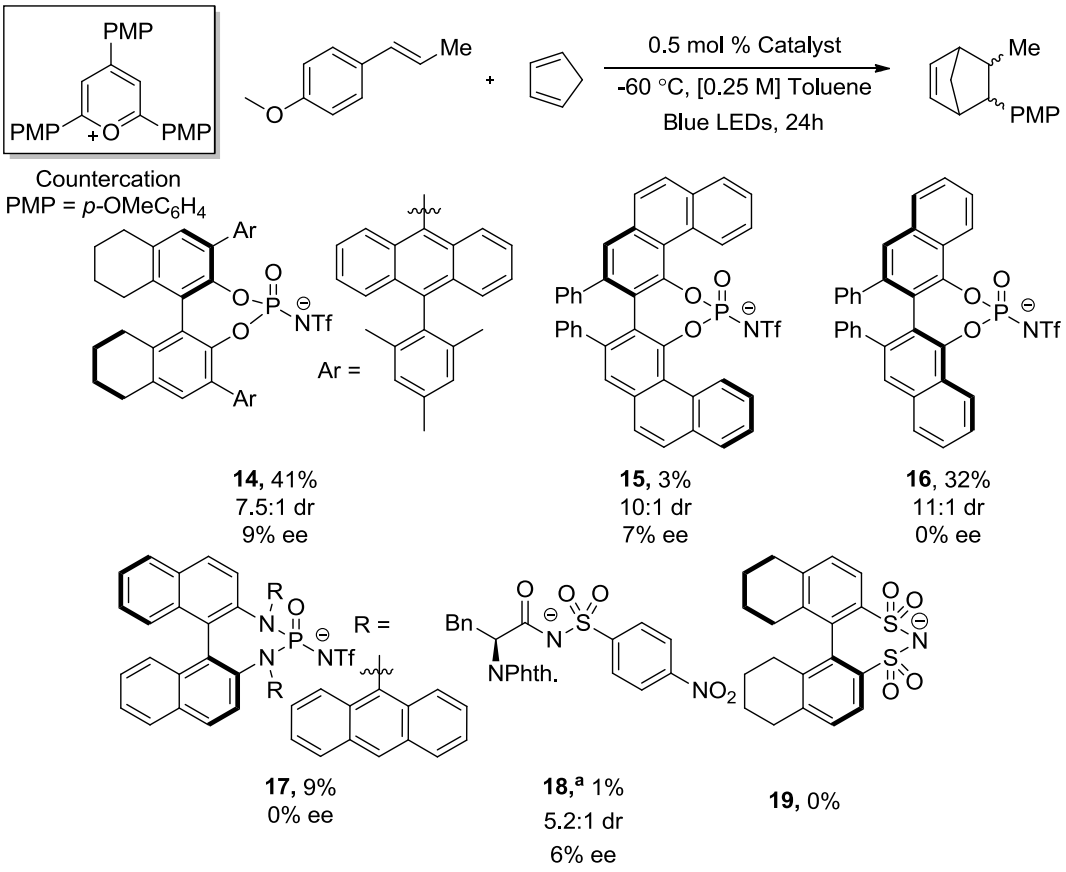

[a]Run with 5 mol % catalyst and irradiated with fluorescent white light

Moving away from the BINOL scaffold, we looked at chiral catalysts derived from expensive, yet commercially available VAPOL (**15**) and VANOL (**16**). These compounds possessed unique backbone structures that extend out over the anionic moiety instead of relying on substituents that branched out. Unfortunately, we observed very low yield using catalyst **15** and decent yield with catalyst **16** but absolutely no enantioinduction.

We then tried a different tact by exchanging the oxygen linkers in the BINOL scaffold to nitrogen linkers, which would allow for the substitution at nitrogen and hopefully create a chiral pocket closer to the ion pair. Synthesized according to literature procedure we evaluated the anthracenyl substituted chiral catalyst **17**, and observed a disappointing 9% yield with no enantioselectivity.

Given that chiral counteranion synthesis is arduous and time-consuming we wanted to try to take advantage of amino acids as potential catalyst scaffolds. Synthesis of chiral catalyst **18** derived from L-alanine was very straightforward and obtained in high yield in just three steps. Its performance as a catalyst for the cation radical Diels-Alder reaction however was poor in terms of reactivity and selectivity; therefore no other amino acid based catalysts were pursued.

Lastly, we evaluated the disulfonimide BINOL catalyst **19**, a scaffold reported recently by the List group. List and coworkers employed the 3,3' arylsubstituted disulfimide for highly selective Mukaiyama aldol reactions.[5] They propose that the chiral acid imparts such great enantiocontrol because the acid is more deeply embedded than the phosphoric acid counterpart. We experienced difficulty synthesizing the disulfimide with substituents at the 3,3' position, however we were able to evaluate the unsubstituted catalyst and unfortunately did not observe any desired product.

We also tried different substituents on the para position of the triaryl oxopyryliums including methoxy, methyl and fluoro groups. We did not observe any clear advantage of using one substitution over the other, so we mainly employed the *p*-OMe substituted oxopyrylium for consistency between our optimization reactions. Though none of the catalysts we tested provided

the results we hoped for, they may be of use in other settings. It is probable that the key to success, as defined by high yield and selectivity, for this transformation still lies in the identification of a chiral catalyst with the right nucleophilicity and chiral environment.

2.4 Miscellaneous Optimization Strategies

Because we were only using 0.5 mol % catalyst in our reactions, we proposed to add additional chiral Brønsted acid to the reaction mixture that could potentially become deprotonated and increase the amount of free chiral counteranion present in solution. We tested a side by side comparison of a reaction with 5 mol % chiral **8a** catalyst and one with 5 mol % chiral catalyst in addition to 5 mol % of the corresponding chiral Brønsted acid. We observed very similar yields and selectivities leading us to abandon this course of investigation. We tested the chiral Brønsted acid's ability to catalyze the reaction by itself and found that it was an incompetent catalyst as expected (**Figure 2.15**).

Figure 2.15 Effect of Additional Chiral Brønsted Acid

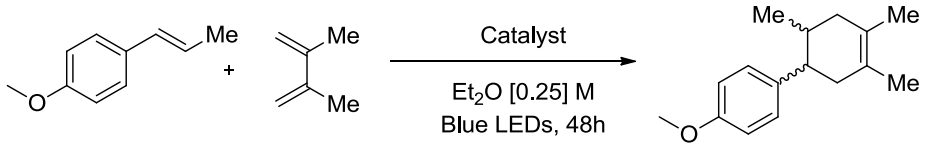

Catalyst **8a**:

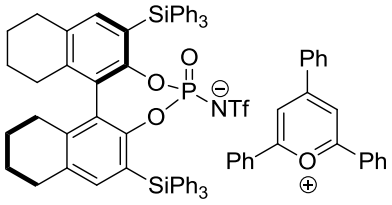

Catalyst	Yield	%ee
5 mol % $SiPh_3$ Bronsted Acid	0%	--
5 mol % $SiPh_3$ Bronsted Acid + 5 mol % **8a**	14%	4%
5 mol % **8a**	16%	3%

Another aspect to consider for this transformation was the light source. In the early stage of our investigations we used four fluorescent light bulbs situated at the bottom of a cryobath. However we realized that it may be advantageous to irradiate the reactions with more focused wavelengths, tuned to the absorption wavelength of the catalyst. The absorption wavelength for the triphenyloxopyrylium tetrafluoroborate is ~412 nm so we imagined that our chiral catalysts would absorb in a similar range. We evaluated blue and violet light-emitting diodes (LEDs) and

fluorescent white light in the racemic reaction with TPT. We indeed observed a considerable increase in yield with the blue LEDs over violet and white light (**Figure 2.16**). Following this experiment, all of our reactions were irradiated with blue LEDs.

Figure 2.16 Effect of Light Sources on the Racemic Reaction

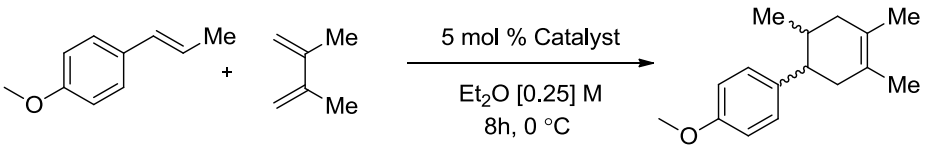

Catalyst:

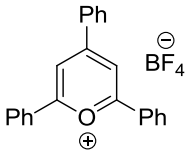

Light Source	GC Yield
Blue LEDs	30%
Violet LEDs	3%
White Fluorescent Lamp	3%

Throughout our investigations we were diligent in setting up the reactions under an atmosphere of nitrogen. However, we wanted to probe the effect of oxygen on our reaction (**Figure 2.17**). We found that the addition of oxygen had a pronounced deleterious effect on the yield of the reaction while the selectivities stayed relatively constant. We propose that oxidative cleavage of the anethole reaction partner occurs competitively in the presence of oxygen accounting for the observed loss in yield.

Figure 2.17 Effect of Oxygen as an Additive

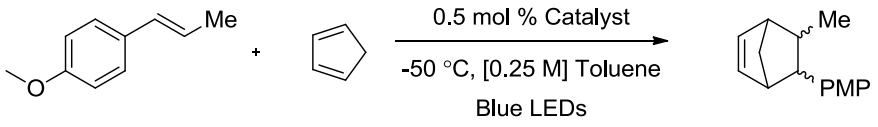

Catalyst:

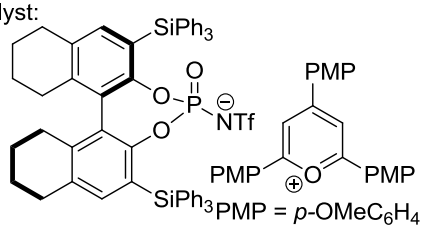

Entry	Conditions	GC Yield	Selectivity
1	Sealed off under N_2	66%	8:1 dr, 27% ee
2	Under air balloon	10%	7:1 dr, 33% ee
3	Under O_2 balloon	4%	6:1 dr, 26% ee

Summary

In this chapter our attempts to develop a practical method for the enantioselective cation radical Diels-Alder reaction through chiral anion catalysis has been detailed. While synthetically relevant levels of reactivity and enantiocontrol were not reached, our work serves as a valuable contribution for the advancement of this novel strategy for enantioinduction. We have synthesized a library of enantiopure chiral acids that other research groups exploring the field of counteranion-directed catalysis may find helpful. Ultimately, we struggled to find a set of conditions that would allow for reactivity without sacrificing enantioselectivity and vice versa.

REFERENCES

(1) Pabon, R. A.; Bellville, D. J.; Bauld, N. L. Cation Radical Diels-Alder Reactions of Electron-Rich Dienophiles. *J. Am. Chem. Soc.* 1983, *105*, 5158–5159.

(2) Schepp, N. P.; Johnston, L. J. Reactivity of Radical Cations. Effect of Radical Cation and Alkene Structure on the Absolute Rate Constants of Radical Cation Mediated Cycloaddition Reactions1. *J. Am. Chem. Soc.* 1996, *118*, 2872–2881.

(3) Uraguchi, D.; Terada, M. Chiral Brønsted Acid-Catalyzed Direct Mannich Reactions via Electrophilic Activation. *J. Am. Chem. Soc.* 2004, *126*, 5356–5357.

(4) Shapiro, N. D.; Rauniyar, V.; Hamilton, G. L.; Wu, J.; Toste, F. D. Asymmetric Additions to Dienes Catalysed by a Dithiophosphoric Acid. *Nature* 2011, *470*, 245–249.

(5) García-García, P.; Lay, F.; García-García, P.; Rabalakos, C.; List, B. A Powerful Chiral Counteranion Motif for Asymmetric Catalysis. *Angew. Chem. Int. Ed.* 2009, *48*, 4363–4366.

CHAPTER 3: BACKGROUND FOR THE DEVELOPMENT OF AN ANTI-MARKOVNIKOV HYDROAMINATION REACTION OF ALKENES

Introduction

Carbon-nitrogen bonds are ubiquitous in highly valuable biologically active compounds. The most direct way to form these bonds is through the addition of an amine to an alkene in the hydroamination reaction. The hydroamination reaction is advantageous because it employs simple and commercially available starting materials and is completely atom economical. Challenges associated with the hydroamination reaction include the repulsion between the alkene pi-electrons and the nitrogen lone pair as well as the regioselectivity of the addition of the amine.

The majority of existing hydroamination reactions furnish products with amine substitution at the more substituted carbon center as governed by Markovnikov's rule, which places the cationic charge generated *in situ* at the most stabilized carbon, either by substitution or electronics. Relatively few methods exist for the direct anti-Markovnikov hydroamination reaction and as will be shown, many require precious metals and are limited to activated alkene partners. In this chapter, previous reports of anti-Markovnikov hydroamination reactions of alkenes will be discussed.

3.1 Anti-Markovnikov Hydroamination Reactions Catalyzed by Transition Metals

Transition metal catalysis dominates the arena of anti-Markovnikov hydroamination. Ni, Cu, Ru, Rh, and Ln have all been shown to be effective catalysts for this transformation by a number of research groups.

Ni-catalyzed Anti-Markovnikov Hydroamination Reactions

Nickel complexes have demonstrated some utility in the hydroamination of activated olefins, though with very limited substrate scope. In 2002, Togni and Fadini employed tridentate phosphines as chiral ligands in the Ni(II) catalyzed anti-Markovnikov addition of anilines and morpholine to electron deficient alkenes (**Figure 3.1**).[1] Yields for the hydroamination with anilines ranged from 26% to 91% yield, with increased electron density providing higher yields while ortho substitution on the anilines led to lower yields. Reactions with morpholine as the amine coupling partner gave uniformly good yields. Based on prior computational studies, the authors propose that the reactions proceed via olefin activation followed by nucleophilic attack by the amine.

Figure 3.1 Ni-catalyzed Anti-Markovnikov Hydroamination Reaction of Activated Olefins

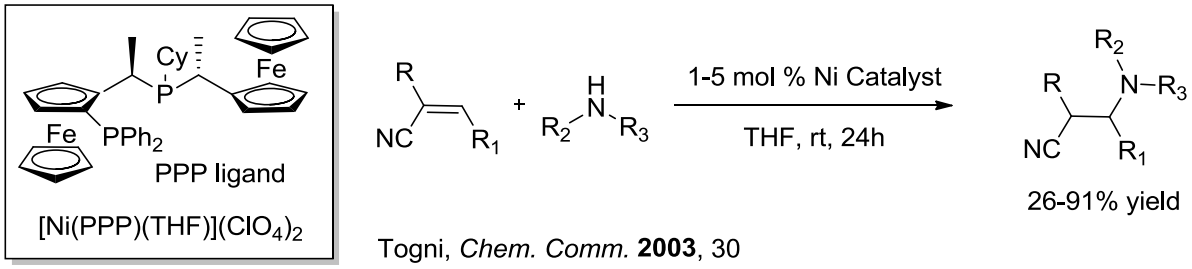

Togni, *Chem. Comm.* **2003**, 30

Zargarian and co-workers published a similar Ni catalyzed hydroamination of acrylonitrile and phenylaniline using diphosphine pincer ligands in 2009 (**Figure 3.2)**.[2] The study evaluated the reactivity of pincer-type complexes with various substitution patterns, obtaining up to 95% yield in their target transformation. The researchers present two possible pathways by which activation occurs either by coordination to the olefin or the nitrile. They speculate that the process undergoes a Lewis acid promoted mechanism, whereby indirect activation of the olefin is followed by nucleophilic attack then proton transfer.

Figure 3.2 Ni-catalyzed Anti-Markovnikov Hydroamination Reaction of Acrylonitrile

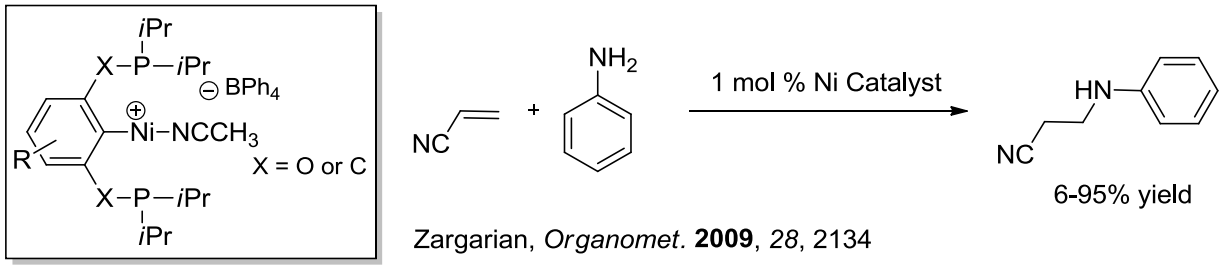

Zargarian, *Organomet.* **2009**, *28*, 2134

Cu-catalyzed Anti-Markovnikov Hydroamination Reactions

The Gunnoe group reported an anti-Markovnikov hydroamination of electron poor olefins using Cu(I) complexes (**Figure 3.3)**.[3] Given the limited nature of the substrate scope in this 2006 report, the transformation can also be thought of as a conjugate Michael addition. The proposed mechanism involves nucleophilic addition of the amido ligand to the alkene to give a zwitterionic intermediate followed by proton transfer to form a copper amido complex. A second proton transfer to regenerate the copper anilido complex completes the catalytic cycle and releases the desired product. In 2008, Gunnoe and co-workers report an expanded substrate scope that includes vinyl arenes. Though the method has not found general utility, its advantage lies in the low cost of Cu in contrast to the more costly Rh and Ru catalysts.[4]

Figure 3.3 Cu-catalyzed Anti-Markovnikov Hydroamination of Electron Deficient Olefins

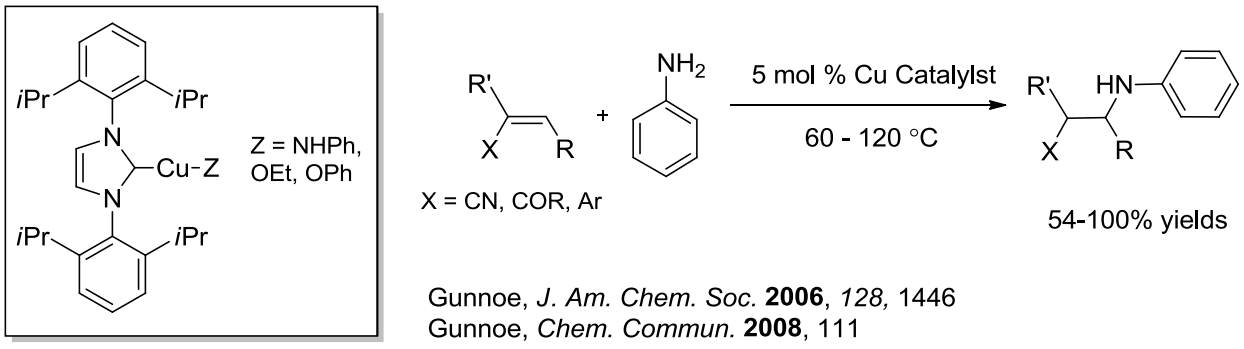

Gunnoe, *J. Am. Chem. Soc.* **2006**, *128,* 1446
Gunnoe, *Chem. Commun.* **2008**, 111

Recently, Buchwald and co-workers published an important advance for Cu catalyzed anti-Markovnikov hydroamination reactions. Using a catalytic amount of $Cu(OAc)_2$, a phosphine ligand and

diethoxymethylsilane as a stoichiometric hydride-transfer reagent, they are able to promote the addition of hydroxylamines to unactivated aliphatic alkene substrates (**Figure 3.4)**.[5] The reaction derives its regioselectivity from the insertion of a CuH species that places the Cu on the less sterically hindered terminal carbon. Following hydride migration, oxidative addition of the Cu intermediate into the hydroxylamine then reductive elimination affords the desired tertiary amine products in high yields. The transformation is tolerant to a variety of functional groups including halides, epoxides, protected alcohols and heterocyclic amines.

Figure 3.4 CuH-catalyzed Anti-Markovnikov Hydroamination of Unactivated Alkenes

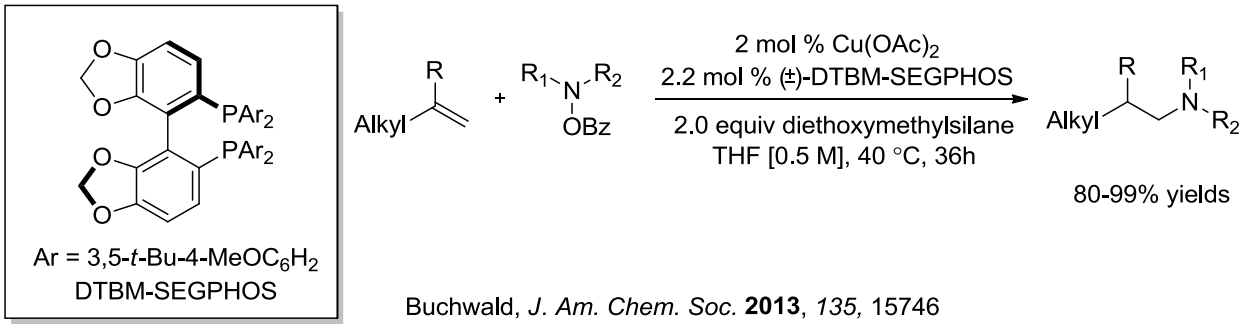

Buchwald, *J. Am. Chem. Soc.* **2013**, *135,* 15746

Rh and Ru-catalyzed Anti-Markovnikov Hydroamination Reactions

In 1999, Beller and colleagues reported the first anti-Markovnikov hydroamination of styrenes using a cationic Rh catalyst (**Figure 3.5)**.[6] However, only small amounts of the hydroamination product were observed while the major product was the enamine arising from the oxidative amination reaction. The enamine to alkylamine product ratio ranged from 2.1:1 to 10.5:1. Combined yields were higher for electron rich styrenyl substrates over electron poor substrates. The authors also observed ethylbenzene as a major side product and sought to probe rhodium's ability to hydrogenate not only the styrene but the enamine product. Additional experiments demonstrated that enamine hydrogenation was not occurring and led them to propose a separate catalytic pathway for the formation of the hydroamination product. The mechanism is proposed to proceed through oxidative insertion of the Rh complex then addition across the alkene or coordination of rhodium to the olefin followed by subsequent nucleophilic addition

of the amine to give an alkyl rhodium species. From this intermediate, β-hydride elimination can occur to produce the enamine product or protonolysis of the complex can furnish the alkyl amine product. In the former case, the *in situ* generated rhodium dihydride species can go on to hydrogenate excess styrene.

Figure 3.5 Rh-catalyzed Anti-Markovnikov Hydroamination of Styrenes, Beller *et al.*

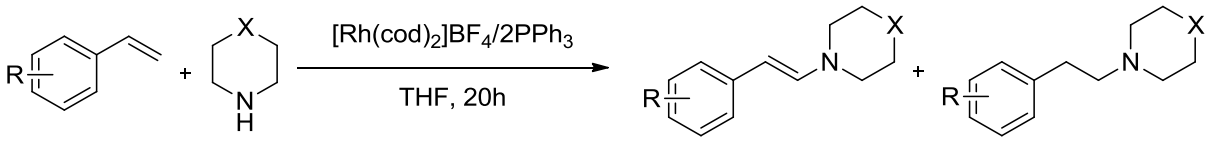

Beller, *Chem. Eur. J.* **1999**, *5,* 1306

In 2003, Hartwig and co-workers reported the same transformation but were able to favor formation of the amine product using a modified Rh catalyst (**Figure 3.6**).[7] They obtained product mixtures in good to high yields at elevated temperatures. In their reported mechanism after initial olefin coordination or amine oxidative addition, they invoke the formation of a rhodium metallacycle, at which point reductive elimination to form the alkyl amine is favored. Alternatively, the metallacycle may also be opened by coordination of another alkene and from this intermediate, reductive elimination or β-hydride elimination can take place.

Figure 3.6 Rh-catalyzed Anti-Markovnikov Hydroamination of Styrenes, Hartwig *et al.*

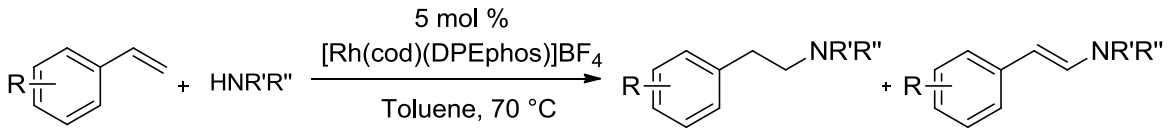

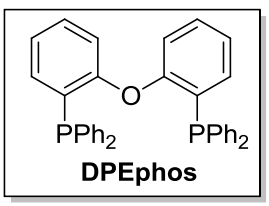

Hartwig, *J. Am. Chem. Soc.* **2003**, *125*, 5608

The following year, the Hartwig group overcame the competing oxidative hydroamination problem by switching to a ruthenium catalyst (**Figure 3.7)**.[8] After optimization, they report the anti-Markovnikov hydroamination of various cyclic amines with terminal styrenes in 40-96% yield. Mechanistic investigations revealed the formation of a π-arene complex between the ruthenium complex and the aryl group of the styrene. This coordination effectively activates the olefin to nucleophilic attack by the amine while circumventing the undesired β-hydride elimination pathway.[9]

Figure 3.7 Ru-catalyzed Anti-Markovnikov Hydroamination of Styrenes, Hartwig *et al.*

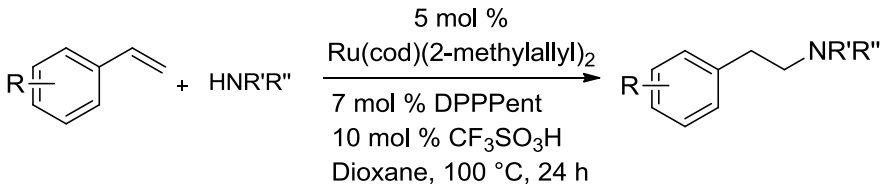

Hartwig, *J. Am. Chem. Soc.* **2004**, *126*, 2702 40-96% yields

In 2006, Hartwig and Takemiya report the extension of this method to include intramolecular examples, which to the best of our knowledge is the sole example of an intramolecular anti-Markovnikov hydroamination outside of our own report (**Figure 3.8**).[10] They obtained the products in good yields and saw only negligible amounts of the enamine side product.

Figure 3.8 Rh-catalyzed Intramolecular Anti-Markovnikov Hydroamination of Styrenes

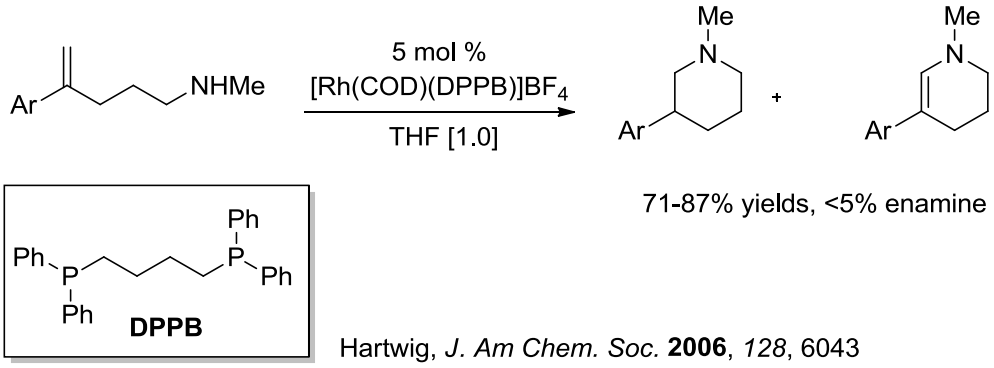

Hartwig, *J. Am Chem. Soc.* **2006**, *128*, 6043

La-catalyzed Anti-Markovnikov Hydroamination of Vinylarenes

The Marks lab reported an organolanthanide catalyzed anti-Markovnikov hydroamination of vinylarenes with primary alkylamines in high yields and regioselectivities (**Figure 3.9**).[11] Electron rich and neutral arenes produced higher yields, which is attributed to their ability to stabilize the lanthanide through the arene π-electrons. The reaction is proposed to begin with coordination of the amine to the metal catalyst followed by insertion of the La-N across the olefin. Protonolysis of the lanthanide complex releases the catalyst and the desired arylethylamine.

Figure 3.9 La-catalyzed Anti-Markovnikov Hydroamination of Vinylarenes

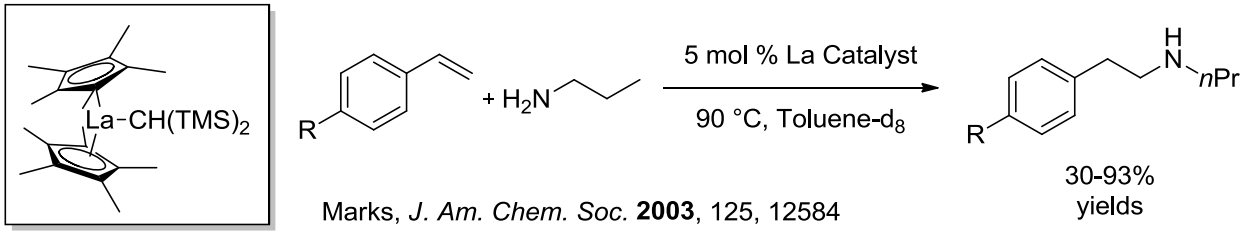

Alkaline Earth Metal-Catalyzed Anti-Markovnikov Hydroamination of Vinylarenes

In 2012, heavy alkaline earth metals joined the field of catalysts for the anti-Markovnikov hydroamination of vinylarenes with a report from the Procopiou group (**Figure 3.10**).[12] They proposed that the insertion of the metal-amine across the olefin is oriented such that the metal stabilizes the developing negative charge on the benzylic position. The reaction was successfully catalyzed by calcium, strontium complexes and even barium catalysts albeit with very long reaction times. The researchers also suggested that the transition state involved coordination of multiple amine substrate molecules to the metal, forming an organized framework of hydrogen bonds. This method is limited by the large excess of styrene required for productive reaction.

Figure 3.10 Ca, Sr, Ba-catalyzed Anti-Markovnikov Hydroamination of Vinylarenes

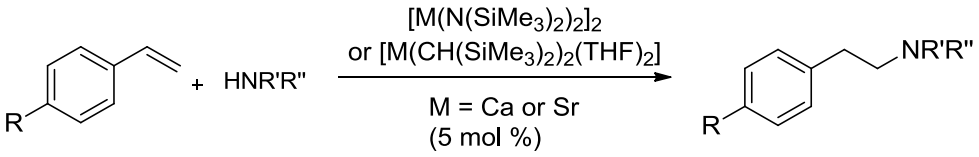

Procopiou, *J. Am. Chem. Soc.* **2012**, *134*, 2193 49-95% yields

3.2 Anti-Markovnikov Hydroamination Promoted by an Organic Sensitizer

While numerous groups have reported transition metal catalyzed hydroamination strategies, purely organic approaches have been relatively less explored. To the best of our knowledge, there exists just one such report from the Yamashita lab, in which UV-light activated dicyanobenzene (DCB) is used to promote the anti-Markovnikov hydroamination of styrenes with ammonia and other primary amines (**Figure 3.11**).[13] Though the method avoids expensive transition metals, it suffers from the requirement of a stoichiometric amount of sensitizer. The desired alkylamine products are obtained in a range of yields along with an undesired side product in which cyanobenzene is incorporated.

The mechanism involved excitation of DCB by UV light which then abstracts a single electron from the alkene forming a radical cation-radical anion pair. Subsequent nucleophilic addition of the amine, deprotonation then reduction of the radical furnishes the desired product. Alternately, radical combination of the radical intermediate with cyanobenzene followed by loss of a cyano group leads to the undesired product.

Figure 3.11 Photoamination of Styrenes Promoted by Dicyanobenzene

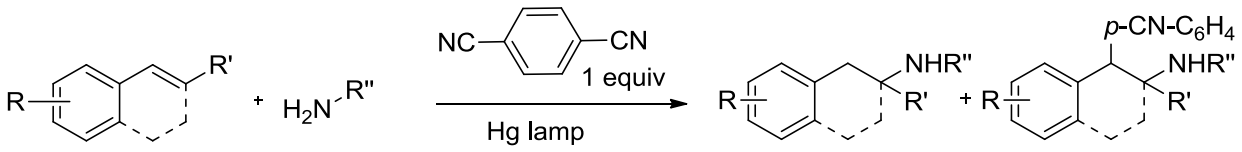

Yamashita, *Tetrahedron* **1994**, 50, 9275 6-68% yield

3.3 Formal Anti-Markovnikov Hydroamination Reactions

Given the challenges associated with developing direct anti-Markovnikov alkene hydroaminations, formal indirect methods have also been explored. These reports generally rely on hydroboration-amination strategies and are highly regioselective though multiple steps are required. In 2012, the Shenvi lab demonstrated an elegant stereoselective formal anti-Markovnikov hydroamination to form polysubstituted indolizidines, an important class of pharmacologically active compounds (**Figure 3.12**).[14] The intramolecular reaction forms two new carbon-nitrogen bonds and sets four stereocenters. The first step involves hydroboration of both internal alkenes and coordination of the amine to boron followed by an iodine mediated alkyl shift from boron onto nitrogen. Oxidation of the borate with hydrogen peroxide furnishes an intermediate alcohol, which was subjected to Mitsunobu conditions to form the second C-N bond.

Figure 3.12 Formal Intramolecular Anti-Markovnikov Hydroamination

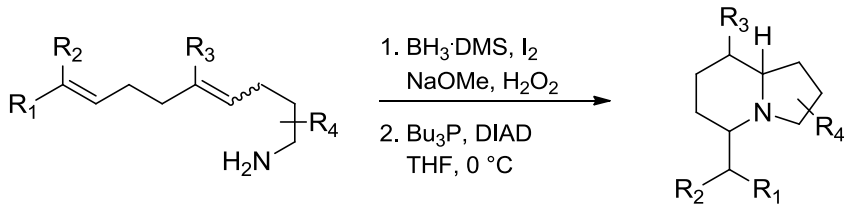

Shenvi, *J. Am Chem. Soc.* **2012,** *134*, 2012 34-54% yields

In the same year, Gojko Lalic and colleagues reported an intermolecular anti-Markovnikov hydroamination of terminal alkenes also taking advantage of an initial hydroboration step (**Figure 3.13**).[15] Advantageously, the procedure is a one-pot process beginning with hydroboration of the alkene. Addition of a benzoyl hydroxylamine, a Cu(I) catalyst and lithium *tert*-butoxide effects the transmetallation from boron to copper, then electrophilic amination of the alkyl copper intermediate forms the desired amination product in excellent yields. The reaction is tolerant to a wide array of functional groups including alkyl, aryl, halide, ester, protected alcohol and cyano groups. Notably, this method provides access to sterically

hindered tertiary amines that can be challenging to synthesize via traditional reductive amination or alkylation strategies.

Figure 3.13 Formal Intermolecular Anti-Markovnikov Hydroamination

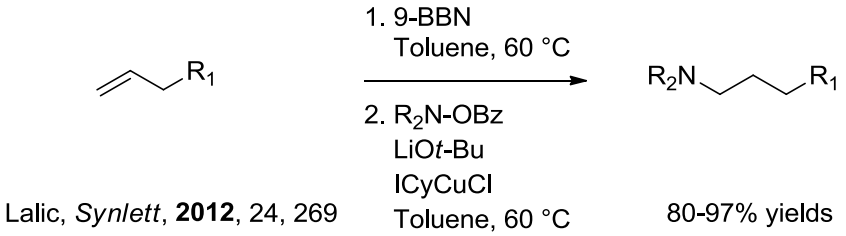

There are relatively few reported methods for the anti-Markovnikov hydroamination reaction of alkenes and the majority rely on transition metal catalysis. Generally, the scope of each strategy has been limited to acrylonitriles, acrylate esters and vinyl arenes and are required to be present in a large excess. The formation of undesired side products either from oxidative amination or incorporation of the sensitizer has also been a challenge in this area. Given the value of gaining access to anti-Markovnikov hydroamination protocols in industrial and drug discovery processes, there exists a need for the development of new efficient strategies. In the next section, we will discuss our proposal to develop a novel catalyst system for the anti-Markovnikov hydroamination of alkenes.

3.4 Research Proposal for an Anti-Markovnikov Hydroamination Reaction

We saw an opportunity to develop a method for the anti-Markovnikov hydroamination drawing on precedent in the area of organic photocatalysis. Our laboratory has found great utility in employing organic single electron photo-oxidants to generate radical cation intermediates. These intermediates are susceptible to nucleophilic addition and inherently give rise to anti-Markovnikov regioselectivity. Our aim was to identify a photoredox catalyst system to generate cation radical intermediates from alkenes that can be intercepted by protected amine nucleophiles. As photo-induced electron transfer for the generation of radical cation intermediates has already been discussed in chapter 1, the following section will focus on the addition of nucleophiles to these reactive intermediates.

3.5 Precedent for the Photocatalyzed Addition of Nucleophiles to Radical Cations

Among the first to explore the reactivity of photolytically generated radical cation intermediates was the Arnold group. In 1973, they reported the irradiation of *p*-cyanobenzoate with 1,1-diphenylethylene in the presence of alcoholic solvents to form ether products with anti-Markovnikov selectivity.[16] Subsequent reports from the Arnold[17,18] and Gassman[19] lab employ dicyanobenzene as a sensitizer to promote the anti-Markovnikov addition of alcoholic nucleophiles. Further exploration of these photochemical nucleophile-olefin combination aromatic substitution (photo-NOCAS) reactions using density functional theory (DFT) calculations led to the proposed mechanism (**Figure 3.14**). Initial irradiation excites DCB to its singlet excited state followed by single electron transfer from the olefin, then the radical cation intermediate is intercepted by the alcohol nucleophile. The β–alkoxy radical undergoes coupling with the 1,4-cyanobenzene radical anion, then loss of the cyano group and aromatization furnishes the product. The regioselectivity can be rationalized by the formation of a three-membered nucleophile-radical cation intermediate which ruptures at the weaker C-O bond to form the more stable radical intermediate.

Figure 3.14 Proposed Mechanism of Photo-NOCAS Reactions

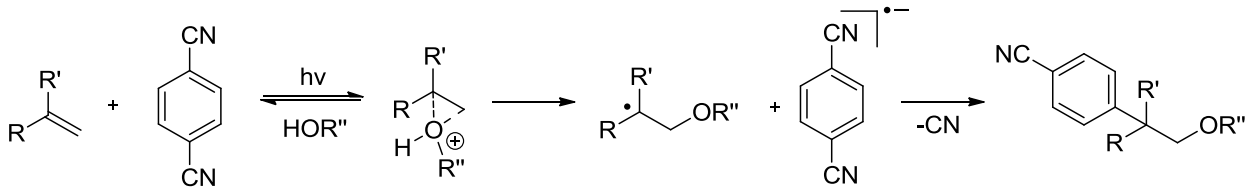

Similar reports of photochemical anti-Markovnikov alcohol additions have been reported by the Mizuno[20] and Inoue[21] research labs with diphenyl alkenols and chiral sensitzers, respectively. These reports, as well as the previously discussed research from the Yamashita lab,[13] are valuable precedents for photolytic anti-Markovnikov addition of nucleophiles but are quite limited in yield and scope. They also suffer from undesired incorporation of the sensitizer and require harsh ultraviolet (UV)-light for the

excitation of the single electron oxidants. Given these disadvantages, our group proposed to explore another class of photo-oxidants to access a broader range of alkenes.

In 2013, Hamilton and Nicewicz report a direct catalytic method for the anti-Markovnikov hydroetherification of alkenols using a 9-mesityl-10-methyl acridinium catalyst and 2-phenylmalononitrile (PMN) as a hydrogen atom source (**Figure 3.15**).[22] The acridinium catalyst

Figure 3.15 Anti-Markovnikov Hydroetherification Catalyzed by an Organic Photoredox System

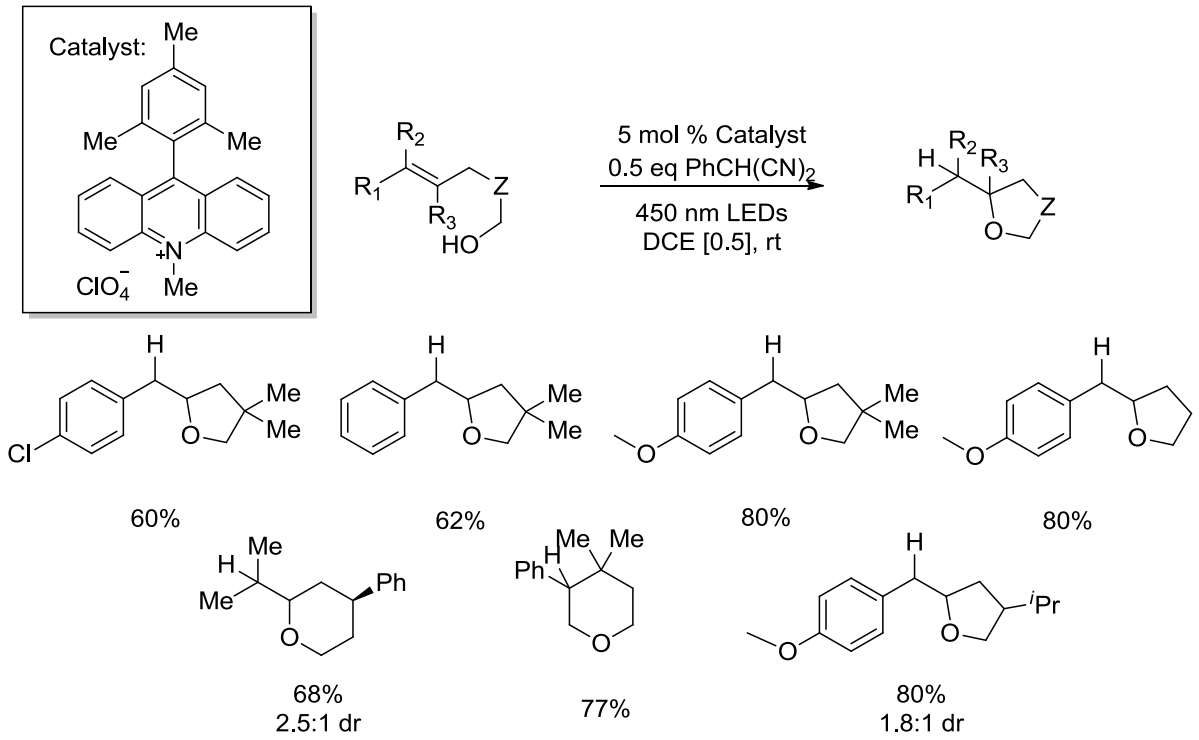

Hamilton and Nicewicz, *J. Am. Chem. Soc.* **2012**, *134,* 18577

developed by the Fukuzumi lab was an attractive photo-oxidant for its high excited state oxidation potential (+2.06 V vs. saturated calomel electrode [SCE]) and its absorption in the visible light range (λ = 430). Initial investigations revealed that reaction of just alkenols and acridinium catalyst resulted in low yields. However introduction of an additive to act as a hydrogen atom transfer reagent improved yields to synthetically useful levels. The researchers evaluated a number of hydrogen atom transfer donors based on their homolytic bond dissociation energies (BDEs). Compounds that possessed sufficiently low BDEs

were chosen to encourage hydrogen atom transfer. Ultimately, 2-phenylmalononitrile proved to be the best transfer reagent with a BDE of 77 kcal/mol.

Using this novel catalyst system, substituted tetrahydrofurans are obtained from styrenyl and trisubstituted alkenols in good yields. The proposed mechanism for this transformation begins with excitation of the acridinium catalyst by visible blue light (450 nm) followed by single electron oxidation of the alkene. Intramolecular nucleophilic addition of the alcohol to the radical cation forms a transient three-membered intermediate then rupture of the weaker C-O bond furnishes the radical intermediate. Subsequent hydrogen atom transfer from PMN gives the desired product and a phenylmalononitrile radical, which can be reduced by the acridinium radical then protonation regenerates the H-atom transfer reagent (**Figure 3.16**). We believed that we could use this catalyst system to develop an analogous anti-Markovnikov hydroamination reaction.

Figure 3.16 Proposed Mechanism for the Anti-Markovnikov Hydroetherification of Alkenols

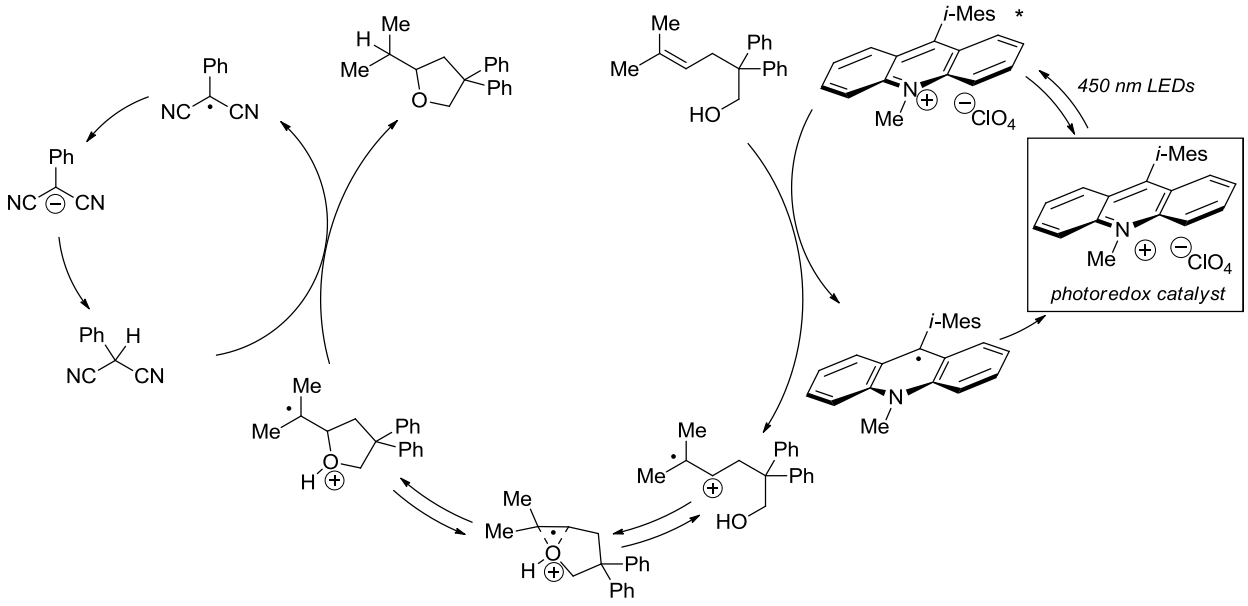

Hamilton and Nicewicz, *J. Am. Chem. Soc.* **2012**, *134,* 18577

Summary

This chapter has provided an overview of existing methods for the anti-Markovnikov hydroamination reactions as well as their advantages and drawbacks. We proposed to introduce a new method to this arena by building on previous success in our lab with a novel organic photoredox catalyst system. This transformation can provide direct access to pharmacologically valuable compounds.

REFERENCES

(1) Fadini, L.; Togni, A. Ni(II) Complexes Containing Chiral Tridentate Phosphines as New Catalysts for the Hydroamination of Activated Olefins. *Chem. Commun.* **2003**, 30–31.

(2) Castonguay, A.; Spasyuk, D. M.; Madern, N.; Beauchamp, A. L.; Zargarian, D. Regioselective Hydroamination of Acrylonitrile Catalyzed by Cationic Pincer Complexes of Nickel(II). *Organometallics* **2009**, *28*, 2134–2141.

(3) Munro-Leighton, C.; Blue, E. D.; Gunnoe, T. B. Anti-Markovnikov N−H and O−H Additions to Electron-Deficient Olefins Catalyzed by Well-Defined Cu(I) Anilido, Ethoxide, and Phenoxide Systems. *J. Am. Chem. Soc.* **2006**, *128*, 1446–1447.

(4) Munro-Leighton, C.; Delp, S. A.; Alsop, N. M.; Blue, E. D.; Gunnoe, T. B. Anti-Markovnikov Hydroamination and Hydrothiolation of Electron-Deficient Vinylarenes Catalyzed by Well-Defined Monomeric copper(I) Amido and Thiolate Complexes. *Chem. Commun.* **2007**, 111–113.

(5) Zhu, S.; Niljianskul, N.; Buchwald, S. L. Enantio- and Regioselective CuH-Catalyzed Hydroamination of Alkenes. *J. Am. Chem. Soc.* **2013**, *135*, 15746–15749.

(6) Beller, M.; Trauthwein, H.; Eichberger, M.; Breindl, C.; Herwig, J.; Müller, T. E.; Thiel, O. R. The First Rhodium-Catalyzed Anti-Markovnikov Hydroamination: Studies on Hydroamination and Oxidative Amination of Aromatic Olefins. *Chemistry – A European Journal* **1999**, *5*, 1306–1319.

(7) Utsunomiya, M.; Kuwano, R.; Kawatsura, M.; Hartwig, J. F. Rhodium-Catalyzed Anti-Markovnikov Hydroamination of Vinylarenes. *J. Am. Chem. Soc.* **2003**, *125*, 5608–5609.

(8) Utsunomiya, M.; Hartwig, J. F. Ruthenium-Catalyzed Anti-Markovnikov Hydroamination of Vinylarenes. *J. Am. Chem. Soc.* **2004**, *126*, 2702–2703.

(9) Takaya, J.; Hartwig, J. F. Mechanistic Studies of Ruthenium-Catalyzed Anti-Markovnikov Hydroamination of Vinylarenes: Intermediates and Evidence for Catalysis through Π-Arene Complexes. *J. Am. Chem. Soc.* **2005**, *127*, 5756–5757.

(10) Takemiya, A.; Hartwig, J. F. Rhodium-Catalyzed Intramolecular, Anti-Markovnikov Hydroamination. Synthesis of 3-Arylpiperidines. *J. Am. Chem. Soc.* **2006**, *128*, 6042–6043.

(11) Ryu, J.-S.; Li, G. Y.; Marks, T. J. Organolathanide-Catalyzed Regioselective Intermolecular Hydroamination of Alkenes, Alkynes, Vinylarenes, Di- and Trivinylarenes, and Methylenecyclopropanes. Scope and Mechanistic Comparison to Intramolecular Cyclohydroaminations. *J. Am. Chem. Soc.* **2003**, *125*, 12584–12605.

(12) Brinkmann, C.; Barrett, A. G. M.; Hill, M. S.; Procopiou, P. A. Heavier Alkaline Earth Catalysts for the Intermolecular Hydroamination of Vinylarenes, Dienes, and Alkynes. *J. Am. Chem. Soc.* **2012**, *134*, 2193–2207.

(13) Yamashita, T.; Yasuda, M.; Isami, T.; Tanabe, K.; Shima, K. Photoinduced Nucleophilic Addition of Ammonia and Alkylamines to Methoxy-Substituted Styrene Derivatives. *Tetrahedron* **1994**, *50*, 9275–9286.

(14) Pronin, S. V.; Tabor, M. G.; Jansen, D. J.; Shenvi, R. A. A Stereoselective Hydroamination Transform To Access Polysubstituted Indolizidines. *J. Am. Chem. Soc.* **2012**, *134*, 2012–2015.

(15) Rucker, R. P.; Whittaker, A. M.; Dang, H.; Lalic, G. Synthesis of Tertiary Alkyl Amines from Terminal Alkenes: Copper-Catalyzed Amination of Alkyl Boranes. *J. Am. Chem. Soc.* **2012**, *134*, 6571–6574.

(16) Neunteufel, R. A.; Arnold, D. R. Radical Ions in Photochemistry. I. 1,1-Diphenylethylene Cation Radical. *J. Am. Chem. Soc.* **1973**, *95*, 4080–4081.

(17) McManus, K. A.; Arnold, D. R. The Photochemical Nucleophile–olefin Combination, Aromatic Substitution (photo-NOCAS) Reaction. Part 10: Intramolecular Reactions Involving Alk-4-Enols and 1,4-Dicyanobenzene. *Can. J. Chem.* **1995**, *73*, 2158–2169.

(18) Arnold, D. R.; Chan, M. S. W.; McManus, K. A. Photochemical Nucleophile–olefin Combination, Aromatic Substitution (photo-NOCAS) Reaction, Part 12. Factors Controlling the Regiochemistry of the Reaction with Alcohol as the Nucleophile. *Canadian Journal of Chemistry* **1996**, *74*, 2143–2166.

(19) Gassman, P. G.; Bottorff, K. J. Anti-Markovnikov Addition of Nucleophiles to a Non-Conjugated Olefin via Single Electron Transfer Photochemistry. *Tetrahedron Letters* **1987**, *28*, 5449–5452.

(20) Mizuno, K.; Tamai, T.; Nishiyama, T.; Tani, K.; Sawasaki, M.; Otsuji, Y. Intramolecular Photocyclization of Ω, Ω-Diphenyl-(ω−1)-Alken-1-Ols by an Exciplex Quenching Mechanism. *Angewandte Chemie International Edition in English* **1994**, *33*, 2113–2115.

(21) Asaoka, S.; Kitazawa, T.; Wada, T.; Inoue, Y. Enantiodifferentiating Anti-Markovnikov Photoaddition of Alcohols to 1,1-Diphenylalkenes Sensitized by Chiral Naphthalenecarboxylates. *J. Am. Chem. Soc.* **1999**, *121*, 8486–8498.

(22) Hamilton, D. S.; Nicewicz, D. A. Direct Catalytic Anti-Markovnikov Hydroetherification of Alkenols. *J. Am. Chem. Soc.* **2012**, *134*, 18577–18580.

CHAPTER 4: DEVELOPMENT OF AN ANTI-MARKOVNIKOV HYDROAMINATION OF ALKENES CATALYZED BY A NOVEL PHOTOREDOX SYSTEM

Introduction

As detailed in the previous chapter, there exists a need for a facile, direct route for the regioselective construction of carbon-nitrogen bonds. To meet this need, we have developed a transition metal-free catalytic anti-Markovnikov hydroamination of alkenes using a unique photoredox system. In this chapter, the reaction development and scope of the intra- and intermolecular anti-Markovnikov hydroamination reaction of alkenes will be discussed.

4.1 Initial Development of an Anti-Markovnikov Hydroamination Reaction of Alkenes

In our initial investigations, we hoped to take advantage of the conditions developed by Hamilton and Nicewicz for the anti-Markovnikov hydroetherification. We believed that we could effect the anti-Markovnikov hydroamination through a similar pathway, though we realized that in modifying the alcohol moiety to an amine there were some challenges and opportunities. Because amines are trivalent, the nitrogen could be substituted with different functionalities to manipulate its nucleophilicity. However, secondary amines, particularly electron rich amines, have been shown to be susceptible to single electron oxidation at nitrogen to give nitrogen radical cations. In fact, this reactivity has been successfully used in other reaction manifolds.

We began by synthesizing diphenyl isoprenylamine according to literature procedure and submitting it to the photocatalytic system successfully used in the anti-Markovnikov hydroetherification reaction. Unfortunately we did not observe any productive reactivity. We tried adding a variety of organic and inorganic base additives for the initial deprotonation of the primary amine to increase its

nucleophilicity. We also evaluated potential additives that had been previously reported as electron shuttles. None of these adjustments to the reaction conditions resulted in any appreciable formation of desired product (**Table 2**).

Table 2. Optimization of the Anti-Markovnikov Hydroamination of Isoprenylamine

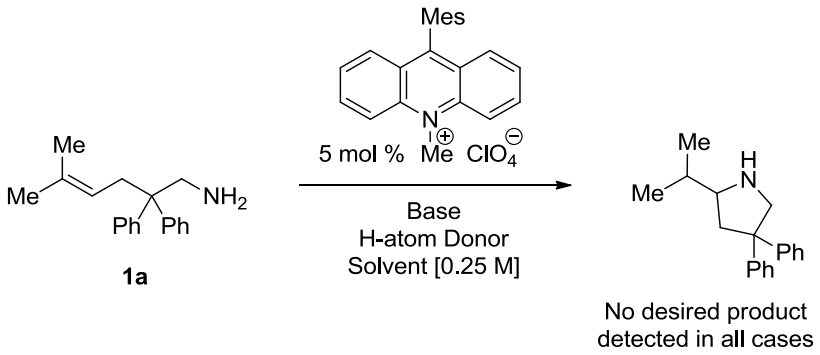

H-Atom Donor	Base	Solvent	Additive
PMN (1.5 equiv)	2,6-lutidine (1.0 equiv)	TFE/MeCN (1:1), MeOH, DCE	None
PMN (1.5 equiv)	2,6-lutidine (None, 0.2 equiv, 3.0 equiv)	DCE	None
PMN (1.5 equiv)	$KHSO_4$ (1 equiv)	DCE	None
PMN (1.5 equiv)	NaOAc (1 equiv)	DCE	None
9-phenylfluorene (1.5 equiv)	2,6-lutidine (None, 0.2 equiv, 1.0 equiv)	DCE	None
PMN (1.5 equiv)	2,6-lutidine (1.0 equiv)	DCE	Benzoic acid (0.9 equiv)
PMN (1.5 equiv)	2,6-lutidine (1.0 equiv)	DCE	Triphenylbenzene (0.2, 1.0 equiv)

Given the lack of reactivity observed with primary unprotected amines, we turned our attention to exploring different protecting groups. Using diphenyl isoprenyl amine as a scaffold, we evaluated a number of sterically and electronically diverse protecting groups (**Figure 4.1**). In moving to secondary amines, we found that the addition of base was not required to observe reactivity. We were pleased to find that the installation of electron rich protecting groups resulted in low to modest amounts of product. Electron withdrawing protecting groups were also tolerated as the *p*-toluenesulfonyl protecting group gave a 16% yield.

Figure 4.1 Evaluation of Various Protecting Groups on Isoprenyl Amine Substrate

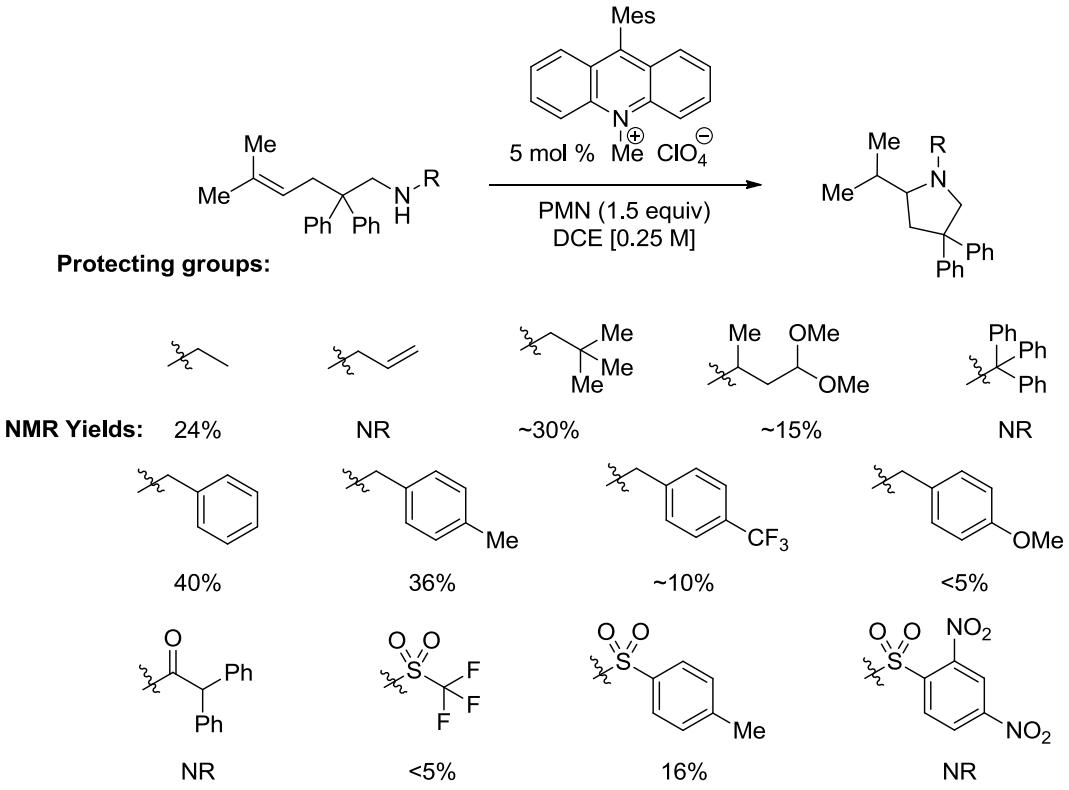

Initially, the benzylamine substrate seemed quite promising with a yield of 40%, though even minor substitutions on the arene with electron donating or withdrawing groups had a negative effect on the yields. Given the sensitivity to substitution, we proposed that the nucleophilicity of the amine was important to reactivity. Further investigation of the benzylamine substrate revealed that an undesired side product was also being formed in the course of the reaction.

After ^{1}H NMR characterization, we determined that the side product was a primary amine with phenylmalononitrile incorporated into the structure (**Figure 4.2**). Running the reaction on a large scale, we obtained 44% desired product along with 30% undesired side product. We propose that the electron rich benzylamine could undergo single electron oxidation at nitrogen. This amine radical cation could be susceptible to deprotonation at the neighboring alpha carbon, followed by addition of the phenylmalononitrile anion. The exploration of protecting groups signaled to us that for productive

reactivity the amine should be sufficiently nucleophilic for the addition but that as the protecting group increases in electron density beyond a certain point, it may participate in unproductive single electron pathways.

Figure 4.2 Detection of Undesired Side Product with Isoprenyl Benzylamine Substrate

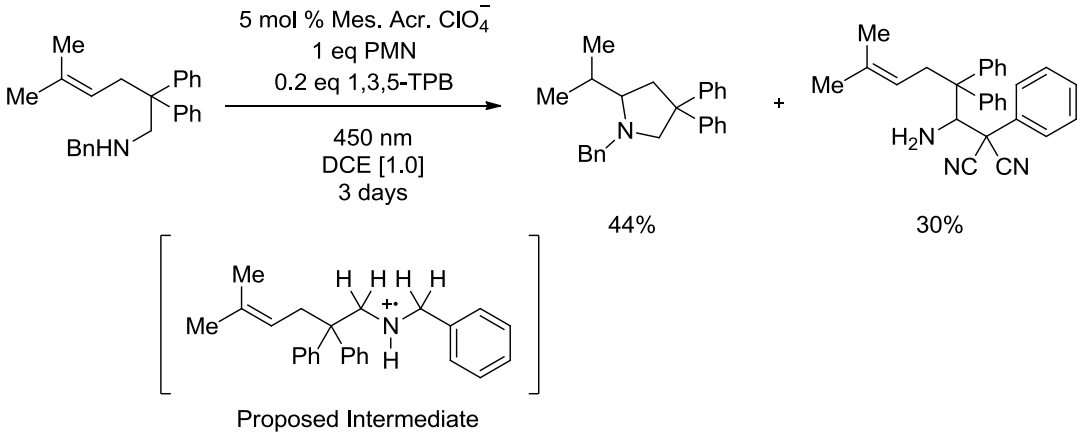

Though yields were promising with the benzyl protected amines, we decided to pursue the more electron withdrawing *p*-toluenesulfonyl (Ts) protecting group to avoid side reactions. Interestingly, while the Ts protecting group gave only a low yield for the isoprenyl substrate, moving to a *p*-methoxy styrenyl substrate, which is more electron rich and more easily oxidized, we observed a good yield of 50%. At this point we focused our efforts on evaluating a range of hydrogen atom donors to optimize the reaction yields (**Figure 4.3**). The hydrogen atom donors evaluated had relatively similar bond dissociation energies ranging between 75-79 kcal/mol. We found that sulfinic acid and 9-cyanofluorene both provided an increase in yield, while exchanging the cyano group for an ester on the fluorene led to a slightly decreased yield.

The best yield was obtained with thiophenol (PhSH) and upon further screening of PhSH loading, we could use just 0.2 equivalents of the H-atom donor to obtain the product in good yields. Interestingly, we observed a minor side product in the reactions with styrenyl substrates that we identified to be the deprotected pyrrolidine. We are unsure about the mechanism of deprotection, though current methods of

Ts group deprotection include treatment with a strong acid or strong reducing metal. It is possible that loss of the Ts group occurs through a single electron reduction or even by a strong acid like the aminium intermediate before it is deprotonated. Thiophenol was also found to be the most efficient H-atom donor for the isoprenylamine substrate as well, with 0.2 equivalents furnishing the product in 70% yield after 96h.

Figure 4.3 Evaluation of H-atom Donors for a Styrenyl Substrate

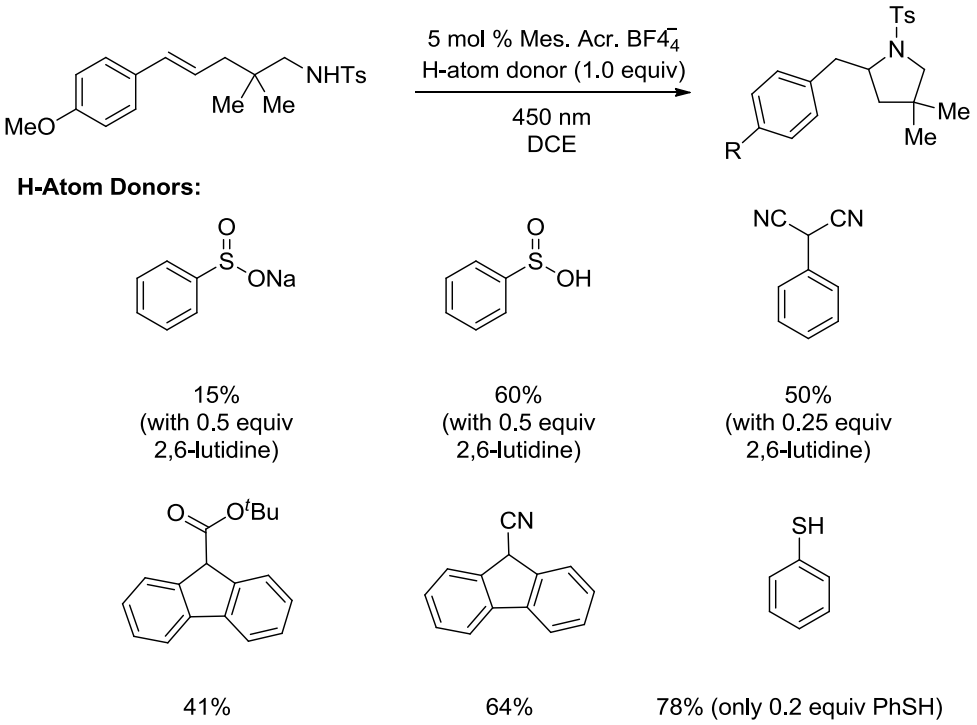

In our optimization reactions we found that the addition of up to 2.0 equivalents of 2,6-lutidine or completely omitting base had no effect on the yields, so we decided move forward without base in our system. We evaluated other solvents such as dichloromethane, nitromethane, acetonitrile and toluene but saw poor reactivity in each solvent. After identifying our optimized conditions, we revisited the identity of the protecting group on the amine using the isoprenylamine as our test substrate (**Figure 4.4**). We observed a low yield for the benzylamine, with many side products, which is in keeping with our hypothesis that more electron rich amines are susceptible to oxidation at the nitrogen, leading to undesired

side product formation. No protecting group resulted in essentially no reaction. We were pleased to see that the electron withdrawing *tert*-butylcarbonyl (Boc) protecting group gave the desired product in 65% yield. Boc protecting groups are advantageous for the ease of their removal but we opted not to use the Boc group in our evaluation of substrates as rotamers made for rather difficult characterization by nuclear magnetic resonance (NMR) spectroscopy. We also performed a series of control reactions and confirmed that blue light, hydrogen atom donor and photocatalyst were all required for product formation.

Figure 4.4 Control and Optimization Studies of Isoprenyl Substrate

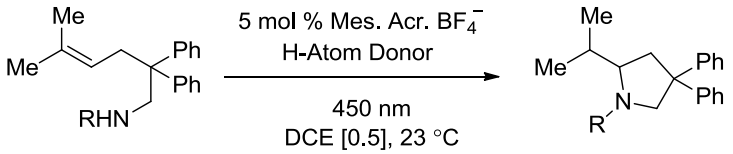

R	H-Atom Donor	Time	NMR Yield
1a, H	0.2 equiv PhSH	96h	**1b**, <5%
2a, Bn	0.2 equiv PhSH	96h	**2b**, 15%
3a, Boc	0.2 equiv PhSH	96h	**3b**, 65%
4a, Ts	0.2 equiv PhSH	96h	**4b**, 70%
Ts	none	96h	<5%
Ts	0.2 equiv PhSH without photocatalyst	24h	<5%
Ts	0.2 equiv PhSH without light	24h	<5%

4.2 Scope of the Intramolecular Anti-Markovnikov Hydroamination Reaction

We then explored the scope of the intramolecular anti-Markovnikov hydroamination reaction (**Figure 4.5**).[1] Styrenyl substrates **5a-10a** furnished the desired pyrrolidines in high yields. The presence of electron withdrawing or donating groups on the arene had little effect on the yield as the reactions with *p*-fluoro and *p*-methoxy substituted styrenyl substrates proceeded in 89% and 88% yield, respectively. Substitution of the ortho position of the styrene was also tolerated, though it required a slightly longer reaction time for completion (**8a,** 69% yield**)**. We also observed that the absence of geminal dimethyl

substitution in the backbone of the structure was not required for reactivity and gave the desired product in good yield (**9a,** 79% yield). Mono-substitution in the chain with an isopropyl group led to a similarly good yield with a low level of diastereoselectivity (**10a,** 88%, 1.6:1 dr). We were also able to effect 6-exo cyclizations with styrenes with and without substitution in the backbone (**11a &12a**, 79% and 60%). As mentioned earlier, for styrenyl substrates, the deprotected pyrrolidines are formed as the minor side product, though reprotection or deprotection could easily circumvent this issue to give a single product. Trisubstituted alkenyl substrates gave good yields though required longer reaction times of 96h.

Figure 4.5 Scope of the Intramolecular Anti-Markovnikov Hydroamination Reaction

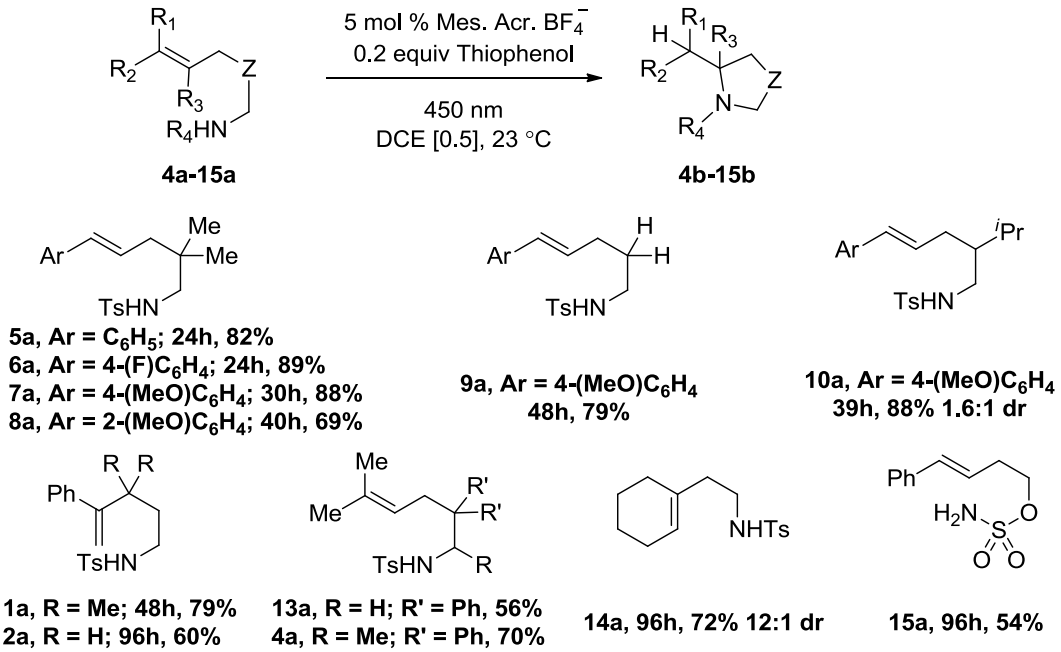

Substitution at the carbon alpha to the amine was tolerated and gave product **13b** in a modest 56% yield with 3:1 dr. A cyclic alkene substrate underwent 5-exo cyclization to produce the bicyclic product **14b** in 72% yield and 12:1 dr. These substrates are notable in that they provide access to non-activated alkene partners, which is a limitation for existing anti-Markovnikov hydroamination methods. We demonstrated one example without the Ts protecting group on the amine, replacing it with a

sulfamate and obtaining the product **15b** in a decent 54% yield. Deprotection of this type of substrate could provide access to valuable 1,3-amino alcohols.

4.3 Mechanistic Investigations of the Anti-Markovnikov Hydroamination Reaction

At the outset of our investigations we presumed that the anti-Markovnikov hydroamination reaction was going through a similar mechanism as the hydroetherification, but with thiophenol instead acting as the H-atom donor. We probed alternative pathways that could be operative. We considered the possibility that thiophenol was acting as a hydrogen atom shuttle, working in concert with a nitrogen centered radical. To this end we submitted the isoprenylamine substrate to two different thermal radical initiators in the presence of thiophenol. However, we observed no reactivity in both cases, suggesting that a nitrogen centered radical intermediate in the case of a Ts-protected amine was unlikely (**Figure 4.6**).

Figure 4.6 Probing Mechanistic Pathways for the Anti-Markovnikov Hydroamination

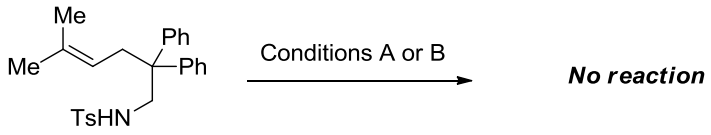

Conditions: A) (*t*-BuO)$_2$ (0.5 equiv), PhSH (0.15 equiv), C_6H_6 [0.4 M],140 °C, 96h.
B) AIBN (0.2 equiv), PhSH (0.2 equiv), DCE [0.5 M], 85 °C, 96h.

A report from the Yoon lab in 2013[2] demonstrated that benzyl mercaptan could participate in light activated Ru catalyzed thiol-ene reactions with terminal styrenes. To explore whether an acridinium catalyzed thiol-ene reaction could be occurring followed by nucleophilic substitution by the pendant amine we synthesized the tertiary Ts, Boc-amine. Exposing the fully substituted amine substrate to light, 5 mol % acridinium catalyst and 1 equivalent of thiophenol resulted in no reaction, making the thiol-ene pathway unlikely (**Figure 4.7**).

Figure 4.7 Probing Thiol-Ene Pathway for the Anti-Markovnikov Hydroamination

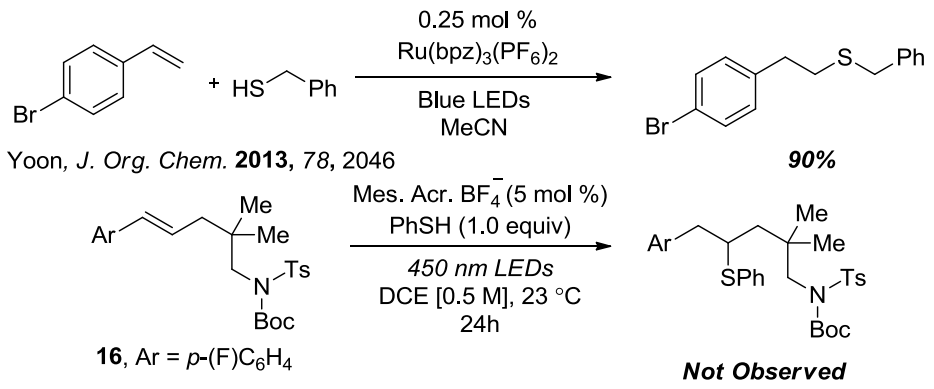

Based on our observations we proposed the following mechanism for the intramolecular anti-Markovnikov hydroamination reaction (**Figure 4.8**). Initial excitation of the acridinium catalyst to its excited state is followed by single electron oxidation of the olefin furnishing the radical cation intermediate and the reduced acridine radical. Nucleophilic addition of the amine to the cationic charge on the anti-Markovnikov position gives the distonic cation radical intermediate. Hydrogen atom transfer from thiophenol and deprotonation of the amine releases the desired product. Reduction of the thiyl radical by the acridine radical to the thiolate is then followed by protonation to regenerate the thiophenol hydrogen atom donor.

In our exploration of this method, we were pleased to find that it could be extended to intermolecular reactions. We were able to obtain the anti-Markovnikov products of the reaction between two cyclic alkenes and trifluoromethanesulfonamide in decent yields with the addition of 0.25 equivalents of 2,6-lutidine (**Figure 4.9**). To the best of our knowledge these examples represent the first organocatalytic method for the intermolecular anti-Markovnikov hydroamination of alkenes. Development and expansion of this method will be discussed in the following section.

Figure 4.8 Proposed Mechanism for the Anti-Markovnikov Hydroamination of Alkenes

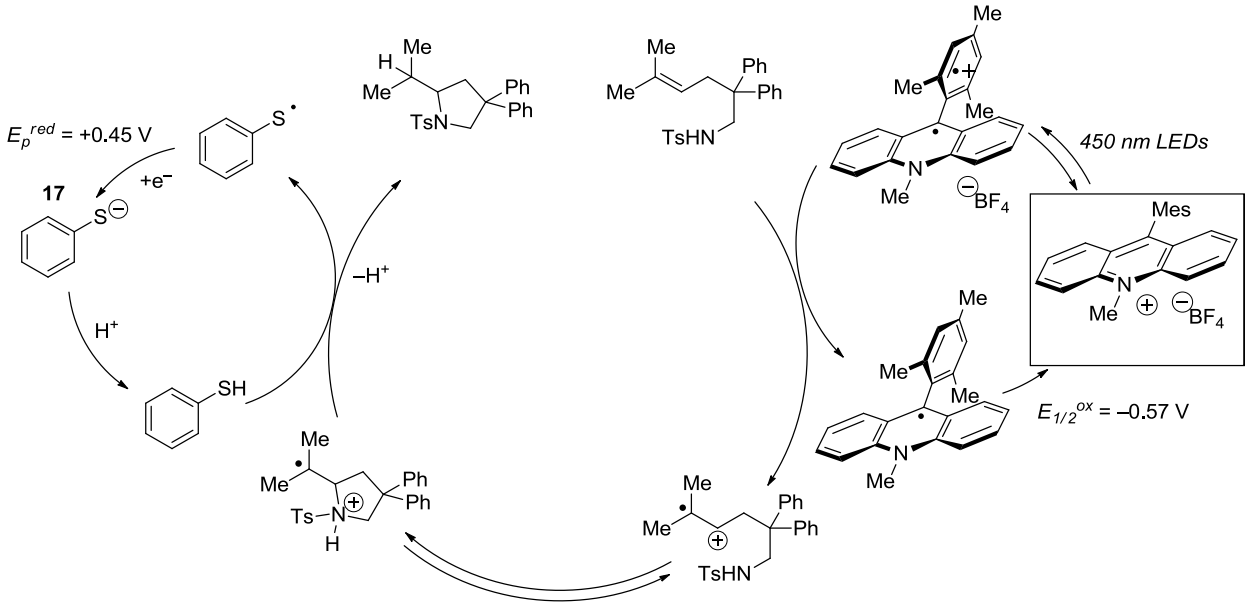

Figure 4.9 First Examples of Intermolecular Anti-Markovnikov Hydroamination

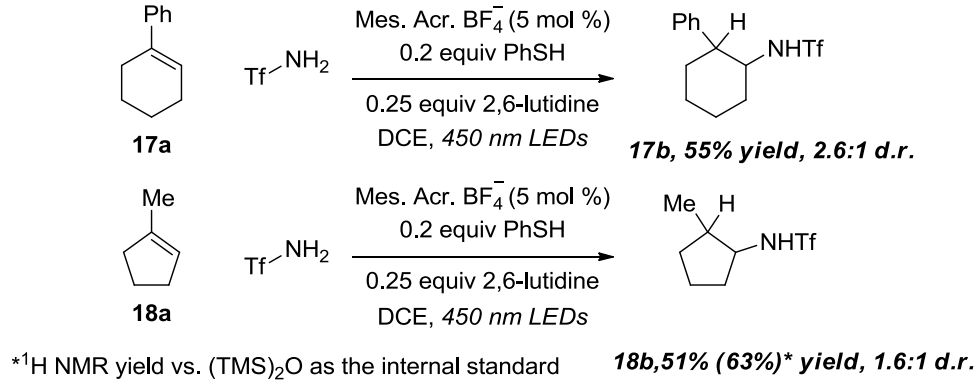

4.4 Development of the Intermolecular Anti-Markovnikov Hydroamination Reaction

Encouraged by initial results for the intermolecular anti-Markovnikov hydroamination reaction, we sought to optimize the reaction conditions for this transformation. Namita Manohar, an undergraduate student in our lab, joined the project and assisted in running optimization reactions and final reactions for our manuscript. Using β-methylstyrene as our test substrate with trifluoromethanesulfonamide, we re-

evaluated the H-atom donors: phenyl malononitrile, 9-cyanofluorene and thiophenol. Of the three, we found that thiophenol was the most efficient hydrogen atom transfer reagent. We then explored how different substitution patterns on thiophenols affected product yields (**Figure 4.10**).

We found that *p*-nitrothiophenol gave the lowest yield of 60%, potentially because its electron deficiency is unfavorable for hydrogen atom donation. Thiophenol gave an 86% yield while dimethylthiophenol gave the product in a slightly lower yield of 78%, perhaps due to the steric hindrance from the two neighboring methyl groups. Interestingly, the addition of diphenyl disulfide as a hydrogen atom donor furnished the desired secondary amine in an excellent yield of 91%.

Figure 4.10 H-Atom Donor Screen for Intermolecular Hydroamination Reaction

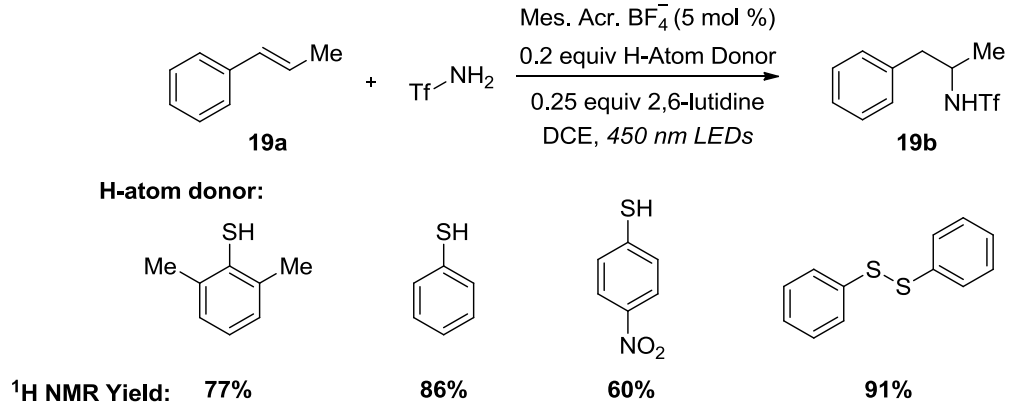

With our optimized hydrogen atom donor in hand, we screened for loading of diphenyl disulfide (**Figure 4.11**). We observed that 5 mol % of disulfide gave a low yield, while increasing the loading to

Figure 4.11 Screening of Diphenyl Disulfide Loading

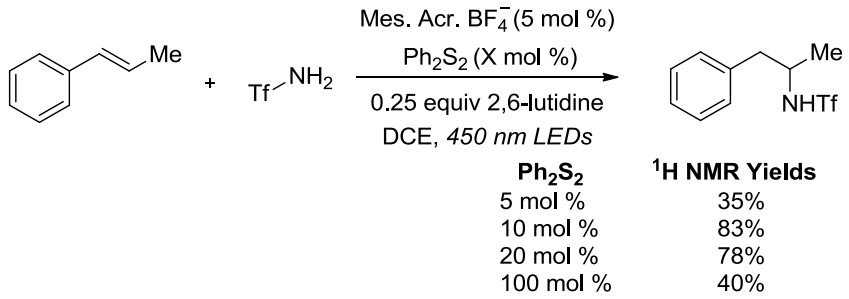

10 mol % and 20 mol % gave similarly good yields. The presence of 1.0 equivalent of disulfide led to a decreased yield.

We have observed the presence of diphenyl disulfide in the crude reaction mixtures, leading us to speculate that there exists an equilibrium between thiophenol and disulfide. Work by Nathan Romero in our lab suggests that diphenyl disulfide can be homolyzed by visible light, in the presence and absence of our photooxidant, to give the corresponding thiyl radical. In addition to producing the highest yield in our H-atom donor screen, diphenyl disulfide is also a desirable additive because it is an odorless solid whereas thiophenol is a very pungent liquid. This observation led us to propose a modified mechanism in which thiyl radical is generated *in situ*, then gains an electron from the acridine radical intermediate followed by protonation to form thiophenol (**Figure 4.12**).

Figure 4.12 Proposed Mechanism for the Intermolecular Hydroamination Reaction

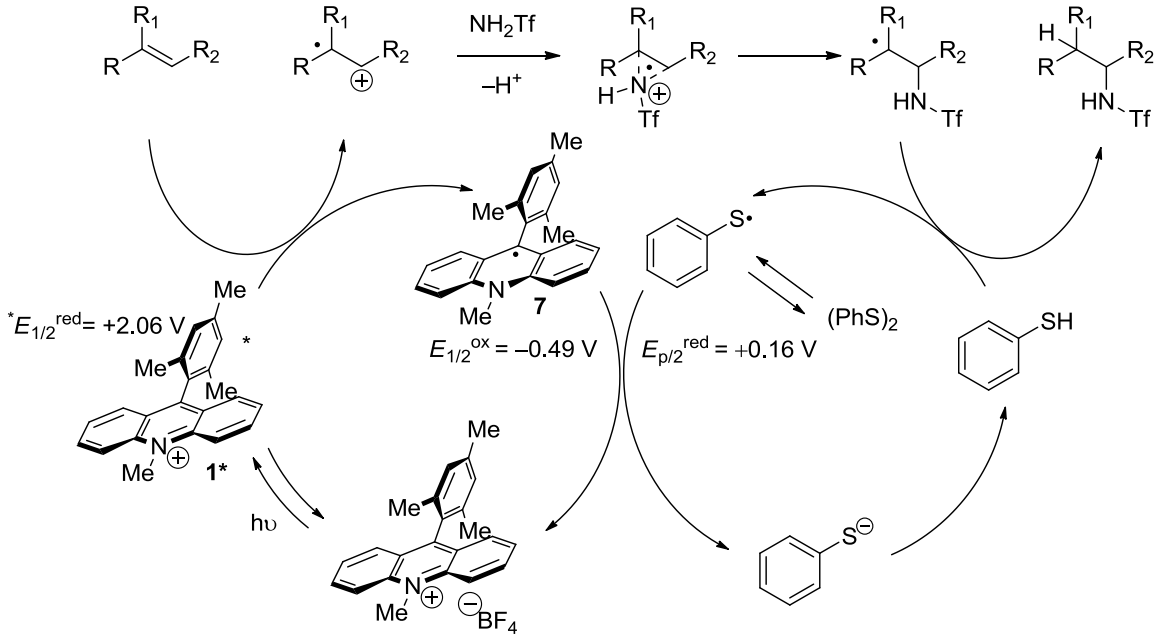

To complete the optimization of this reaction, we then investigated base loading and concentration as summarized in **Table 3**. We decided to switch to dichloromethane (DCM) from dichloroethane (DCE) because it gave a marginally better yield and is a slightly more common solvent.

We also found that we could decrease the catalyst loading from 5 mol % to 1 mol % with no appreciable loss in yield. In our screening, we found that 25 mol % of 2,6-lutidine and [0.5 M] DCM was optimal for our reaction conditions. We saw decreased yields upon going to [1.0 M] likely because the increased concentration was unfavorable for solubility.

Table 3. Optimization of Concentration and Base Loading for the Intermolecular anti-Markovnikov Hydroamination Reaction

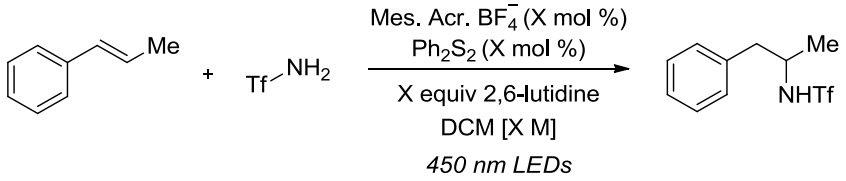

Catalyst Loading	Disulfide Loading	2,6-lutidine Loading	Concentration	^{1}H NMR Yield
5 mol %	20 mol %	None	[0.5 M]	**64%**
5 mol %	20 mol %	15 mol %	[0.5 M]	**59%**
5 mol %	20 mol %	25 mol %	[0.5 M]	**91%**
5 mol %	20 mol %	50 mol %	[0.5 M]	**77%**
5 mol %	20 mol %	100 mol %	[0.5 M]	**36%**
1 mol %	10 mol %	25 mol %	[0.1 M]	**65%**
1 mol %	10 mol %	25 mol %	[0.25 M]	**62%**
1 mol %	10 mol %	25 mol %	[0.5 M]	**80%**
1 mol %	10 mol %	25 mol %	[1.0 M]	**30%**

Following the optimization of various reaction parameters, we turned our attention to evaluating different amine nucleophiles (**Figure 4.13**). We found that *p*-toluenesulfonamide and

Figure 4.13 Screening of Amine Nucleophiles with β-Methylstyrene

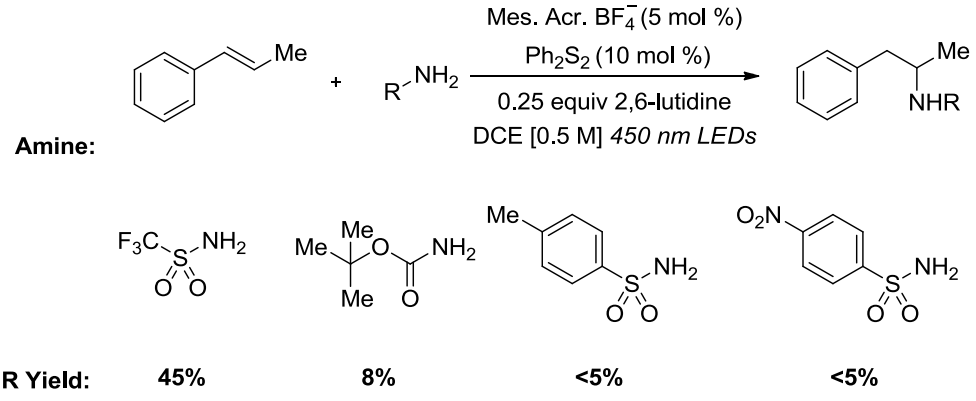

p-nitrobenzenesulfonamide were not competent reaction partners, while *tert*-butylcarbamate did react with β–methyl styrene to give the desired product in low yield. Trifluoromethanesulfonamide has a pKa of ~9.7[3] in dimethyl sulfoxide (DMSO) and is more acidic than the other amine nucleophiles. The parent benzene sulfonamide has a reported pKa of ~24.2[4] in DMSO and ethyl carbamate has a pKa of ~16,[5] which can be used to estimate the acidities of the amines we investigated. It is likely that only amines within a certain pKa range that is sufficiently nucleophilic will lead to product formation in our reaction conditions.

4.5 Scope of the Intermolecular Anti-Markovnikov Hydroamination Reaction

We recognized that our method would provide access to a class of phenethylamine compounds, which are highly valuable for their bioactivity. To this end, we began screening styrenyl substrates as the alkene partner with trifluoromethane sulfonamide as the amine nucleophile (**Figure 4.14**). Our optimized reaction conditions included 1 mol % mesityl acridinium tetrafluoroborate catalyst, 10 mol % diphenyl disulfide, 25 mol % 2,6-lutidine, 1.0 equivalent of alkene and 1.5 equivalents of trifluoromethane sulfonamide in a [0.5 M] solution of dichloromethane.

Figure 4.14 Scope of Intermolecular Anti-Markovnikov Hydroamination Reactions with Styrenes

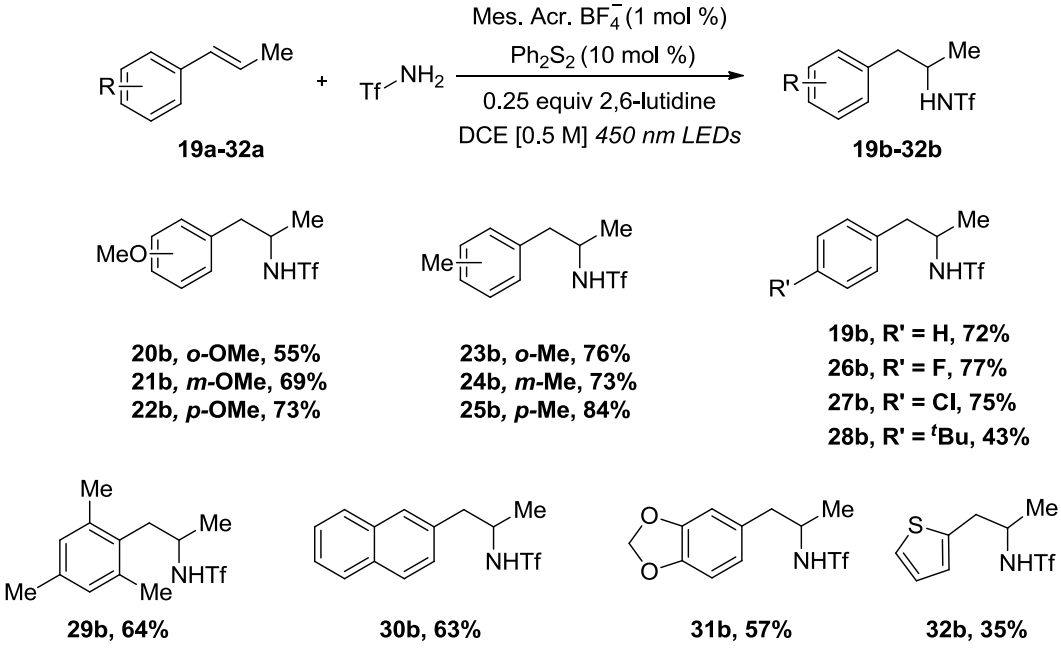

We found that the *p*-methoxy substituted styrenes went to completion with the fastest reaction times and were formed in good yields. Slightly less electron rich methyl substituted styrenes also gave the desired products in high yields. In both methoxy and methyl substituted styrenes, substitution at the para position of the arene gave the highest yields. The electron neutral β-methylstyrene and electron deficient *p*-F and *p*-Cl substituted styrenes were tolerated and high yielding. Bulky mesityl styrene and *tert*-butyl substituted styrene reacted only in modest yields and in the latter case we observed the formation of many oligomeric side products. We also extended the scope to include bicyclic styrenes, with naphthalene and isosafrole performing as competent alkene partners. Heteroaromatic substitution was also tolerated as demonstrated by thiophene though in low yield and prolonged reaction times.

We then turned our attention to evaluating alkenes with more challenging oxidation potentials and substitution patterns. We observed that our reaction tolerated ester, protected amine and even free alcohol moieties. Alkenyl substrates also underwent reaction in good yields with 1-phenyl cyclohexene and 1-methyl cyclopentene reacting to give the anti-Markovnikov products in 50% and 85% yield, respectively, with a mild level of diastereoselection. Due to its volatility, 3.0 equivalents of 2-methyl-2-butene was employed and the amine product was formed in 72% yield as determined by ^{1}H NMR with an internal standard (**Figure 4.15**).

Figure 4.15 Scope of the Anti-Markovnikov Hydroamination Reactions with Alkenes

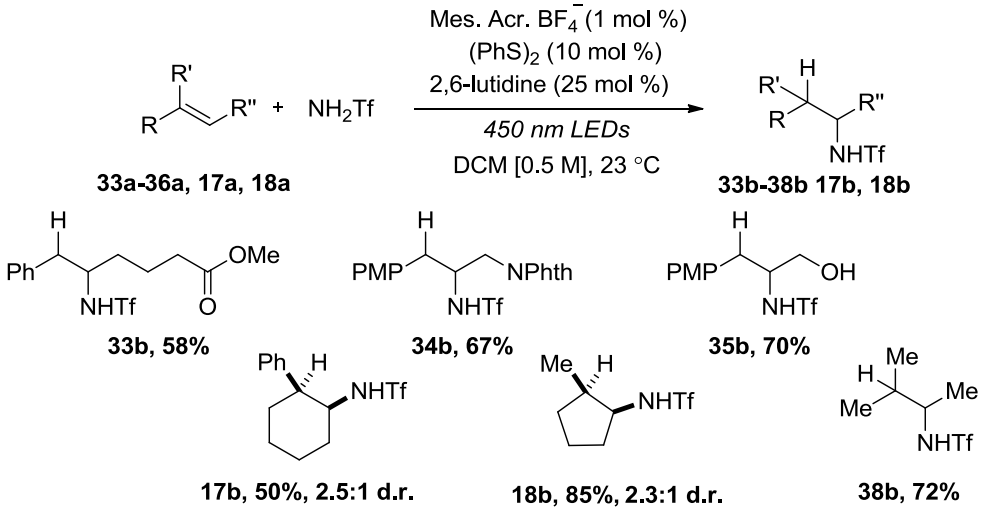

We were pleased to discover that heterocyclic amines could act as nucleophiles in our reaction, providing direct access to compounds highly sought after by medicinal chemists (**Figure 4.16**). We found that pyrazole and 1,2,3-triazole gave the desired product in good yields, 83% and 80%, respectively. 1,2,3-triazole reacted with *p*-OMe styrene to give the product in a 2:1 mixture of regioisomers with preferential substitution at the N1 position, as expected due to its statistical advantage and increased electron density. Imidazole and indazole both reacted to give the amine products in similarly decent yields. We attribute the lowered yield observed in the reaction with imidazole to its poor solubility and unfortunately, attempts to increase solubility through various solvents were unsuccessful. Indazole reacted with *o*-OMe styrene to give a single regioisomer with substitution at the N2 position, as previously reported for alkylations with indazole under non-basic conditions. 1,1-disubstituted styrenes were also reactive towards 1,2,3-triazole though no reaction was observed with trifluoromethane sulfonamide.

Figure 4.16 Scope of the Intermolecular Anti-Markovnikov Hydroamination Reactions with Heterocyclic Amines

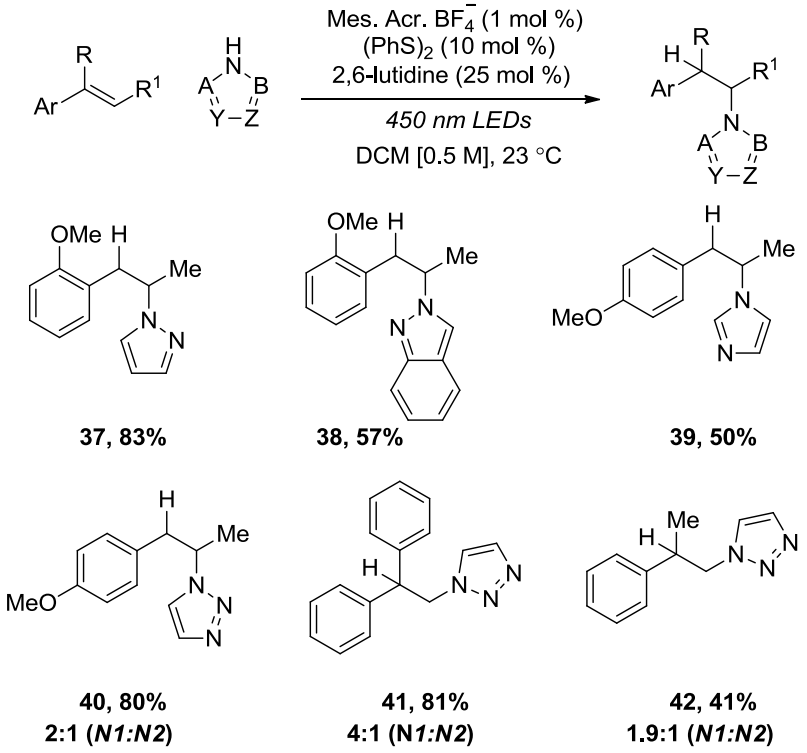

Summary

We have developed an efficient method for the anti-Markovnikov hydroamination reaction of alkenes. Using a novel organic photoredox catalyst system developed by our lab, this method offers direct access to valuable biologically active amines with complete regioselectivity. The scope of our transformation is complementary to existing methods, as it includes non-activated alkenyl partners as well as heteroaromatic amine nucleophiles. In total we have demonstrated 38 examples in 35%-89% yield. Based on previous literature and our own observations we have proposed a mechanism for this transformation, with deeper investigations ongoing in our lab.

REFERENCES

(1) Nguyen, T. M.; Nicewicz, D. A. Anti-Markovnikov Hydroamination of Alkenes Catalyzed by an Organic Photoredox System. *J. Am. Chem. Soc.* **2013**, *135*, 9588–9591.

(2) Tyson, E. L.; Ament, M. S.; Yoon, T. P. Transition Metal Photoredox Catalysis of Radical Thiol-Ene Reactions. *J. Org. Chem.* **2013**, *78*, 2046–2050.

(3) Bordwell, F. G.; Algrim, D. Nitrogen Acids. 1. Carboxamides and Sulfonamides. *J. Org. Chem.* **1976**, *41*, 2507–2508.

(4) Bordwell, F. G.; Fried, H. E.; Hughes, D. L.; Lynch, T. Y.; Satish, A. V.; Whang, Y. E. Acidities of Carboxamides, Hydroxamic Acids, Carbohydrazides, Benzenesulfonamides, and Benzenesulfonohydrazides in DMSO Solution. *J. Org. Chem.* **1990**, *55*, 3330–3336.

(5) Bordwell, F. G.; Fried, H. E. Heterocyclic Aromatic Anions with 4n + 2 .pi.-Electrons. *J. Org. Chem.* **1991**, *56*, 4218–4223.

APPENDIX 1: SUPPORTING INFO FOR CATION RADICAL DIELS-ALDER REACTIONS

General Procedure 1: To a clean dry 1 dram vial was added catalyst and purged with N_2. Dichloromethane (sparged for ~10 min with N_2) was added then dienophile (freshly distilled over CaH) and then diene (freshly distilled) was added to the reaction mixture. The reaction was irradiated with the specified light source and then quenched with a TEMPO solution (~5mg/0.2 mL). Products were purified via silica gel chromatography with 1% EtOAc/Hexanes.

5-(4-methoxyphenyl)-6-methylbicyclo[2.2.1]hept-2-ene (A).

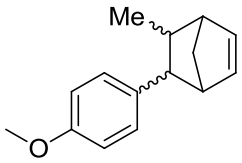

Prepared via General Procedure 1 and spectral data were in agreement with reported literature.[1]

4'-methoxy-2,4,5-trimethyl-1,2,3,6-tetrahydro-1,1'-biphenyl (D).

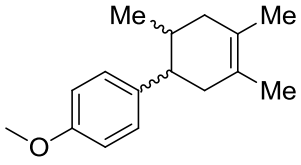

Prepared via General Procedure 1 and spectral data were in agreement with reported literature.[2]

5-ethyl-6-(4-methoxyphenyl)bicyclo[2.2.1]hept-2-ene (E).

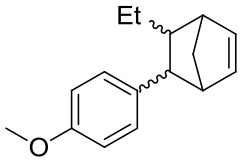

Prepared via General Procedure 1. **^{1}H NMR Major set of diastereomers** (400MHz, $CDCl_3$) δ = 7.08 (d, *J* = 8.7 Hz, 2 H), 6.76 (d, *J* = 8.7 Hz, 2 H), 6.30 (dd, *J* = 3.0, 5.3 Hz, 1 H), 5.85 (dd, *J* = 2.8, 5.5 Hz, 1 H), 3.76 (s, 3 H), 2.90 (br. s., 1 H), 2.73 (t, *J* = 3.6 Hz, 1 H), 2.64 (br. s., 1 H), 1.67 - 1.54 (m, 2 H), 1.51 - 1.42 (m, 4 H), 0.93 - 0.87 (m, 3 H); ^{1}H NMR (400MHz , $CDCl_3$) δ = 7.20 (d, *J* = 8.7 Hz, 2 H), 6.83 (d, *J*

= 8.7 Hz, 2 H), 6.11 - 6.05 (m, 1 H), 5.73 - 5.60 (m, 1 H), 3.78 (s, 3 H), 2.02 (br. s., 1 H), 1.97 - 1.90 (m, 1 H), 1.69 (s, 1 H), 1.60 - 1.53 (m, 2 H), 1.41 (br. s., 2 H), 1.17 - 1.06 (m, 2 H), 0.85 (t, *J* = 7.4 Hz, 3 H).

General Procedure 2:

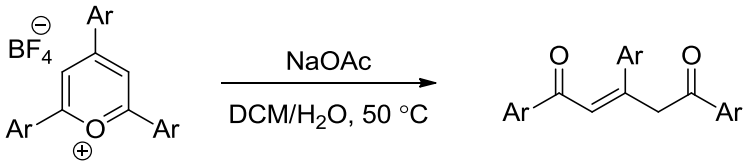

To a clean dry RBF was added triaryloxopyrylium tetrafluoroborate and sodium acetate. Then the solids were dissolved in a 1:1 mixture of DCM/H_2O. Equipped with reflux condenser and heated to 50 °C overnight. Cooled to room temperature then the organic and aqueous layers separated, then the aqueous layer was extracted with DCM 3x, organic layers combined and washed with brine, dried over Na_2SO_4 and concentrated in vacuo. Chromatographed in 25% EtOAc/Hexanes to give the desired product.

1,3,5-triphenylpent-2-ene-1,5-dione (B).

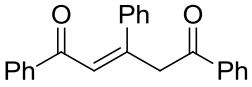

Prepared according to General Procedure 2 and spectral data were in agreement with literature values.[3]

1,3,5-tris(4-methoxyphenyl)pent-2-ene-1,5-dione (C).

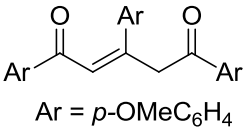

Prepared according to General Procedure 2. **^{1}H NMR** (400MHz , $CDCl_3$) δ = 8.08 (d, *J* = 8.8 Hz, 2 H), 8.01 (d, *J* = 8.8 Hz, 6 H), 7.53 (d, *J* = 8.8 Hz, 2 H), 7.42 (s, 1 H), 7.01 - 6.90 (m, 6 H), 4.86 (s, 2 H), 3.90 (s, 3 H), 3.89 (s, 3 H), 3.85 (s, 3 H); ^{13}C NMR (101MHz , $CDCl_3$) δ = 195.1, 189.4, 163.5, 163.2, 160.6, 151.7, 134.3, 132.3, 130.6, 128.3, 121.8, 114.1, 113.7, 55.5, 42.3.

3,3'-SiPh$_3$-H8-BINOL N-trifyl phosphoramide (7).

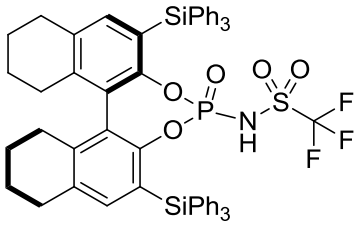

Prepared according to literature procedure and spectral data were in agreement with reported.[4]

3,3'-SiPh$_3$-H8-BINOL N-trifyl phosphoramide tri-(p-OMeC6H4)oxopyrlium (8e).

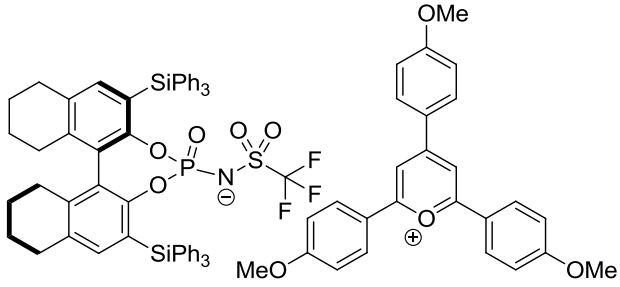

To a clean dry 20 mL scintillation vial was added N-trifylphosphoramide **7** (1.0 equiv) and ene dione **C**. Dissolved in a small amount of EtOH and heated with heat gun until all solids were in solution. Allowed mixture to cool slowly and precipitates formed. Filtered and washed with hexanes then recrystallized from DCM/Hexanes to give the desired product. **^{1}H NMR** (400MHz , $CDCl_3$) δ = 8.14 - 8.05 (m, 6 H), 7.57 - 7.45 (m, 10 H), 7.20 - 6.99 (m, 12 H), 6.98 - 6.93 (m, 2 H), 6.80 (d, *J* = 8.8 Hz, 2 H), 3.81 (s, 6 H), 3.71 (s, 3 H), 2.78 - 2.51 (m, 6 H), 2.41 - 2.19 (m,23 H), 1.83 - 1.54 (m, 8 H); **^{13}C NMR** (101MHz , $CDCl_3$) δ = 167.5, 166.2, 165.0, 162.0, 136.7, 133.1, 130.5, 127.7, 123.9, 121.2, 115.7, 110.6, 55.8, 29.2, 27.7, 22.8

REFERENCES

(1) Bauld, N. L.; Gao, D. Approaching a Possible Stepwise/concerted Mechanistic Crossover Point in the Cation Radical Cycloadditions of Cis- and Trans-Anethole. *J. Chem. Soc. Perkin Trans. 2* **2000**, 931–934.

(2) Yueh, W.; Bauld, N. L. Mechanistic Aspects of Aminium Salt-Catalyzed Diels-Alder Reactions: The Substrate Ionization Step. *J. Phys. Org. Chem.* **1996**, *9*, 529–538.

(3) Song, M.; Fan, C. A Rapid Approach Toward Synthesis of 1,3,5-Triarylpent-2-Ene-1,5-Diones Catalyzed by KF/Al2O3 and PEG-400 Using Microwave Irradiation. *Lett. Org. Chem.* **2013**, *10*, 27–30.

(4) Rueping, M.; Nachtsheim, B. J.; Koenigs, R. M.; Ieawsuwan, W. Synthesis and Structural Aspects of N-Triflylphosphoramides and Their Calcium Salts—Highly Acidic and Effective Brønsted Acids. *Chem. – Eur. J.* **2010**, *16*, 13116–13126.

Compound **C**

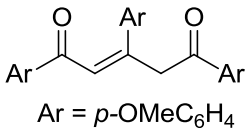
O
Ar
O
Ar
Ar
Ar = p-OMeC6H4

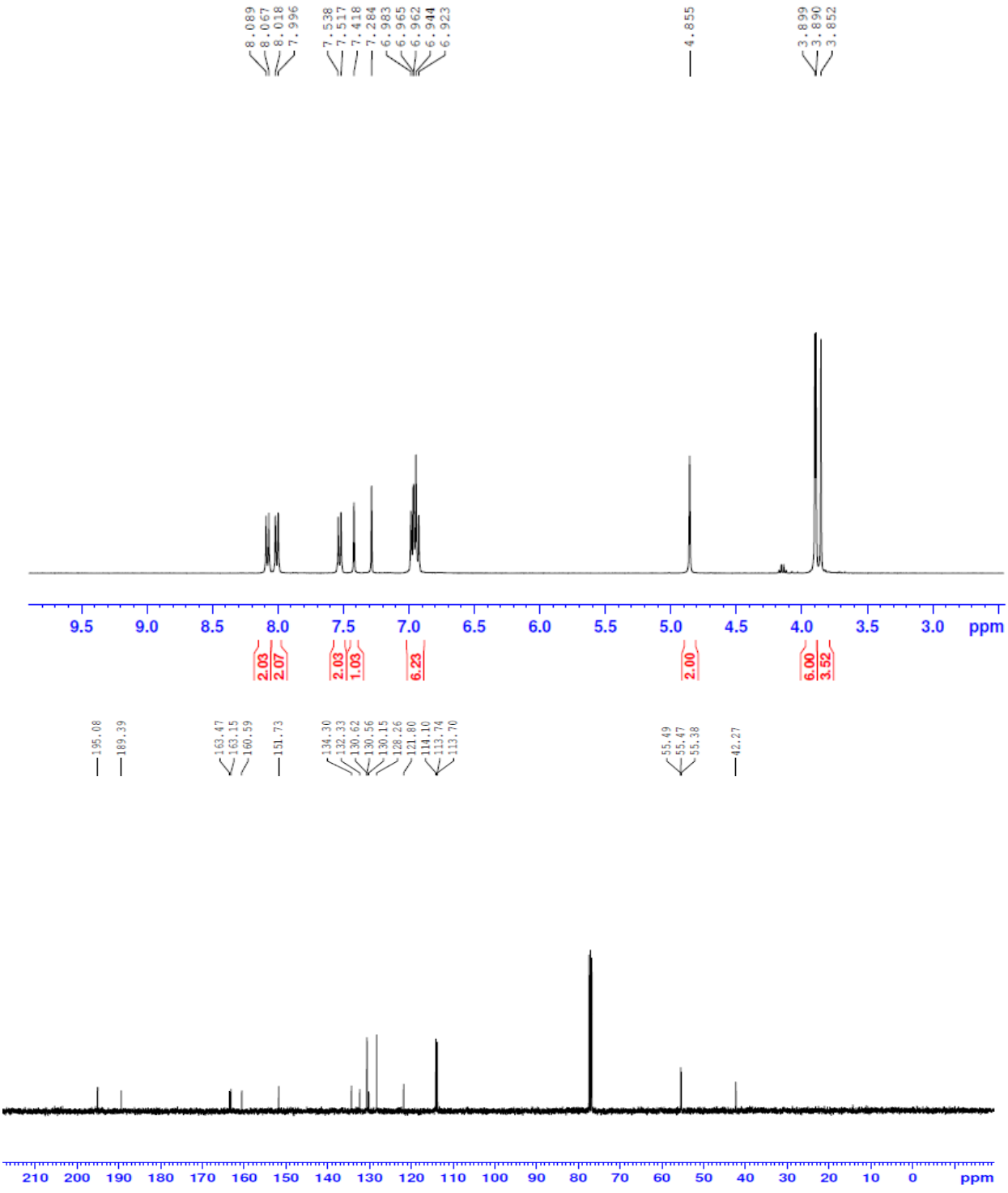
8.089
8.067
8.018
7.996
7.538
7.517
7.418
7.284
6.983
6.965
6.962
6.944
6.923
4.855
3.899
3.890
3.852
9.5
9.0
8.5
8.0
7.5
7.0
6.5
6.0
5.5
5.0
4.5
4.0
3.5
3.0
ppm
2.03
2.07
2.03
1.03
6.23
2.00
6.00
3.52
195.08
189.39
163.47
163.15
160.59
151.73
134.30
132.33
130.62
130.56
130.15
128.26
121.80
114.10
113.74
113.70
55.49
55.47
55.38
42.27
210
200
190
180
170
160
150
140
130
120
110
100
90
80
70
60
50
40
30
20
10
0
ppm

Compound **E**

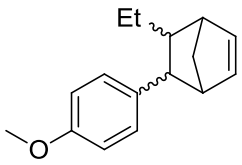
Et
O

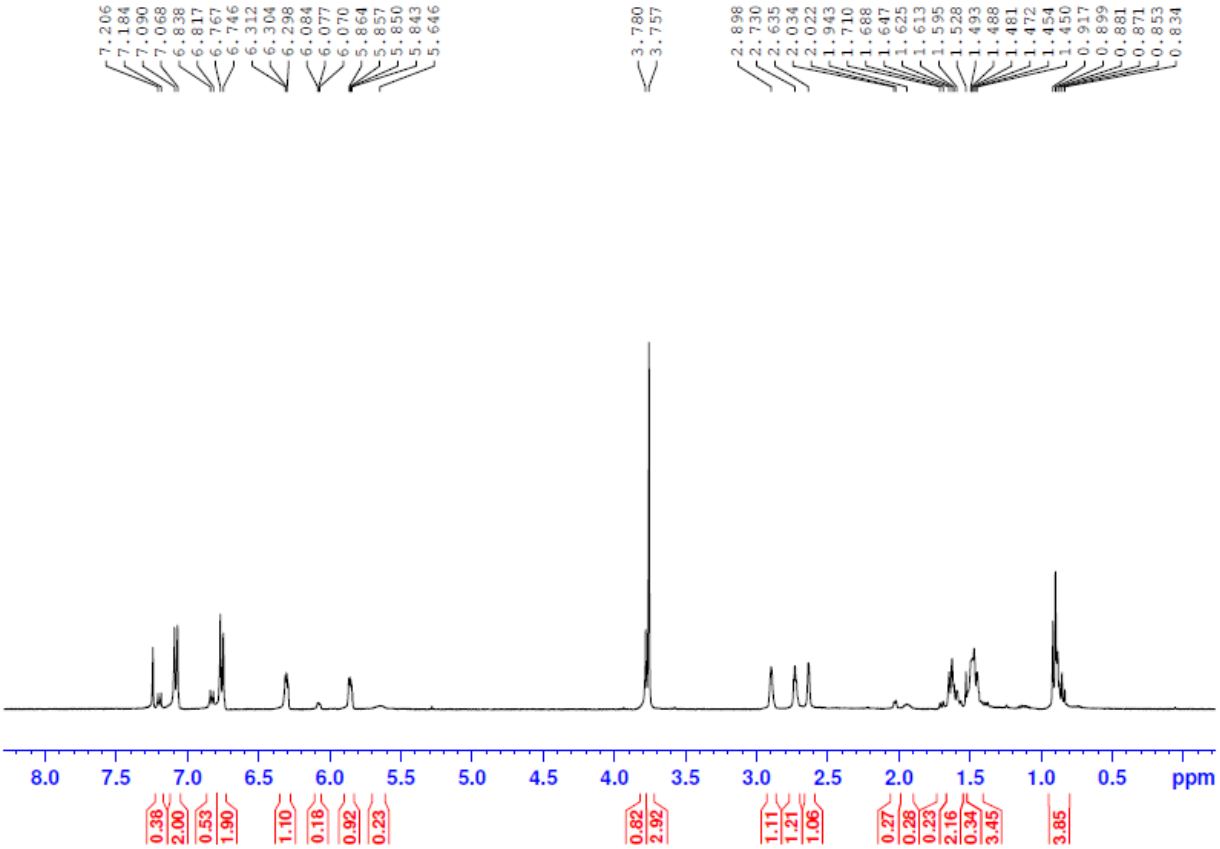
7.206
7.184
7.090
7.068
6.838
6.817
6.767
6.746
6.312
6.304
6.298
6.084
6.077
6.070
5.864
5.857
5.850
5.843
5.646
3.780
3.757
2.898
2.730
2.635
2.034
2.022
1.943
1.710
1.688
1.647
1.625
1.613
1.595
1.528
1.493
1.488
1.481
1.472
1.454
1.450
0.917
0.899
0.881
0.871
0.853
0.834
8.0
7.5
7.0
6.5
6.0
5.5
5.0
4.5
4.0
3.5
3.0
2.5
2.0
1.5
1.0
0.5
ppm
0.38
2.00
0.53
1.90
1.10
0.18
0.92
0.23
0.82
2.92
1.11
1.21
1.06
0.27
0.28
0.23
2.16
0.34
3.45
3.85

Compound **8e**

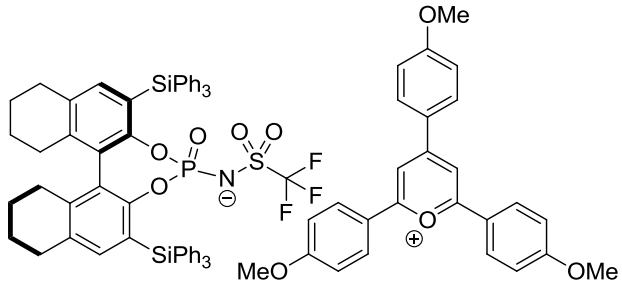
OMe
SiPh3
SiPh3
MeO
OMe


8.114
8.091
8.069
7.616
7.599
7.537
7.531
7.501
7.493
7.487
7.482
7.150
7.137
7.084
7.079
7.016
6.978
6.956
6.814
6.792
3.812
3.713
2.695
2.650
2.632
2.617
2.602
2.588
2.360
2.270
1.764
1.686
1.664
1.650
1.643
1.629
1.599
1.587

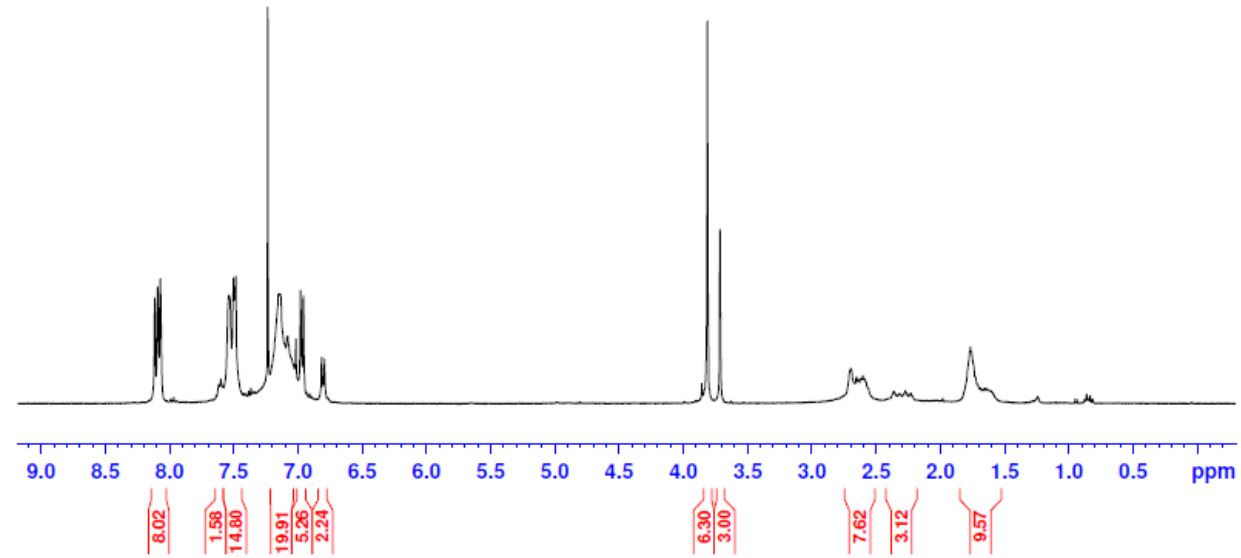
9.0
8.5
8.0
7.5
7.0
6.5
6.0
5.5
5.0
4.5
4.0
3.5
3.0
2.5
2.0
1.5
1.0
0.5
ppm
8.02
1.58
14.80
19.91
5.26
2.24
6.30
3.00
7.62
3.12
9.57

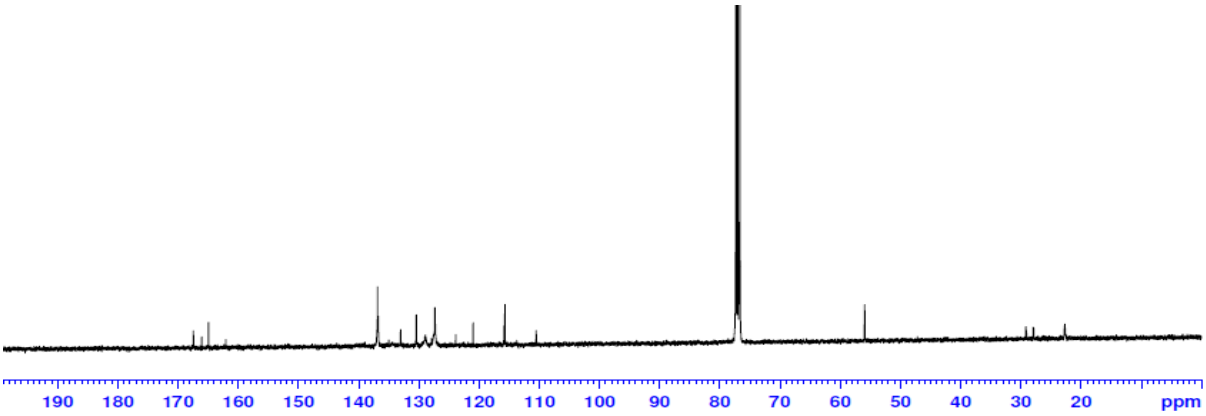
190
180
170
160
150
140
130
120
110
100
90
80
70
60
50
40
30
20
ppm

Racemic GC Trace of Compound D:

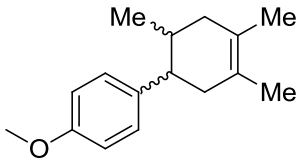

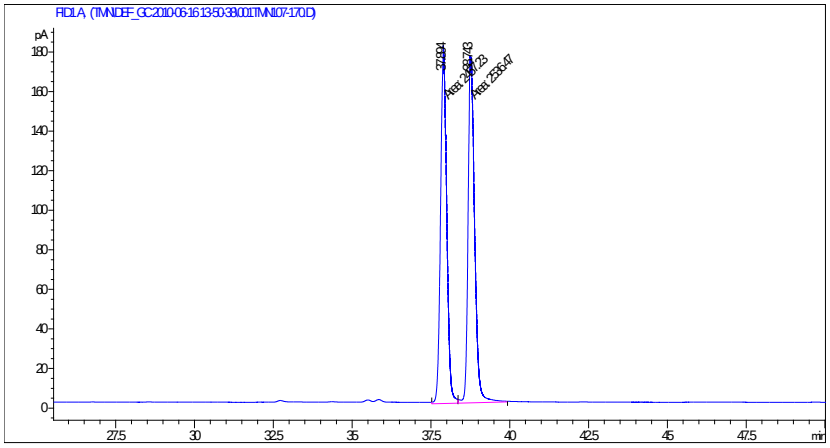

Chiral GC Trace for Figure 2.4 (Entry 4):

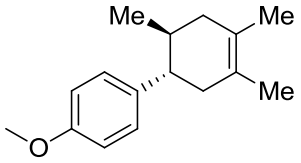

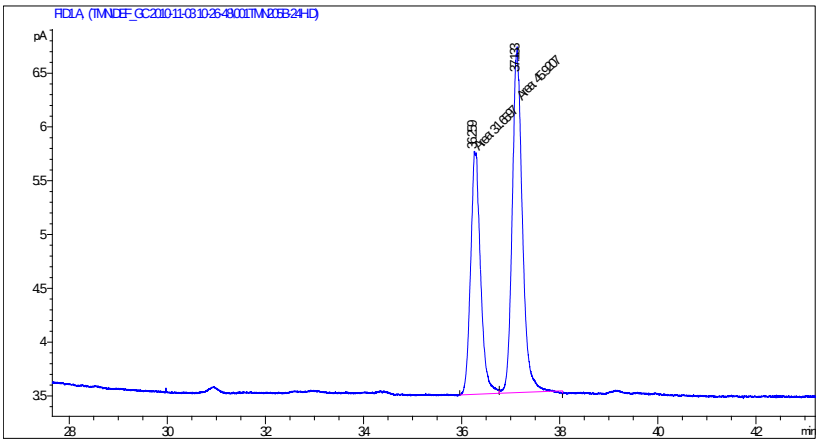

Chiral GC Trace for Figure 2.4 (Entry 5):

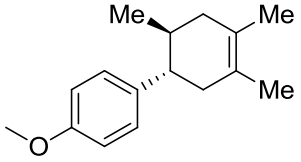

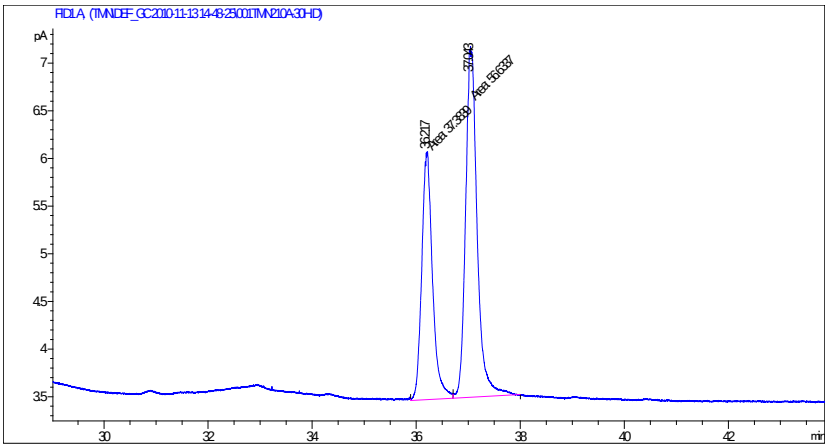

Chiral GC Trace for Table 3 (Entry 1):

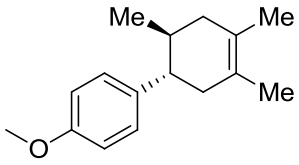

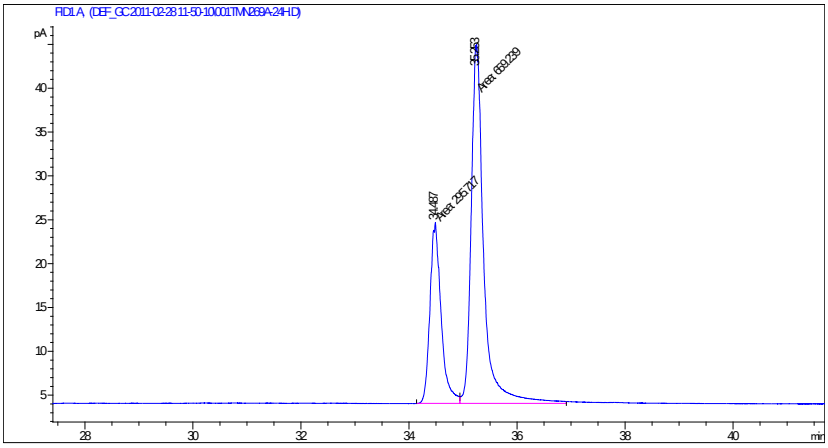

Chiral GC Trace for Table 3 (Entry 2):

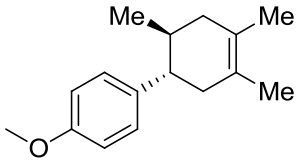

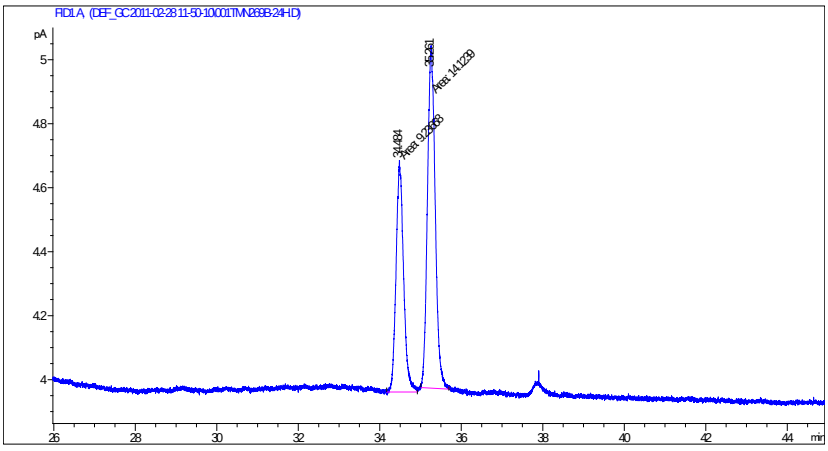

Chiral GC Trace for Table 3 (Entry 4):

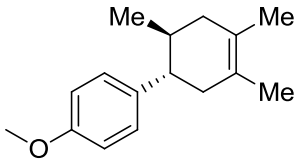

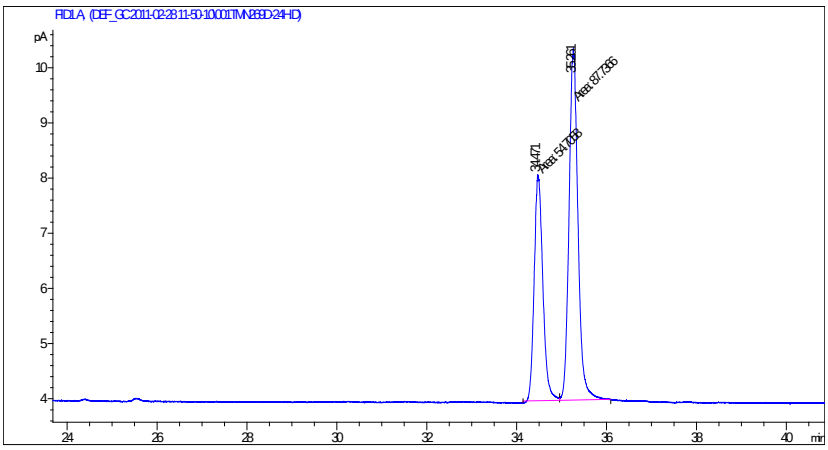

Chiral GC Trace for Figure 2.5 (Entry 3):

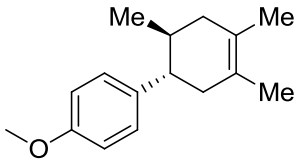

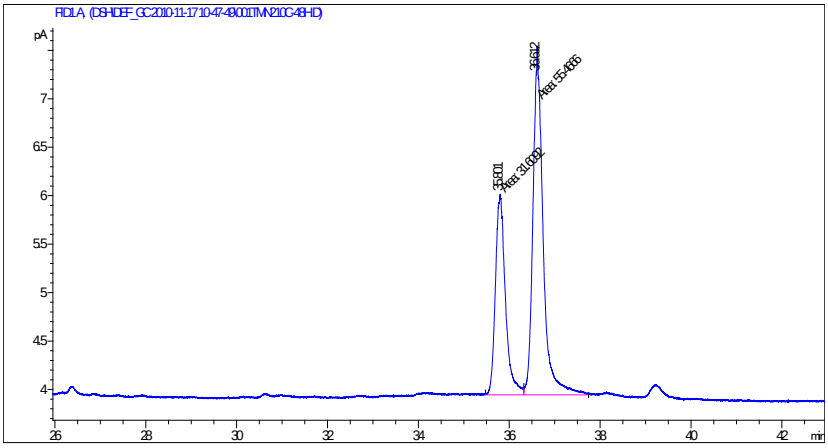

Chiral GC Trace for Figure 2.6 (Entry 1):

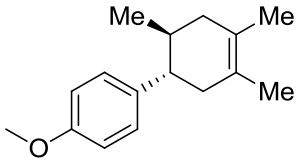

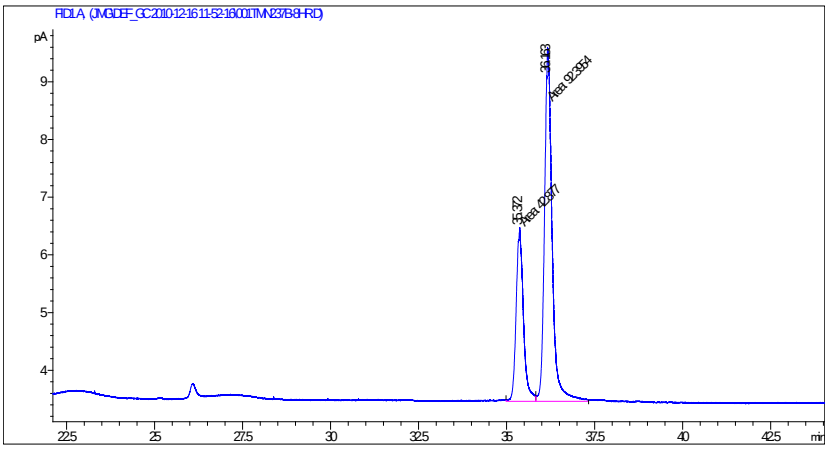

Chiral GC Trace for Figure 2.6 (Entry 2):

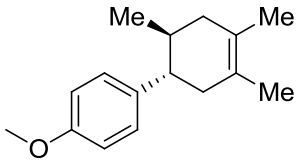

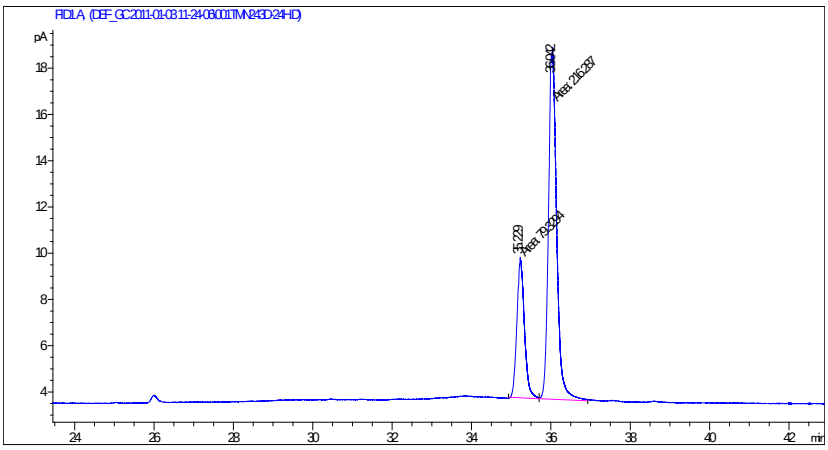

Chiral GC Trace for Figure 2.6 Entry 3):

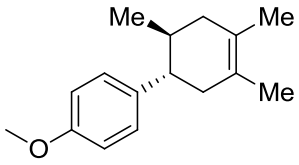

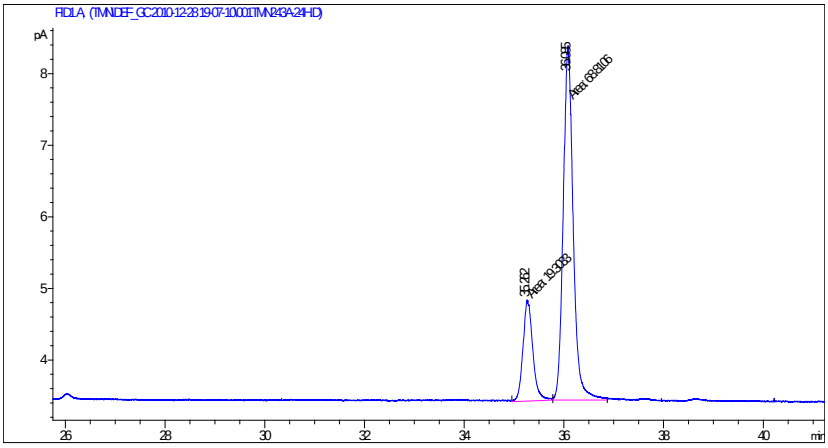

Chiral GC Trace for Figure 2.6 (Entry 4):

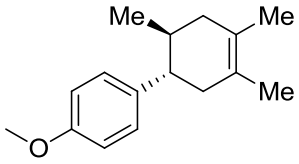

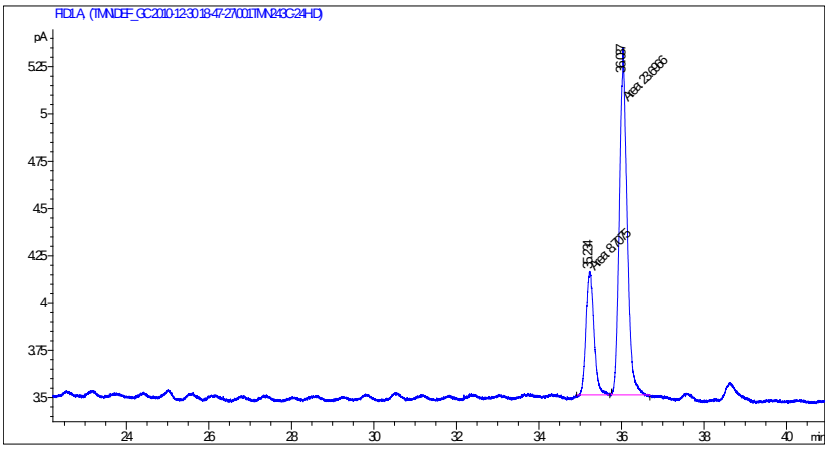

Chiral GC Trace for Figure 2.9 (Entry 1):

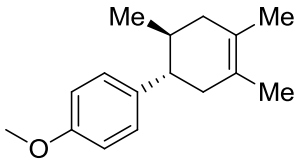

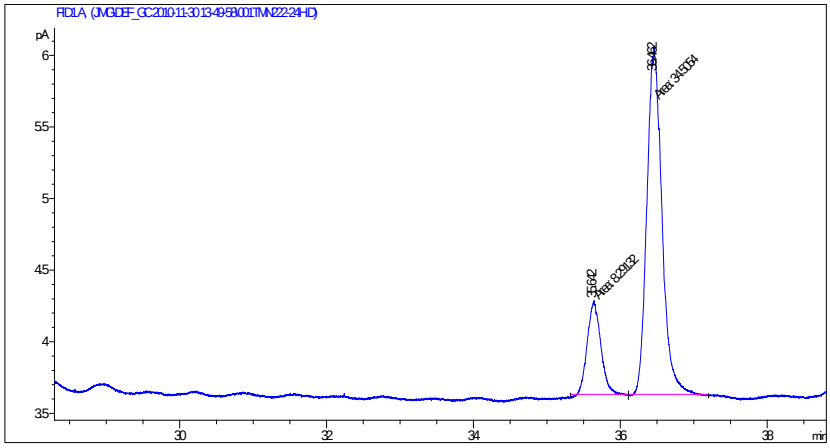

Racemic GC Trace for Compound A:

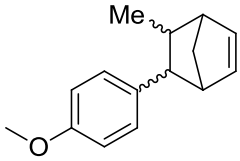

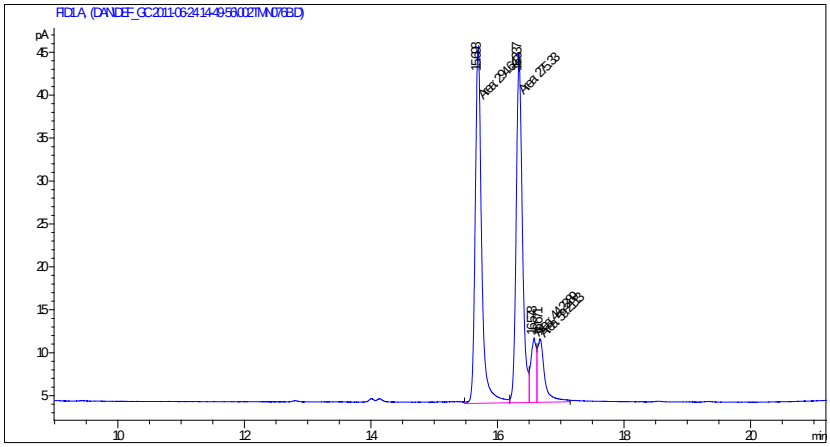

Chiral GC Trace for Figure 2.10 (Entry 3):

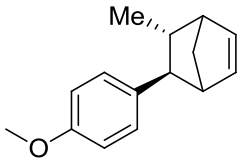

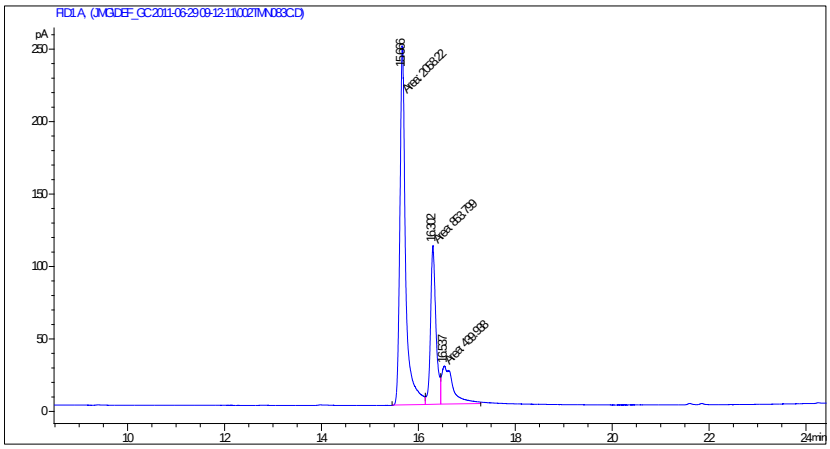

Chiral GC Trace for Figure 2.10 (Entry 4):

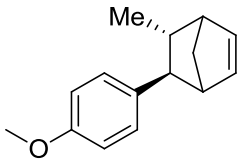

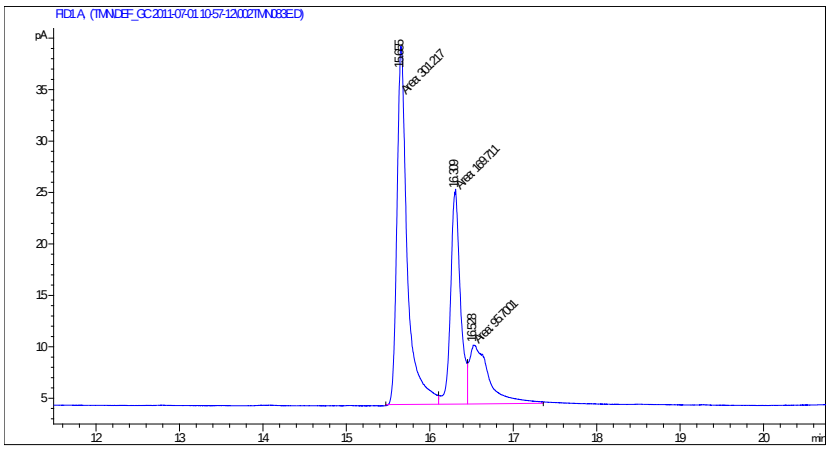

Racemic GC Trace for Compound E:

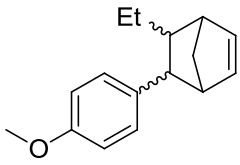

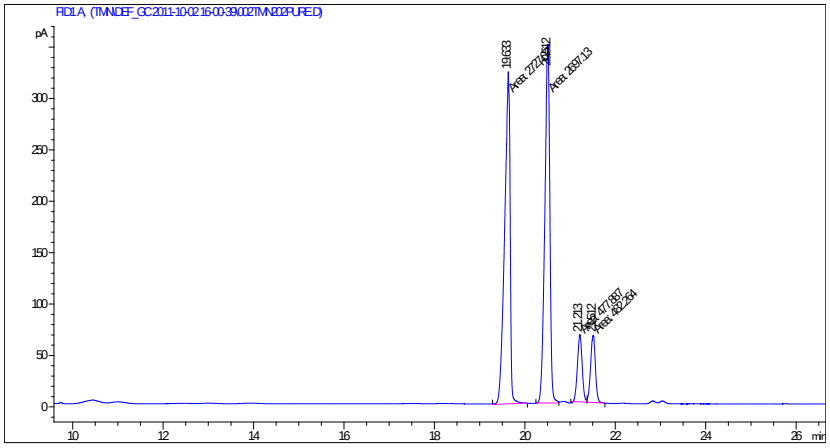

Chiral GC Trace for Figure 2.11:

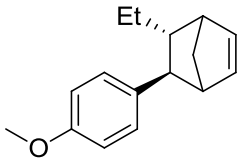

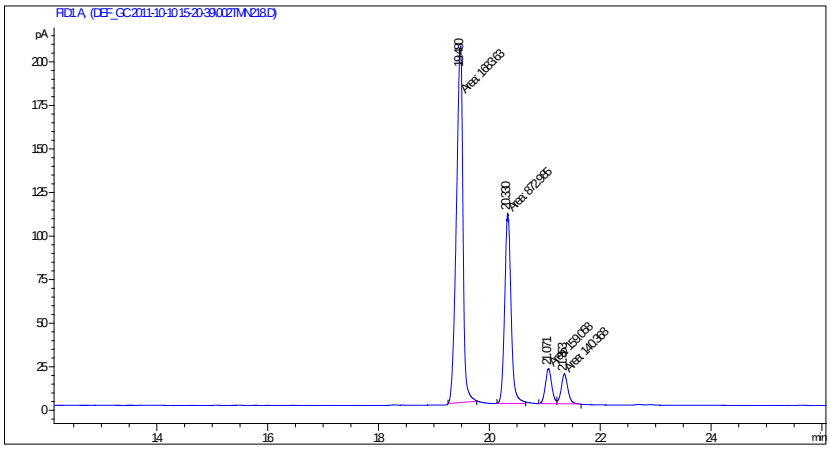

Racemic GC Trace for Compound A:

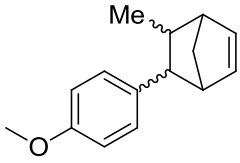

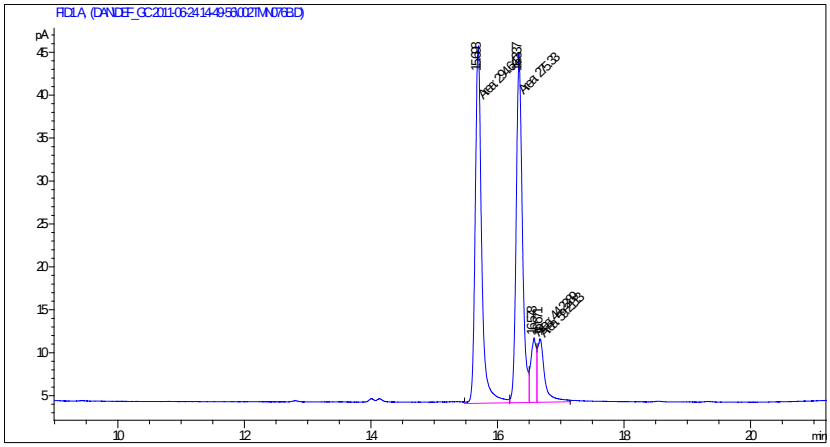

Chiral GC Trace for Figure 2.12 (Catalyst 12):

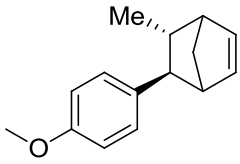

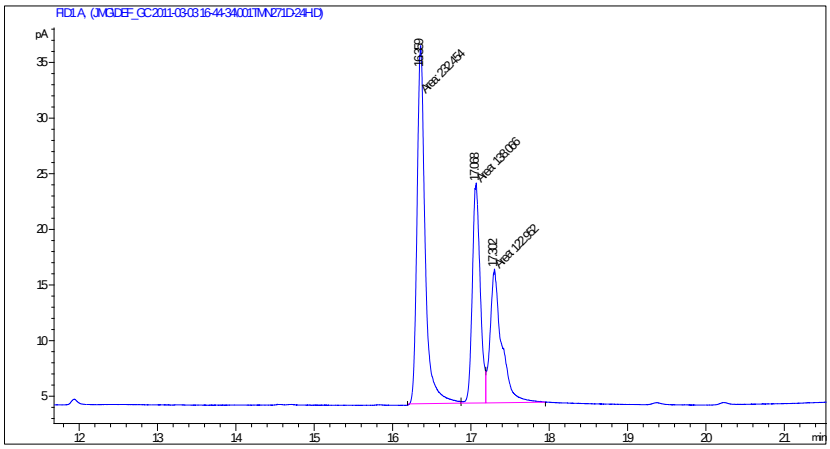

Racemic GC Trace for Compound E:

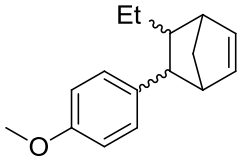

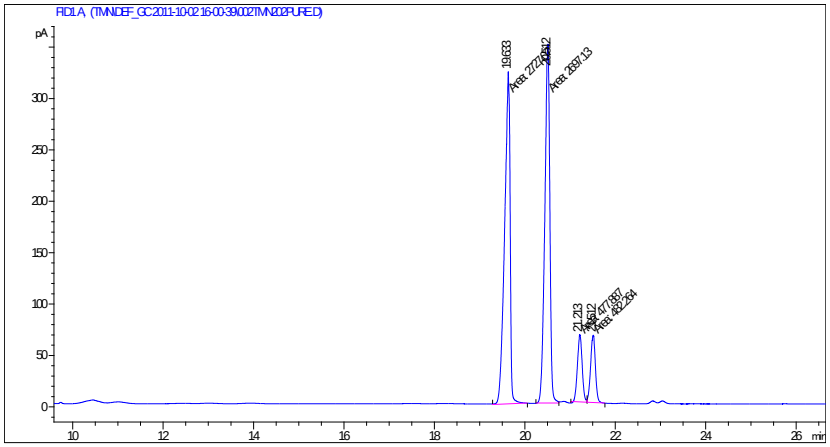

Chiral GC Trace for Figure 2.13 (Entry 1):

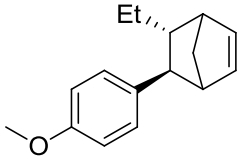

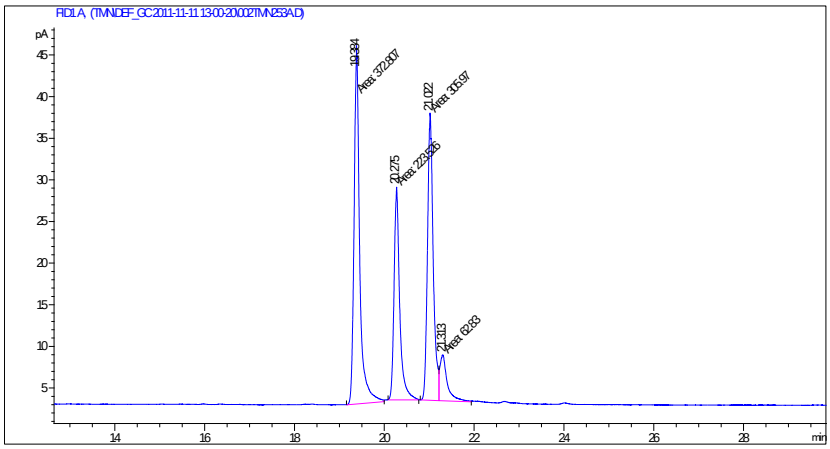

Chiral GC Trace for Figure 2.13 (Entry 2):

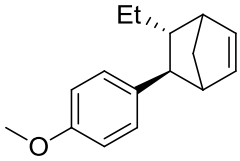

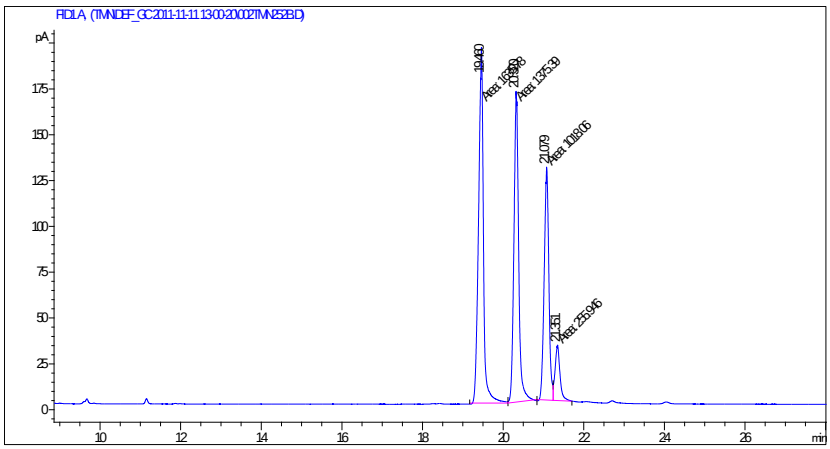

Chiral GC Trace for Figure 2.13 (Entry 3):

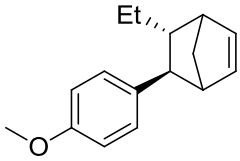

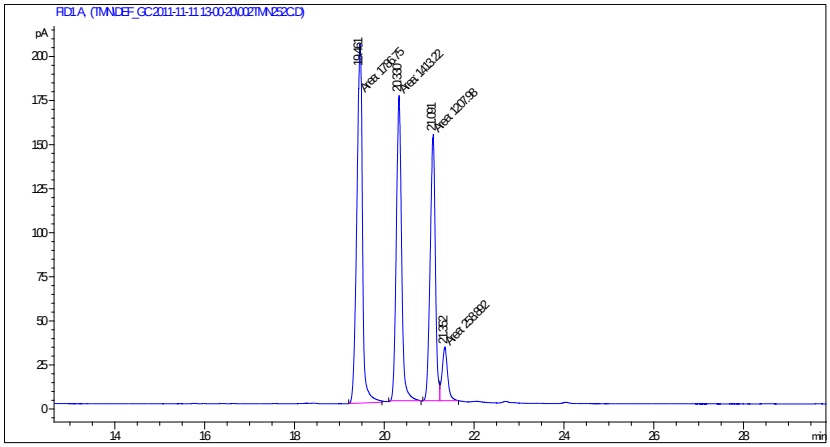

Chiral GC Trace for Figure 2.13 (Entry 4):

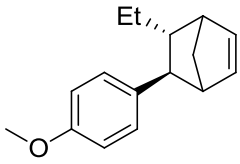

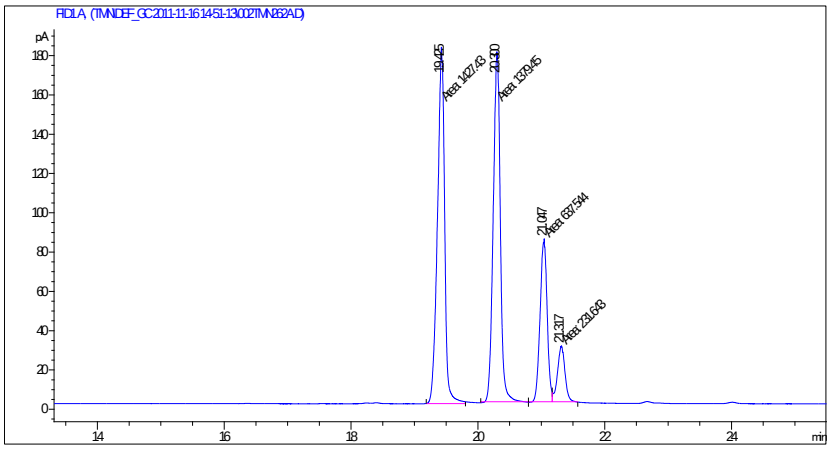

Chiral GC Trace for Figure 2.13 (Entry 5):

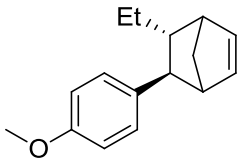

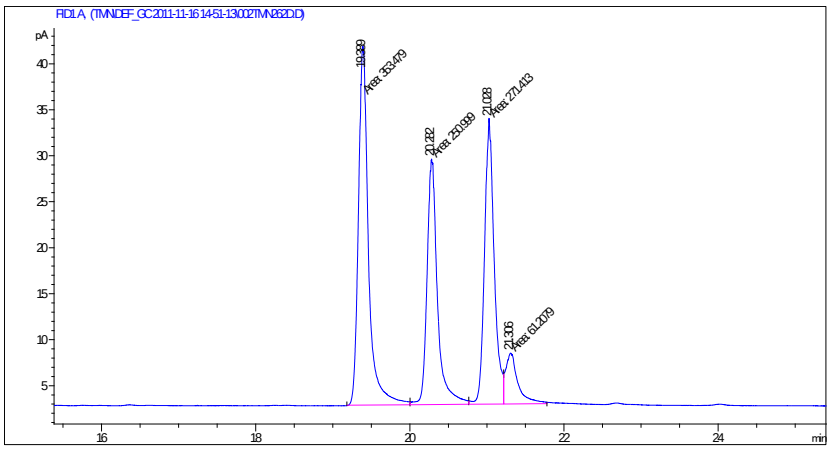

Chiral GC Trace for Figure 2.13 (Entry 6):

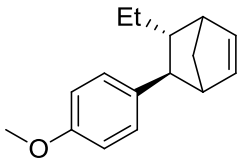

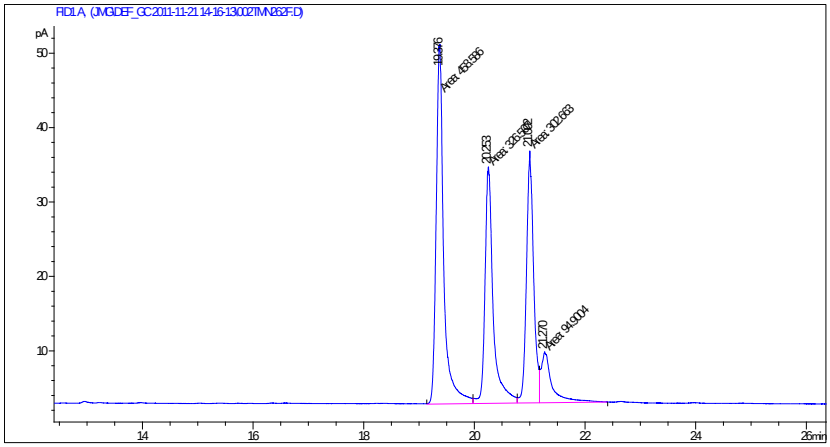

Racemic GC Trace for Compound A:

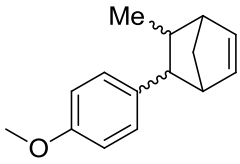

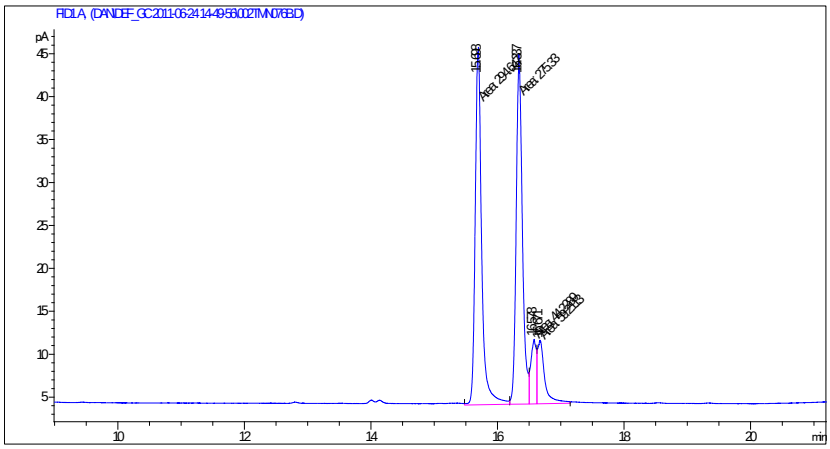

Chiral GC Trace for Figure 2.17 (Entry 1):

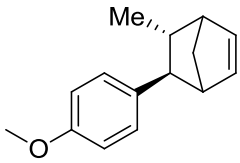

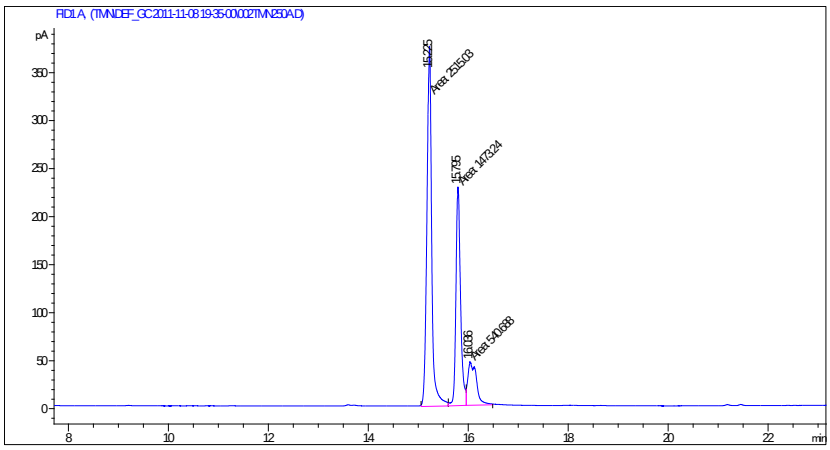

Chiral GC Trace for Figure 2.17 (Entry 2):

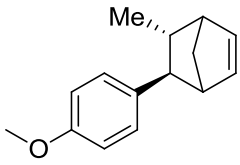

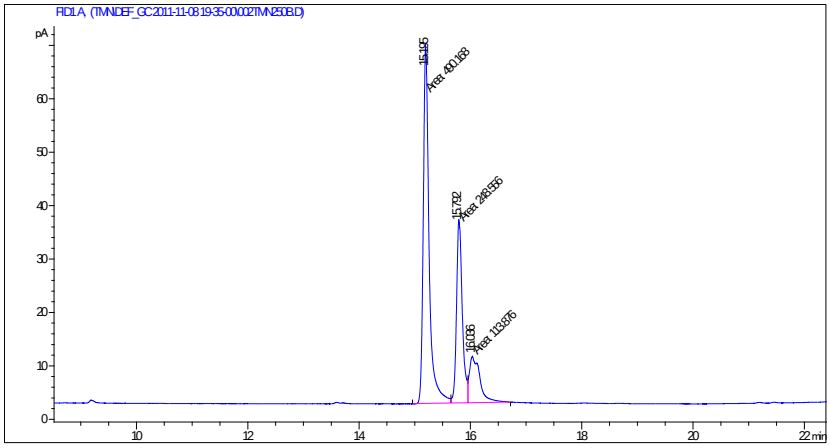

Chiral GC Trace for Figure 2.17 (Entry 3):

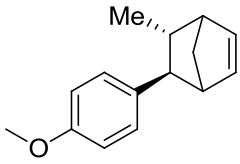

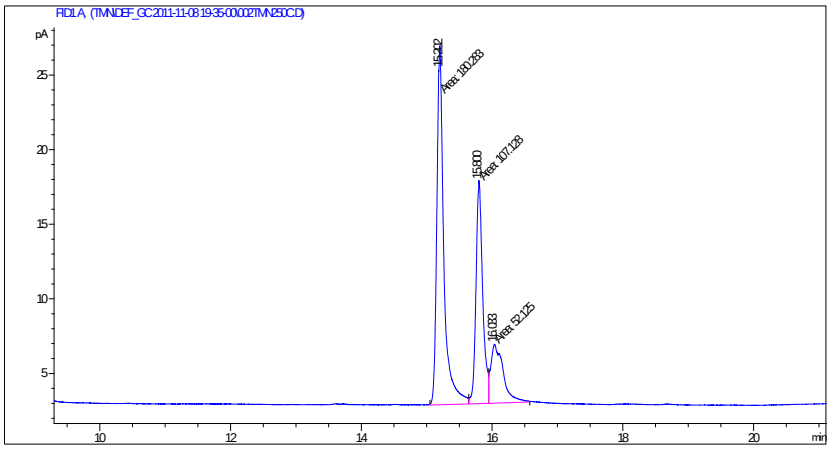

APPENDIX 2: SUPPORTING INFO FOR ANTI-MARKOVNIKOV HYDROAMINATION REACTIONS

General Methods:

Infrared (IR) spectra were obtained using a Jasco 260 Plus Fourier transform infrared spectrometer. Proton and carbon magnetic resonance spectra (^{1}H NMR and ^{13}C NMR) were recorded on a Bruker model DRX 400 (^{1}H NMR at 400 MHz and 600 MHz and ^{13}C NMR at 100 MHz) spectrometer with solvent resonance as the internal standard (^{1}H NMR: $CDCl_3$ at 7.24 ppm; ^{13}C NMR: $CDCl_3$ at 77.0 ppm). ^{1}H NMR data are reported as follows: chemical shift, multiplicity (s = singlet, d = doublet, t = triplet, dd = doublet of doublets, ddt = doublet of doublet of triplets, ddd = doublet of doublet of doublets, dddd = doublet of doublet of doublet of doublets m = multiplet, brs = broad singlet), coupling constants (Hz), and integration. Mass spectra were obtained using a Micromass (now Waters Corporation, 34 Maple Street, Milford, MA 01757) Quattro-II, Triple Quadrupole Mass Spectrometer, with a Z-spray nano-Electrospray source design, in combination with a NanoMate (Advion 19 Brown Road, Ithaca, NY 14850) chip based electrospray sample introduction system and nozzle. Thin layer chromatography (TLC) was performed on SiliaPlate 250 μm thick silica gel plates provided by Silicycle. Visualization was accomplished with short wave UV light (254 nm) or cerium ammonium molybdate solution followed by heating. Flash chromatography was performed using SiliaFlash P60 silica gel (40-63 μm) purchased from Silicycle. Tetrahydrofuran, diethyl ether, dichloromethane, and toluene were dried by passage through a column of neutral alumina under nitrogen prior to use. Irradiation of photochemical reactions was carried out using a 15W PAR38 blue LED floodlamp purchased from EagleLight (Carlsbad, CA). All other reagents were obtained from commercial sources and used without further purification unless otherwise noted. Cyclic voltammograms were obtained with a glassy carbon working electrode, $Ag/AgNO_3$ reference electrode, a platinum wire auxiliary and a BAS CV-27 potentiostat using 1 mM solutions of analyte in acetonitrile with 0.1 M tetrabutylammonium hexafluorophosphate as supporting electrolyte at a scan rate of 0.1V/s.

Oxidation potential is reported as the half-wave oxidation potential, taken as the midpoint between the onset of the sloping curve and the minima of the curve.

Preparation of Acridinium Photocatalyst (Catalyst A):

The photocatalyst used in this study, *N*-Me-9-mesityl acridinium tetrafluoroborate, was synthesized by the method of Fukuzumi et al.[1] Tetrafluoroboric acid (diethyl ether complex) was substituted for perchloric acid during the hydrolysis. The spectral data matched the values reported in the literature for the perchlorate and hexafluorophosphate salts. **^{1}H NMR** (600 MHz, $CDCl_3$) δ 8.60 (d, *J* = 9.0 Hz, 2H), 8.37 (t, *J* = 9.0 Hz, 2H), 7.84 (s, 4H), 7.23 (s, 2H), 4.81 (s, 3H), 2.46 (s, 3H), 1.68 (s, 6H).

Oxidation Potentials of Substrates vs. Ag/$AgNO_3$:

Substrate	$E_{p/2}$	Substrate	$E_{p/2}$
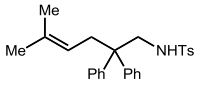	1.23 V	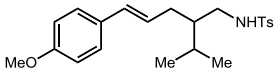	0.77 V
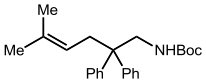	1.31 V	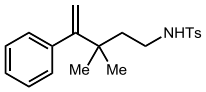	1.44 V
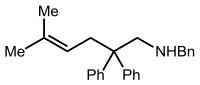	0.77 V	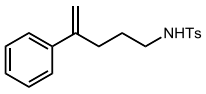	1.29 V
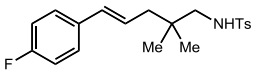	1.04 V	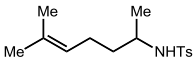	1.27 V
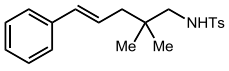	1.03 V	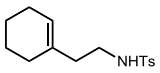	1.38 V
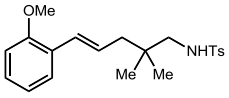	0.88 V	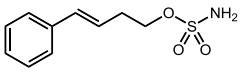	1.31 V
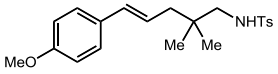	0.83 V	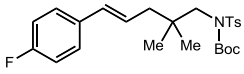	1.32 V
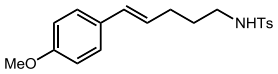	1.02 V		

Optimization Studies (equivalents of thiophenol):

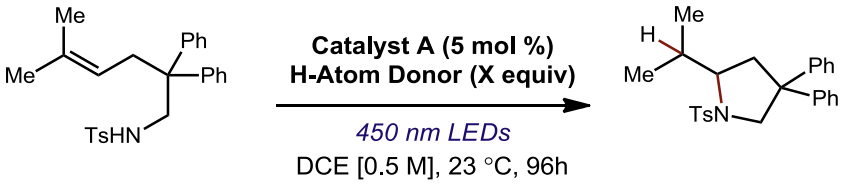

Entry	H-Atom Donor	Yield (by ^{1}H NMR)
1	0.2 equiv PhSH	70%
2	0.5 equiv PhSH	66%
3	0.75 equiv PhSH	54%
4	1.0 equiv PhSH	41%
5	2.0 equiv PhSH	19%

5-methyl-2,2-diphenylhex-4-en-1-amine (1a). Prepared according to a published procedure; spectral data were in agreement with literature values.[2]

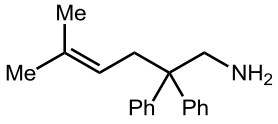

N-Benzyl-5-methyl-2,2-diphenylhex-4-en-1-amine (2a).

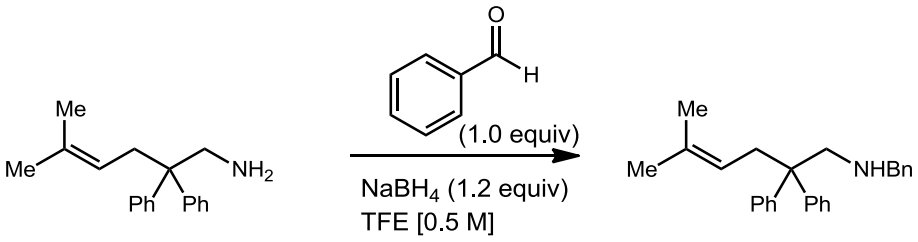

To a clean dry RBF was added a magnetic stir bar, 5-methyl-2,2-diphenylhex-4-en-1-amine[2] (1.0 equiv, prepared from literature procedure) and benzaldehyde (1.0 equiv), dissolved in TFE [0.5 M] under nitrogen. Reaction mixture was heated to 40 °C for ~1 h then sodium borohydride was added. Allowed to stir at 40 °C for ~3 h then heating was discontinued, reaction mixture was filtered through cotton then concentrated in vacuo. Title compound was purified by silica gel chromatography using 10%

EtOAc/Hexanes to give a colorless oil in 56% yield. **^{1}H NMR** (400 MHz, $CDCl_3$) δ = 7.33 - 7.18 (m, 5 H), 7.18 - 7.12 (m, 5 H), 4.76 - 4.69 (m, 1 H), 3.69 (s, 2 H), 3.15 (s, 2 H), 2.92 (d, *J* = 7.3 Hz, 2 H), 1.53 (s, 3 H), 1.46 (s, 3 H); **^{13}C NMR** (100 MHz, $CDCl_3$) δ = 147.3, 140.8, 134.0, 128.3, 127.9, 126.7, 125.9, 120.4, 55.7, 54.3, 50.9, 35.8, 26.0, 17.9; **IR** (thin film): 3065, 3058, 3025, 2966, 2912, 2852, 2359, 1943, 1868, 1800, 1749, 1716, 1698, 1683, 1670, 1540, 1495, 1444, 1375, 1361 cm^{-1}; **LRMS** (ESI): Calculated for $[M+H^+]$ = 356.52; found 356.19

***tert*-Butyl (5-methyl-2,2-diphenylhex-4-en-1-yl)carbamate (3a).**

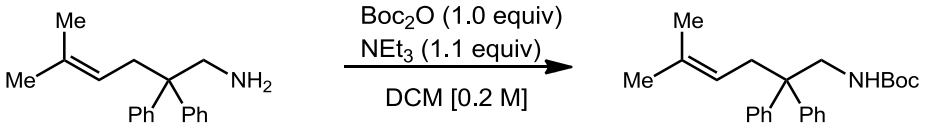

To a clean dry RBF was added a magnetic stir bar and 5-methyl-2,2-diphenylhex-4-en-1-amine[2] (1.0 equiv, prepared from literature procedure) and dissolved in DCM [0.2 M] under nitrogen. Reaction mixture was cooled to -78 °C and freshly distilled triethylamine added then boc anhydride added quickly. Allowed to stir at -78 °C for ~30 min then warmed to 0 °C. After 1 h, saturated ammonium chloride solution was added, the aqueous layer was extracted 3x with DCM, organic layers were combined and washed with brine solution, dried over Na_2SO_4 and concentrated in vacuo. Purified via silica gel chromatography with 10% EtOAc/Hexanes to give the desired product as a white solid in 68% yield. **^{1}H NMR** (400 MHz, $CDCl_3$) δ = 7.30 - 7.24 (m, 4 H), 7.22 - 7.11 (m, 6 H), 4.82 (t, *J* = 6.8 Hz, 1 H), 4.12 (br. s., 1 H), 3.80 (d, *J* = 5.9 Hz, 2 H), 2.77 (d, *J* = 7.1 Hz, 2 H), 1.56 (s, 3 H), 1.39 (s, 3 H), 1.35 (s, 9 H); **^{13}C NMR** (100 MHz, $CDCl_3$) δ = 155.8, 145.7, 134.8, 128.2, 126.3, 119.3, 50.8, 47.4, 35.9, 28.4, 27.4, 26.0, 17.7; **IR** (thin film): 3442, 2925, 1718, 1498, 1445, 1390, 1365, 1233 cm^{-1}; **LRMS** (ESI): Calculated for $[M+H^+]$ = 366.51; found 366.24

General Procedure A: Protection of primary amines with tosylchloride

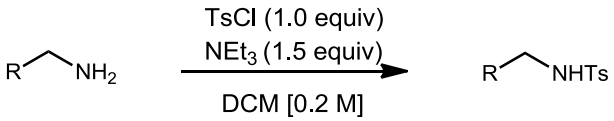

To a clean dry RBF was added a magnetic stir bar and the primary amine (1 equiv) under nitrogen at RT. Dissolved in DCM [0.2 M] and freshly distilled triethylamine (1.5 equiv) then tosylchloride added. Allowed to stir at room temperature overnight, then H_2O added and aqueous layer was extracted 3x with DCM, organic layers washed with brine solution, dried over Na_2SO_2 and concentrated in vacuo. Final substrates were purified by silica gel chromatography using the conditions listed.

4-Methyl-*N*-(5-methyl-2,2-diphenylhex-4-en-1-yl)benzenesulfonamide (4a).

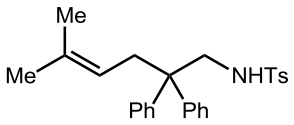

Prepared via general procedure A from 5-methyl-2,2-diphenylhex-4-en-1-amine[2] (prepared from reported literature procedure). Purified in 10% EtOAc/Hex to give a white solid in 51% yield. **^{1}H NMR** (400 MHz, $CDCl_3$) δ = 7.57 (d, *J* = 8.0 Hz, 2 H), 7.33 - 7.16 (m, 8H), 7.11 - 7.02 (m, 4 H), 4.77 - 4.69 (m, 1 H), 3.87 (t, *J* = 6.1 Hz, 1 H), 3.50 (d, *J* = 6.3 Hz, 2 H), 2.81 (d, *J* = 7.0 Hz, 2 H), 2.42 (s, 3 H), 1.58 - 1.53 (m, 3 H), 1.38 (s, 3 H); **^{13}C NMR** (100 MHz, $CDCl_3$) δ = 144.8, 143.4, 136.1, 135.5, 129.7, 128.1, 127.2, 126.6, 118.5, 50.2, 49.7, 35.6, 26.0, 21.5, 17.9; **IR** (thin film): 3276, 3058, 2919, 1671, 1598, 1496, 1445, 1406, 1330, 1266 cm^{-1}; **LRMS** (ESI): Calculated for $[M+H^+]$ = 420.58; found 420.26

General Procedure B: Preparation of N-tosylamines via amide coupling/reduction sequence

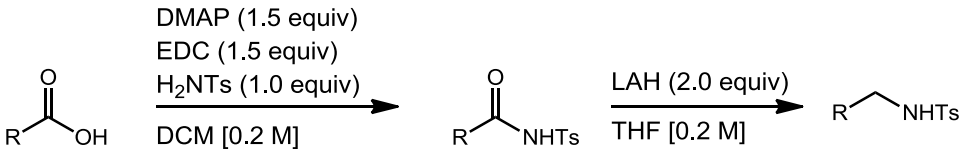

To a clean dry RBF was added a magnetic stir bar, the starting carboxylic acid (1.0 equiv), dimethylaminopyridine (1.5 equiv) and tosylamine (1.0 equiv) under nitrogen at ambient temperature. Dissolved in DCM [0.2 M] then EDC (1.5 equiv) was added. Reaction was stirred at RT overnight. Then 4N HCl was added, phases were separated then aqueous layer extracted three times with DCM. Organic portions were combined and washed with brine solution, dried over Na_2SO_4 and concentrated in vacuo. Reaction mixtures were then taken onto the reduction step as a crude reaction mixture.

To a clean dry RBF was added a magnetic stir bar, the starting amide (1.0 equiv) and lithium aluminium hydride (2.0 equiv) under nitrogen. Reaction was cooled to 0 °C and slowly dissolved in THF [0.2 M]. Reaction was monitored by TLC and upon complete consumption of starting material, mixture was cooled to 0 °C and a saturated solution of sodium potassium tartrate was added slowly. The reaction was allowed to warm to RT and stirred for ~20 min. Then phases were separated and aqueous layer extracted three times with diethyl ether, and organic layers combined and washed with brine solution. Dried over Na_2SO_4 and concentrated in vacuo. Final substrates were purified by silica gel chromatography using the conditions listed.

***(E)-N*-(2,2-Dimethyl-5-phenylpent-4-en-1-yl)-4-methylbenzenesulfonamide (5a).**

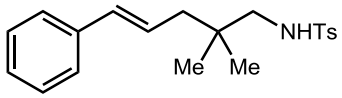

Prepared using general procedure B starting from (*E*)-2,2-dimethyl-5-phenylpent-4-enoic acid[3] (prepared from reported literature procedure). Title compound was purified in 10% EtOAc/Hexanes to give a white solid in 33% yield over two steps. The alkenol was found as a major by-product. **^{1}H NMR** (400 MHz, $CDCl_3$) δ = 7.75 (d, *J* = 8.3 Hz, 2 H), 7.30 - 7.16 (m, 7 H), 6.34 (d, *J* = 15.6 Hz, 1 H), 6.15 - 6.04 (m, 1 H), 5.02 (t, *J* = 6.8 Hz, 1 H), 2.70 (d, *J* = 7.0 Hz, 2 H), 2.37 (s, 3 H), 2.10 (d, *J* = 7.5 Hz, 2 H), 0.90 (s, 6 H); **^{13}C NMR** (100 MHz, $CDCl_3$) δ = 143.3, 137.5, 137.0, 133.0, 129.7, 128.5, 127.1, 126.1, 52.8, 42.9, 34.8, 25.1, 21.5; **IR** (thin film): 3275, 3025, 2956, 1653, 1597, 1576, 1493, 1457, 1410, 1368, 1321, 1265 cm^{-1}; **LRMS** (ESI): Calculated for $[M+H^+]$ =344.48; found 344.24

***(E)-N*-(5-(4-Fluorophenyl)-2,2-dimethylpent-4-en-1-yl)-4-methylbenzenesulfonamide(6a).**

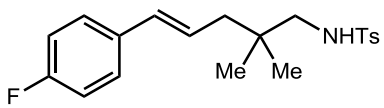

Prepared using general procedure B starting from (*E*)-5-(4-fluorophenyl)-2,2-dimethylpent-4-enoic acid[3] (prepared from reported literature procedure). Title compound was purified in 10% EtOAc/Hexanes to give a white solid in 33% yield over two steps. The alkenol was found as a major by-product. **^{1}H NMR**

(400 MHz, $CDCl_3$) δ = 7.72 - 7.68 (dd, 2 H), 7.28 - 7.22 (m, 4 H), 6.96 (dd, *J* = 8.7 Hz, 2 H), 6.30 (d, *J* = 16.1 Hz, 1 H), 6.06 - 5.96 (m, 1 H), 4.34 - 4.27 (m, 1 H), 2.71 (d, *J* = 7.0 Hz, 2 H), 2.39 (s, 3 H), 2.11 - 2.07 (m, 2 H), 0.89 (s, 6 H); **^{13}C NMR** (100 MHz, $CDCl_3$) δ = 163.2, 160.8, 143.3, 137.0, 133.7, 131.8, 129.7, 127.4, 125.8, 115.4, 115.2, 52.7, 42.8, 34.8, 25.1, 21.5; **IR** (thin film): 3284, 3031, 2961, 1652, 1600, 1508, 1471, 1417, 1325, 1266, 1227 cm^{-1}; **LRMS** (ESI): Calculated for $[M+H^+]$ = 362.47; found 362.04

***(E)-N*-(5-(4-Methoxyphenyl)-2,2-dimethylpent-4-en-1-yl)-4-methylbenzenesulfonamide (7a).**

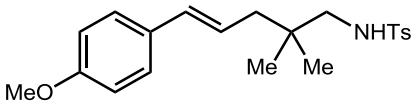

Prepared using general procedure B starting from *(E)*-5-(4-methoxyphenyl)-2,2-dimethylpent-4-enoic acid[3] (prepared from reported literature procedure). Title compound was purified in 10% EtOAc/Hexanes to give a white solid in 25% yield over two steps. The alkenol was found as a major by-product. **^{1}H NMR** (400 MHz, $CDCl_3$) δ = 7.77 (d, *J* = 8.3 Hz, 2 H), 7.32 - 7.27 (m, 2 H), 7.25 (d, *J* = 8.5 Hz, 2 H), 6.85 (d, *J* = 8.5 Hz, 2 H), 6.31 (d, *J* = 15.6 Hz, 1 H), 6.04 - 5.92 (m, 1 H), 4.91 (t, *J* = 6.8 Hz, 1 H), 3.82 (s, 3 H), 2.73 (d, *J* = 7.0 Hz, 2 H), 2.42 (s, 3 H), 2.11 (d, *J* = 7.5 Hz, 2 H), 0.92 (s, 6 H); **^{13}C NMR** (100 MHz, $CDCl_3$) δ = 158.9, 143.3, 136.9, 132.3, 130.3, 129.7, 127.2, 123.7, 113.9, 55.6, 52.8, 42.9, 34.8, 25.1, 21.5, 19.9; **IR** (thin film): 3283, 3030, 2960, 2836, 1770, 1651, 1607, 1576, 1509, 1465, 1419, 1368, 1325, 1247 cm^{-1}; **LRMS** (ESI): Calculated for $[M+H^+]$ = 374.51; found 374.22

***(E)-N*-(5-(2-Methoxyphenyl)-2,2-dimethylpent-4-en-1-yl)-4-methylbenzenesulfonamide (8a).**

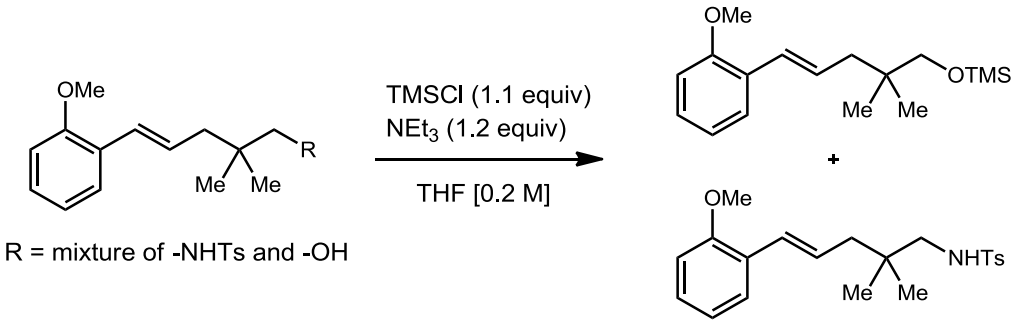

Prepared using general procedure B starting from (*E*)-5-(2-methoxyphenyl)-2,2-dimethylpent-4-enoic acid[3] (prepared from reported literature procedure). Desired product was obtained as an inseparable mixture with the alkenol by-product. To a clean dry RBF was added a magnetic star bar and the amine/alcohol mixture and dissolved in THF [0.2 M] under nitrogen. Then freshly distilled triethylamine (1.2 equiv) and TMSCl (1.1 equiv) added and allowed to stir overnight at room temperature. Then H_2O was added and layers separated. The aqueous layer was extracted 3x with Et_2O, organic layers combined and washed with brine solution, dried over Na_2SO_4 and concentrated in vacuo. Purified by silica gel chromatography with 25% EtOAc/Hexanes to give the title compound in 19% yield over three steps. **^{1}H NMR** (400 MHz, $CDCl_3$) δ = 7.72 (d, *J* = 8.1 Hz, 2 H), 7.30 (dd, *J* = 1.5, 7.6 Hz, 1 H), 7.23 - 7.14 (m, 3 H), 6.91 - 6.81 (m, 2 H), 6.65 (d, *J* = 15.9 Hz, 1 H), 6.13 - 6.03 (m, 1 H), 4.79 (t, *J* = 6.8 Hz, 1 H), 3.81 (s, 3 H), 2.70 (d, *J* = 6.8 Hz, 2 H), 2.38 - 2.35 (m, 3 H), 2.11 (d, *J* = 7.6 Hz, 2 H), 0.90 (s, 6 H); **^{13}C NMR** (100 MHz, $CDCl_3$) δ = 156.4, 143.3, 137.0, 129.7, 128.2, 127.7, 127.1, 126.8, 126.6, 126.5, 120.6, 110.9, 55.5, 52.9, 43.6, 34.8, 25.2, 21.5; **IR** (thin film): 3283, 2960, 1715, 1488, 1463, 1436, 1327, 1242 cm^{-1}; **LRMS** (ESI): Calculated for [$M+H^+$] = 374.51; found 374.16

***(E)-N*-(5-(4-Methoxyphenyl)pent-4-en-1-yl)-4-methylbenzenesulfonamide (9a).**

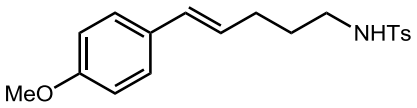

Prepared via general procedure A from (*E*)-5-(4-methoxyphenyl)pent-4-en-1-amine[4] (prepared from reported literature procedure). Purified by silica gel chromatography in 15% EtOAc/Hex to give a colorless oil in 25% yield. **^{1}H NMR (cis)** (400 MHz, $CDCl_3$) δ = 7.69 (d, *J* = 8.3 Hz, 2 H), 7.28 - 7.22 (m, 2 H), 7.12 (d, *J* = 8.5 Hz, 2 H), 6.87 - 6.81 (m, 2 H), 6.32 (d, *J* = 11.5 Hz, 1 H), 5.41 (td, *J* = 7.2, 11.6 Hz, 1 H), 4.66 (t, *J* = 6.1 Hz, 1 H), 3.78 (s, 3 H), 2.93 (qd, *J* = 6.7, 13.0 Hz, 2 H), 2.38 (s, *J* = 2.3 Hz, 3 H), 2.27 (dq, *J* = 1.5, 7.4 Hz, 2 H), 1.63 - 1.54 (m, 2 H) **^{1}H NMR (trans)** (400 MHz, $CDCl_3$) δ = 7.73 (d, *J* = 8.3 Hz, 2 H), 7.28 - 7.23 (m, 2 H), 7.19 (d, *J* = 8.8 Hz, 2 H), 6.81 - 6.76 (m, 2 H), 6.23 (d, *J* = 15.8 Hz, 1 H), 5.95 - 5.84 (m, 1 H), 4.77 (t, *J* = 6.1 Hz, 1 H), 3.77 (s, 3 H), 2.98 - 2.92 (m, 2 H), 2.38 (s, 3 H), 2.19 -

2.11 (m, 2 H), 1.67 - 1.57 (m, 2 H); **^{13}C NMR (mix of isomers)** (100 MHz, $CDCl_3$) δ = 143.4, 137.0, 130.3, 130.0, 129.7, 129.4, 127.9, 127.0, 113.9, 113.7, 55.3, 42.9, 42.6, 29.8, 29.3, 25.6, 21.5; **IR** (thin film): 3280, 3005, 2933, 1607, 1575, 1509, 1456, 1323 cm^{-1}; **LRMS** (ESI): Calculated for [$M+H^+$] = 346.46; found 346.11

***(E)-N*-(2-Isopropyl-5-(4-methoxyphenyl)pent-4-en-1-yl)-4-methylbenzenesulfonamide (10a).**

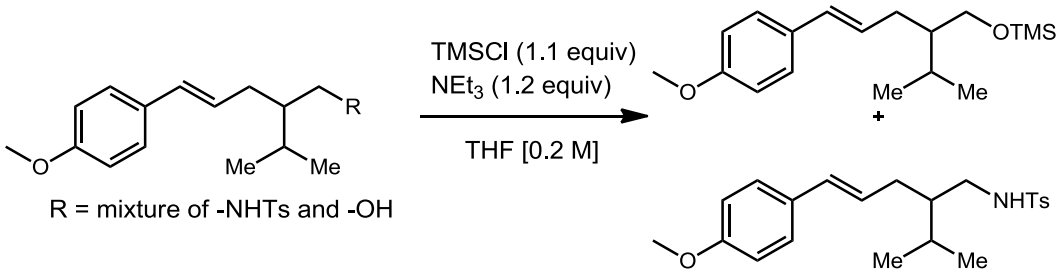

Prepared using general procedure B starting from (*E*)-2-isopropyl-5-(4-methoxyphenyl)pent-4-enoic acid[3] (prepared from reported literature procedure). Desired product was obtained as an inseparable mixture with the alkenol. To a clean dry RBF was added a magnetic star bar and the amine/alcohol mixture and dissolved in THF [0.2 M] under nitrogen. Then freshly distilled triethylamine (1.2 equiv) and TMSCl (1.1 equiv) added and allowed to stir overnight at room temperature. Then H_2O was added and layers separated. The aqueous layer was extracted 3x with Et_2O, organic layers combined and washed with brine solution, dried over Na_2SO_4 and concentrated in vacuo. Purified by silica gel chromatography with 20% EtOAc/Hexanes to give the title compound in 18% yield over three steps. **^{1}H NMR** (400 MHz, $CDCl_3$) δ = 7.67 (d, *J* = 8.3 Hz, 2 H), 7.20 (t, *J* = 8.6 Hz, 4 H), 6.82 (d, *J* = 8.6 Hz, 2 H), 6.24 (d, *J* = 16.4 Hz, 1 H), 5.87 (td, *J* = 7.6, 15.5 Hz, 1 H), 4.27 (br. s., 1 H), 3.79 (s, 3 H), 2.98 - 2.81 (m, 2 H), 2.37 (s, 3 H), 2.28 - 2.19 (m, 1 H), 2.07 - 1.98 (m, 1 H), 1.73 (dd, *J* = 6.5, 12.1 Hz, 1 H), 1.48 - 1.37 (m, 1 H), 0.86 (d, *J* = 3.7 Hz, 3 H), 0.84 (d, *J* = 3.7 Hz, 3 H); **^{13}C NMR** (100 MHz, $CDCl_3$) δ = 158.8, 143.2, 136.9, 131.1, 130.3, 129.7, 127.1, 126.4, 113.9, 55.3, 44.4, 44.0, 32.3, 28.2, 21.5, 19.6, 19.2; **IR** (thin film): 3648, 3566, 3283, 3030, 2958, 2933, 2873, 2737, 1918, 1770, 1716, 1652, 1607, 1576, 1510, 1464, 1325, 1440, 1419, 1388, 1368, 1325, 1304, 1289 cm^{-1}; **LRMS** (ESI): Calculated for [$M+H^+$] = 387.54; found 388.13

***N*-(3,3-Dimethyl-4-phenylpent-4-en-1-yl)-4-methylbenzenesulfonamide (11a).**

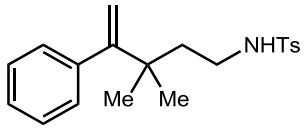

Prepared using general procedure B starting from 3,3-dimethyl-4-phenylpent-4-enoic acid[3] (prepared from reported literature procedure). Title compound was purified by silica gel chromatography in 25% EtOAc/Hexanes to give a white solid in 45% yield over two steps. **^{1}H NMR** (400 MHz, $CDCl_3$) δ = 7.73 (d, *J* = 8.3 Hz, 2 H), 7.31 - 7.26 (m, 2 H), 7.22 - 7.17 (m, 3 H), 6.96 (dd, *J* = 3.0, 6.5 Hz, 2 H), 5.06 (d, *J* = 1.5 Hz, 1 H), 4.82 (d, *J* = 1.3 Hz, 1 H), 4.67 (t, *J* = 6.0 Hz, 1 H), 3.01 - 2.93 (m, 2 H), 2.41 (s, 3 H), 1.53 - 1.47 (m, 2 H), 1.02 (s, 6 H); **^{13}C NMR** (100 MHz, $CDCl_3$) δ = 156.7, 143.4, 142.6, 137.0, 129.7, 128.7, 127.6, 126.9, 114.2, 40.2, 40.0, 38.4, 27.8, 21.6; **IR** (thin film): 3279, 3080 3053, 2967, 2871, 1810, 1717, 1625, 1598, 1573, 1493, 1439, 1362, 1325, 1267, 1230 cm^{-1}; **LRMS** (ESI): Calculated for [$M+H^+$] = 344.48; found 344.18

4-Methyl-*N*-(4-phenylpent-4-en-1-yl)benzenesulfonamide (12a).

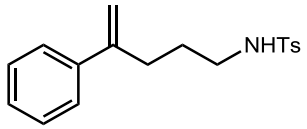

Prepared using general procedure B starting from 4-phenylpent-4-enoic acid[3] (prepared from reported literature procedure). Title compound was purified by silica gel chromatography in 20% EtOAc/Hexanes to give a white solid in 56% yield over two steps. Spectral data were in agreement with literature values.[5] **^{1}H NMR** (400 MHz, $CDCl_3$) δ = 7.73 - 7.64 (m, 2 H), 7.31 - 7.15 (m, 5 H), 5.22 - 5.15 (m, 1 H), 4.95 (t, *J* = 6.0 Hz, 1 H), 4.93 (s, 1 H), 2.87 (q, *J* = 6.8 Hz, 2 H), 2.50 - 2.39 (m, 2 H), 2.34 (s, 3 H), 1.59 - 1.47 (m, 2 H)

4-Methyl-*N*-(6-methylhept-5-en-2-yl)benzenesulfonamide (13a).

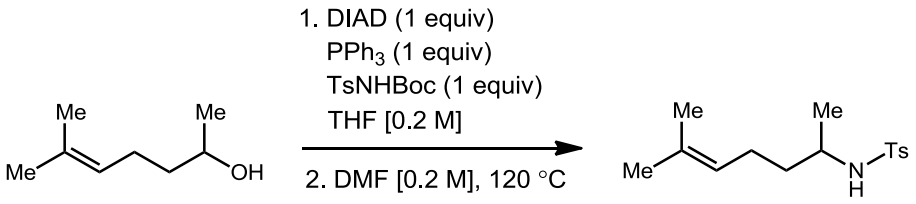

To a clean dry RBF was added a magnetic stir bar, tosylboc amine and triphenylphosphine and solids were dissolved in THF [0.2 M] under nitrogen. Then 6-methylhept-5-en-2-ol (commercially available) was added and reaction was cooled to 0 °C and then DIAD was added and allowed to warm to RT overnight. Then Et_2O was added and aqueous layer was extracted 3x with Et_2O, organic layers were combined and washed with brine solution, dried over Na_2SO_4 and concentrated in vacuo. Purified by silica gel chromatography in 10% EtOAc/Hexanes.

To a clean dry vial was added a magnetic stir bar, tosylboc amine and dissolved in DMF [0.2 M] under nitrogen. The vial was sealed and heated to 120 °C for 48 hours. Heating was discontinued and H_2O was added and then the aqueous layer was extracted 3x with Et_2O, organic layers were combined and washed with brine solution, dried over Na_2SO_4 and concentrated in vacuo. Purified by silica gel chromatography in 10% EtOAc/Hexanes to give the title compound as a colorless oil in 27% yield over 2 steps. Spectral data were in agreement with literature values.[6] **^{1}H NMR** (400 MHz, $CDCl_3$) δ = 7.77 - 7.72 (m, 2 H), 7.25 (d, *J* = 8.3 Hz, 2 H), 4.91 - 4.85 (m, 2 H), 3.31 - 3.19 (m, 1 H), 2.38 (s, 3 H), 1.96 - 1.74 (m, 2 H), 1.59 (s, 3 H), 1.47 (s, 3 H), 1.38 - 1.30 (m, 2 H), 1.00 (d, *J* = 6.5 Hz, 3 H)

***N*-(2-(Cyclohex-1-en-1-yl)ethyl)-4-methylbenzenesulfonamide (14a).**

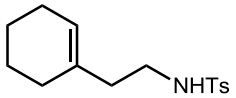

Prepared via general procedure A from commercially available 2-(cyclohex-1-en-1-yl)ethanamine. Purified in 10% EtOAc/Hex to give a white solid in 27% yield. Spectral data were in agreement with literature values.[6] **^{1}H NMR** (400 MHz, $CDCl_3$) δ = 7.71 (d, *J* = 8.3 Hz, 2 H), 7.30 - 7.24 (m, 2 H), 5.33

(br. s., 1 H), 4.58 (t, *J* = 5.6 Hz, 1 H), 2.95 (q, *J* = 6.5 Hz, 2 H), 2.39 (s, 3 H), 2.01 (t, *J* = 6.7 Hz, 2 H), 1.94 - 1.86 (m, 2 H), 1.68 (br. s., 2 H), 1.54 - 1.41 (m, 4 H)

***(E)*-4-Phenylbut-3-en-1-yl sulfamate (15a).**

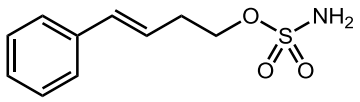

Prepared according to a published procedure;[7] spectral data were in agreement with literature values.[8] **^{1}H NMR** (400 MHz, $CDCl_3$) δ = 7.42 - 7.28 (m, 4 H), 7.27 - 7.20 (m, 1 H), 6.50 (d, *J* = 15.9 Hz, 1 H), 6.16 (td, *J* = 7.0, 15.8 Hz, 1 H), 5.15 (s, 2 H), 4.28 (t, *J* = 6.6 Hz, 2 H), 2.63 (q, *J* = 6.6 Hz, 2 H)

***(E)*-*tert*-Butyl (5-(4-fluorophenyl)-2,2-dimethylpent-4-en-1-yl)(tosyl)carbamate (16).**

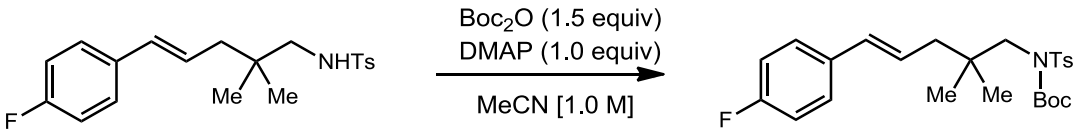

To a clean dry RBF was added a magnetic stir bar and (*E*)-N-(5-(4-fluorophenyl)-2,2-dimethylpent-4-en-1-yl)-4-methylbenzenesulfonamide (1.0 equiv) and DMAP (1.0 equiv) and dissolved in MeCN [1.0 M] under nitrogen. Then boc anhydride was added quickly. Allowed to stir at RT overnight. Water was added, and the aqueous layer extracted 3x with EtOAc, organic layers combined and washed with 1M HCl solution then brine solution, dried over Na_2SO_4 and concentrated in vacuo. Purified via silica gel chromatography with 10% EtOAc/Hexanes to give the desired product as a colorless oil in 64% yield. **^{1}H NMR** (400 MHz, $CDCl_3$) δ = 7.73 - 7.68 (m, 2 H), 7.34 - 7.25 (m, 4 H), 6.99 - 6.93 (m, 2 H), 6.40 - 6.32 (m, 1 H), 6.25 - 6.15 (m, 1 H), 3.87 (s, 2 H), 2.41 (s, 3 H), 2.22 (d, *J* = 7.3 Hz, 2 H), 1.22 (s, 9 H), 1.02 (s, 6 H); **^{13}C NMR** (100 MHz, $CDCl_3$) δ = 151.6, 144.0, 137.9, 133.9, 131.5, 129.3, 127.6, 126.6, 115.4, 115.2, 84.1, 56.2, 44.2, 36.7, 27.6, 25.3, 21.6; **IR** (thin film): 3674, 3648, 3028, 3617, 3566, 3437, 3039, 2979, 2932, 2825, 2392, 1808, 1730, 1652, 1636, 1599, 1588, 1508, 1472, 1434, 1395, 1354, 1276, 1225 cm^{-1}; **LRMS** (ESI): Calculated for [M+Na] = 484.59; found 484.15

General Procedure C: Anti-Markovnikov hydroamination reactions

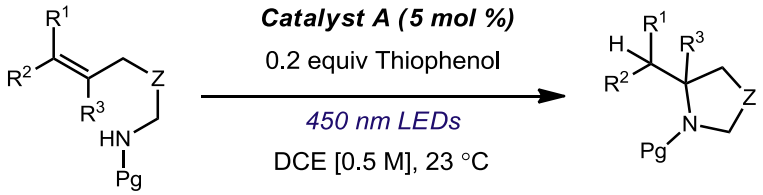

To a clean flame-dried 1 dram vial was added a magnetic stir bar, N-Me-mesityl acridinium catalyst (5.0 mol %) and protected amine substrate (100 mg). Reaction vessel was purged with nitrogen then dichloroethane (sparged for 15 min, [0.5M]) was added, then thiophenol (0.2 equiv). Reaction was sealed with Teflon tape then irradiated with blue LED lamp at room temperature until reaction was complete monitoring by TLC. Reactions were quenched with a solution of TEMPO (~5 mg) in dichloromethane (0.2 mL) and concentrated in vacuo. The final products were purified by silica gel chromatography using the conditions listed.

2-Isopropyl-4,4-diphenylpyrrolidine (1b).

Prepared using general procedure **C** on a 100 mg scale with 0.2 equiv thiophenol, and dichloroethane [0.5 M]. Irradiated for 96h then purified in 3% EtOAc/Hexanes to give a white solid in 65% isolated yield. ^{1}H NMR was very complex, to confirm identity isolated material was submitted to deprotection with TFA. To a clean dry RBF was added a magnetic stir bar and *tert*-butyl 2-isopropyl-4,4-diphenylpyrrolidine-1-carboxylate and dissolved in DCM:TFA (1:1) under nitrogen at room temperature. After 3 h, saturated sodium bicarbonate added, aqueous layer extracted 3x with DCM, organic layers combined and washed with brine solution, dried over na2SO4 and concentrated in vacuo. Purified by silica gel chromatography in 50% EtOAc/Hexanes to give the desired 2-isopropyl-4,4-diphenylpyrrolidine. Spectral data were in agreement with literature values.[9] **^{1}H NMR** (400 MHz, $CDCl_3$) δ = 7.33 - 7.24 (m, 4 H), 7.23 - 7.11 (m, 6 H), 3.73 (dd, *J* = 1.7, 11.2 Hz, 1 H), 3.33 (d, *J* = 11.2 Hz, 1 H), 2.90 - 2.82 (m, 1 H), 2.70 (ddd, *J* = 1.7,

6.5, 12.6 Hz, 1 H), 2.06 (dd, *J* = 9.8, 12.7 Hz, 1 H), 1.71 - 1.60 (m, 1 H), 1.28 (d, *J* = 16.1 Hz, 1 H), 0.94 (d, *J* = 6.6 Hz, 3 H), 0.88 (d, *J* = 6.6 Hz, 3 H)

2-Benzyl-4,4-dimethyl-1-tosylpyrrolidine (5b).

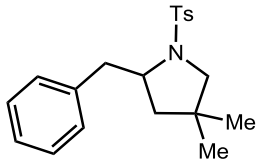

Prepared using general procedure **C** on a 100 mg scale with 0.2 equiv thiophenol, and dichloroethane [0.5 M]. Irradiated for 24h then purified in 2% EtOAc/Hexanes to give a white solid in 82% isolated yield (average of two trials). **^{1}H NMR** (400 MHz, $CDCl_3$) δ = 7.79 (d, *J* = 8.0 Hz, 2 H), 7.33 (d, *J* = 8.3 Hz, 2 H), 7.29 (d, *J* = 7.3 Hz, 2 H), 7.25 - 7.19 (m, 3 H), 3.84 - 3.75 (m, 1 H), 3.58 (dd, *J* = 3.5, 13.1 Hz, 1 H), 3.13 (s, 2 H), 2.78 (dd, *J* = 9.8, 13.1 Hz, 1 H), 2.43 (s, 3 H), 1.54 - 1.42 (m, 2 H), 0.99 (s, 3 H), 0.46 (s, 3 H); **^{13}C NMR** (100 MHz, $CDCl_3$) δ = 143.3, 138.5, 135.3, 129.6, 129.5, 128.4, 127.6, 126.4, 61.7, 61.6, 45.7, 42.9, 37.2, 26.5, 25.8, 21.6; **IR** (thin film): 3061, 3027, 2960, 1288, 2873, 1599, 1540, 1494, 1245, 1454, 1390, 1347, 1303, 1224 cm^{-1}; **LRMS** (ESI): Calculated for $[M+H^+]$ = 344.48; found 344.12

2-(4-Fluorobenzyl)-4,4-dimethyl-1-tosylpyrrolidine (6b).

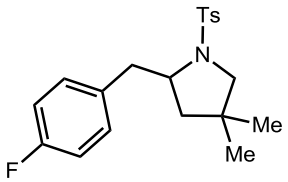

Prepared using general procedure **C** on a 100 mg scale with 0.2 equiv thiophenol, and dichloroethane [0.5 M]. Irradiated for 24h then purified in 2% EtOAc/Hexanes to give a white solid in 89% isolated yield (average of two trials). **^{1}H NMR** (400 MHz, $CDCl_3$) δ = 7.75 (d, *J* = 8.3 Hz, 2 H), 7.30 (d, *J* = 8.5 Hz, 2 H), 7.20 - 7.13 (m, 2 H), 7.00 - 6.92 (m, 2 H), 3.78 - 3.69 (m, 1 H), 3.43 (dd, *J* = 3.4, 13.4 Hz, 1 H), 3.07 (q, *J* = 10.5 Hz, 2 H), 2.80 (dd, *J* = 9.5, 13.3 Hz, 1 H), 2.40 (s, 3 H), 1.43 (d, *J* = 8.0 Hz, 2 H), 0.94 (s, 3 H), 0.41 (s, 3 H); **^{13}C NMR** (100 MHz, $CDCl_3$) δ = 143.4, 135.2, 134.0, 131.1, 131.0, 129.6, 127.5, 115.3,

115.1, 61.6, 61.4, 45.5, 41.7, 37.2, 26.4, 25.8, 21.6; **IR** (thin film): 2962, 1597, 1508, 1465, 1330, 1302, 1218 cm^{-1}; **LRMS** (ESI): Calculated for $[M+H^+]$ = 362.47; found 362.10

2-(4-Methoxybenzyl)-4,4-dimethyl-1-tosylpyrrolidine (7b).

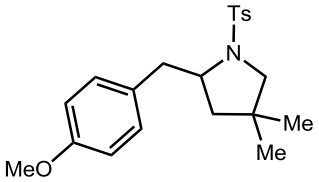

Prepared using general procedure **C** on a 100 mg scale with 0.2 equiv thiophenol, and dichloroethane [0.5 M]. Irradiated for 30h then purified in 5% EtOAc/Hexanes to give a colorless oil in 88% isolated yield (average of two trials). **^{1}H NMR** (400 MHz, $CDCl_3$) δ = 7.76 (d, *J* = 8.0 Hz, 2 H), 7.30 (d, *J* = 8.3 Hz, 2 H), 7.12 (d, *J* = 8.5 Hz, 2 H), 6.81 (d, *J* = 8.5 Hz, 2 H), 3.87 - 3.76 (m, 3 H), 3.75 - 3.68 (m, 1 H), 3.45 (dd, *J* = 3.4, 13.2 Hz, 1 H), 3.13 - 3.04 (m, 2 H), 2.72 (dd, *J* = 9.7, 13.2 Hz, 1 H), 2.40 (s, 3 H), 1.52 - 1.42 (m, 2 H), 1.02 - 0.92 (m, 3 H), 0.42 (s, 3 H); **^{13}C NMR** (100 MHz, $CDCl_3$) δ = 158.2, 143.3, 135.3, 130.5, 129.6, 127.5, 113.8, 61.7, 55.2, 45.7, 41.8, 37.2, 26.5, 25.8, 21.4; **IR** (thin film): 2958, 2872, 1683, 1612, 1582, 1511, 1464, 1390, 1346, 1302, 1247 cm^{-1}; **LRMS** (ESI): Calculated for $[M+H^+]$ = 374.51; found 374.15

2-(2-Methoxybenzyl)-4,4-dimethyl-1-tosylpyrrolidine (8b).

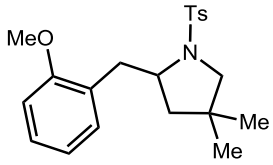

Prepared using general procedure **C** on a 100 mg scale with 0.2 equiv thiophenol, and dichloroethane [0.5 M]. Irradiated for 40h then purified in 5% EtOAc/Hexanes to give a white solid in 69% isolated yield (average of two trials). **^{1}H NMR** (400 MHz, $CDCl_3$) δ = 7.80 (d, *J* = 8.3 Hz, 2 H), 7.30 (d, *J* = 8.1 Hz, 2 H), 7.20 - 7.12 (m, 2 H), 6.89 - 6.80 (m, 2 H), 3.85 (s, 3 H), 3.83 - 3.76 (m, 1 H), 3.72 (dd, *J* = 3.9, 12.7 Hz, 1 H), 3.22 - 3.16 (m, 1 H), 3.11 - 3.06 (m, 1 H), 2.68 (dd, *J* = 10.3, 12.7 Hz, 1 H), 2.40 (s, 3 H), 1.48 (dd, *J* = 8.2, 12.8 Hz, 1 H), 1.34 (dd, *J* = 7.1, 12.7 Hz, 1 H), 0.99 (s, 3 H), 0.42 (s, 3 H); **^{13}C NMR** (100

MHz, $CDCl_3$) δ = 157.7, 143.1, 135.0, 131.2, 129.4, 127.7, 127.7, 127.2, 120.5, 110.4, 62.1, 60.0, 55.3, 45.8, 37.5, 37.0, 26.7, 26.1, 21.6; **IR** (thin film) 2958, 2872, 1732, 1716, 1698, 1683, 1670, 1652, 1599, 1540, 1507, 1493, 1438, 1396, 1304, 1244 cm^{-1}; **LRMS** (ESI): Calculated for $[M+H^+]$ = 374.51; found 374.16

2-(4-Methoxybenzyl)-1-tosylpyrrolidine (9b).

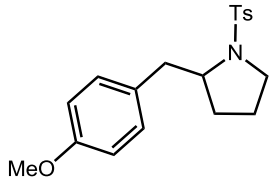

Prepared using general procedure C on a 100 mg scale with 0.2 equiv thiophenol, and dichloroethane [0.5 M]. Irradiated for 48h then purified in 5% EtOAc/Hexanes to give a colorless oil in 79% isolated yield (average of two trials). **^{1}H NMR** (400 MHz, $CDCl_3$) δ = 7.73 (d, *J* = 8.3 Hz, 2 H), 7.28 (d, *J* = 8.0 Hz, 2 H), 7.16 - 7.10 (m, 2 H), 6.81 (d, *J* = 8.5 Hz, 2 H), 3.77 (s, 3 H), 3.74 (d, *J* = 3.8 Hz, 1 H), 3.39 - 3.31 (m, 1 H), 3.16 - 3.05 (m, 2 H), 2.69 (dd, *J* = 9.4, 13.4 Hz, 1 H), 2.40 (s, 3 H), 1.65 - 1.54 (m, 2 H), 1.47 - 1.34 (m, 2 H); **^{13}C NMR** (100 MHz, $CDCl_3$) δ = 158.3, 143.3, 134.8, 130.6, 130.5, 129.7, 127.5, 113.8, 61.7, 55.3, 49.3, 41.7, 29.8, 23.8, 21.5; **IR** (thin film): 2953, 2835, 1612, 1597, 1583, 1511, 1399, 1339, 1247 cm^{-1}; **LRMS** (ESI): Calculated for $[M+H^+]$ = 346.46; found 346.12

4-Isopropyl-2-(4-methoxybenzyl)-1-tosylpyrrolidine (10b).

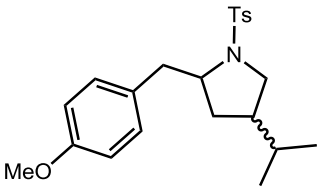

Prepared using general procedure C on a 100 mg scale with 0.2 equiv thiophenol, and dichloroethane [0.5 M]. Irradiated for 39h then purified in 8% EtOAc/Hexanes to give a white solid in 88% isolated yield (average of two trials) in a 1.6:1 dr. **^{1}H NMR (major)** (400 MHz, $CDCl_3$) δ = 7.73 (d, *J* = 3.2, 8.1 Hz, 2 H), 7.33 - 7.27 (m, 2 H), 7.16 - 7.09 (m, 2 H), 6.85 - 6.78 (m, 2 H), 3.80 (d, *J* = 2.7 Hz, 1 H), 3.76 (s, 3

H), 3.71 - 3.63 (m, 1 H), 3.62 - 3.51 (m, 1 H), 3.30 (dd, *J* = 3.4, 13.4 Hz, 1 H), 2.85 - 2.71 (m, 1 H), 2.41 (s, 3 H), 1.79 (td, *J* = 6.4, 12.8 Hz, 1 H), 1.27 - 1.10 (m, 2 H), 0.70 (t, *J* = 7.3 Hz, 6 H) **^{1}H NMR (minor)** (400 MHz, $CDCl_3$) δ = 7.74 - 7.70 (m, 2 H), 7.30 (d, *J* = 5.1 Hz, 2 H), 7.14 (d, *J* = 6.6 Hz, 2 H), 6.84 - 6.81 (m, 2 H), 3.76 (s, 3 H), 3.72 - 3.63 (m, 1 H), 3.62 - 3.51 (m, 1 H), 3.11 (dd, *J* = 3.4, 13.4 Hz, 1 H), 2.69 - 2.54 (m, 1 H), 2.40 (s, 3 H), 1.73 - 1.65 (m, 1 H), 1.21-1.14 (m, 1H), 1.03 - 0.90 (m, 2 H), 0.78 (d, *J* = 6.6 Hz, 3 H), 0.74 (d, *J* = 6.6 Hz, 3 H) **^{13}C NMR (mix of isomers** (100 MHz, $CDCl_3$) δ = 158.2, 143.3, 135.3, 134.4, 130.7, 130.6, 130.5, 130.3, 129.7, 129.6, 127.5, 127.4, 113.9, 113.8, 62.5, 62.1, 55.3, 55.2, 53.4, 45.4, 44.1, 42.1, 41.9, 36.8, 34.0, 31.8, 31.2, 21.6, 21.5, 21.4, 21.3, 21.1, 21.0 **IR** (thin film): 3060, 3030, 2959, 2871, 2835, 1749, 1716, 1683, 1652, 1613, 1597, 1558, 1540, 1494, 1456, 1386, 1302, 1247 cm^{-1}; **LRMS** (ESI): Calculated for $[M+H^+]$ = 388.54; found 388.13

4,4-Dimethyl-3-phenyl-1-tosylpiperidine (11b).

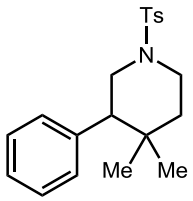

Prepared using general procedure C on a 100 mg scale with 0.2 equiv thiophenol, and dichloroethane [0.5 M]. Irradiated for 48h then purified in 4% EtOAc/Hexanes to give a white solid in 79% isolated yield (average of two trials). **^{1}H NMR** (400 MHz, $CDCl_3$) δ = 7.65 (d, *J* = 8.3 Hz, 2 H), 7.33 (d, *J* = 8.0 Hz, 2 H), 7.27 - 7.19 (m, 3 H), 7.01 (d, *J* = 7.8 Hz, 2 H), 3.67 (d, *J* = 12.0 Hz, 1 H), 3.61 (d, *J* = 10.5 Hz, 1 H), 2.80 - 2.67 (m, 2 H), 2.58 (dt, *J* = 2.8, 12.3 Hz, 1 H), 2.44 (s, 3 H), 1.71 (dt, *J* = 4.5, 13.1 Hz, 1 H), 1.52 - 1.45 (m, 1 H), 0.79 (s, 3 H), 0.67 (s, 3 H); **^{13}C NMR** (100 MHz, $CDCl_3$) δ = 143.5, 139.5, 133.6, 129.7, 129.1, 127.9, 126.9, 51.6, 46.4, 42.8, 39.7, 32.5, 29.9, 21.6, 19.3; **IR** (thin film): 2948, 1597, 1455, 1389, 1340, 1223 cm^{-1}; **LRMS** (ESI): Calculated for $[M+H^+]$ = 344.48; found 344.06

3-Phenyl-1-tosylpiperidine (12b).

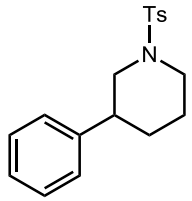

Prepared using general procedure C on a 100 mg scale with 0.2 equiv thiophenol, and dichloroethane [0.5 M]. Irradiated for 96h then purified in 5% EtOAc/Hexanes to give a colorless oil in 60% isolated yield (average of two trials). Spectral data were in agreement with literature values.[10] **^{1}H NMR** (400 MHz, $CDCl_3$) δ = 7.62 (d, *J* = 8.3 Hz, 2 H), 7.33 - 7.26 (m, 4 H), 7.25 - 7.19 (m, 1 H), 7.16 (d, *J* = 7.0 Hz, 2 H), 3.91 - 3.81 (m, 2 H), 2.92 - 2.81 (m, 1 H), 2.42 (s, 3 H), 2.32 - 2.17 (m, 2 H), 1.93 (d, *J* = 13.3 Hz, 1 H), 1.87 - 1.70 (m, 2 H), 1.48 - 1.35 (m, 1 H)

2-Isopropyl-4,4-diphenyl-1-tosylpyrrolidine (4b).

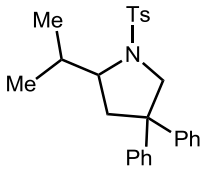

Prepared using general procedure **C** on a 100 mg scale with 0.2 equiv thiophenol, and dichloroethane [0.5 M]. Irradiated for 96h then purified in 3% EtOAc/Hexanes to give a colorless oil in 70% isolated yield (average of two trials). **^{1}H NMR** (400 MHz, $CDCl_3$) δ = 7.42 (d, *J* = 8.3 Hz, 2 H), 7.22 (d, *J* = 7.8 Hz, 2 H), 7.15 (d, *J* = 7.3 Hz, 1 H), 7.10 (dd, *J* = 1.9, 10.2 Hz, 4 H), 7.06 - 7.00 (m, 5 H), 4.47 (dd, *J* = 1.8, 11.0 Hz, 1 H), 3.91 (d, *J* = 11.0 Hz, 1 H), 3.74 (s, 1 H), 2.75 - 2.67 (m, 1 H), 2.57 - 2.47 (m, 1 H), 2.33 (s, 3 H), 2.23 (dd, *J* = 10.4, 12.9 Hz, 1 H), 0.88 (d, *J* = 7.0 Hz, 3 H), 0.74 (d, *J* = 6.8 Hz, 3 H); **^{13}C NMR** (100 MHz, $CDCl_3$) δ = 146.3, 144.3, 142.5, 136.7, 129.3, 128.6, 128.5, 126.7, 126.7, 126.5, 126.5, 126.1, 64.5, 59.9, 52.4, 36.9, 30.0, 21.5, 19.4, 14.7; **IR** (thin film): 3058, 2962, 1598, 1495, 1447, 1389, 1336, 1304, 1265, 1235 cm^{-1}; **LRMS** (ESI): Calculated for $[M+H^+]$ = 420.58; found 420.15

(2*S*, 5*S*)-2-Isopropyl-5-methyl-1-tosylpyrrolidine (13b).

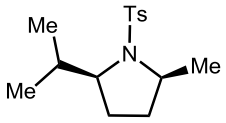

Prepared using general procedure C on a 100 mg scale with 0.2 equiv thiophenol, and dichloroethane [0.5 M]. Irradiated for 96h then purified in 3% EtOAc/Hexanes to give a colorless oil in 56% isolated yield (average of two trials) in 3:1 dr. Spectral data were in agreement with literature values.[11] **^{1}H NMR (major)** (400 MHz, $CDCl_3$) δ = 7.71 - 7.67 (m, 2 H), 7.27 (d, *J* = 7.8 Hz, 2 H), 3.71 - 3.63 (m, 1 H), 3.43 - 3.36 (m, 1 H), 2.40 (s, 3 H), 2.11 - 2.00 (m, 1 H), 1.62 (td, *J* = 6.1, 12.1 Hz, 1 H), 1.56 - 1.45 (m, 1 H), 1.44 - 1.34 (m, 1 H), 1.31 - 1.23 (m, 4 H), 0.96 (d, *J* = 7.0 Hz, 3 H), 0.90 (d, *J* = 6.8 Hz, 3 H)

1-Tosyloctahydro-1H-indole (14b).

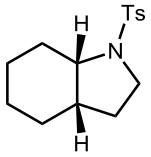

Prepared using general procedure C on a 100 mg scale with 0.2 equiv thiophenol, and dichloroethane [0.5 M]. Irradiated for 96h then purified in 5% EtOAc/Hexanes to give a colorless oil in 72% isolated yield (average of two trials) in 12:1 dr. Spectral data were in agreement with literature values.[12] **^{1}H NMR major** (400 MHz, $CDCl_3$) δ = 7.72 - 7.65 (m, 2 H), 7.29 - 7.22 (m, 2 H), 3.56 - 3.42 (m, 2 H), 3.19 - 3.09 (m, 1 H), 2.42 - 2.35 (m, 3 H), 1.91 - 1.69 (m, 3 H), 1.63 - 1.46 (m, 5 H), 1.39 - 1.23 (m, 2 H), 1.23 - 1.11 (m, 1 H)

4-Benzyl-1,2,3-oxathiazinane 2,2-dioxide (15b).

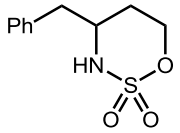

Prepared using general procedure C on a 100 mg scale with 0.2 equiv thiophenol, and dichloroethane [0.5 M]. Irradiated for 96h then purified in 20 % EtOAc/Hexanes to give an off-white solid 54% isolated yield

(average of two trials). **^{1}H NMR** (400 MHz, $CDCl_3$) δ = 7.36 - 7.29 (m, 2 H), 7.28 - 7.24 (m, 1 H), 7.18 - 7.14 (m, 2 H), 4.66 (dt, *J* = 2.8, 12.0 Hz, 1 H), 4.48 (ddd, *J* = 1.8, 4.9, 11.6 Hz, 1 H), 4.10 (d, *J* = 10.0 Hz, 1 H), 4.03 - 3.90 (m, 1 H), 2.92 (dd, *J* = 5.9, 13.7 Hz, 1 H), 2.77 (dd, *J* = 7.3, 13.7 Hz, 1 H), 1.81 - 1.62 (m, 2 H) **^{13}C NMR** (100 MHz, $CDCl_3$) δ = 135.4, 129.4, 129.0, 127.4, 72.0, 56.5, 41.1, 29.0 3 **IR** (thin film): 3259, 3086, 3062, 2965, 2925, 2855, 1698, 1683, 1670, 1636, 1602, 1558, 1523, 1497, 1455, 1420, 1360, 1267, 1239, 1220 cm^{-1}; **LRMS** (ESI): Calculated for $[M+H^+]$ = 227.28; found 227.99

Procedure for Control Reactions:

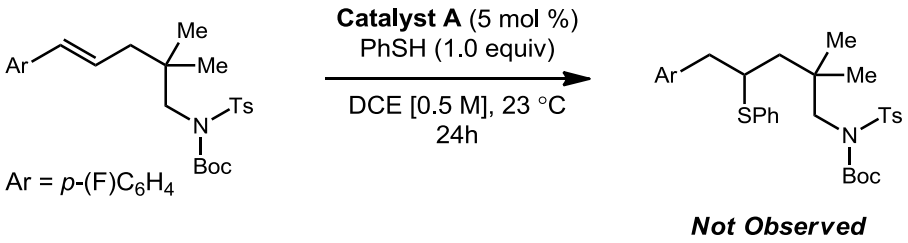

Figure 4.7: To a clean flame-dried 1 dram vial was added a magnetic stir bar, N-Me-mesityl acridinium catalyst (5.0 mol %), *(E)-tert*-butyl (5-(4-fluorophenyl)-2,2-dimethylpent-4-en-1-yl)(tosyl)carbamate (100 mg). Reaction vessel was purged with nitrogen then dichloroethane (sparged for 15 min, [0.5M]) was added then thiophenol was added (1.0 equiv). Reaction was sealed with teflon tape then irradiated with blue LED lamp at room temperature for 24 hours. Reaction was quenched with a solution of TEMPO (~5 mg) in dichloromethane (0.2 mL) and concentrated in vacuo. Only unchanged starting material was observed by ^{1}H NMR.

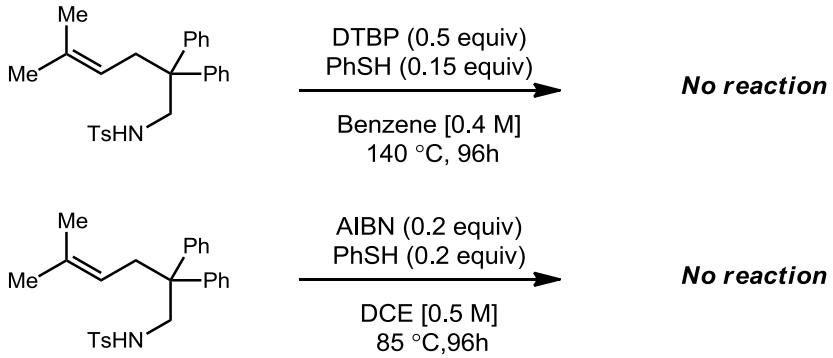

Figure 4.6, Conditions A: To a clean dry 20 mL scintillation vial was added a magnetic stir bar, 4-Methyl-*N*-(5-methyl-2,2-diphenylhex-4-en-1-yl)benzenesulfonamide (1 equiv) , benzene [0.4 M], di-*tert*-butyl peroxide (0.5 equiv) and thiophenol (0.15 equiv) under nitrogen. Reaction vessel was sealed and heated to 140 °C for 96 hours, then heating was discontinued and reaction mixture was quenched with TEMPO solution, and concentrated in vacuo. Only unchanged starting material was observed by ^{1}H NMR.

Figure 4.6, Conditions B: To a clean dry 20 mL scintillation vial was added a magnetic stir bar, 4-Methyl-*N*-(5-methyl-2,2-diphenylhex-4-en-1-yl)benzenesulfonamide (1 equiv) , dichloroethane [0.5 M], azobisisobutyronitrile (0.2 equiv) and thiophenol (0.2 equiv) under nitrogen. Reaction vessel was sealed and heated to 85°C for 96 hours, then heating was discontinued and reaction mixture was quenched with TEMPO solution, and concentrated in vacuo. Only unchanged starting material was observed by ^{1}H NMR.

1,1,1-trifluoro-N-(2-phenylcyclohexyl)methanesulfonamide (17b).

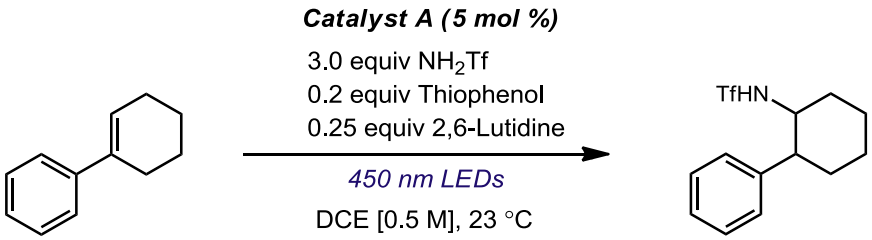

To a clean dry 2 dram vial was added a magnetic stirbar, catalyst A (5 mol %), commercially available 1-phenylcyclohexene **17a** (1 equiv) and $TfNH_2$ (3.0 equiv). Vial with solids were then brought into the glovebox where 2,6-lutidine (0.25 equiv) and dichloroethane [0.5 M] were added. Reaction vessel was sealed and taken out of the glovebox, then thiophenol (0.2 equiv, freshly sparged) was added. Irradiated for 96h then purified in 5% EtOAc/Hexanes to give a white solid in 55% isolated yield (average of two trials) in 2.6:1 dr. **^{1}H NMR (inseparable mixture of diastereomers)** (400 MHz, $CDCl_3$) δ = 7.36 - 7.29 (m, 4 H), 7.26 (s, 2 H), 7.19 - 7.13 (m, 4 H), 4.67 (br s, 1 H), 4.33 (br s, 1H), 3.95-3.89 (m, 1 H), 3.01 -

2.93 (m, 1 H), 2.43 - 2.31 (m, 1 H), 2.09-1.38 (m, 17 H); **^{13}C NMR** (100 MHz, $CDCl_3$) δ = 141.5, 141.3, 128.8, 128.6, 127.7, 127.6, 127.4, 127.2, 60.0, 57.5, 51.1, 45.8, 35.5, 34.3, 32.6, 25.6, 25.2, 25.0, 19.8; **^{19}F NMR** (376 MHz, $CDCl_3$) δ = -77.68 (minor), -77.79 (major); **IR** (thin film): 3313, 2928, 1421, 1357, 1224 cm^{-1}; **LRMS** (ESI): Calculated for [M+H_2O] = 325.35; found 325.20

1,1,1-trifluoro-N-(2-methylcyclopentyl)methanesulfonamide (18b).

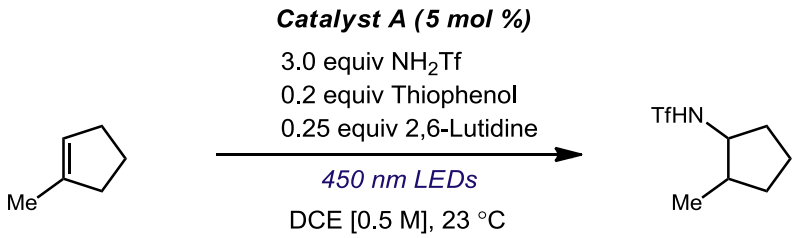

To a clean dry 2 dram vial was added a magnetic stirbar, catalyst A (5 mol %), commercially available 1-methylcyclopentene **18a** (1 equiv) and $TfNH_2$ (3.0 equiv). Vial with solids were then brought into the glovebox where 2,6-lutidine (0.25 equiv) and dichloroethane [0.5 M] were added. Reaction vessel was sealed and taken out of the glovebox, then thiophenol (0.2 equiv, freshly sparged) was added. Irradiated for 96h then purified in 5% EtOAc/Hexanes to give a colorless oil in 51% isolated yield (average of two trials, obtained an average 63% yield by NMR using hexamethyldisiloxane as an internal standard) in 1.5:1 dr. **^{1}H NMR (inseparable mixture of diastereomers)** (400 MHz, $CDCl_3$) δ = 5.04 (br s, 2 H), 3.86 (m, 2 H), 3.34 (quint, *J* = 7.3 Hz, 2 H), 2.20 – 1.43 (m, 8 H), 1.31 – 1.14 (m, 4 H), 1.05 (d, *J* = 6.4 Hz, 3 H), 0.97 (d, *J* = 6.8 Hz, 3 H); **^{13}C NMR** (100 MHz, $CDCl_3$) δ = 121.2, 118.1, 63.4, 60.3, 41.5, 40.5, 37.1, 33.2, 32.4, 31.6, 31.0, 22.9, 21.3, 21.0, 17.2, 14.3; **^{19}F NMR** (376 MHz, $CDCl_3$) δ = -77.54 (major), -77.71 (minor); **IR** (thin film): 3647, 3565, 3303, 2965, 2878, 1622, 1444, 1375, 1269, 1232 cm^{-1}; **LRMS** (ESI): Calculated for [M+H+K] = 271.34; found 271.16

Preparation of Alkene Substrates in Figure 4.14:

(*E*)-1-methoxy-2-(prop-1-en-1-yl)benzene (20a): Prepared according to a published procedure[13]; spectral data were in agreement with literature values.[14]

(*E*)-1-methoxy-3-(prop-1-en-1-yl)benzene (21a): Prepared according to a published procedure; spectral data were in agreement with literature values.[15]

(*E*)-1-methyl-2-(prop-1-en-1-yl)benzene (23a): Prepared according to a published procedure; spectral data were in agreement with literature values.[16]

(*E*)-1-methyl-3-(prop-1-en-1-yl)benzene (24a): Prepared according to a published procedure; spectral data were in agreement with literature values.[17]

(*E*)-1-methyl-4-(prop-1-en-1-yl)benzene (25a): Prepared according to a published procedure; spectral data were in agreement with literature values.[17]

(*E*)-1-fluoro-4-(prop-1-en-1-yl)benzene (26a): Prepared according to a published procedure; spectral data were in agreement with literature values.[18]

(*E*)-1-chloro-4-(prop-1-en-1-yl)benzene (27a): Prepared according to a published procedure; spectral data were in agreement with literature values.[19]

(*E*)-1-(tert-butyl)-4-(prop-1-en-1-yl)benzene (28a): Prepared according to a published procedure; spectral data were in agreement with literature values.[20]

(*E*)-1,3,5-trimethyl-2-(prop-1-en-1-yl)benzene (29a): Prepared according to a published procedure; spectral data were in agreement with literature values.[21]

(*E*)-2-(prop-1-en-1-yl)naphthalene (30a): Prepared according to a published procedure; spectral data were in agreement with literature values.[22]

(*E*)-2-(prop-1-en-1-yl)thiophene (32a): Prepared according to a published procedure; spectral data were in agreement with literature values.[23]

(*E*)-methyl-6-(4-methoxyphenyl)hex-5-enoate (33a): Prepared according to a published procedure; spectral data were in agreement with literature values.[24]

(*E*)-2-(3-(4-methoxyphenyl)allyl)isoindoline-1,3-dione (34a):Prepared according to a published procedure; spectral data were in agreement with literature values.[25]

(*E*)-3-(4-methoxyphenyl)prop-2-en-1-ol (35a): Prepared according to a published procedure; spectral data were in agreement with literature values.[26]

General Procedure X: Anti-Markovnikov Intermolecular Hydroamination Reactions

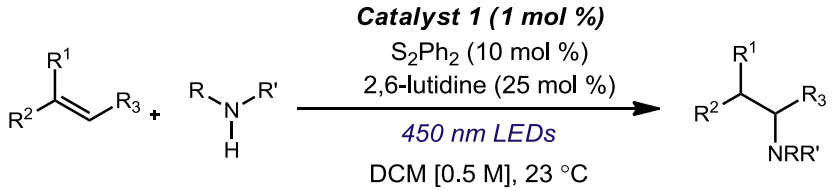

To a clean flame-dried 2 dram vial was added a magnetic stir bar, N-Me-mesityl acridinium catalyst (1.0 mol %), diphenyldisulfide (10 mol %) and amine (1.5 equiv). Reaction vessel was purged with nitrogen then 2,6-lutidine (25 mol %), starting alkene (1.0 equiv) and dichloromethane (sparged for 15 min, [0.5 M]) was added. Reaction was sealed with Teflon tape then irradiated with a blue LED lamp at room temperature. Reactions were quenched with a solution of TEMPO (~5 mg) in dichloromethane (0.2 mL) and concentrated in vacuo. The final products were purified by silica gel chromatography using the conditions listed.

1,1,1-trifluoro-N-(1-(2-methoxyphenyl)propan-2-yl)methanesulfonamide (20b).

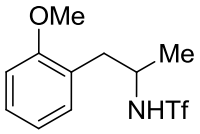

Prepared using general procedure **X** on a 100 mg scale with catalyst 1 (1 mol %), trifluoromethanesulfonamide (1.5 equiv), diphenyldisulfide (10 mol %), 2,6-lutidine (25 mol %) and dichloromethane [0.5 M]. Irradiated for 48h then purified in 10% EtOAc/Hexanes to give a yellow oil in 55% isolated yield (average of two trials). **^{1}H NMR** (400 MHz, $CDCl_3$) δ = 1.50 - 1.69 (m, 3 H), 3.10 - 3.26 (m, 2 H), 4.09 - 4.20 (m, 3 H), 4.21 - 4.33 (m, 1 H), 5.38 - 6.31 (m, 1 H), 7.21 - 7.30 (m, 2 H), 7.43 (d, *J*=7.34 Hz, 1 H), 7.59 (t, *J*=7.83 Hz, 1 H); **^{13}C NMR** (100 MHz, $CDCl_3$) δ = 22.71, 37.97, 53.56,

55.40, 110.74, 121.17, 125.04, 128.74, 131.57, 157.15; **IR** (thin film): 3750, 3648, 3807, 3071, 2939, 2840, 1683, 1603, 1558, 1495, 1457, 1372; **LRMS** (ESI): Calculated for [M+H_2O]= 315.3; found 315.24.

1,1,1-trifluoro-N-(1-(3-methoxyphenyl)propan-2-yl)methanesulfonamide (21b).

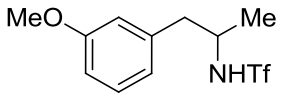

Prepared using general procedure **X** on a 100 mg scale with catalyst 1 (1 mol %), trifluoromethanesulfonamide (1.5 equiv), diphenyldisulfide (10 mol %), 2,6-lutidine (25 mol %) and dichloromethane [0.5 M]. Irradiated for 48h then purified in 10% EtOAc/Hexanes to give a yellow oil in 69% isolated yield (average of two trials). **^{1}H NMR** (400 MHz, $CDCl_3$) δ = 1.22 (d, *J*=6.60 Hz, 3 H), 2.78 (t, *J*=5.62 Hz, 2 H), 3.78 (s, 3 H), 3.84 - 3.93 (m, 1 H), 4.47 - 4.53 (m, 1 H), 6.82 - 6.87 (m, 2 H), 7.04 - 7.09 (m, 2 H), 7.23 (s, 1 H); **^{13}C NMR** (100 MHz, $CDCl_3$) δ =21.39, 43.79, 52.97, 55.24, 112.50, 115.43, 121.94, 129.81, 137.47, 159.87; **IR** (thin film): 3627, 3305, 2439, 2839, 2416, 1715, 1602, 1436, 1368; **LRMS** (ESI): Calculated for [M+H^+] = 298.29; found 298.14.

1,1,1-trifluoro-N-(1-(4-methoxyphenyl)propan-2-yl)methanesulfonamide (22b).

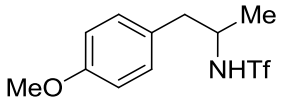

Prepared using general procedure **X** on a 100 mg scale with catalyst 1 (1 mol %), trifluoromethanesulfonamide (1.5 equiv), diphenyldisulfide (10 mol %), 2,6-lutidine (25 mol %) and dichloromethane [0.5 M]. Irradiated for 48h then purified in 10 % EtOAc/Hexanes to give a yellow oil in 73% isolated yield (average of two trials). **^{1}H NMR** (400 MHz, $CDCl_3$) 1.12 - 1.29 (m, 3 H), 2.68 - 2.90 (m, 2 H), 3.66 - 3.82 (m, 3 H), 3.84 - 3.98 (m, 1 H), 4.80 (d, *J*=7.34 Hz, 1 H), 6.63 - 6.77 (m, 3 H), 6.77 - 6.85 (m, 1 H), 7.18 - 7.27 (m, 1 H); **^{13}C NMR** (100 MHz, $CDCl_3$) δ = 21.20, 42.85, 53.19, 55.29, 114.19, 121. 15, 127.98, 130.61, 158; **IR** (thin film): 3902, 3870, 3838, 3819, 3801, 3734, 3716, 3307, 3034,

2839, 1770, 1698, 1671, 1585, 1436, 1373, 1361, 1231; **LRMS** (ESI): Calculated for [M+H_2O] = 315.3; found 315.18.

1,1,1-trifluoro-N-(1-(o-tolyl)propan-2-yl)methanesulfonamide (23b).

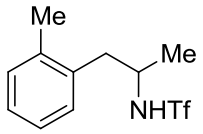

Prepared using general procedure **X** on a 100 mg scale with catalyst 1 (1 mol %), trifluoromethanesulfonamide (1.5 equiv), diphenyldisulfide (10 mol %), 2,6-lutidine (25 mol %) and dichloromethane [0.5 M]. Irradiated for 72h then purified in 10% EtOAc/Hexanes to give a yellow oil in 76% isolated yield (average of two trials). **^{1}H NMR** (400 MHz, $CDCl_3$) δ = 7.19 - 7.12 (m, 3 H), 7.07 (d, *J* = 5.4 Hz, 1 H), 3.94 (br. s., 1 H), 2.97 (d, *J* = 7.1 Hz, 1 H), 2.80 (br. s., 1 H), 2.33 (s, 3 H), 1.27 (d, *J* = 6.4 Hz, 3 H); **^{13}C NMR** (100 MHz, $CDCl_3$) δ = 136.6, 135.0, 131.0, 130.9, 127.4, 126.3, 52.7, 42.5, 22.5, 19.7; **IR** (thin film): 3307, 3067, 3019, 2980, 2876, 2351, 1918, 1844, 1792, 1732, 1698, 1670, 1635, 1576, 1540, 1434, 1372, 1230; **LRMS** (ESI): Calculated for [M+H^+] = 282.29; found 282.23.

1,1,1-trifluoro-N-(1-(m-tolyl)propan-2-yl)methanesulfonamide (24b).

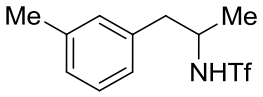

Prepared using general procedure **X** on a 100 mg scale with catalyst 1 (1 mol %), trifluoromethanesulfonamide (1.5 equiv), diphenyldisulfide (10 mol %), 2,6-lutidine (25 mol %) and dichloromethane [0.5 M]. Irradiated for 72h then purified in 5% EtOAc/Hexanes to give a yellow oil in 73% isolated yield (average of two trials). **^{1}H NMR** (400 MHz, $CDCl_3$) δ = 7.23 - 7.18 (m, 1 H), 7.07 (d, *J* = 7.6 Hz, 3 H), 6.98 - 6.92 (m, 6 H), 4.57 - 4.42 (m, 1 H), 3.99 - 3.87 (m, 1 H), 2.88 - 2.74 (m, 2 H), 2.33 (s, 3 H), 1.24 (d, *J* = 6.8 Hz, 3 H); **^{13}C NMR** (100 MHz, $CDCl_3$) δ =; **IR** (thin film): 3565, 3307,

2979, 2928, 1867, 1828, 1792, 1744, 1732, 1683, 1670, 1609, 1590, 1546, 1507, 1457, 1372, 1288, 1230; **LRMS** (ESI): Calculated for $[M+H^+]$ = 282.29; found 282.22.

1,1,1-trifluoro-N-(1-(p-tolyl)propan-2-yl)methanesulfonamide (25b).

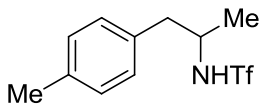

Prepared using general procedure **X** on a 100 mg scale with catalyst 1 (1 mol %), trifluoromethanesulfonamide (1.5 equiv), diphenyldisulfide (10 mol %), 2,6-lutidine (25 mol %) and dichloromethane [0.5 M]. Irradiated for 72h then purified in 10% EtOAc/Hexanes to give a yellow solid in 84% isolated yield (average of two trials). **^{1}H NMR** (400 MHz, $CDCl_3$) δ = 7.15 - 7.11 (m, 2 H), 7.06 - 7.01 (m, 2 H), 4.48 (br. s., 1 H), 3.92 (d, *J* = 5.1 Hz, 1 H), 2.87 - 2.75 (m, 2 H), 2.32 (s, 3 H), 1.23 (d, *J* = 6.6 Hz, 3 H); **^{13}C NMR** (100 MHz, $CDCl_3$) δ = 136.9, 132.8, 129.6, 129.5, 53.1, 43.5, 21.5, 21.1; **IR** (thin film): 3749, 3734, 3710, 3689, 3628, 3566, 3299, 2980, 2740, 1683, 1636, 1576, 1558, 1457, 1427, 1326, 1227; **LRMS** (ESI): Calculated for $[M+H^+]$ = 282.29 ; found 282.22.

1,1,1-trifluoro-N-(1-phenylpropan-2-yl)methanesulfonamide (19b).

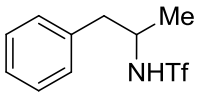

Prepared using general procedure **X** on a 100 mg scale with catalyst 1 (1 mol %), trifluoromethanesulfonamide (1.5 equiv), diphenyldisulfide (10 mol %), 2,6-lutidine (25 mol %) and dichloromethane [0.5 M]. Irradiated for 72h then purified in 10 % EtOAc/Hexanes to give a yellow oil in 72% isolated yield (average of two trials). **^{1}H NMR** (400 MHz, $CDCl_3$) δ = 7.35 - 7.28 (m, 2 H), 7.28 - 7.24 (m, 1 H), 7.15 (d, *J* = 6.8 Hz, 2 H), 4.54 (br. s., 1 H), 3.94 (br. s., 1 H), 2.90 - 2.77 (m, 2 H), 1.24 (d, *J* = 6.6 Hz, 3 H); **^{13}C NMR** (100 MHz, $CDCl_3$) δ= 21.67, 44.12, 53.34, 127.23, 128.82, 129.74, 136.25;

IR (thin film): 3642, 3565, 3308, 3066, 3031, 2980, 2935, 1951, 1886, 1810, 1603, 1586, 1432, 1230; **LRMS** (ESI): Calculated for [M+H_2O] = 285.27; found 285.16.

1,1,1-trifluoro-N-(1-(4-fluorophenyl)propan-2-yl)methanesulfonamide (26b).

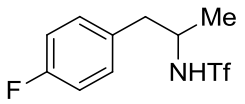

Prepared using general procedure **X** on a 100 mg scale with catalyst 1 (1 mol %), trifluoromethanesulfonamide (1.5 equiv), diphenyldisulfide (10 mol %), 2,6-lutidine (25 mol %) and dichloromethane [0.5 M]. Irradiated for 96h then purified in 5% EtOAc/Hexanes to give a yellow solid in 77% isolated yield (average of two trials). **^{1}H NMR** (400 MHz, $CDCl_3$) δ = 7.15 - 7.09 (m, 2 H), 7.05 - 6.96 (m, 2 H), 4.56 - 4.41 (m, 1 H), 3.90 (d, *J* = 5.9 Hz, 1 H), 2.82 (dd, *J* = 6.5, 7.7 Hz, 2 H), 1.24 (d, *J* = 6.6 Hz, 3 H); **^{13}C NMR** (100 MHz, $CDCl_3$) δ = 163.3, 160.8, 132.0, 131.0, 115.6, 53.4, 43.0, 21.3; **IR** (thin film): 3648, 3566, 3310, 2981, 2936, 1771, 1732, 1716, 1698, 1652, 1558, 1456, 1367, 1227; **LRMS** (ESI): Calculated for [M+H_2O] = 303.26; found 303.13.

N-(1-(4-chlorophenyl)propan-2-yl)-1,1,1-trifluoromethanesulfonamide (27b).

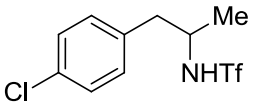

Prepared using general procedure **X** on a 100 mg scale with catalyst 1 (1 mol %), trifluoromethanesulfonamide (1.5 equiv), diphenyldisulfide (10 mol %), 2,6-lutidine (25 mol %) and dichloromethane [0.5 M]. Irradiated for 72h then purified in 10% EtOAc/Hexanes to give a white solid in 75% isolated yield (average of two trials). **^{1}H NMR** (400 MHz, $CDCl_3$) δ = 7.33 - 7.26 (m, 2 H), 7.15 - 7.05 (m, 2 H), 4.59 (d, *J* = 9.0 Hz, 1 H), 3.96 - 3.84 (m, 1 H), 2.91 - 2.73 (m, 2 H), 1.24 (d, *J* = 6.8 Hz, 3 H); **^{13}C NMR** (100 MHz, $CDCl_3$) δ = 134.5, 133.3, 130.9, 128.9, 53.1, 43.3, 21.3; **IR** (thin film): 3307,

2981, 1761, 1683, 1652, 1540, 1494, 1457, 1428, 1360, 1320, 1226; **LRMS** (ESI): Calculated for [M+ H_2O] = 319.71; found 319.11.

N-(1-(4-(tert-butyl)phenyl)propan-2-yl)-1,1,1-trifluoromethanesulfonamide (28b).

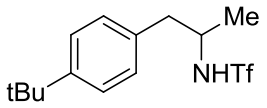

Prepared using general procedure **X** on a 100 mg scale with catalyst 1 (1 mol %), trifluoromethanesulfonamide (1.5 equiv), diphenyldisulfide (10 mol %), 2,6-lutidine (25 mol %) and dichloromethane [0.5 M]. Irradiated for 72h then purified in 10% EtOAc/Hexanes to give a yellow oil in 43% isolated yield (average of two trials). **^{1}H NMR** (400 MHz, $CDCl_3$) δ = 7.34 (d, *J* = 8.1 Hz, 2 H), 7.08 (d, *J* = 8.1 Hz, 2 H), 4.03 - 3.85 (m, 1 H), 2.83 (br. s., 2 H), 1.30 (s, 9 H), 1.25 (d, *J* = 6.6 Hz, 3 H); **^{13}C NMR** (100 MHz, $CDCl_3$) δ = 150.2, 132.8, 129.5, 125.7, 53.1, 43.5, 34.5, 31.4, 21.8; **IR** (thin film): 3567, 3307, 3094, 3026, 2964, 2864, 2871, 1792, 1771, 1698, 1652, 1635, 1558, 1513, 1457, 1432, 1372, 1269; **LRMS** (ESI): Calculated for [M+ H_2O] = 341.37; found 341.21.

1,1,1-trifluoro-N-(1-mesitylpropan-2-yl)methanesulfonamide (29b).

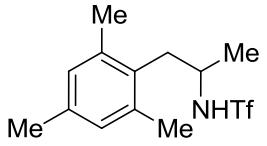

Prepared using general procedure **X** on a 100 mg scale with catalyst 1 (1 mol %), trifluoromethanesulfonamide (1.5 equiv), diphenyldisulfide (10 mol %), 2,6-lutidine (25 mol %) and dichloromethane [0.5 M]. Irradiated for 72h then purified in 10% EtOAc/Hexanes to give an orange oil in 64% isolated yield (average of two trials. **^{1}H NMR** (400 MHz, $CDCl_3$) δ = 6.85 (s, 2 H), 3.93 (br. s., 1 H), 2.98 (br. s., 1 H), 2.81 (br. s., 1 H), 2.29 (s, 6 H), 2.24 (s, 3 H), 1.24 (d, *J* = 5.6 Hz, 3 H); **^{13}C NMR** (100 MHz, $CDCl_3$) δ = 136.8, 136.3, 130.8, 129.5, 52.5, 38.0, 22.1, 20.9, 20.6; **IR** (thin film): 3302, 2932,

2737, 1732, 1716, 1683, 1614, 1577, 1558, 1434, 1371, 1283, 1230; **LRMS** (ESI): Calculated for [M+H$^+$] = 310.35; found 310.18.

1,1,1-trifluoro-N-(1-(naphthalen-2-yl)propan-2-yl)methanesulfonamide (30b).

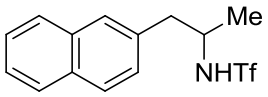

Prepared using general procedure **X** on a 100 mg scale with catalyst 1 (1 mol %), trifluoromethanesulfonamide (1.5 equiv), diphenyldisulfide (10 mol %), 2,6-lutidine (25 mol %) and dichloromethane [0.5 M]. Irradiated for 72h then purified in 10% EtOAc/Hexanes to give a yellow oil in 63% isolated yield (average of two trials). **^{1}H NMR** (400 MHz, $CDCl_3$) δ = 7.86 - 7.76 (m, 18 H), 7.61 (s, 1 H), 7.52 - 7.43 (m, 12 H), 7.29 (dd, *J* = 1.6, 8.4 Hz, 6 H), 4.86 (d, *J* = 7.6 Hz, 1 H), 4.08 - 3.95 (m, 1 H), 3.09 - 3.01 (m, 1 H), 2.98 - 2.88 (m, 1 H), 1.26 (d, *J* = 6.6 Hz, 3 H); **^{13}C NMR** (100 MHz, $CDCl_3$) δ = 133.5, 133.5, 132.5, 128.5, 128.3, 127.7, 127.6, 127.6, 126.4, 126.0, 121.2, 53.1, 44.0, 21.3; **IR** (thin film): 3820, 3801, 3734, 3648, 3305, 3056, 3022, 2980, 2876, 2360, 1771, 1683, 1633, 1558, 1508, 1433, 1371, 1286, 1271; **LRMS** (ESI): Calculated for [M+H$^+$] = 318.33; found 318.17.

N-(1-(benzo[d][1,3]dioxol-5-yl)propan-2-yl)-1,1,1-trifluoromethanesulfonamide (31b).

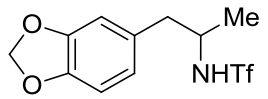

Prepared using general procedure **X** on a 100 mg scale with catalyst 1 (1 mol %), trifluoromethanesulfonamide (1.5 equiv), diphenyldisulfide (10 mol %), 2,6-lutidine (25 mol %) and dichloromethane [0.5 M]. Irradiated for 96h then purified in 10% EtOAc/Hexanes to give a white solid in 63% isolated yield (average of two trials). **^{1}H NMR** (400 MHz, $CDCl_3$) δ = 6.75 (d, *J* = 7.8 Hz, 1 H), 6.66 - 6.56 (m, 2 H), 5.92 (s, 2 H), 4.84 (d, *J* = 8.1 Hz, 1 H), 3.91 - 3.77 (m, 1 H), 2.84 - 2.66 (m, 2 H), 1.23 (d, *J* = 6.6 Hz, 3 H); **^{13}C NMR** (100 MHz, $CDCl_3$) δ = 147.9, 146.7, 129.6, 122.7, 121.1, 117.9, 110.0, 108.5, 101.1, 53.2, 43.5, 21.2; **IR** (thin film): 3853, 3828, 3819, 3801, 3749, 3734, 3648, 3305, 3076, 2981,

2901, 2613, 1854, 1749, 1716, 1671, 1491, 1443, 1368; **LRMS** (ESI): Calculated for [M+H$^+$] = 312.28; found 312.12.

1,1,1-trifluoro-N-(1-(thiophen-2-yl)propan-2-yl)methanesulfonamide (32b).

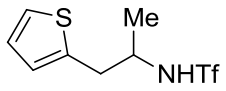

Prepared using general procedure **X** on a 100 mg scale with catalyst 1 (1 mol %), trifluoromethanesulfonamide (1.5 equiv), diphenyldisulfide (10 mol %), 2,6-lutidine (25 mol %) and dichloromethane [0.5 M]. Irradiated for 144h then purified in 25% EtOAc/Hexanes to give a yellow oil in 35% isolated yield (average of two trials). **^{1}H NMR** (400 MHz, $CDCl_3$) δ = 7.20 (d, *J* = 5.1 Hz, 1 H), 6.97 (dd, *J* = 3.4, 5.1 Hz, 1 H), 6.85 (d, *J* = 3.2 Hz, 1 H), 3.99 - 3.89 (m, 1 H), 3.15 - 2.99 (m, 2 H), 1.29 (d, *J* = 6.6 Hz, 3 H); **^{13}C NMR** (100 MHz, $CDCl_3$) δ = 137.1, 127.3, 125.1, 121.1, 118.0, 52.5, 37.5, 21.1; **IR** (thin film): 3710, 3688, 3648, 3628, 3565, 3113, 2981, 2933, 1716, 1698, 1653, 1558, 1506, 1488, 1430, 1373, 1287; **LRMS** (ESI): Calculated for [M+H$^+$] = 274.30; found 274.04.

Methyl -6-(4-methoxyphenyl)-5-(trifluoromethylsulfonamido)hexanoate (33b).

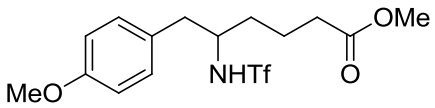

Prepared using general procedure **X** on a 100 mg scale with catalyst 1 (1 mol %), trifluoromethanesulfonamide (1.5 equiv), diphenyldisulfide (10 mol %), 2,6-lutidine (25 mol %) and dichloromethane [0.5 M]. Irradiated for 96h then purified in 10% EtOAc/Hexanes to give a yellow oil in 58% isolated yield (average of two trials). **^{1}H NMR** (400 MHz, $CDCl_3$) δ = 7.29 - 7.34 (m, 2 H), 7.23 - 7.28 (m, 3 H), 7.15 (d, *J*=6.85 Hz, 2 H), 3.72 - 3.83 (m, 2 H), 3.64 (s, 3 H), 2.91 - 2.97 (m, 1 H), 2.82 - 2.88 (m, 1 H), 2.24 - 2.39 (m, 2 H), 1.56 - 1.82 (m, 4 H), 1.36 - 1.47 (m, 1 H); **^{13}C NMR** (100 MHz, $CDCl_3$) δ =174.02, 135.94, 129.58, 127.10, 121.08, 117.89, 57.09, 51.76, 41.86, 33.43, 33.21, 20.58 **IR**

(thin film):3628, 3221, 3030, 2955, 1955, 1887, 1716, 1603, 1558, 1496, 1438, 1374; **LRMS** (ESI): Calculated for $[M+H^+]$ = 354.36; found 354.19.

N-(1-(1,3-dioxoisoindolin-2-yl)-3-(4-methoxyphenyl)propan-2-yl)-1,1,1-trifluoromethanesulfonamide (34b).

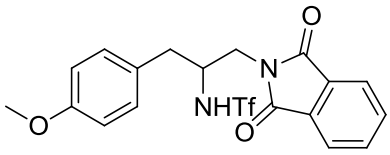

Prepared using general procedure **X** on a 100 mg scale with catalyst 1 (1 mol %), trifluoromethanesulfonamide (1.5 equiv), diphenyldisulfide (10 mol %), 2,6-lutidine (25 mol %) and dichloromethane [0.5 M]. Irradiated for 48h then purified in 15% EtOAc/Hexanes to give a white solid in 67% isolated yield (average of two trials). **^{1}H NMR** (400 MHz, $CDCl_3$) δ = 7.83 (dd, *J* = 3.1, 5.3 Hz, 2 H), 7.71 (dd, *J* = 3.1, 5.3 Hz, 2 H), 7.15 (d, *J* = 8.3 Hz, 2 H), 6.82 (d, *J* = 8.6 Hz, 2 H), 6.17 (d, *J* = 9.3 Hz, 1 H), 4.10 (d, *J* = 5.9 Hz, 1 H), 3.78 - 3.68 (m, 5 H), 3.05 - 2.89 (m, 2 H); **^{13}C NMR** (100 MHz, $CDCl_3$) δ = 168.6, 158.9, 134.4, 131.7, 130.7, 127.0, 123.6, 120.9, 114.3, 56.1, 55.2, 41.2, 39.4; **IR** (thin film): 3853, 3838, 3750, 3710, 3689, 3674, 3648, 3420, 1772, 1706, 1652, 1635, 1616, 1514, 1456, 1434, 1397, 1249, 1230; **LRMS** (ESI): Calculated for $[M+H^+]$ = 443.41; found 443.21.

1,1,1-trifluoro-N-(1-hydroxy-3-(4-methoxyphenyl)propan-2-yl)methanesulfonamide (35b).

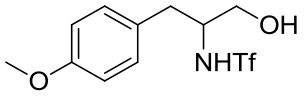

Prepared using general procedure **X** on a 100 mg scale with catalyst 1 (1 mol %), trifluoromethanesulfonamide (1.5 equiv), diphenyldisulfide (10 mol %), 2,6-lutidine (25 mol %) and dichloromethane [0.5 M]. Irradiated for 96h then purified in 20% EtOAc/Hexanes then 50% EtOAc/Hexanes to give a yellow oil in 70% isolated yield (average of two trials). **^{1}H NMR** (400 MHz, $CDCl_3$) δ =7.24 (s, 2 H), 7.10 (d, *J*=8.56 Hz, 2 H), 6.85 (d, *J*=7.34 Hz, 2 H), 5.24 (br. s., 1 H), 3.78 (s, 4

H), 3.58 - 3.71 (m, 2 H), 2.86 - 2.95 (m, 2 H); **^{13}C NMR** (100 MHz, $CDCl_3$) δ =158.26, 130.16, 127.68, 113.82, 62.83, 57.87, 54.89, 37.27; **IR** (thin film): 3734, 3710, 3292, 2551, 2425, 2360, 1999, 1942, 1889, 1771, 1613, 1586, 1517, 1202; **LRMS** (ESI): Calculated for [M+H$^+$] = 314.29; found 314.18.

1,1,1-trifluoro-N-(2-phenylcyclohexyl)methanesulfonamide (17b).

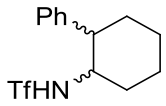

(2.5:1, cis:trans)

Prepared using general procedure **X** on a 100 mg scale with catalyst 1 (1 mol %), trifluoromethanesulfonamide (1.5 equiv), diphenyldisulfide (10 mol %), 2,6-lutidine (25 mol %) and dichloromethane [0.5 M]. Irradiated for 96h then purified in 5% EtOAc/Hexanes to give a white solid in 50% isolated yield in 2.5:1 dr (average of two trials). Assignment of major and minor diastereomers calculated by coupling constants of peaks at 3.00 – 2.95 ppm (ddd, *J* = 3.6, 3.6, 12.8 Hz) and 2.42 – 2.35 ppm (ddd, *J* = 3.6, 11.6, 11.6 Hz). Spectral data were in agreement with literature values.[27]

1,1,1-trifluoro-N-(2-methylcyclopentyl)methanesulfonamide (18b).

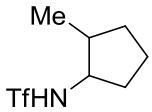

Prepared using general procedure **X** on a 100 mg scale with catalyst 1 (1 mol %), trifluoromethanesulfonamide (1.5 equiv), diphenyldisulfide (10 mol %), 2,6-lutidine (25 mol %) and dichloromethane [0.5 M]. Irradiated for 96h then purified in 5% EtOAc/Hexanes to give a clear oil in 85% isolated yield, 2.3:1 dr (average of two trials). Spectral data were in agreement with literature values.[27]

1,1,1-trifluoro-N-(3-methylbutan-2-yl)methanesulfonamide (36b).

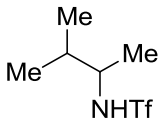

Prepared using general procedure **X** on a 100 mg scale (3.0 equiv alkene) with catalyst 1 (1 mol %), trifluoromethanesulfonamide (1.0 equiv), diphenyldisulfide (10 mol %), 2,6-lutidine (25 mol %) and dichloromethane [0.5 M]. Irradiated for 96h then purified in 10% EtOAc/Hexanes to give a yellow oil in 72% isolated yield (average of two trials). **^{1}H NMR** (400 MHz, $CDCl_3$) δ = 4.83 - 4.39 (m, 1 H), 3.55 (br. s., 1 H), 1.78 (d, *J* = 6.4 Hz, 1 H), 1.24 (d, *J* = 6.8 Hz, 3 H), 0.96 (d, *J* = 4.6 Hz, 6 H); **^{13}C NMR** (100 MHz, $CDCl_3$) δ = 57.5, 33.8, 19.0, 18.2, 18.1; **IR** (thin film): 2924, 2851, 1715, 1583, 1540, 1457, 1373, 1318, 1229; **LRMS** (ESI): Calculated for [M+Na^+] = 242.21 ; found 242.25.

1-(1-(2-methoxyphenyl)propan-2-yl)-1H-pyrazole (37).

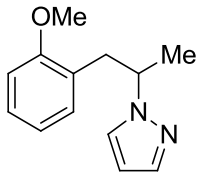

Prepared using general procedure **X** on a 100 mg scale with catalyst 1 (1 mol %), trifluoromethanesulfonamide (1.5 equiv), diphenyldisulfide (10 mol %), 2,6-lutidine (25 mol %) and dichloromethane [0.5 M]. Irradiated for 96h then purified in 10% EtOAc/Hexanes to give a clear oil in 83% isolated yield (average of two trials). **^{1}H NMR** (400 MHz, $CDCl_3$) δ = 7.49 (d, *J* = 1.5 Hz, 1 H), 7.20 - 7.11 (m, 2 H), 6.85 - 6.69 (m, 3 H), 6.10 (t, *J* = 2.0 Hz, 2 H), 4.66 - 4.54 (m, 1 H), 3.84 - 3.78 (m, 3 H), 3.16 - 3.00 (m, 2 H), 1.50 (d, *J* = 6.6 Hz, 3 H); **^{13}C NMR** (100 MHz, $CDCl_3$) δ = 157.5, 138.8, 131.0, 127.9, 126.4, 120.5, 110.1, 104.4, 57.9, 55.3, 38.5, 20.6; **IR** (thin film):3421, 3102, 2978, 2936, 2835, 1897, 1732, 1716, 1698, 1652, 1601, 1558, 1540, 1457, 1398, 1340, 1243, 1210; **LRMS** (ESI): Calculated for [M+H^+] = 217.28; found 217.11.

1-(1-(2-methoxyphenyl)propan-2-yl)-1H-indazole (38).

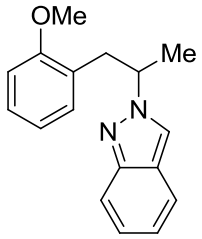

Prepared using general procedure **X** on a 100 mg scale with catalyst 1 (1 mol %), trifluoromethanesulfonamide (1.5 equiv), diphenyldisulfide (10 mol %), 2,6-lutidine (25 mol %) and dichloromethane [0.5 M]. Irradiated for 96h then purified in 10% EtOAc/Hexanes to give a yellow oil in 57% isolated yield (average of two trials). Regioselectivity determined by NOESY NMR experiment. **^{1}H NMR** (400 MHz, $CDCl_3$) δ = 7.78 (dd, *J* = 0.9, 8.7 Hz, 1 H), 7.75 (s, 1 H), 7.60 (td, *J* = 1.1, 8.4 Hz, 1 H), 7.32 - 7.26 (m, 1 H), 7.19 (dt, *J* = 1.8, 7.8 Hz, 1 H), 7.06 (ddd, *J* = 0.7, 6.6, 8.3 Hz, 1 H), 6.89 - 6.81 (m, 2 H), 6.78 - 6.72 (m, 1 H), 4.96 - 4.86 (m, 1 H), 3.82 (s, 3 H), 3.38 - 3.21 (m, 2 H), 1.69 (d, *J* = 6.8 Hz, 3 H); **^{13}C NMR** (100 MHz, $CDCl_3$) δ = 157.5, 148.6, 131.0, 128.1, 126.1, 121.6, 121.2, 121.1, 120.5, 120.2, 117.5, 110.2, 59.8, 55.2, 38.6, 21.0; **IR** (thin film): 3734, 3711, 3648, 3566, 3420, 3060, 2834, 2533, 2483, 2007, 1935, 1782, 1716, 1626, 1601, 1587, 1494, 1455, 1333, 1288, 1242; **LRMS** (ESI): Calculated for $[M+H^+]$ = 267.34; found 267.17.

1-(1-(4-methoxyphenyl)propan-2-yl)-1H-imidazole (39).

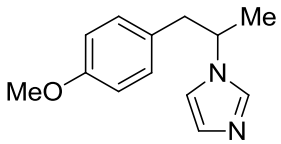

Prepared using general procedure **X** on a 100 mg scale with catalyst 1 (1 mol %), trifluoromethanesulfonamide (3.0 equiv), diphenyldisulfide (10 mol %), 2,6-lutidine (25 mol %) and dichloromethane [0.5 M]. Irradiated for 96h then purified in 5% MeOH/DCM to give a yellow oil in 50% isolated yield (average of two trials). **^{1}H NMR** (400 MHz, $CDCl_3$) δ =7.72 - 7.80 (m, 1 H), 7.50 (s, 1 H),

7.35 (s, 1 H), 7.28 - 7.32 (m, 2 H), 7.24 (s, 2 H), 4.75 (sxt, *J*=6.80 Hz, 1 H), 4.22 (s, 3 H), 3.37 (br. s., 2 H), 1.98 (s, 3 H); **^{13}C NMR** (100 MHz, $CDCl_3$) δ =158.39, 135.77, 129.78, 129.03, 116.50, 113.84, 55.31, 55.10, 43.72, 20.99; **IR** (thin film): 3838, 3801, 3749, 3710, 3689, 3383, 3107, 2934, 2548, 2059, 1889, 1771, 1698, 1652, 1612, 1583, 1455, 1378, 1246; **LRMS** (ESI): Calculated for [M+H$^+$] = 217.28; found 217.12.

2-(1-(4-methoxyphenyl)propan-2-yl)-2H-1,2,3-triazole (40).

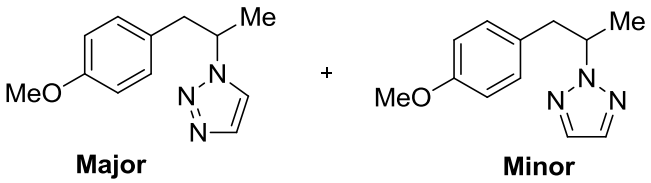

Major **Minor**

Prepared using general procedure **X** on a 100 mg scale with catalyst 1 (1 mol %), trifluoromethanesulfonamide (1.5 equiv), diphenyldisulfide (10 mol %), 2,6-lutidine (25 mol %) and dichloromethane [0.5 M]. Irradiated for 96h then purified in 10% to 20% to 50% to 75% EtOAc/Hexanes to give two separately collected clear oils in 80% isolated yield, 2:1 mix of regioisomers (average of two trials). **Major Regioisomer: ^{1}H NMR** (400 MHz, $CDCl_3$) δ = 7.57 (s, 1 H), 7.26 (s, 1 H), 6.84 (d, *J* = 8.6 Hz, 2 H), 6.72 (d, *J* = 8.6 Hz, 2 H), 4.85 - 4.72 (m, 1 H), 3.71 (s, 3 H), 3.20 - 3.06 (m, 1 H), 3.06 - 2.97 (m, 1 H), 1.57 (d, *J* = 6.8 Hz, 3 H); **^{13}C NMR** (100 MHz, $CDCl_3$) δ = 158.5, 133.2, 130.1, 128.7, 122.2, 113.9, 58.7, 55.2, 42.8, 20.4; **IR** (thin film): 3710, 3673, 3420, 3124, 2836, 1771, 1732, 1716, 1652, 1584, 1513, 1420, 1302, 1280; **LRMS** (ESI): Calculated for [M+H$^+$] = 218.27; found 218.11; **Minor Regioisomer: ^{1}H NMR** (400 MHz, $CDCl_3$) δ = 7.54 (s, 2 H), 6.96 - 6.89 (m, 2 H), 6.79 - 6.72 (m, 2 H), 4.96 - 4.82 (m, 1 H), 3.74 (s, 3 H), 3.25 (dd, *J* = 7.7, 13.8 Hz, 1 H), 3.01 (dd, *J* = 7.0, 13.8 Hz, 1 H), 1.60 - 1.50 (m, 3 H); **^{13}C NMR** (100 MHz, $CDCl_3$) δ = 158.3, 133.5, 130.0, 129.6, 113.8, 63.0, 55.2, 42.2, 20.1; **IR** (thin film): 3125, 2983, 2835, 1733, 1698, 1683, 1652, 1635, 1613, 1540, 1374, 1301, 1248; **LRMS** (ESI): Calculated for [M+H$^+$] = 218.27; found 218.11.

1-(2,2-diphenylethyl)-1H-1,2,3-triazole (41).

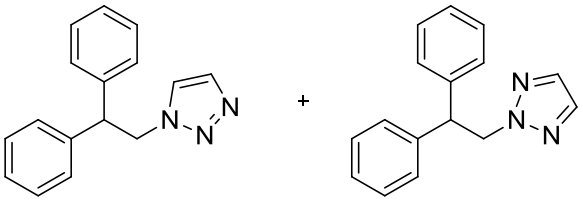

Prepared using general procedure **X** on a 100 mg scale with catalyst 1 (1 mol %), trifluoromethanesulfonamide (1.5 equiv), diphenyldisulfide (10 mol %), 2,6-lutidine (25 mol %) and dichloromethane [0.5 M]. Irradiated for Xh then purified in 10 to 25 to 100% EtOAc/Hexanes to give two white solids in 81% isolated yield, 3.9:1 mix of regioisomers (average of two trials). **Major regioisomer** **^{1}H NMR** (400 MHz, $CDCl_3$) δ = 7.52 (s, 1 H), 7.35 - 7.28 (m, 4 H), 7.27 - 7.20 (m, 5 H), 7.09 (s, 1 H), 5.02 (d, *J* = 8.1 Hz, 2 H), 4.63 (t, *J* = 7.9 Hz, 1 H); **^{13}C NMR** (100 MHz, $CDCl_3$) δ = 140.5, 133.3, 128.9, 127.9, 127.3, 124.1, 54.7, 51.8; **IR** (thin film): 3853, 3801, 3674, 3420, 1771, 1716, 1683, 1635, 1558, 1540, 1495, 1455, 1210; **LRMS** (ESI): Calculated for [M+H$^+$] = 250.31; found 250.20 **Minor regioisomer** **^{1}H NMR** (400 MHz, $CDCl_3$) δ = 7.47 (s, 2 H), 7.30 - 7.14 (m, 10 H), 5.05 (d, *J* = 8.3 Hz, 2 H), 4.93 - 4.84 (m, 1 H); **^{13}C NMR** (100 MHz, $CDCl_3$) δ = 140.9, 134.0, 128.7, 128.0, 127.0, 58.8, 51.1; **IR** (thin film): 3027, 1771, 1698, 1652, 1558, 1540, 1507, 1473, 1418, 1362; **LRMS** (ESI): Calculated for [M+H$^+$] = 250.31; found 250.20.

1-(2-phenylpropyl)-1H-1,2,3-triazole (42).

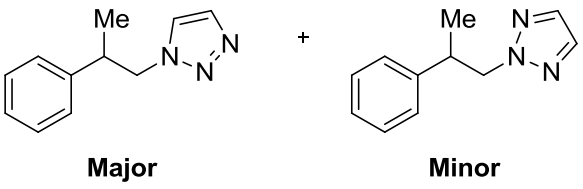

Prepared using general procedure **X** on a 100 mg scale with catalyst 1 (1 mol %), trifluoromethanesulfonamide (1.5 equiv), diphenyldisulfide (10 mol %), 2,6-lutidine (25 mol %) and

dichloromethane [0.5 M]. Irradiated for 72h then purified in 5 to 50% EtOAc/Hexanes to give two white solids in 41% isolated yield as a 1.9:1 mix of regioisomers (average of two trials). **Major regioisomer ^{1}H NMR** (400 MHz, $CDCl_3$) δ = 7.55 (s, 1 H), 7.32 - 7.26 (m, 2 H), 7.23 - 7.20 (m, 1 H), 7.14 - 7.08 (m, 5 H), 4.60 - 4.53 (m, 2 H), 4.46 - 4.39 (m, 2 H), 3.40 - 3.29 (m, 2 H), 1.31 (d, *J* = 7.1 Hz, 3 H); **^{13}C NMR** (100 MHz, $CDCl_3$) δ = 142.4, 133.4, 127.3, 127.1, 123.8, 57.0, 41.0, 18.7; **IR** (thin film): 3853, 3801, 3750, 3689, 3125, 3062, 2968, 2876; **LRMS** (ESI): Calculated for $[M+H^+]$ = 188.11; found 188.12. **Minor regioisomer ^{1}H NMR** (400 MHz, $CDCl_3$) δ = 7.54 (s, 2 H), 7.32 - 7.25 (m, 2 H), 7.23 - 7.16 (m, 3 H), 4.63 - 4.47 (m, 2 H), 3.58 - 3.46 (m, 1 H), 1.21 (d, *J* = 6.8 Hz, 3 H); **^{13}C NMR** (100 MHz, $CDCl_3$) δ = 142.8, 134.0, 128.7, 127.1, 126.9, 61.4, 40.6, 18.6; **IR** (thin film): 3029, 2966, 1733, 1716, 1698, 1652, 1635, 1558, 1520, 1495, 1455, 1418, 1361; **LRMS** (ESI): Calculated for $[M+H^+]$ = 188.11; found 188.12.

REFERENCES

(1) Kotani, H.; Ohkubo, K.; Fukuzumi, S. *J. Am. Chem. Soc.* **2004**, *126*, 15999–16006.

(2) Crimmin, M. R.; Arrowsmith, M.; Barrett, A. G. M.; Casely, I. J.; Hill, M. S.; Procopiou, P. A. J. Am. Chem. Soc. 2009, 131, 9670–9685.

(3) Hamilton, D. S.; Nicewicz, D. A. *J. Am. Chem. Soc.* **2012**, *134*, 18577–18580.

(4) Schlummer, B.; Hartwig, J. F. *Org. Lett.* **2002**, *4*, 1471–1474.

(5) Zhou, L.; Chen, J.; Tan, C. K.; Yeung, Y.-Y. *J. Am. Chem. Soc.* **2011**, *133*, 9164–9167.

(6) Marcotullio, M.; Campagna, V.; Sternativo, S.; Costantino, F.; Curini, M. *Synthesis* **2006**, *2006*, 2760–2766.

(7) Espino, C. G.; Wehn, P. M.; Chow, J.; Du Bois, J. *J. Am. Chem. Soc.* **2001**, *123*, 6935–6936.

(8) Estéoule, A.; Durán, F.; Retailleau, P.; Dodd, R.; Dauban, P. *Synthesis* **2007**, *2007*, 1251–1260.

(9) Chapurina, Y.; Ibrahim, H.; Guillot, R.; Kolodziej, E.; Collin, J.; Trifonov, A.; Schulz, E.; Hannedouche, J. *J. Org. Chem.* **2011**, *76*, 10163–10172.

(10) Verendel, J. J.; Zhou, T.; Li, J.-Q.; Paptchikhine, A.; Lebedev, O.; Andersson, P. G. J. Am. Chem. Soc. 2010, 132, 8880–8881.

(11) Sherman, E. S.; Fuller, P. H.; Kasi, D.; Chemler, S. R. *J. Org. Chem.* **2007**, *72*, 3896–3905.

(12) Klein, J. E. M. N.; Müller-Bunz, H.; Evans, P. *Org. Biomol. Chem.* **2009**, *7*, 986–995.

(13) Green, Ivan R.; October, Natasha, *ARKIVOC* **2010**, 2, 71–96.

(14) Hogan, Anne-Marie L.; Tricotet, Thomas; Meek, Alastair; Khokhar, Shaista S.; O'Shea, Donal F. *J. Org. Chem.* **2008**, 73, 6041 – 6044.

(15) Gaunt, Matthew J.; Spencer, Jonathan B.; Yu, Jinquan *J. Org. Chem.* **2002,** *67*, 4627–4629.

(16) Thimmaiah, Muralidhara; Zhang, Xiang; Fang, Shiyue *Tet. Lett.* **2008**, *49*, 5605–5607.

(17) Tian, H.; She, X.; Yu, H.; Shu, L.; Shi, Y. *J. Org. Chem.* **2007**, *67*, 2435-2446.

(18) Gaunt, Matthew J.; Spencer, Jonathan B.; Yu, Jinquan *J. Org. Chem.* **2002,** 67, 4627–4629.

(19) Engler, T. A.; Combink, K. D.; Ray, J. E. *J. Am. Chem. Soc.* **1998**, *110*, 7931–7933.

(20) Takashi Morimoto, Masao Hirano, Kohki Echigoya, and Takafumi Sato *J. Chem. Soc. Perkin Trans. II* **1986**, 1205–1209.

(21) von Wehrli, R.; Heimgartner, H.; Schmidt, H. *Helv. Acta* **1977**, *6*, 2034–2061.

(22) Taylor, B. L. H.; Swift, E. C.; Waetzig, J. D.; Jarvo, E. R. *J. Am. Chem. Soc.* **2011**, *133*, 389–391.

(23) Lara, M.; Mutti, F. G.; Glueck, S. M.; Kroutil, W. *Eur. J. Org. Chem.* **2008**, 3668–3672.

(24) Werner, E. W.; Sigman, M. S. *J. Am Chem. Soc.* **2010**, *132*, 13981–13983.

(25) Prediger, P.; Barbosa, L. F.; Génisson, Y.; Correia, C. R. D. *J. Org. Chem.* **2011**, *76*, 7737–7749.

(26) Brochu, C.; Molinaro, C.; Charette, A. B *J. Am. Chem. Soc.* **2001,** *123*, 12168–12175.

(27) Nguyen, T. M.; Nicewicz, D. A *J. Am Chem. Soc.* **2013**, *135*, 9588–9591.

Compound **2a**

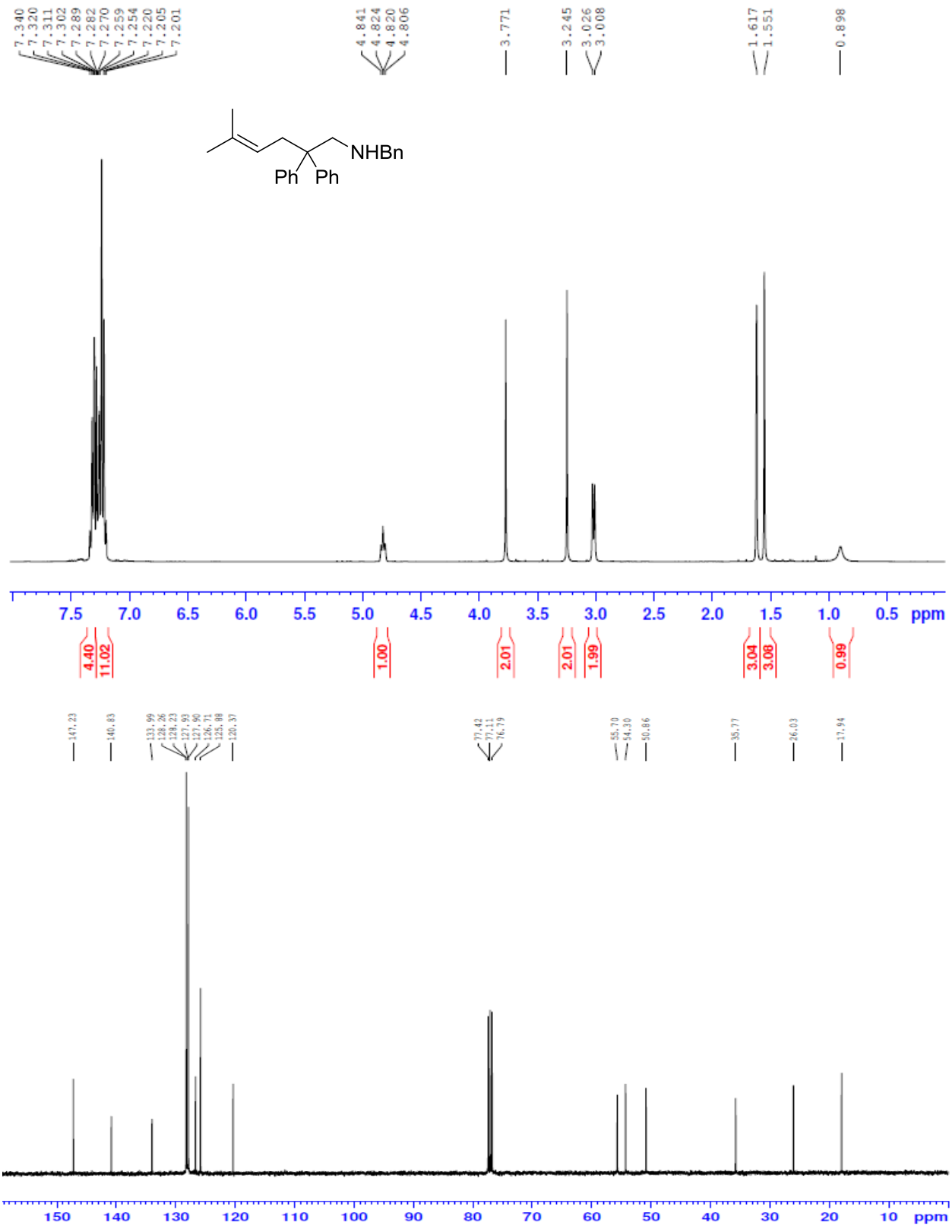
7.340
7.320
7.311
7.302
7.289
7.282
7.270
7.259
7.254
7.220
7.205
7.201
4.841
4.824
4.820
4.806
3.771
3.245
3.026
3.008
1.617
1.551
0.898
NHBn
Ph
Ph
7.5
7.0
6.5
6.0
5.5
5.0
4.5
4.0
3.5
3.0
2.5
2.0
1.5
1.0
0.5
ppm
4.40
11.02
1.00
2.01
2.01
1.99
3.04
3.08
0.99
147.23
140.83
133.99
128.26
128.23
127.93
127.90
126.71
126.08
120.37
77.42
77.11
76.79
55.70
54.30
50.86
35.77
26.03
17.94
150
140
130
120
110
100
90
80
70
60
50
40
30
20
10
ppm

Compound **3a**

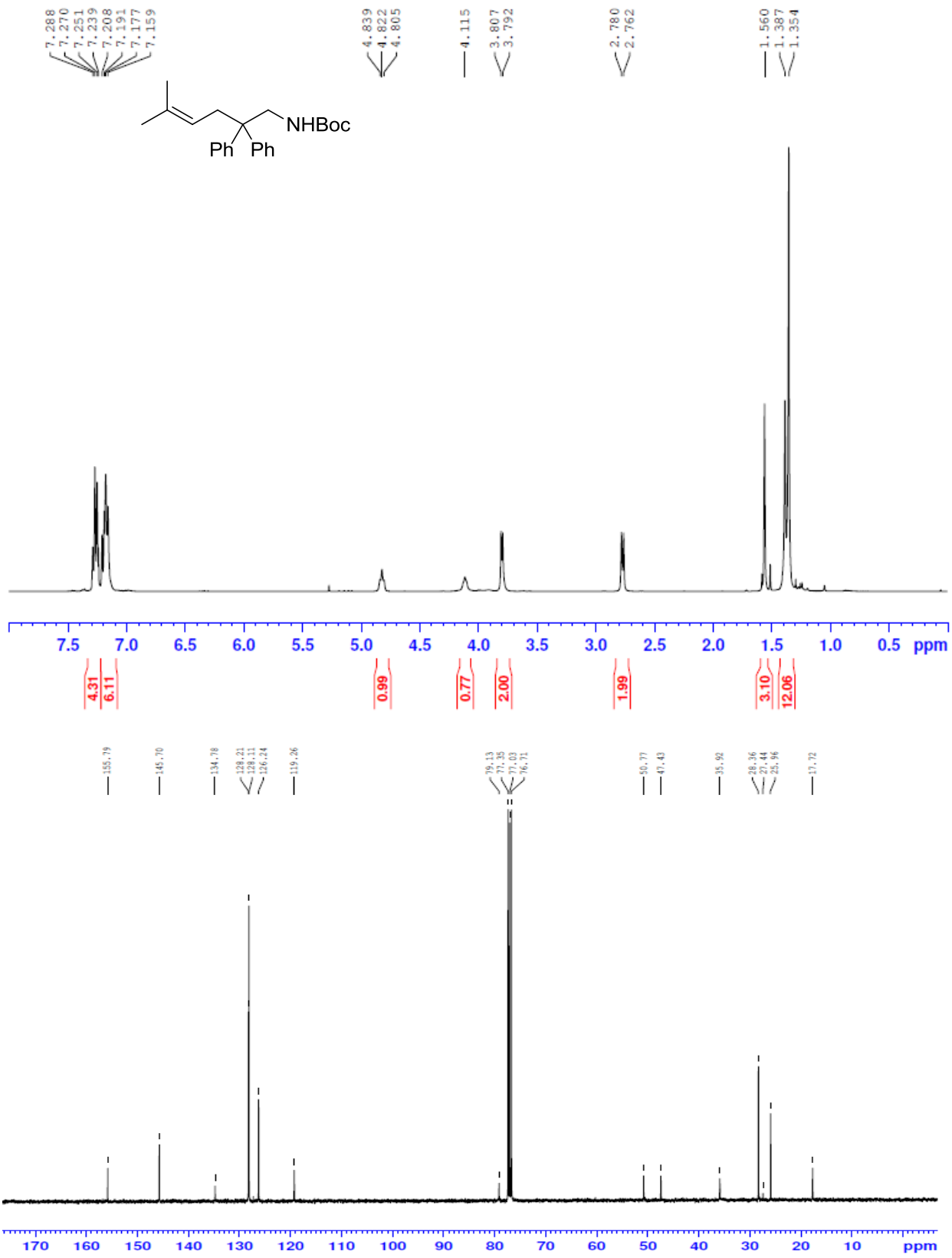
7.288
7.270
7.251
7.239
7.208
7.191
7.177
7.159
4.839
4.822
4.805
4.115
3.807
3.792
2.780
2.762
1.560
1.387
1.354
NHBoc
Ph
Ph
7.5
7.0
6.5
6.0
5.5
5.0
4.5
4.0
3.5
3.0
2.5
2.0
1.5
1.0
0.5
ppm
4.31
6.11
0.99
0.77
2.00
1.99
3.10
12.06
155.79
145.70
134.78
128.21
128.11
126.24
119.26
79.13
77.35
77.03
76.71
50.77
47.43
35.92
28.36
27.44
25.96
17.72
170
160
150
140
130
120
110
100
90
80
70
60
50
40
30
20
10
ppm

Compound **4a**

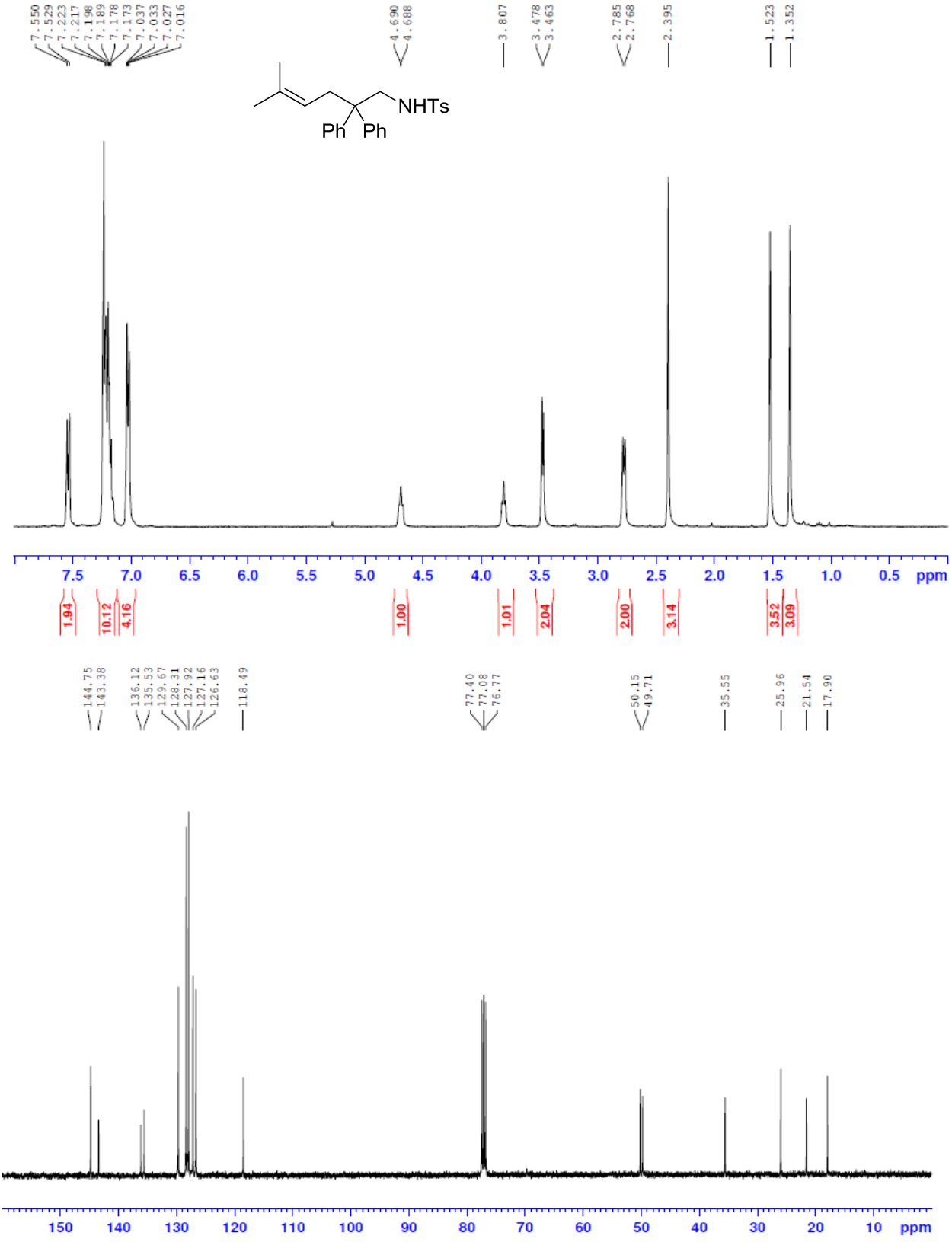
7.550
7.529
7.223
7.217
7.198
7.189
7.178
7.173
7.037
7.033
7.027
7.016
4.690
4.688
3.807
3.478
3.463
2.785
2.768
2.395
1.523
1.352
NHTs
Ph
Ph
7.5
7.0
6.5
6.0
5.5
5.0
4.5
4.0
3.5
3.0
2.5
2.0
1.5
1.0
0.5
ppm
1.94
10.12
4.16
1.00
1.01
2.04
2.00
3.14
3.52
3.09
144.75
143.38
136.12
135.53
129.67
128.31
127.92
127.16
126.63
118.49
77.40
77.08
76.77
50.15
49.71
35.55
25.96
21.54
17.90
150
140
130
120
110
100
90
80
70
60
50
40
30
20
10
ppm

Compound **5a**

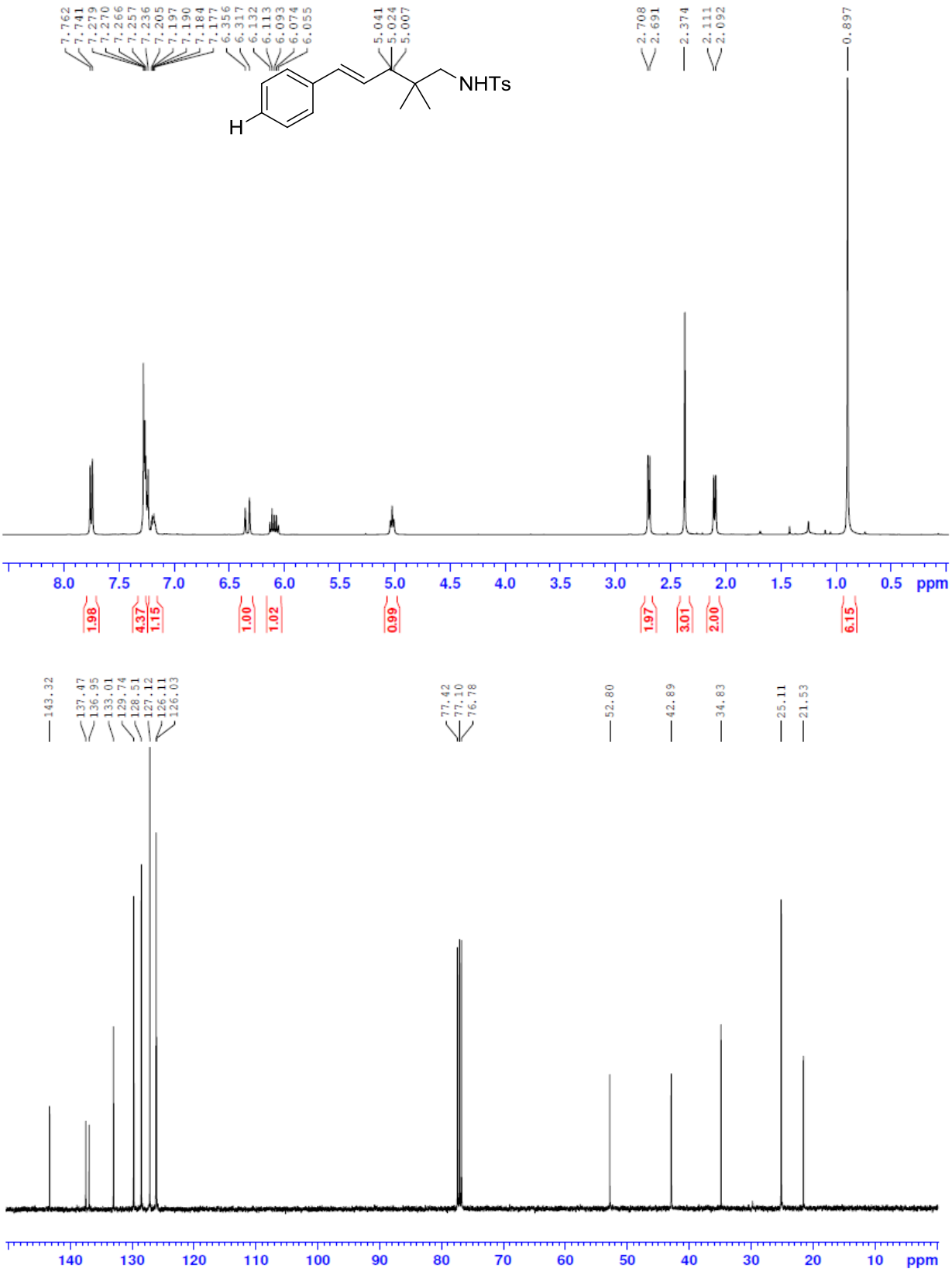
7.762
7.741
7.279
7.270
7.266
7.257
7.236
7.205
7.197
7.190
7.184
7.177
6.356
6.317
6.132
6.113
6.093
6.074
6.055
5.041
5.024
5.007
2.708
2.691
2.374
2.111
2.092
0.897
NHTs
H
8.0
7.5
7.0
6.5
6.0
5.5
5.0
4.5
4.0
3.5
3.0
2.5
2.0
1.5
1.0
0.5
ppm
1.98
4.37
1.15
1.00
1.02
0.99
1.97
3.01
2.00
6.15
143.32
137.47
136.95
133.01
129.74
128.51
127.12
126.11
126.03
77.42
77.10
76.78
52.80
42.89
34.83
25.11
21.53
140
130
120
110
100
90
80
70
60
50
40
30
20
10
ppm

Compound **6a**

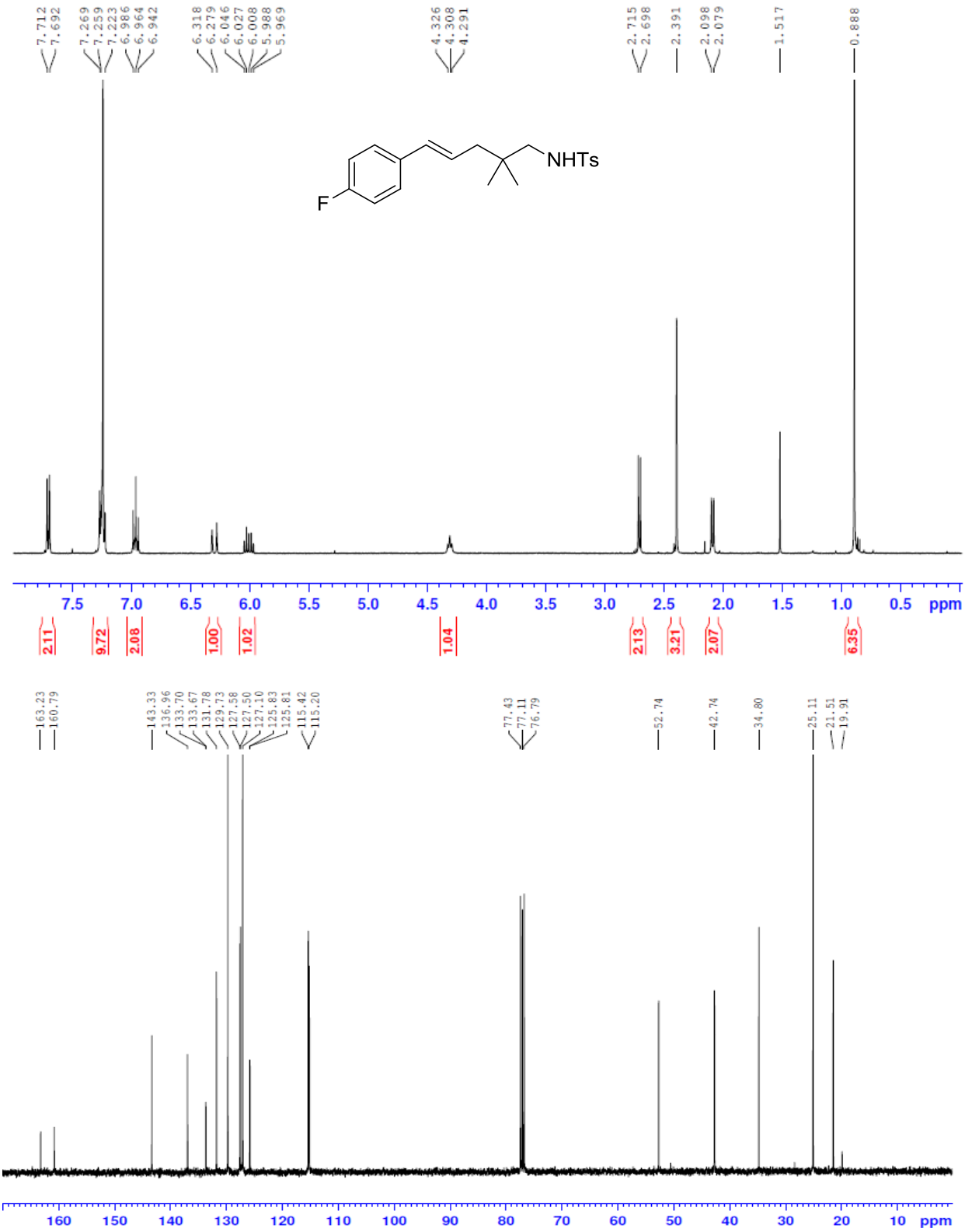
7.712
7.692
7.269
7.259
7.223
6.986
6.964
6.942
6.318
6.279
6.046
6.027
6.008
5.988
5.969
4.326
4.308
4.291
2.715
2.698
2.391
2.098
2.079
1.517
0.888
NHTs
F
7.5
7.0
6.5
6.0
5.5
5.0
4.5
4.0
3.5
3.0
2.5
2.0
1.5
1.0
0.5
ppm
2.11
9.72
2.08
1.00
1.02
1.04
2.13
3.21
2.07
6.35
163.23
160.79
143.33
136.96
133.70
133.67
131.78
129.73
127.58
127.50
127.10
125.83
125.81
115.42
115.20
77.43
77.11
76.79
52.74
42.74
34.80
25.11
21.51
19.91
160
150
140
130
120
110
100
90
80
70
60
50
40
30
20
10
ppm

Compound **7a**

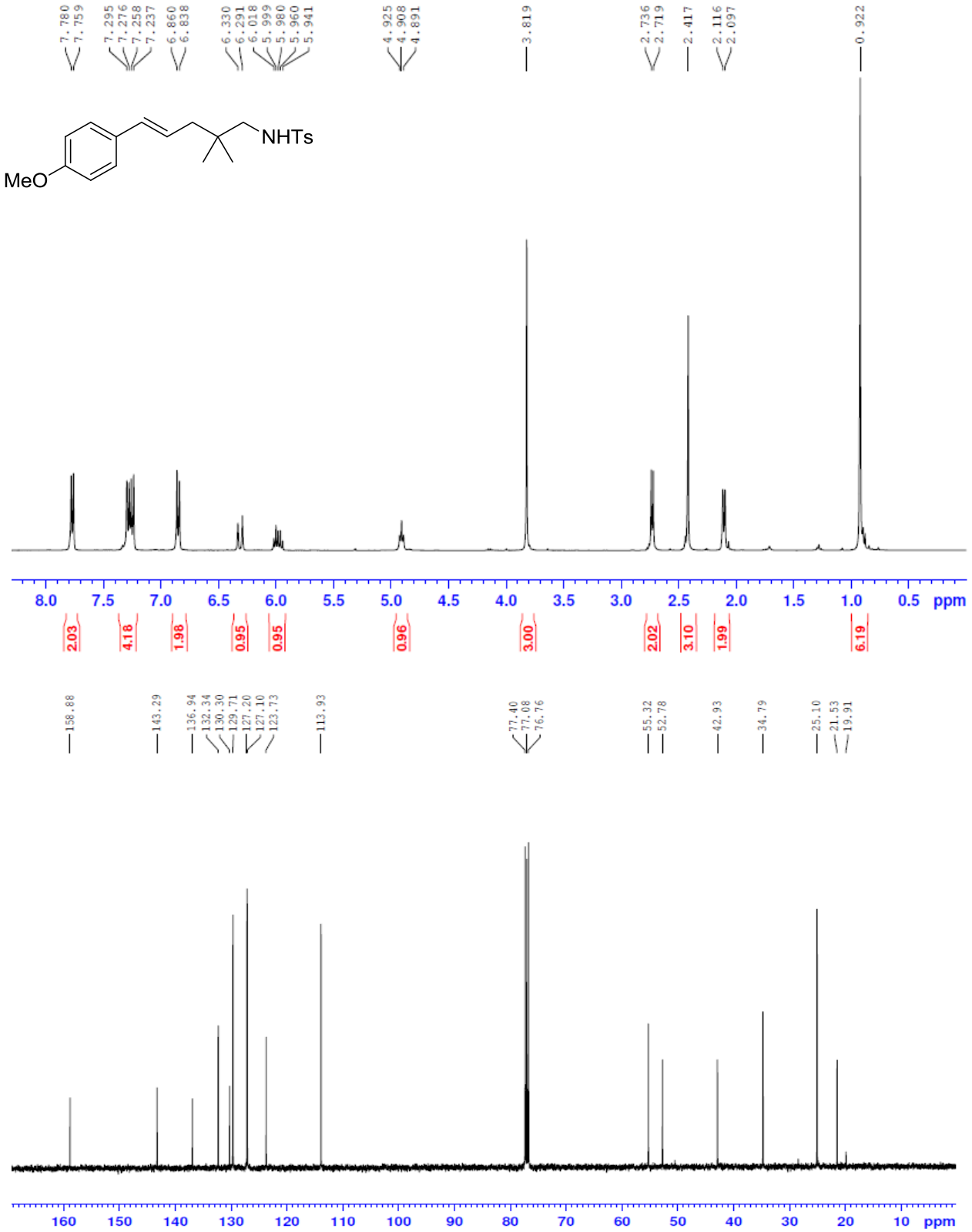
7.780
7.759
7.295
7.276
7.258
7.237
6.860
6.838
6.330
6.291
6.018
5.999
5.980
5.960
5.941
4.925
4.908
4.891
3.819
2.736
2.719
2.417
2.116
2.097
0.922
NHTs
MeO
8.0
7.5
7.0
6.5
6.0
5.5
5.0
4.5
4.0
3.5
3.0
2.5
2.0
1.5
1.0
0.5
ppm
2.03
4.18
1.98
0.95
0.95
0.96
3.00
2.02
3.10
1.99
6.19
158.88
143.29
136.94
132.34
130.30
129.71
127.20
127.10
123.73
113.93
77.40
77.08
76.76
55.32
52.78
42.93
34.79
25.10
21.53
19.91
160
150
140
130
120
110
100
90
80
70
60
50
40
30
20
10
ppm

Compound **8a**

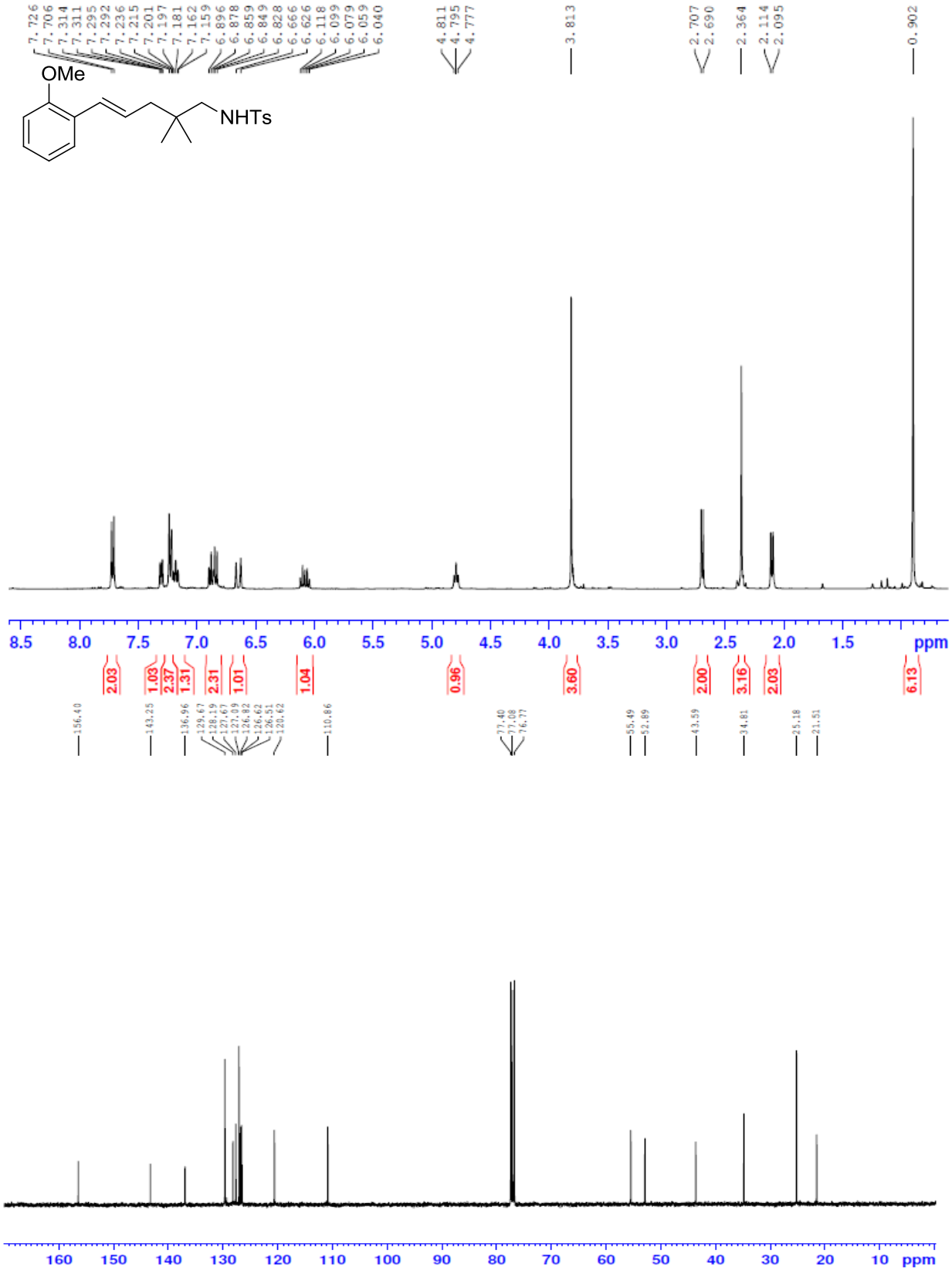
7.726
7.706
7.314
7.311
7.295
7.292
7.236
7.215
7.201
7.197
7.181
7.162
7.159
6.896
6.878
6.859
6.849
6.828
6.666
6.626
6.118
6.099
6.079
6.059
6.040
4.811
4.795
4.777
3.813
2.707
2.690
2.364
2.114
2.095
0.902
OMe
NHTs
8.5
8.0
7.5
7.0
6.5
6.0
5.5
5.0
4.5
4.0
3.5
3.0
2.5
2.0
1.5
ppm
2.03
1.03
2.37
1.31
2.31
1.01
1.04
0.96
3.60
2.00
3.16
2.03
6.13
156.40
143.25
136.96
129.67
128.19
127.69
127.09
126.82
126.62
126.51
120.62
110.86
77.40
77.08
76.77
55.49
52.89
43.59
34.81
25.18
21.51
160
150
140
130
120
110
100
90
80
70
60
50
40
30
20
10
ppm

Compound **9a**

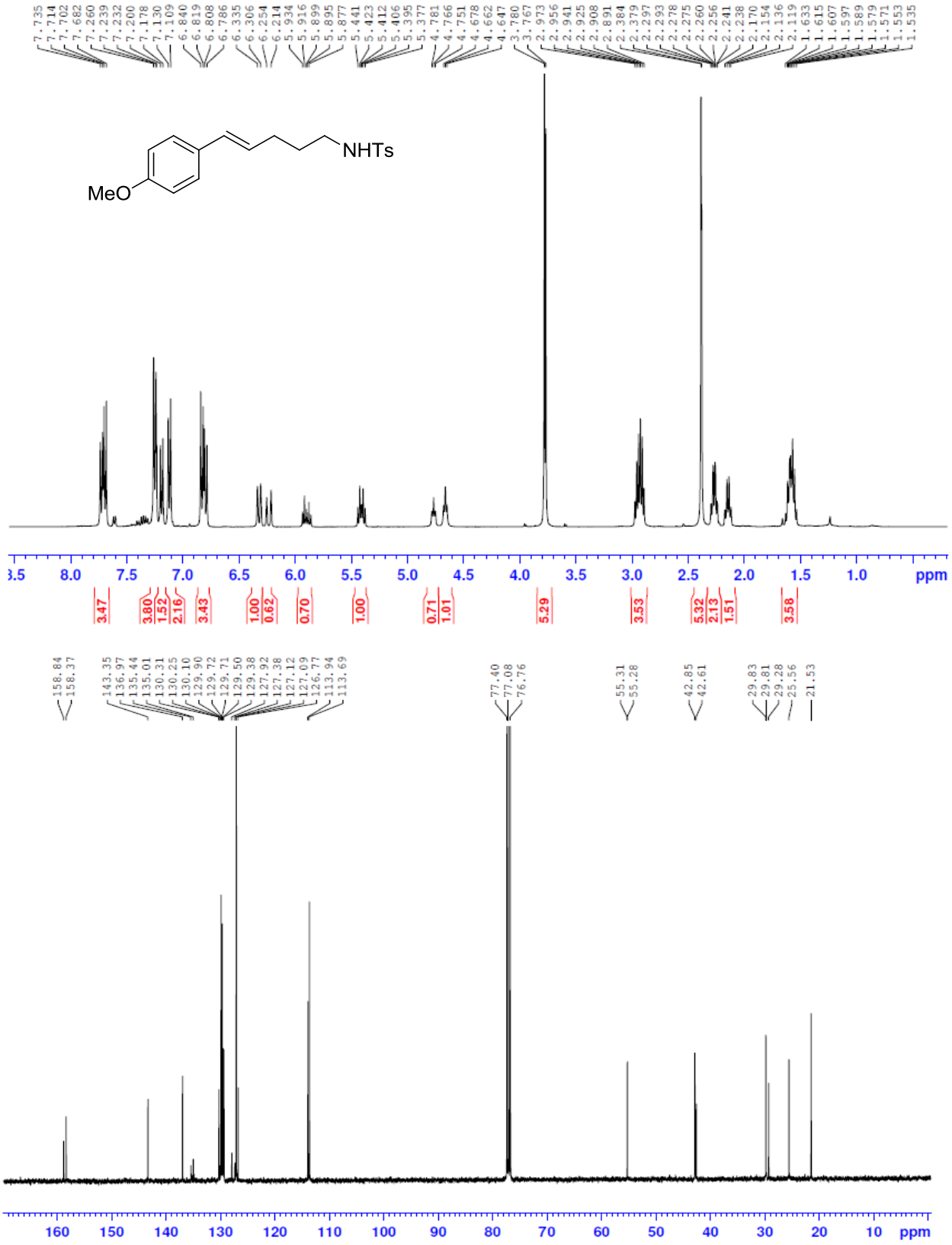

Compound **10a**

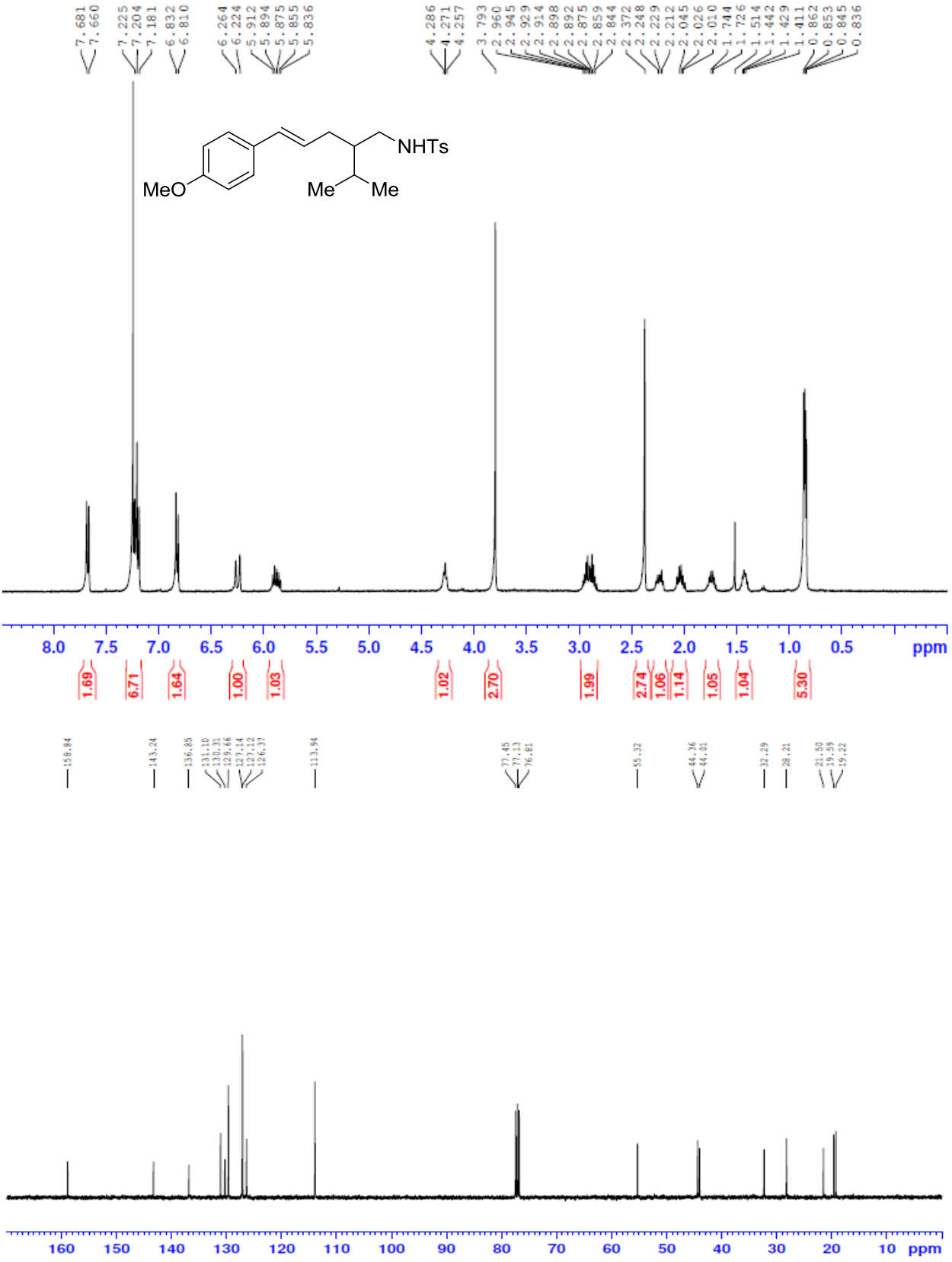

Compound **11a**

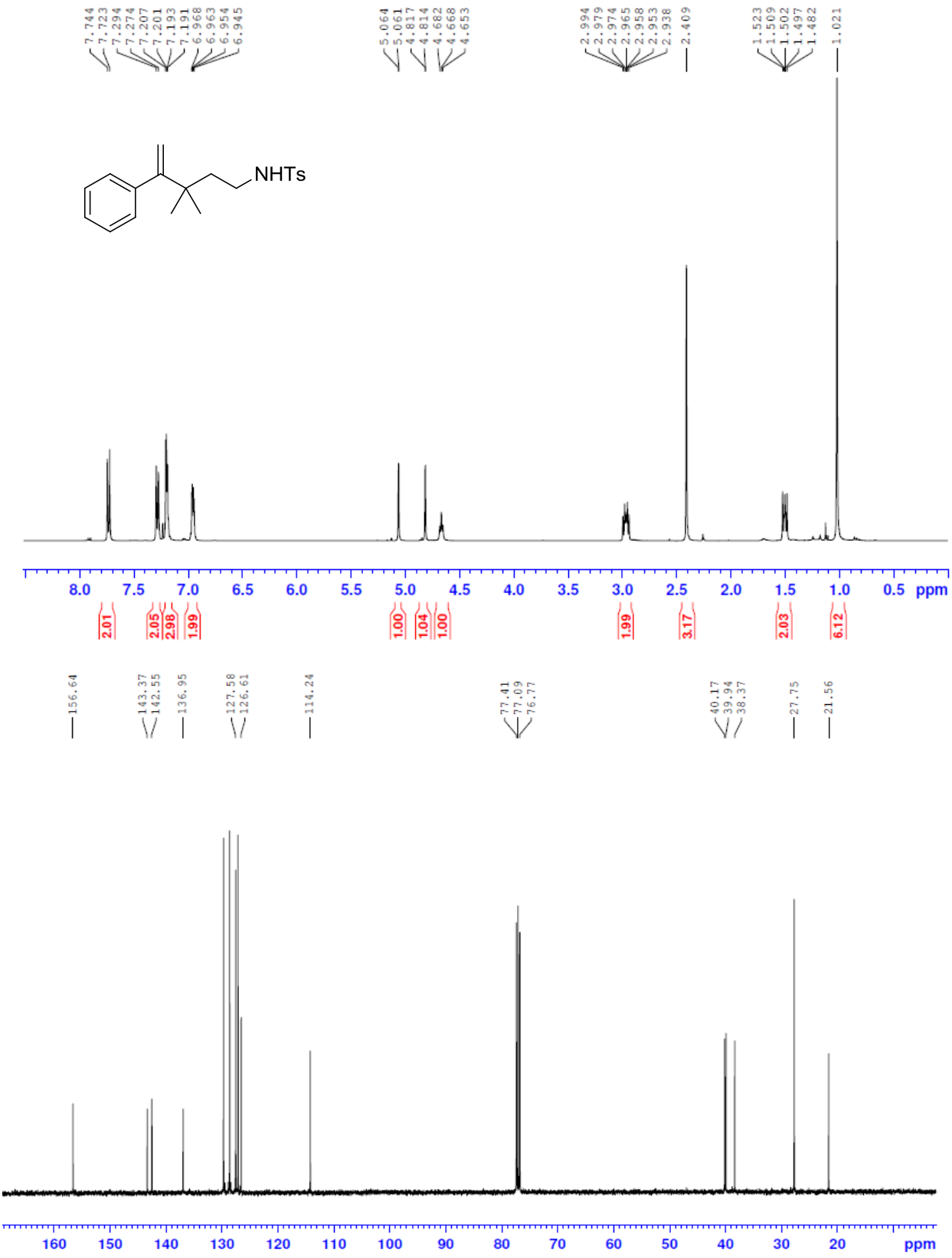

Compound **12a**

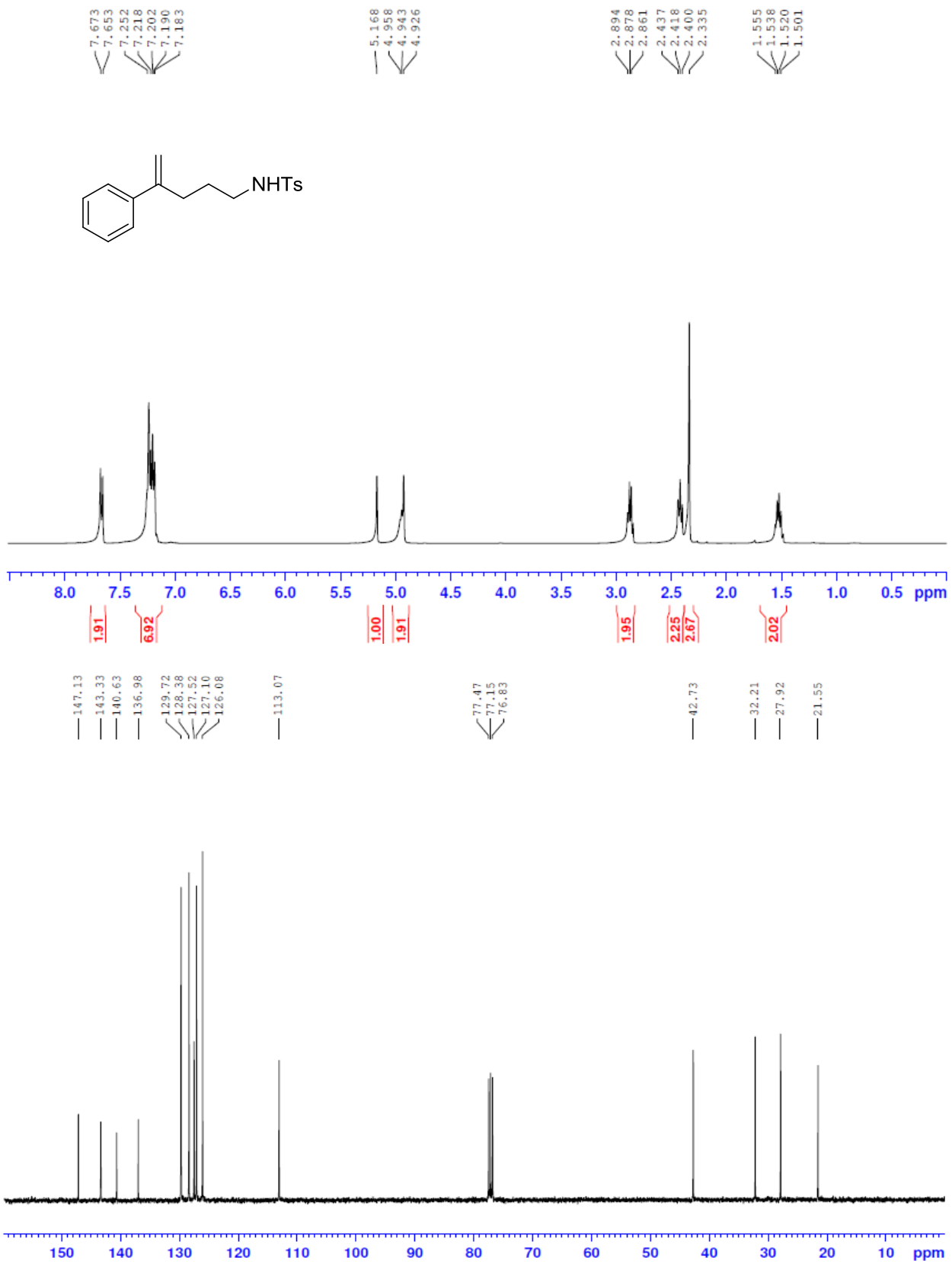

Compound **13a**

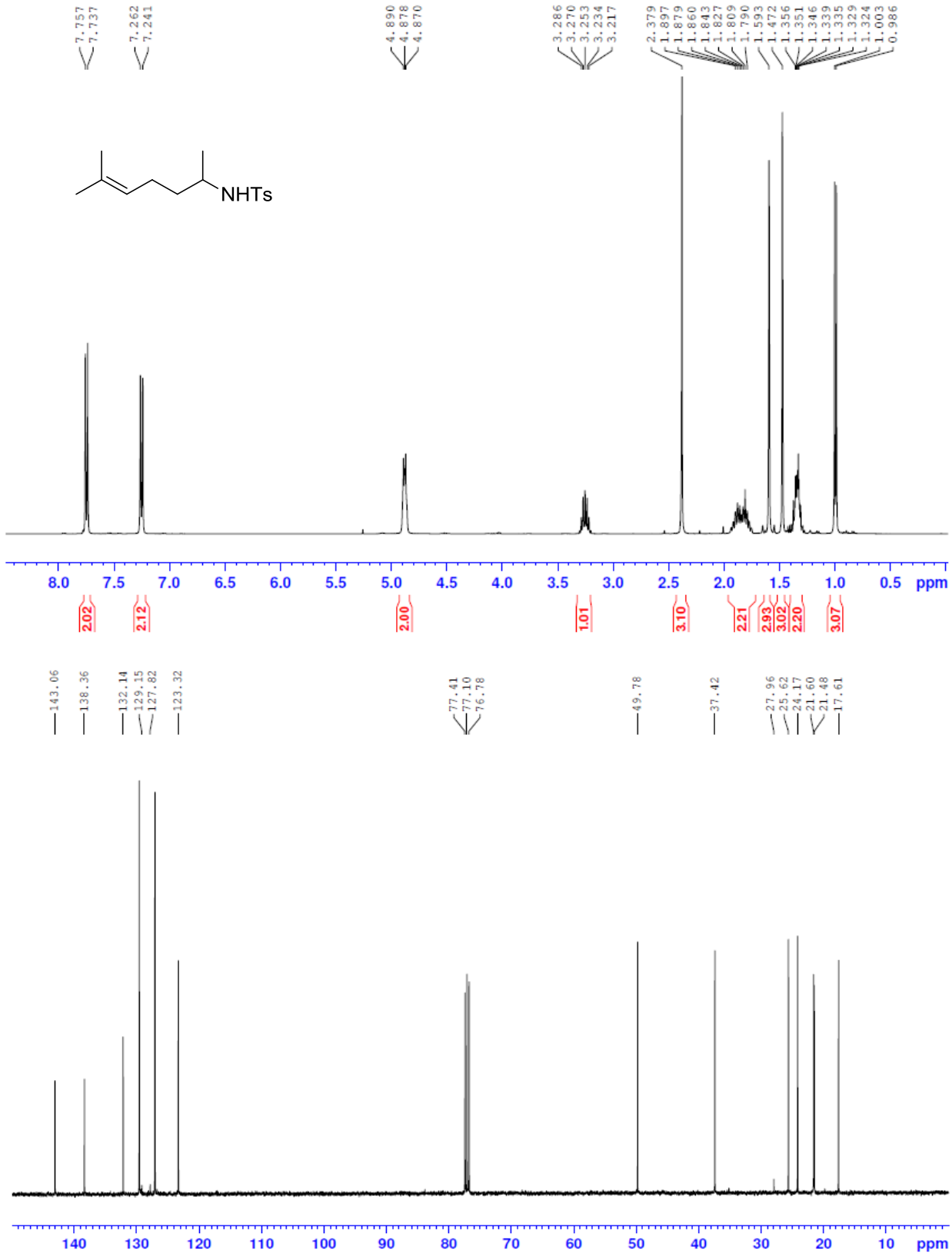

Compound **15a**

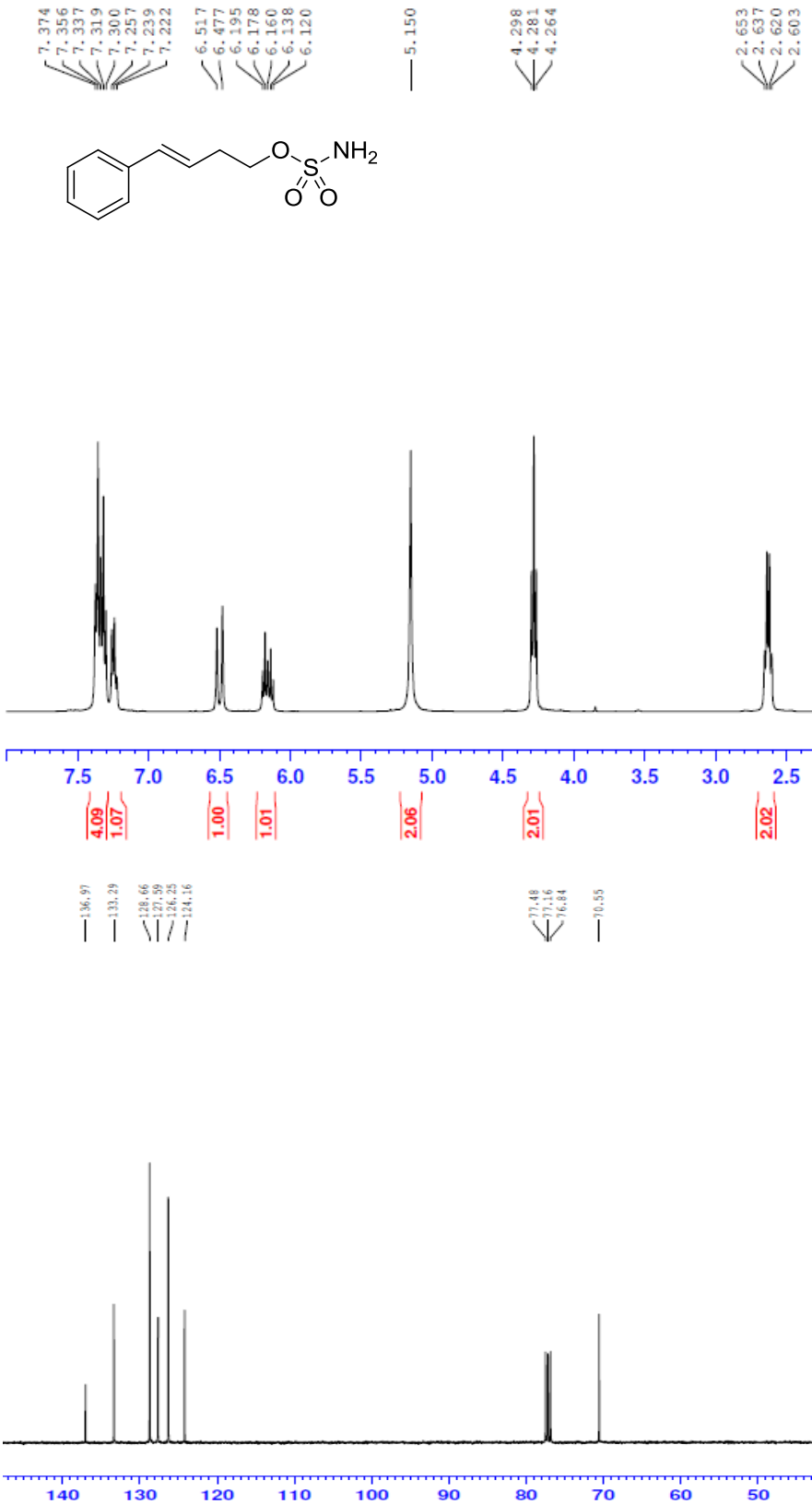

Compound **16**

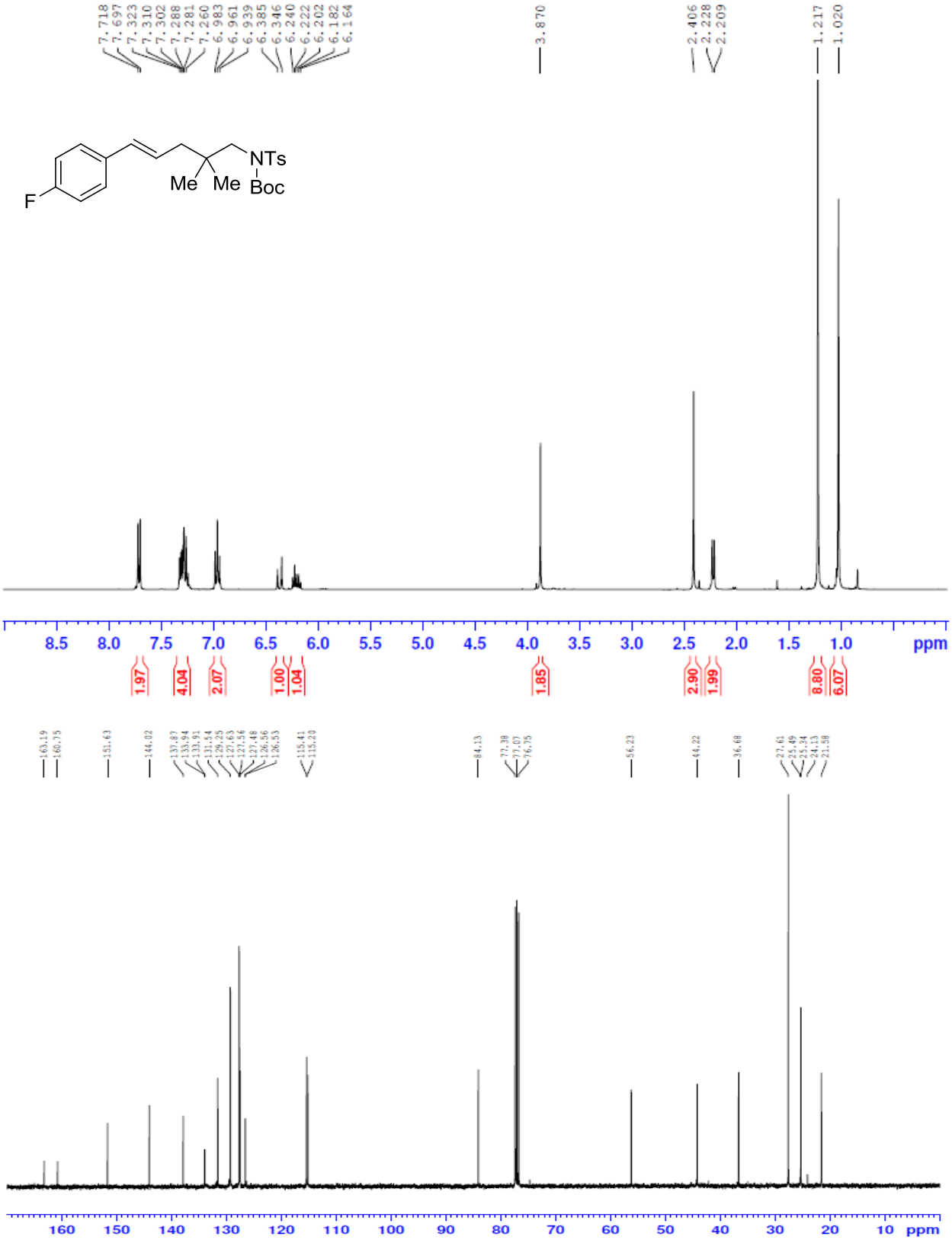
7.718
7.697
7.323
7.310
7.302
7.288
7.281
7.260
6.983
6.961
6.939
6.385
6.346
6.240
6.222
6.202
6.182
6.164
3.870
2.406
2.228
2.209
1.217
1.020
NTs
Me
Me
Boc
F
8.5
8.0
7.5
7.0
6.5
6.0
5.5
5.0
4.5
4.0
3.5
3.0
2.5
2.0
1.5
1.0
ppm
1.97
4.04
2.07
1.00
1.04
1.85
2.90
1.99
8.80
6.07
163.19
160.75
151.63
144.02
137.87
133.94
133.91
131.54
129.25
127.63
127.56
127.48
126.56
126.53
115.41
115.20
84.13
77.38
77.07
76.75
56.23
44.22
36.68
27.61
25.49
25.34
24.13
21.58
160
150
140
130
120
110
100
90
80
70
60
50
40
30
20
10
ppm

Compound **3b**

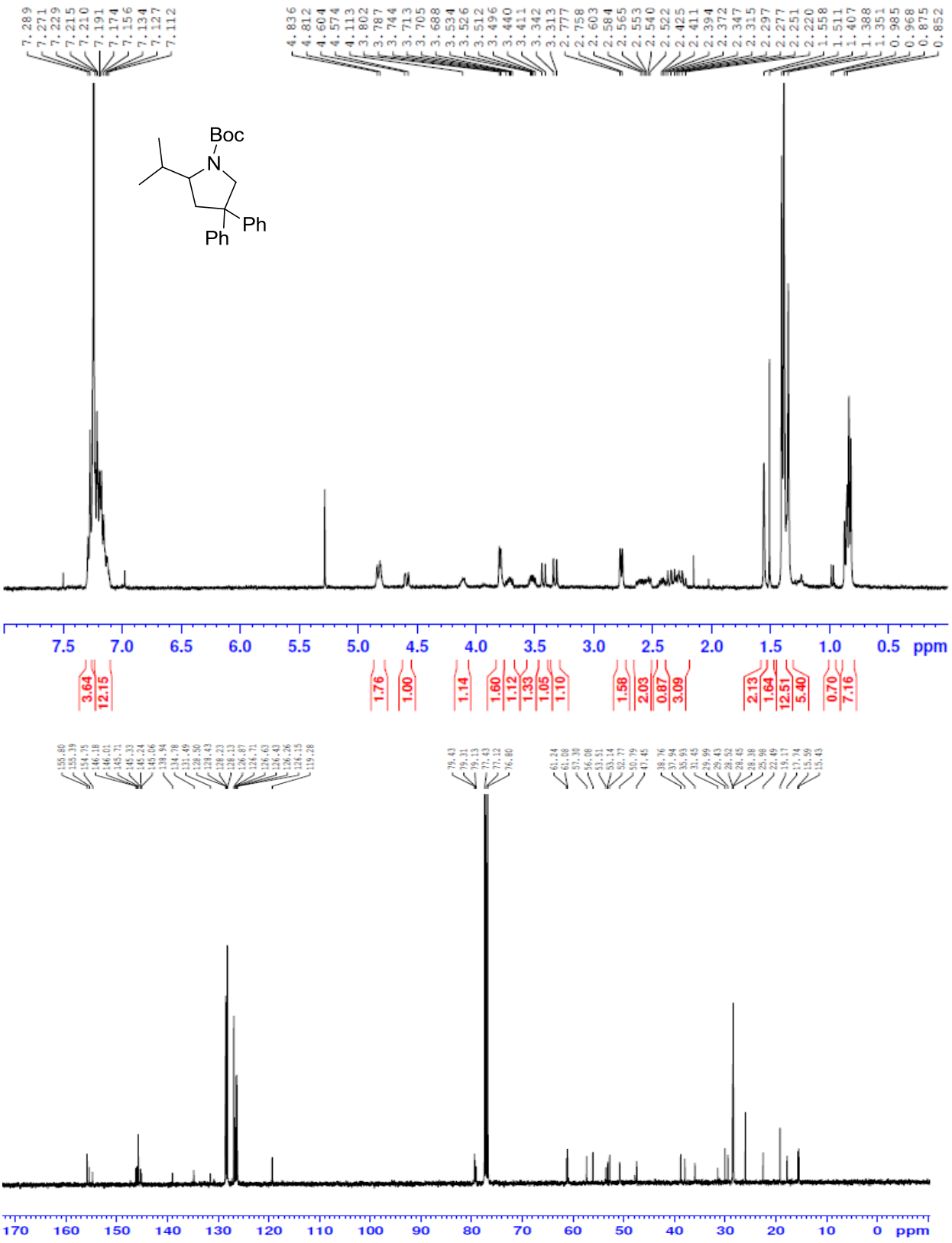

Compound **4b**

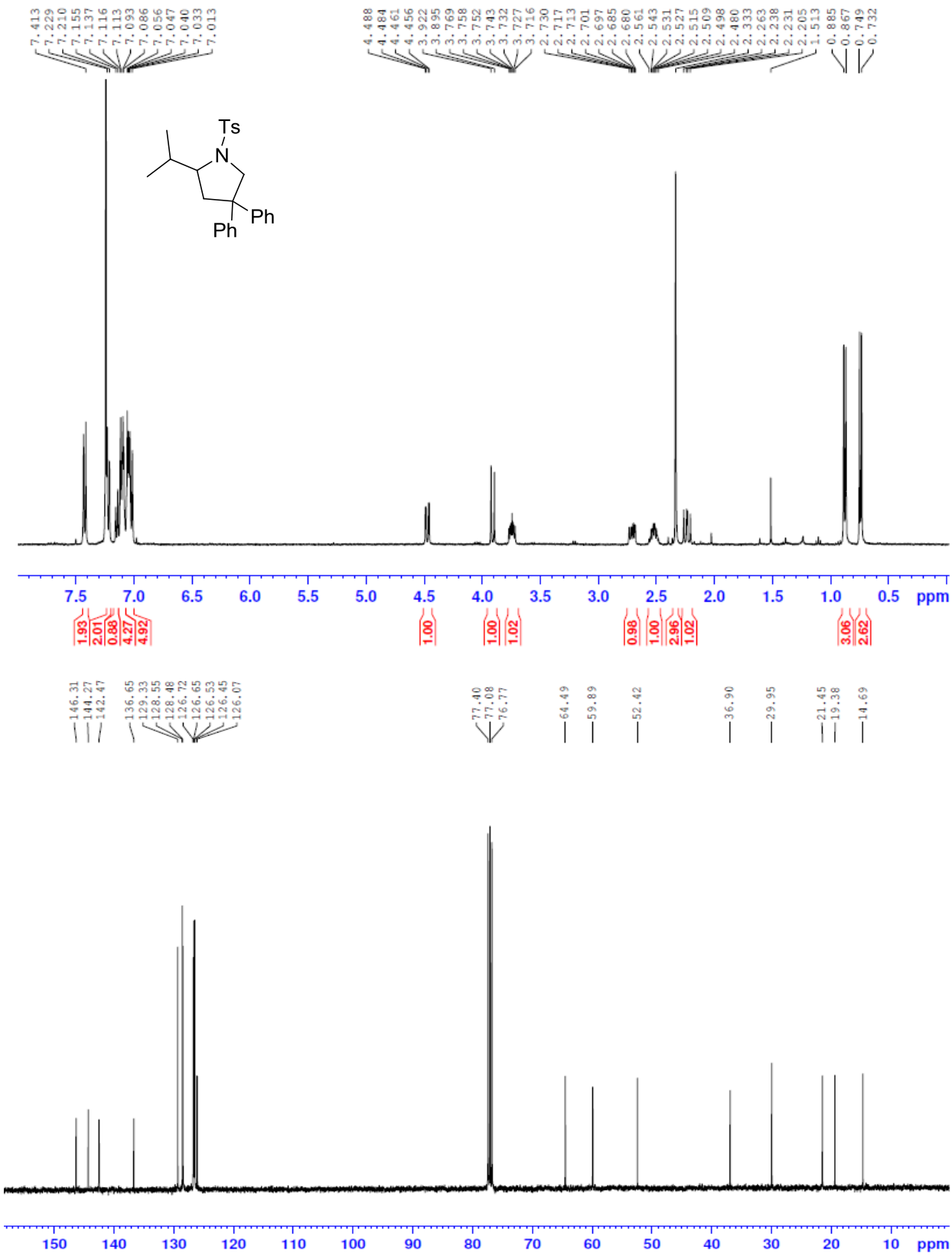
7.413
7.229
7.210
7.155
7.137
7.116
7.113
7.093
7.086
7.056
7.047
7.040
7.033
7.013
4.488
4.484
4.461
4.456
3.922
3.895
3.769
3.758
3.752
3.743
3.732
3.727
3.716
2.730
2.717
2.713
2.701
2.697
2.685
2.680
2.561
2.543
2.531
2.527
2.515
2.509
2.498
2.480
2.333
2.263
2.238
2.231
2.205
1.513
0.885
0.867
0.749
0.732
Ts
N
Ph
Ph
7.5
7.0
6.5
6.0
5.5
5.0
4.5
4.0
3.5
3.0
2.5
2.0
1.5
1.0
0.5
ppm
1.93
2.01
0.88
4.27
4.92
1.00
1.00
1.02
0.98
1.00
2.96
1.02
3.06
2.62
146.31
144.27
142.47
136.65
129.33
128.55
128.48
126.72
126.65
126.53
126.45
126.07
77.40
77.08
76.77
64.49
59.89
52.42
36.90
29.95
21.45
19.38
14.69
150
140
130
120
110
100
90
80
70
60
50
40
30
20
10
ppm

Compound **5b**

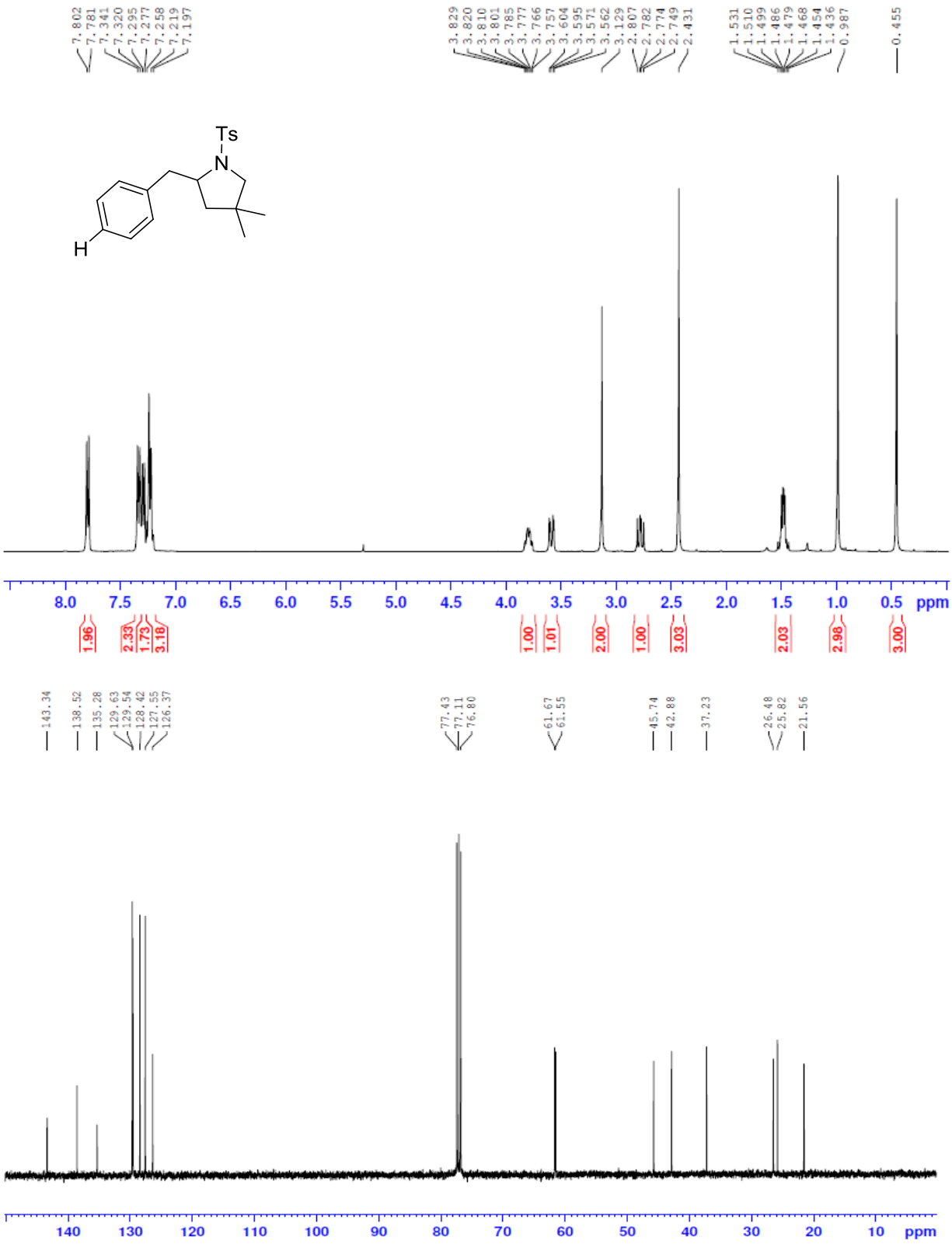
7.802
7.781
7.341
7.320
7.295
7.277
7.258
7.219
7.197
3.829
3.820
3.810
3.801
3.785
3.777
3.766
3.757
3.604
3.595
3.571
3.562
3.129
2.807
2.782
2.774
2.749
2.431
1.531
1.510
1.499
1.486
1.479
1.468
1.454
1.436
0.987
0.455
Ts
N
H
8.0
7.5
7.0
6.5
6.0
5.5
5.0
4.5
4.0
3.5
3.0
2.5
2.0
1.5
1.0
0.5
ppm
1.96
2.33
1.73
3.18
1.00
1.01
2.00
1.00
3.03
2.03
2.98
3.00
143.34
138.52
135.28
129.63
129.54
128.42
127.55
126.37
77.43
77.11
76.80
61.67
61.55
45.74
42.88
37.23
26.48
25.82
21.56
140
130
120
110
100
90
80
70
60
50
40
30
20
10
ppm

Compound **6b**

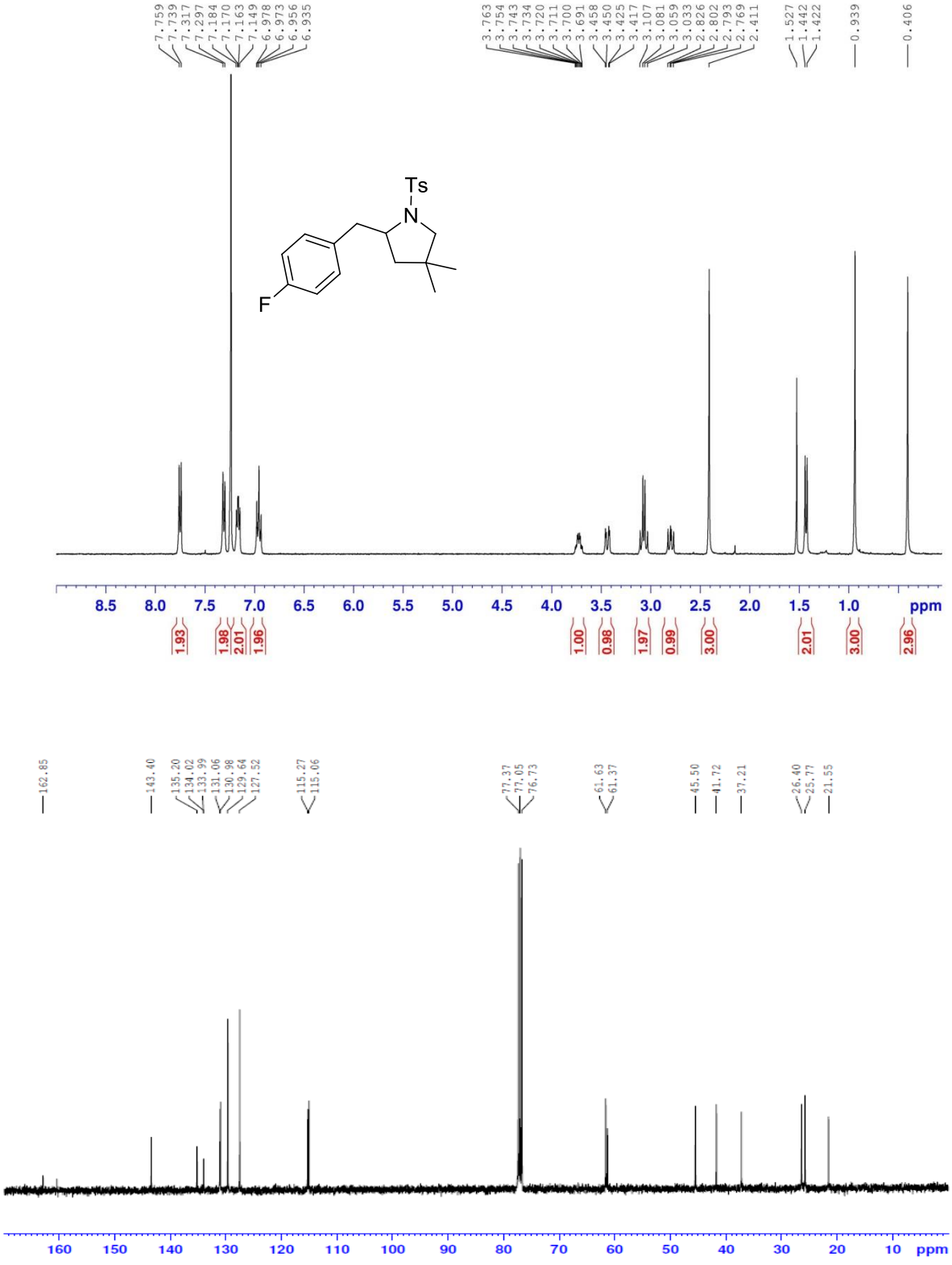
7.759
7.739
7.317
7.297
7.184
7.170
7.163
7.149
6.978
6.973
6.956
6.935
3.763
3.754
3.743
3.734
3.720
3.711
3.700
3.691
3.458
3.450
3.425
3.417
3.107
3.081
3.059
3.033
2.826
2.802
2.793
2.769
2.411
1.527
1.442
1.422
0.939
0.406
Ts
N
F
8.5
8.0
7.5
7.0
6.5
6.0
5.5
5.0
4.5
4.0
3.5
3.0
2.5
2.0
1.5
1.0
ppm
1.93
1.98
2.01
1.96
1.00
0.98
1.97
0.99
3.00
2.01
3.00
2.96
162.85
143.40
135.20
134.02
133.99
131.06
130.98
129.64
127.52
115.27
115.06
77.37
77.05
76.73
61.63
61.37
45.50
41.72
37.21
26.40
25.77
21.55
160
150
140
130
120
110
100
90
80
70
60
50
40
30
20
10
ppm

Compound **7b**

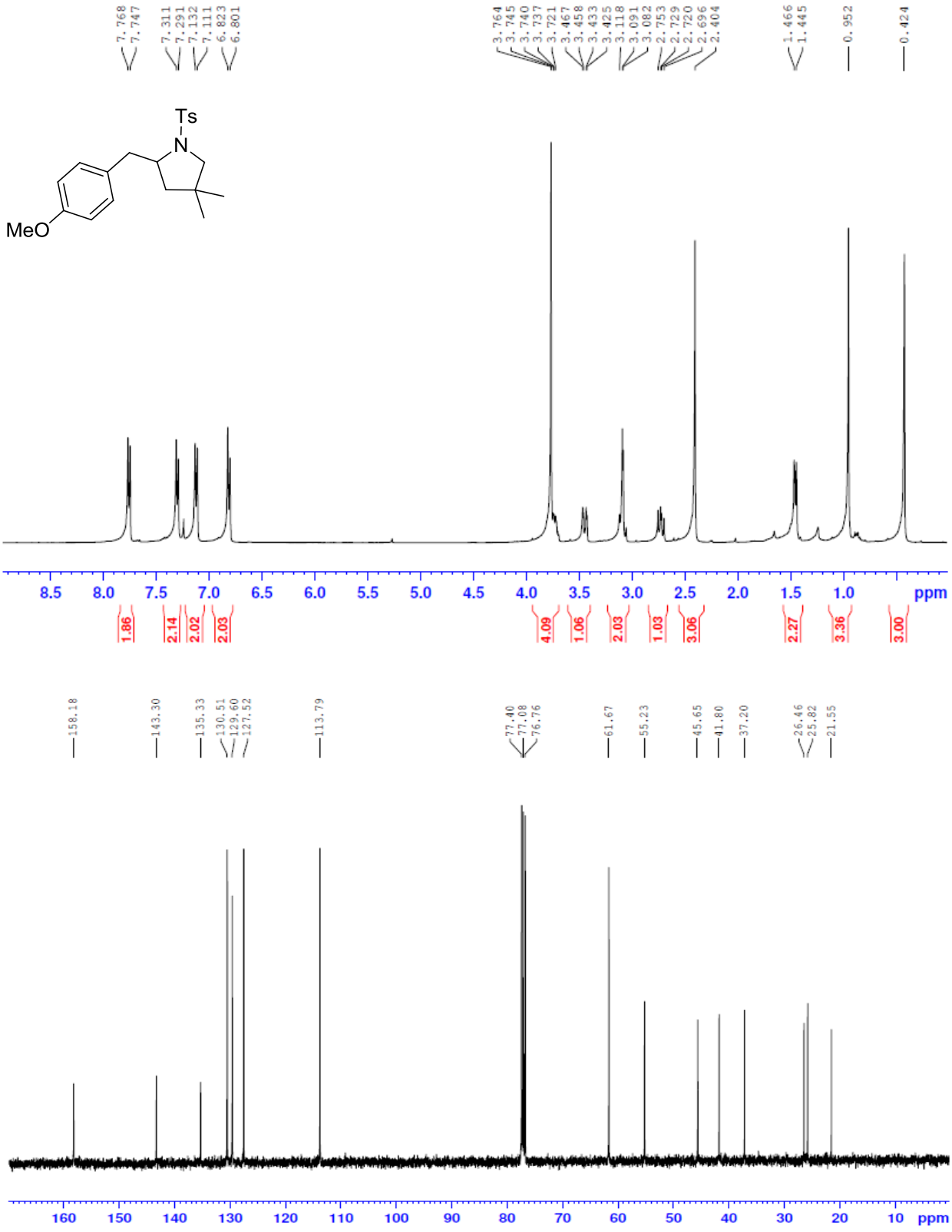
7.768
7.747
7.311
7.291
7.132
7.111
6.823
6.801
3.764
3.745
3.740
3.737
3.721
3.467
3.458
3.433
3.425
3.118
3.091
3.082
2.753
2.729
2.720
2.696
2.404
1.466
1.445
0.952
0.424
Ts
N
MeO
8.5
8.0
7.5
7.0
6.5
6.0
5.5
5.0
4.5
4.0
3.5
3.0
2.5
2.0
1.5
1.0
ppm
1.86
2.14
2.02
2.03
4.09
1.06
2.03
1.03
3.06
2.27
3.36
3.00
158.18
143.30
135.33
130.51
129.60
127.52
113.79
77.40
77.08
76.76
61.67
55.23
45.65
41.80
37.20
26.46
25.82
21.55
160
150
140
130
120
110
100
90
80
70
60
50
40
30
20
10
ppm

Compound **8b**

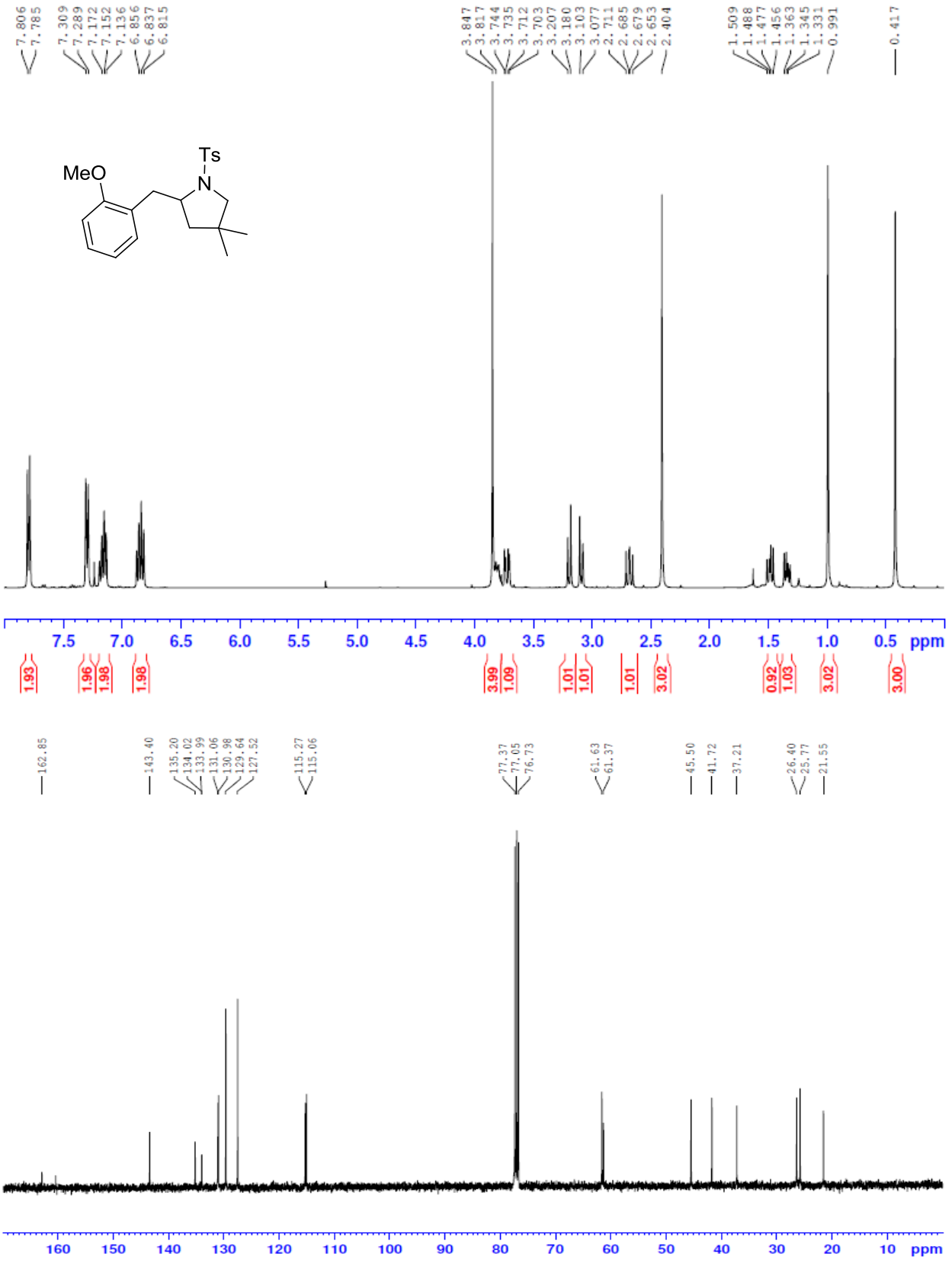
7.806
7.785
7.309
7.289
7.172
7.152
7.136
6.856
6.837
6.815
3.847
3.817
3.744
3.735
3.712
3.703
3.207
3.180
3.103
3.077
2.711
2.685
2.679
2.653
2.404
1.509
1.488
1.477
1.456
1.363
1.345
1.331
0.991
0.417
MeO
Ts
N
7.5
7.0
6.5
6.0
5.5
5.0
4.5
4.0
3.5
3.0
2.5
2.0
1.5
1.0
0.5
ppm
1.93
1.96
1.98
1.98
3.99
1.09
1.01
1.01
1.01
3.02
0.92
1.03
3.02
3.00
162.85
143.40
135.20
134.02
133.99
131.06
130.98
129.64
127.52
115.27
115.06
77.37
77.05
76.73
61.63
61.37
45.50
41.72
37.21
26.40
25.77
21.55
160
150
140
130
120
110
100
90
80
70
60
50
40
30
20
10
ppm

Compound **9b**

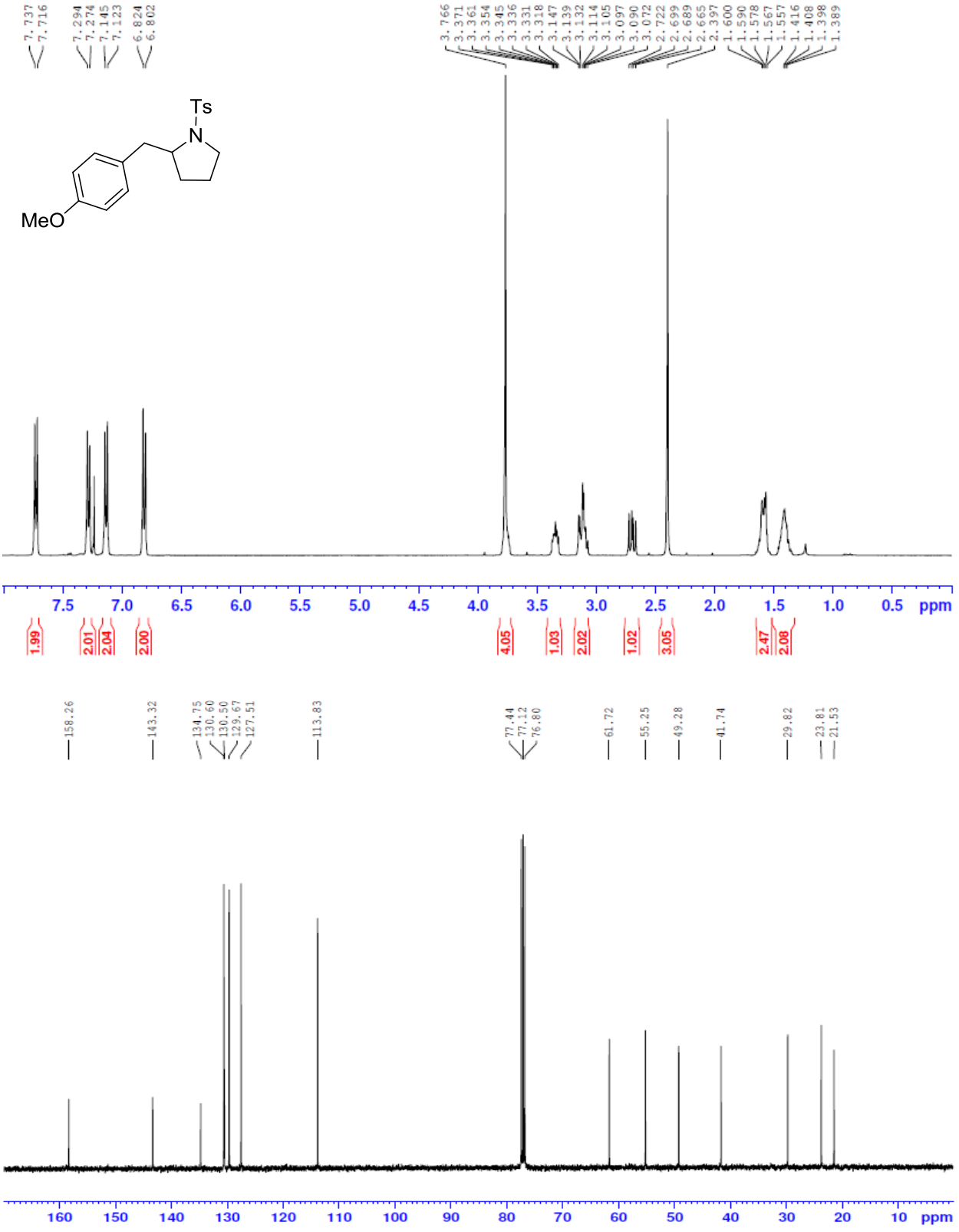
7.737
7.716
7.294
7.274
7.145
7.123
6.824
6.802
3.766
3.371
3.361
3.354
3.345
3.336
3.331
3.318
3.147
3.139
3.132
3.114
3.105
3.097
3.090
3.072
2.722
2.699
2.689
2.665
2.397
1.600
1.590
1.578
1.567
1.557
1.416
1.408
1.398
1.389
Ts
N
MeO
7.5
7.0
6.5
6.0
5.5
5.0
4.5
4.0
3.5
3.0
2.5
2.0
1.5
1.0
0.5
ppm
1.99
2.01
2.04
2.00
4.05
1.03
2.02
1.02
3.05
2.47
2.08
158.26
143.32
134.75
130.60
130.50
129.67
127.51
113.83
77.44
77.22
76.80
61.72
55.25
49.28
41.74
29.82
23.81
21.53
160
150
140
130
120
110
100
90
80
70
60
50
40
30
20
10
ppm

Compound **10b**

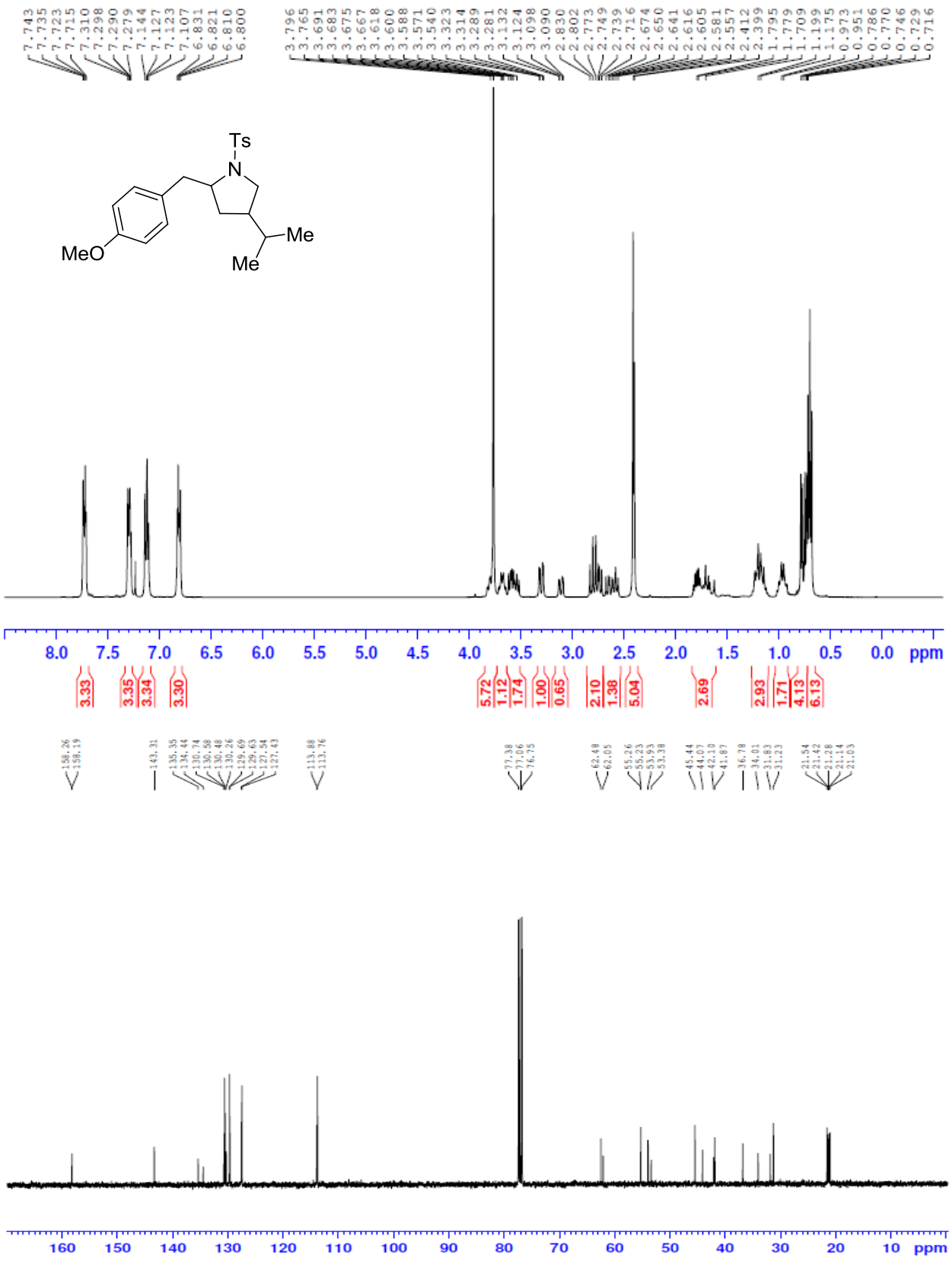

Compound **11b**

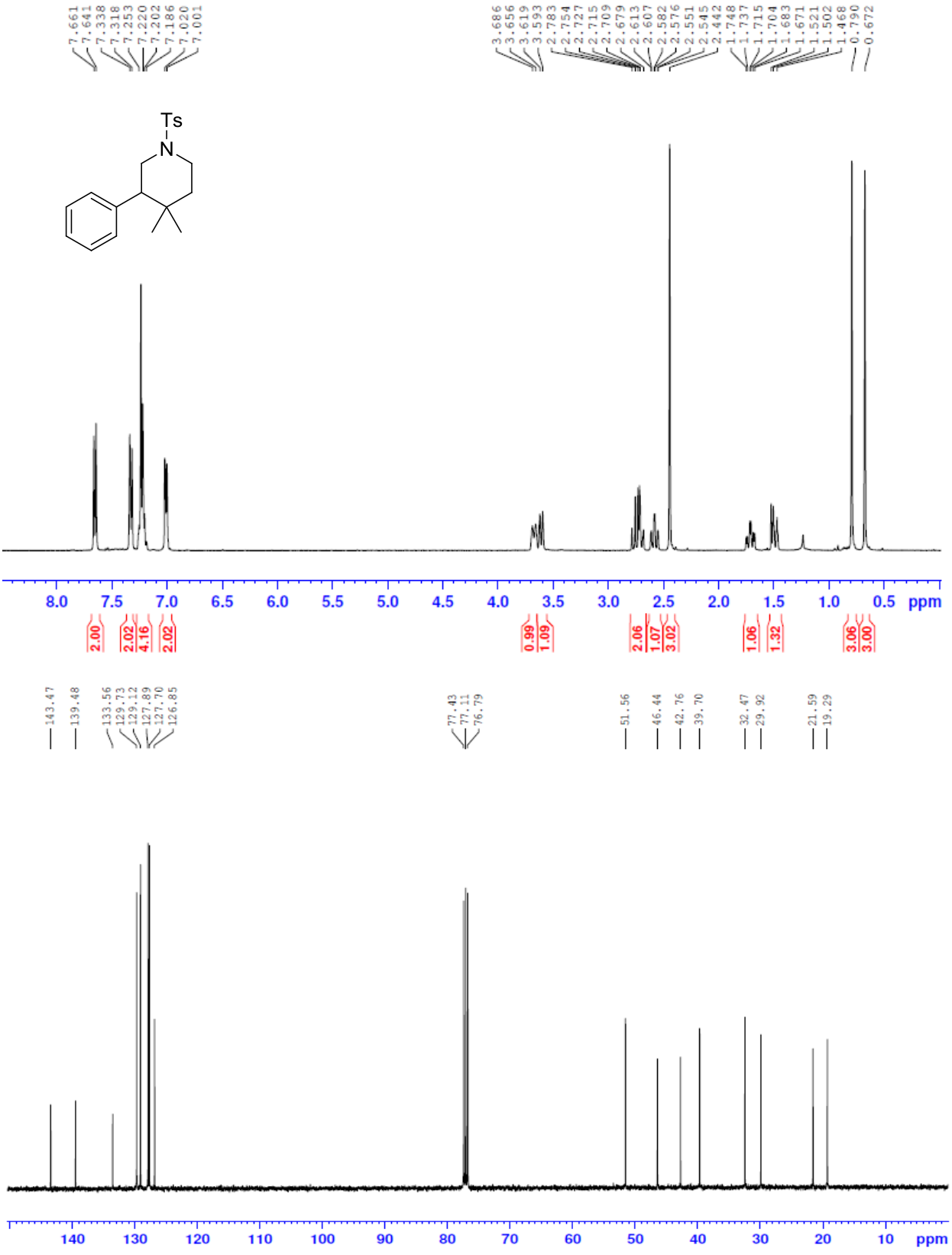

Compound **12b**

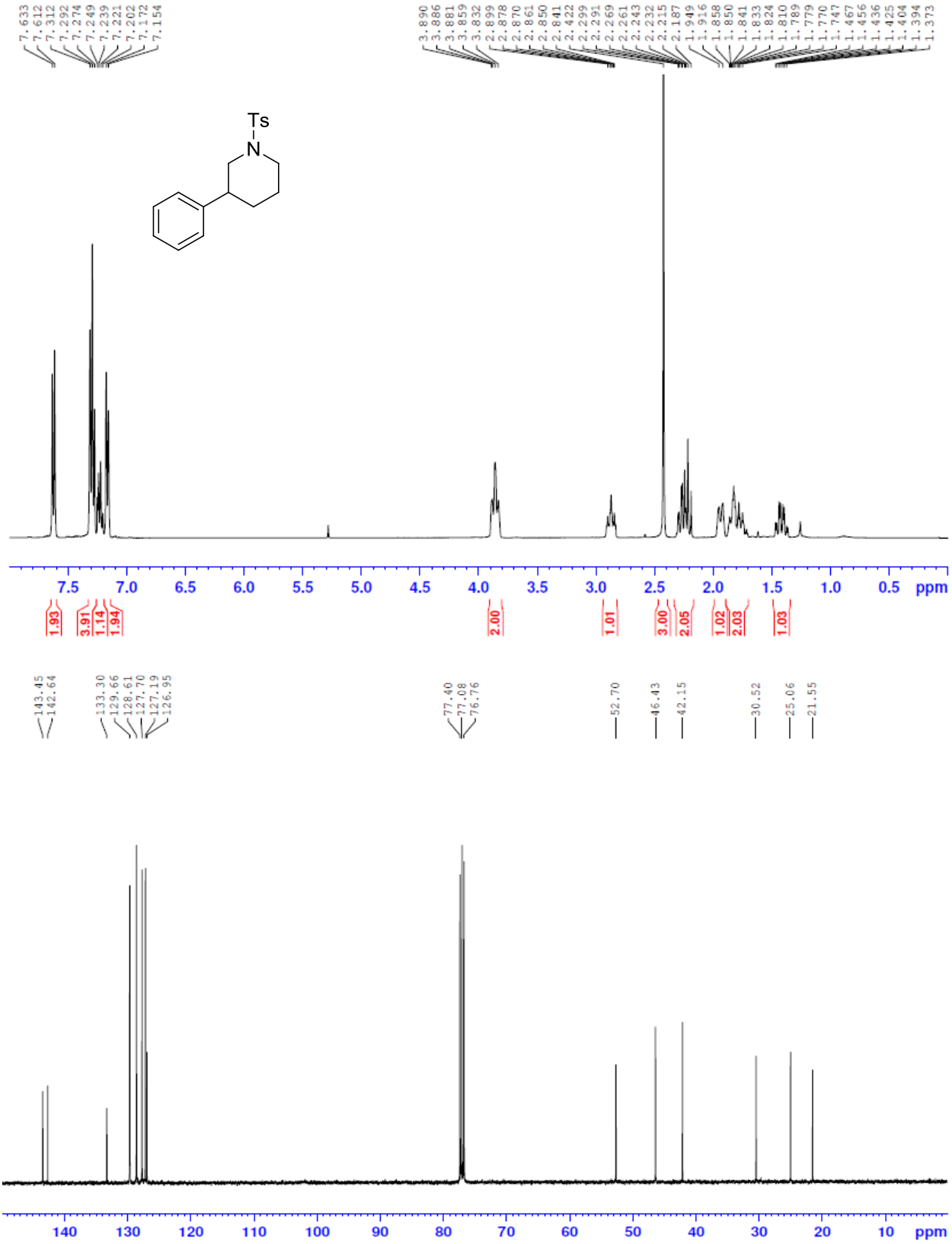

Compound **13b**

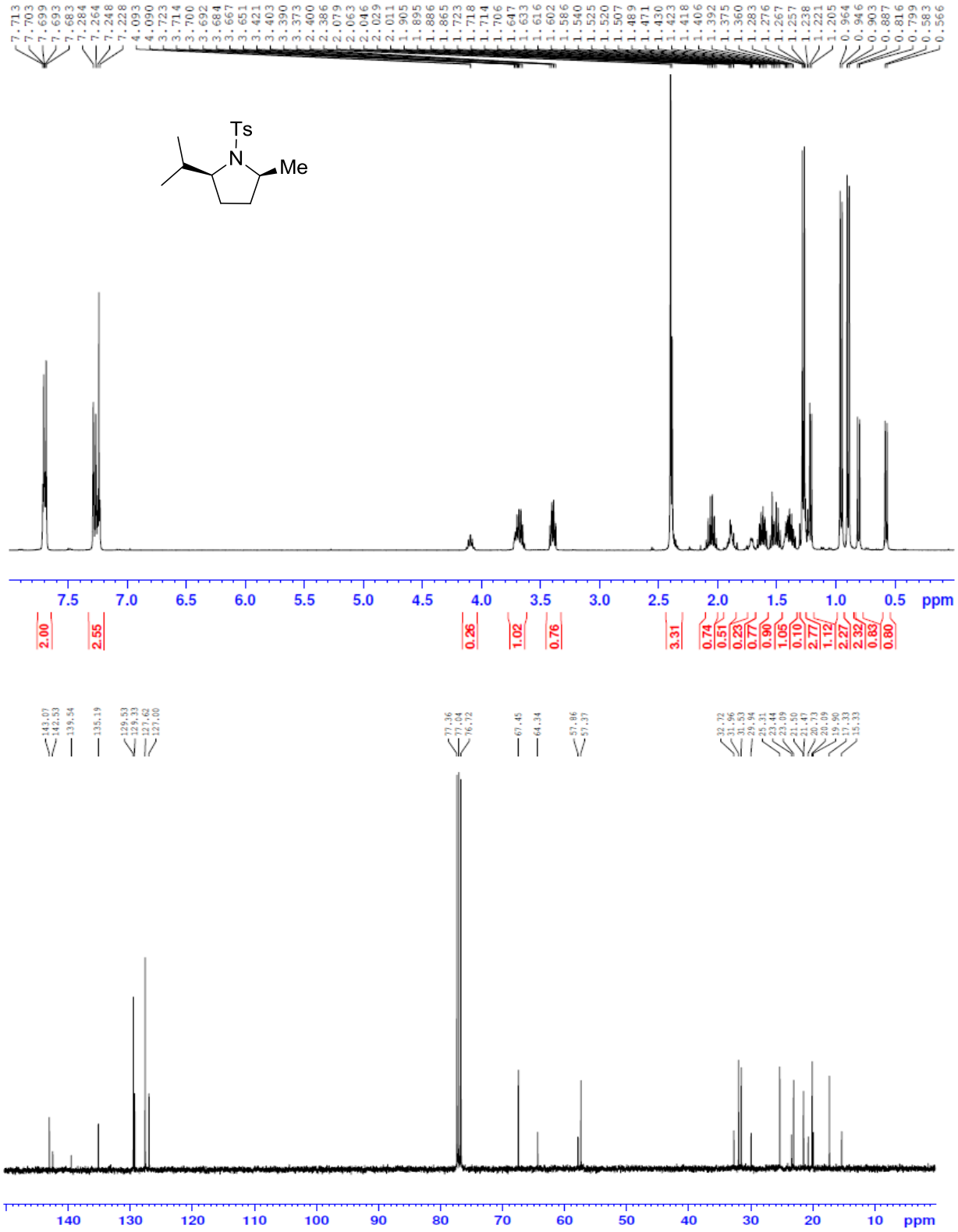

Compound **14b**

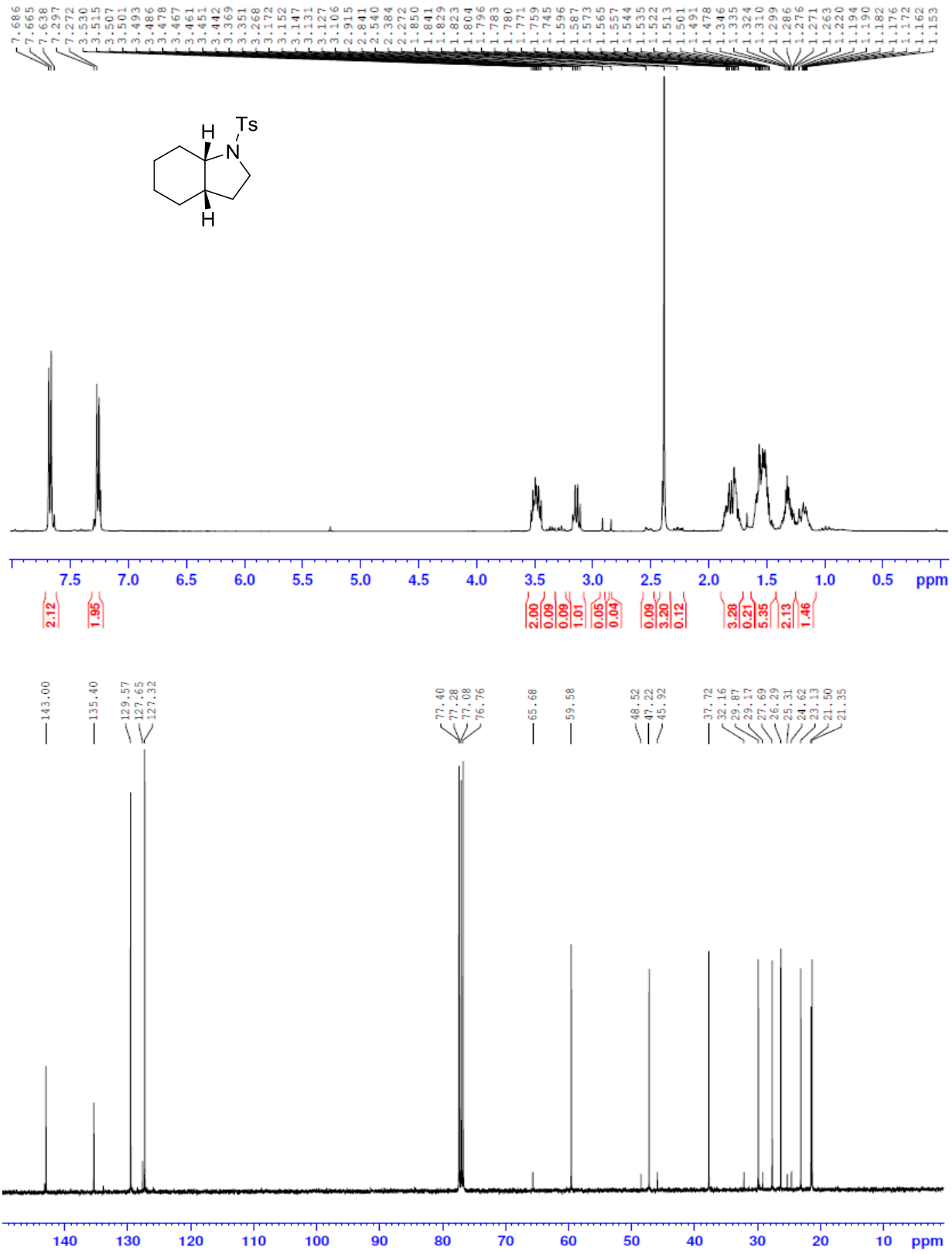

Compound **15b**

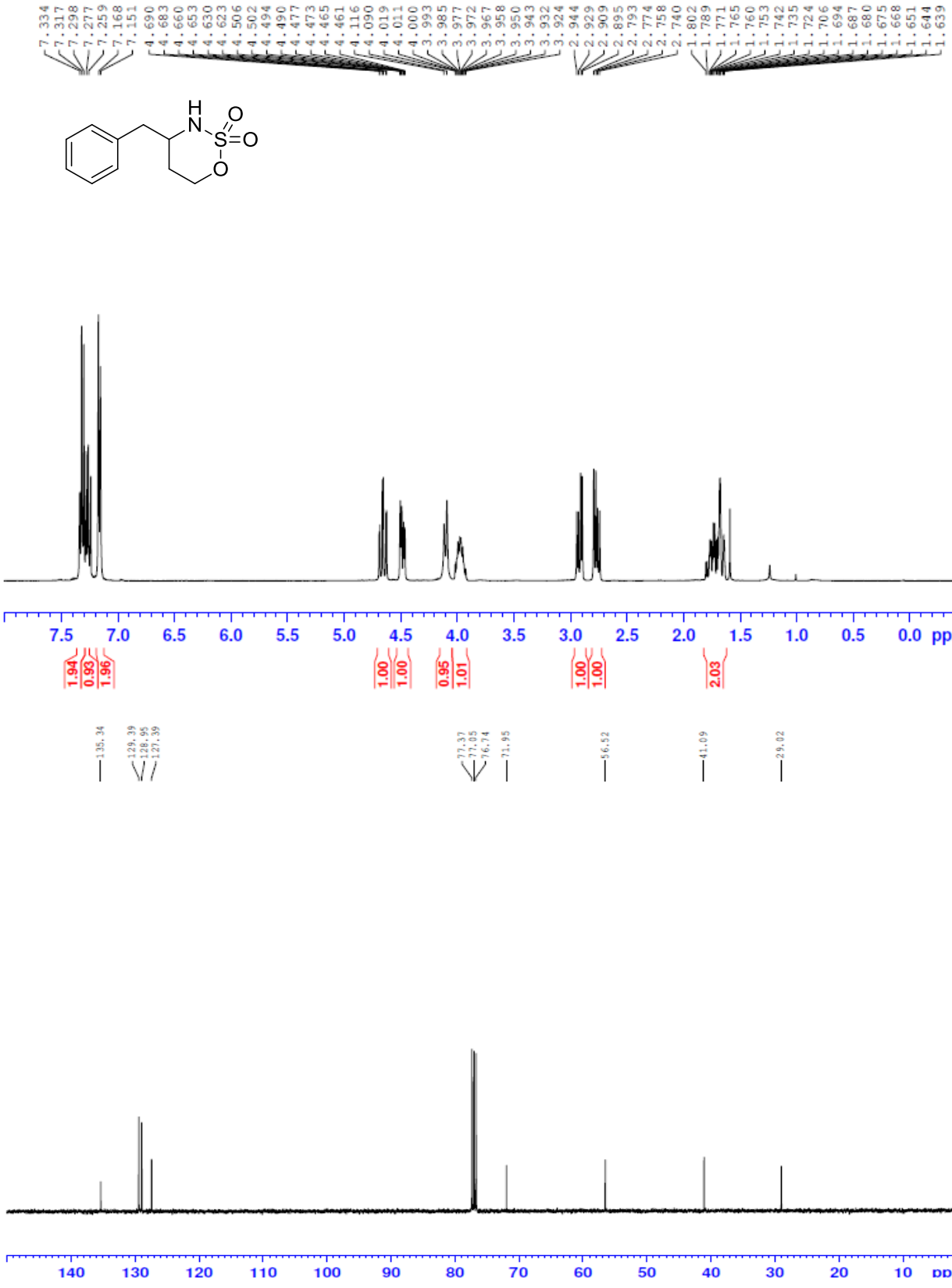

Compound **17b**

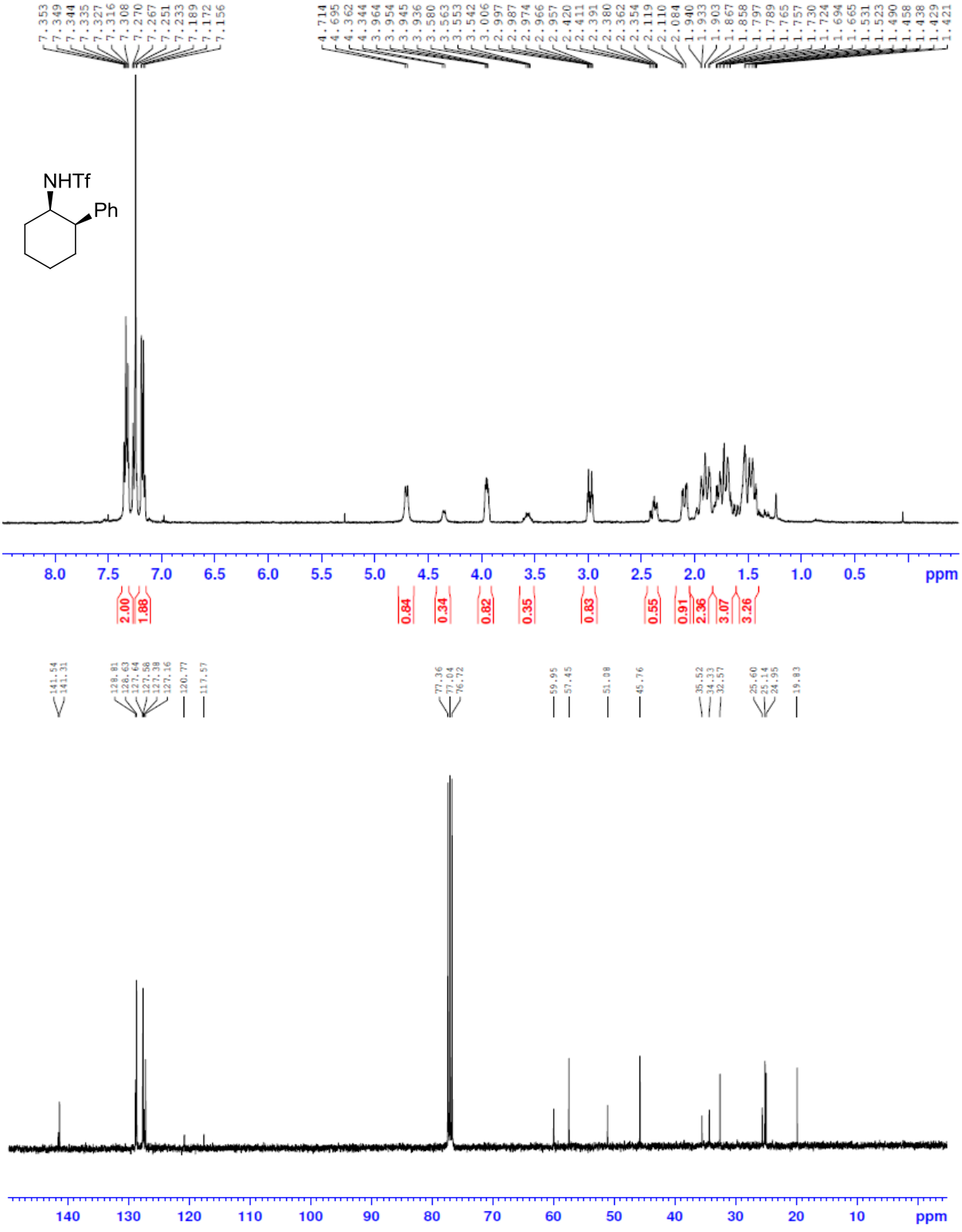

Compound **18b**

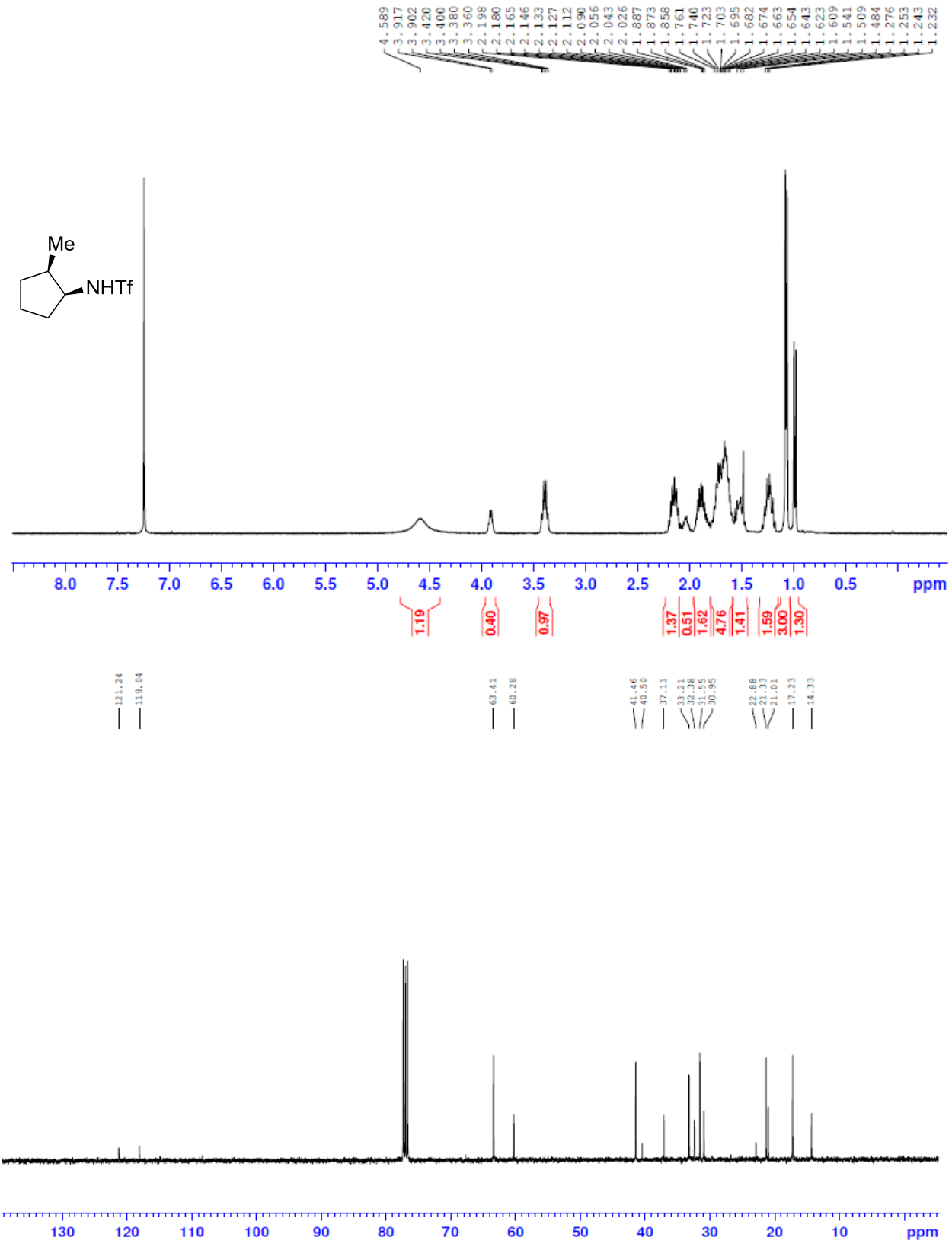

Compound **19b**

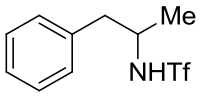

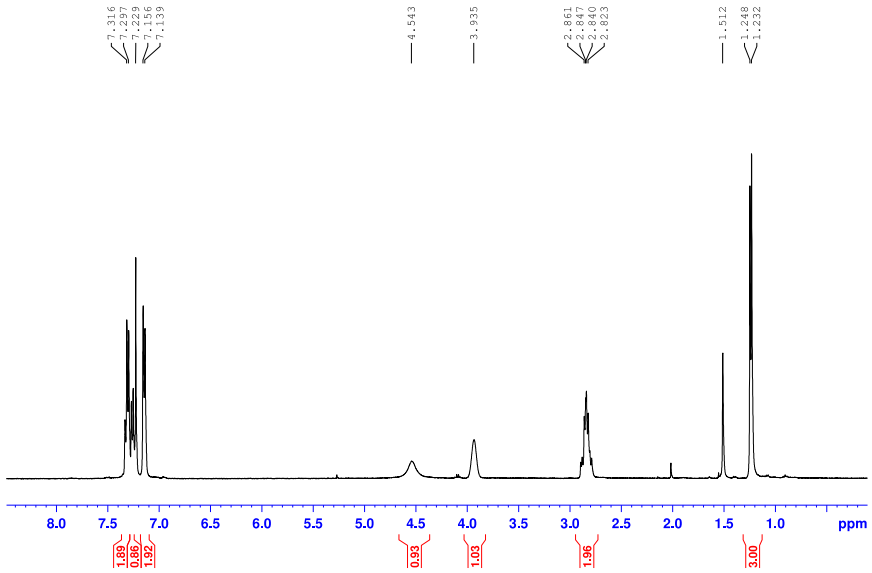

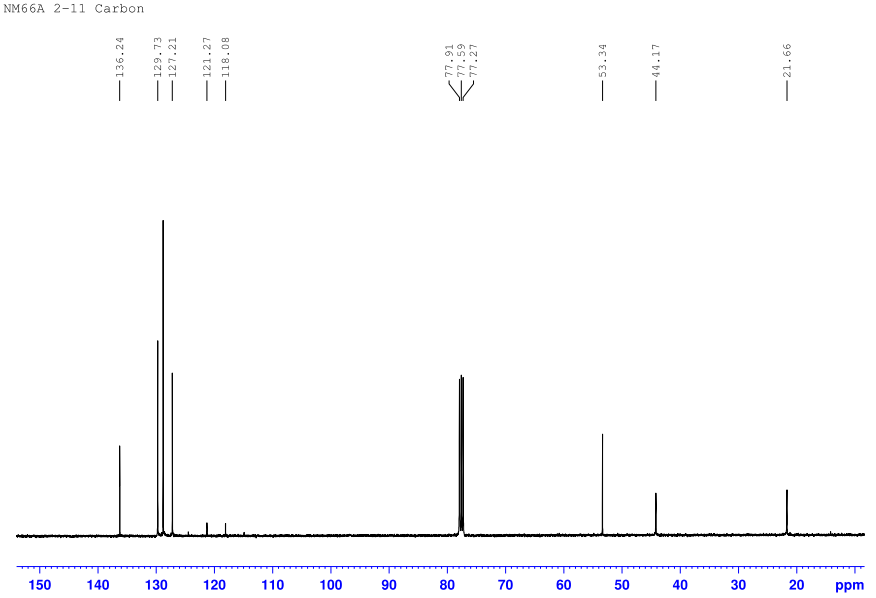

Compound **20b**

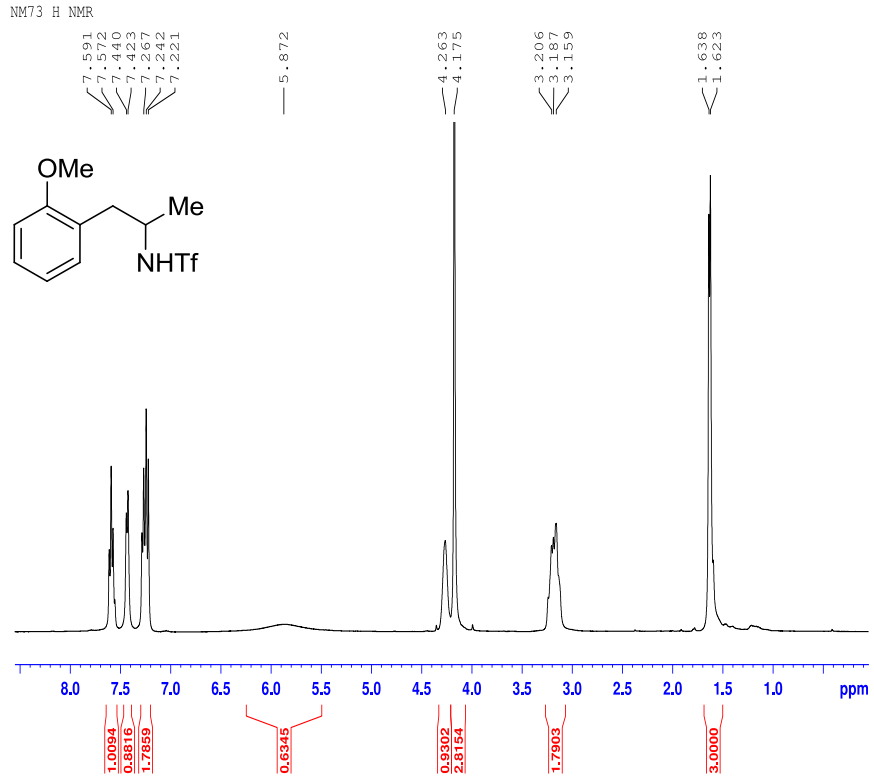

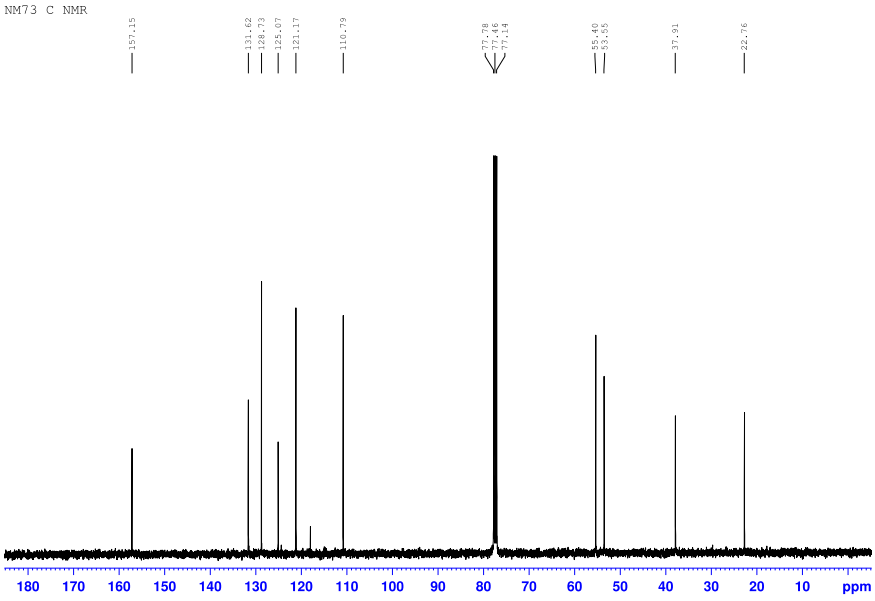

Compound **21b**

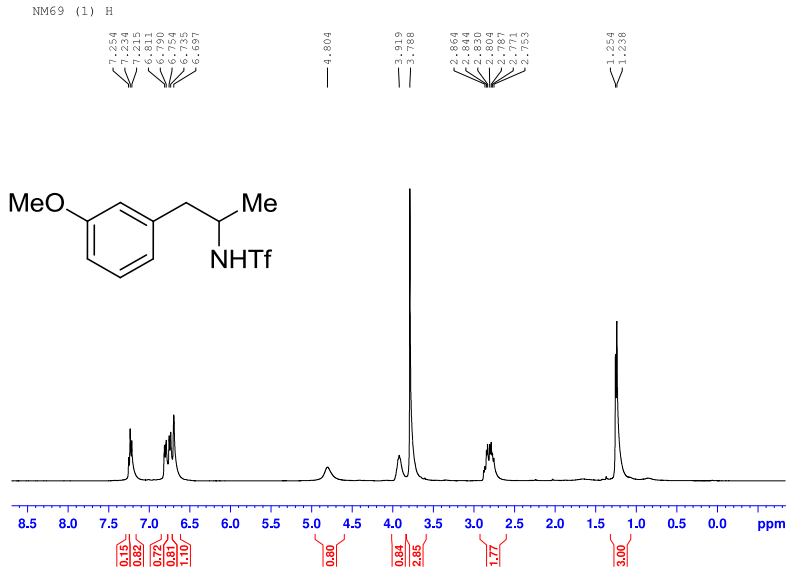

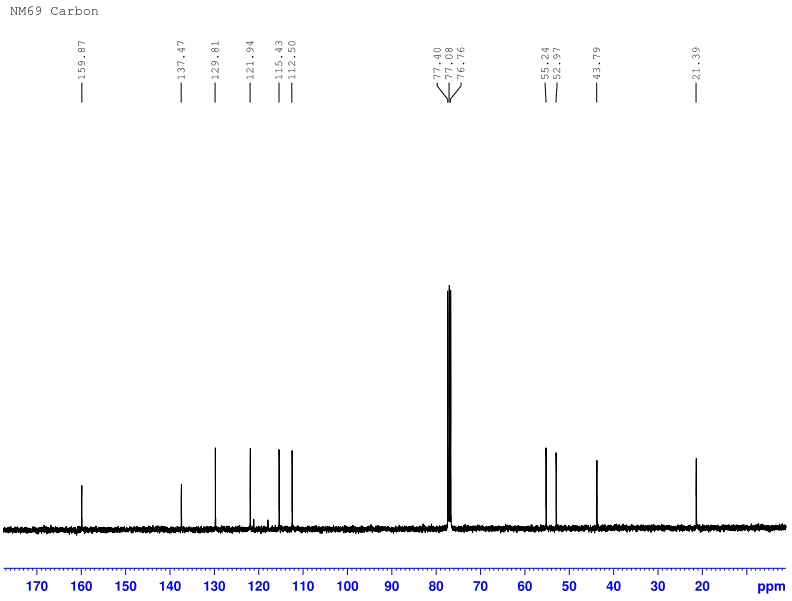

Compound **22b**

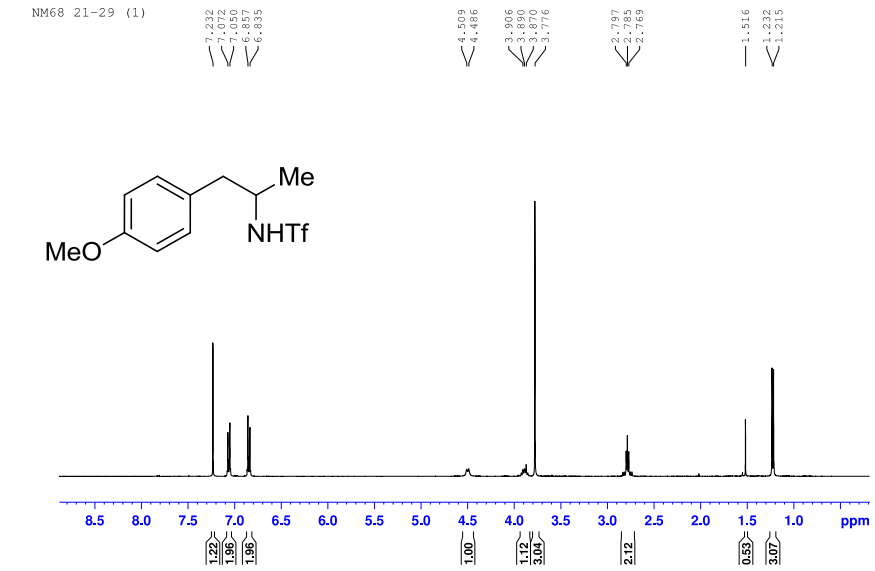

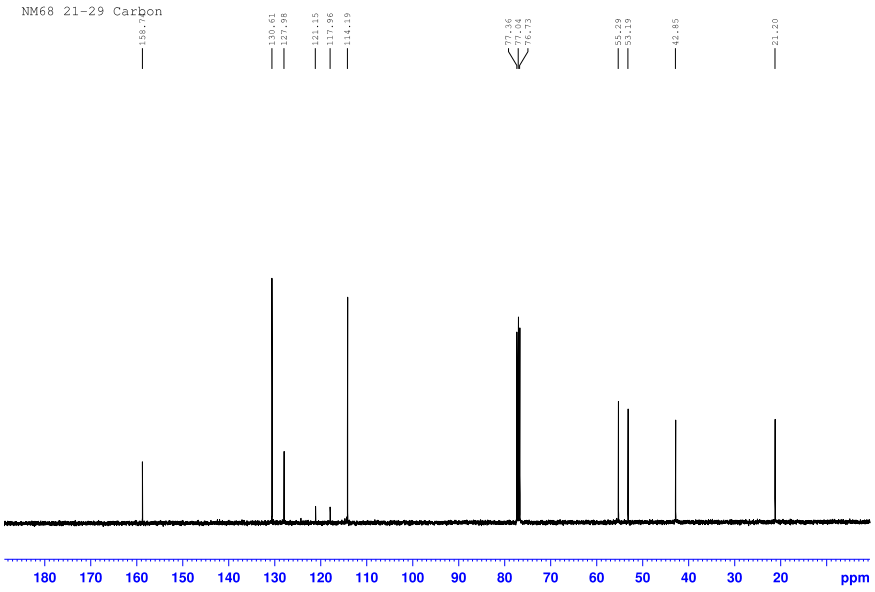

Compound **23b**

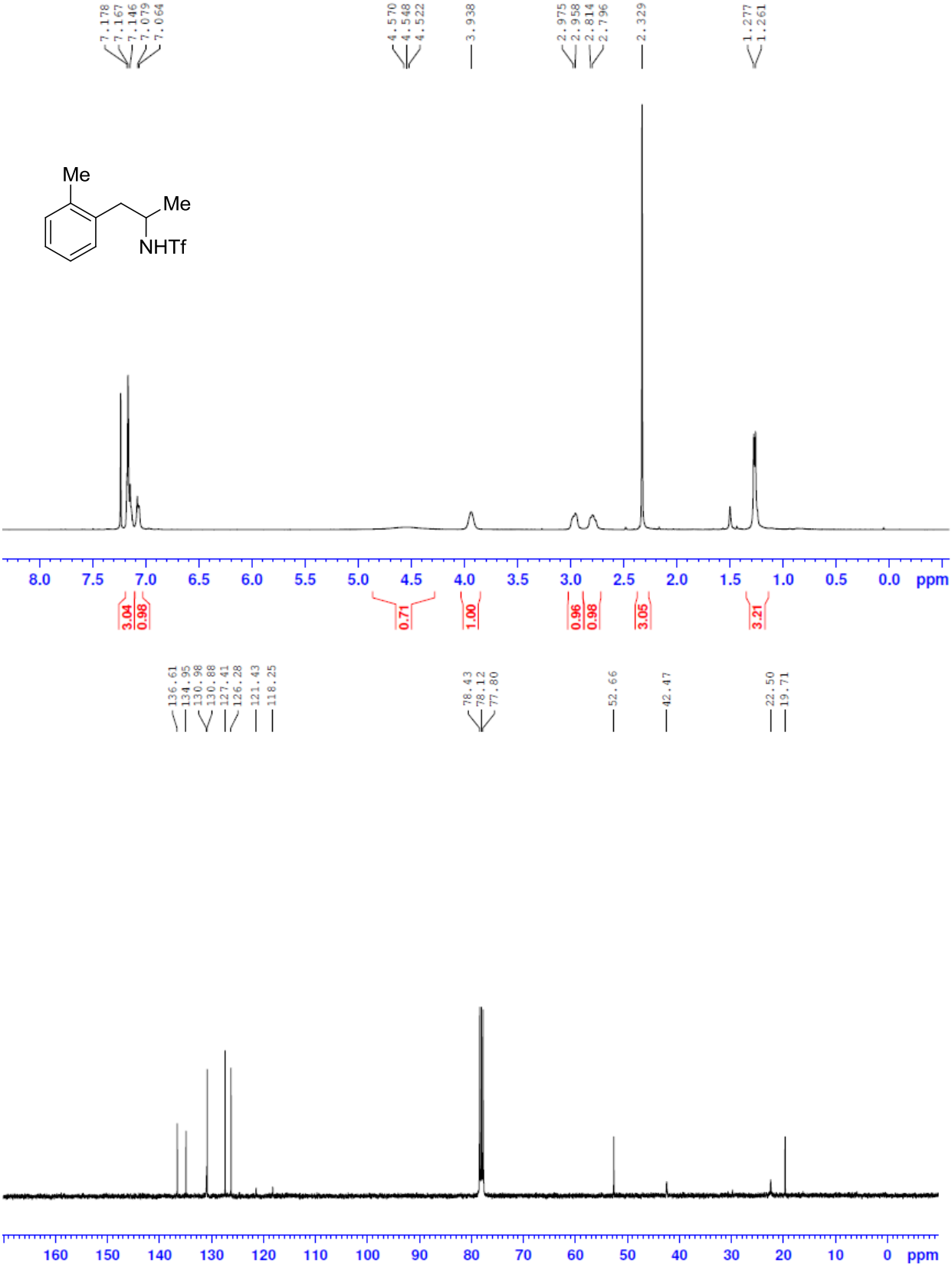

Compound **24b**

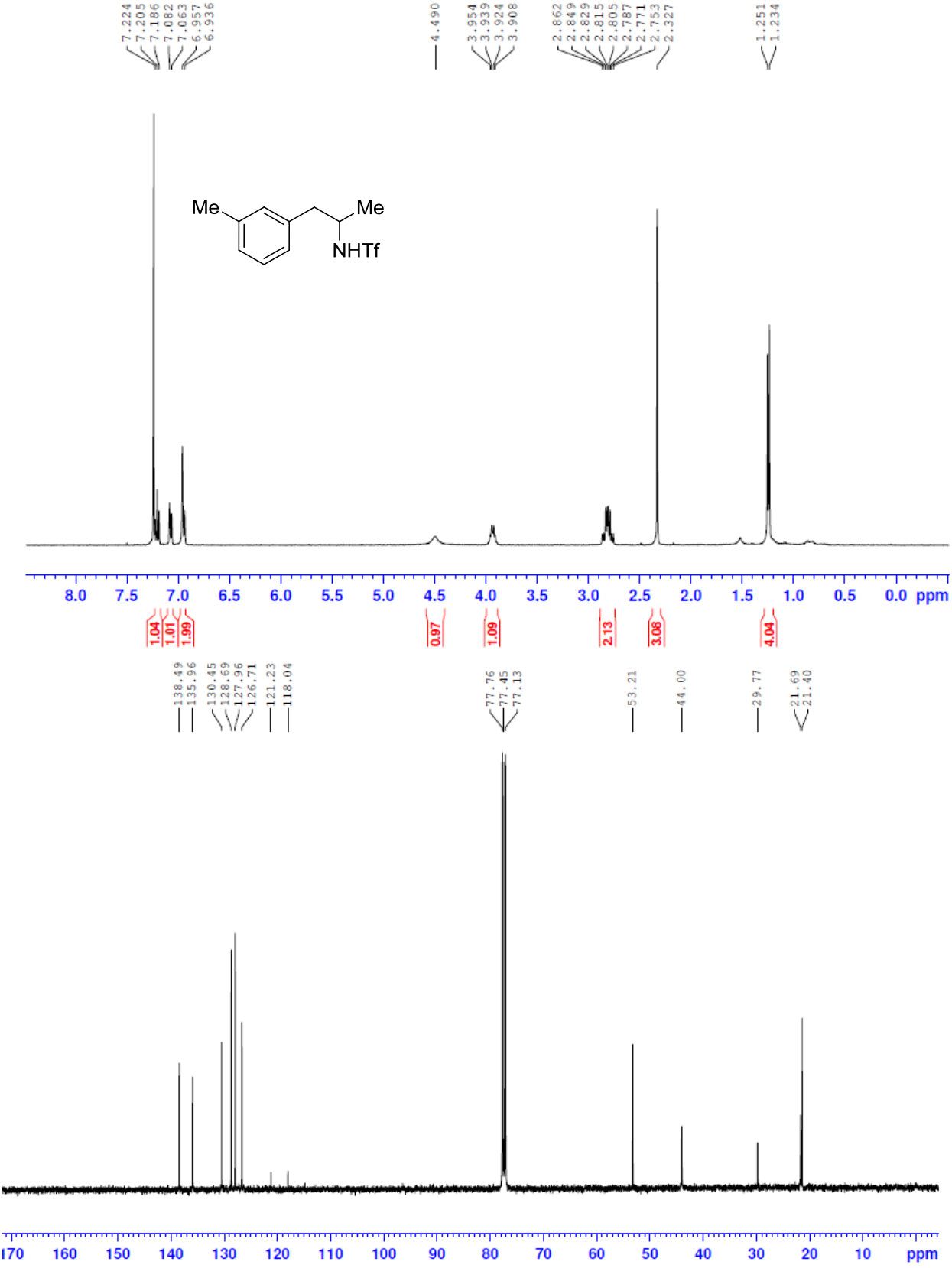

Compound **25b**

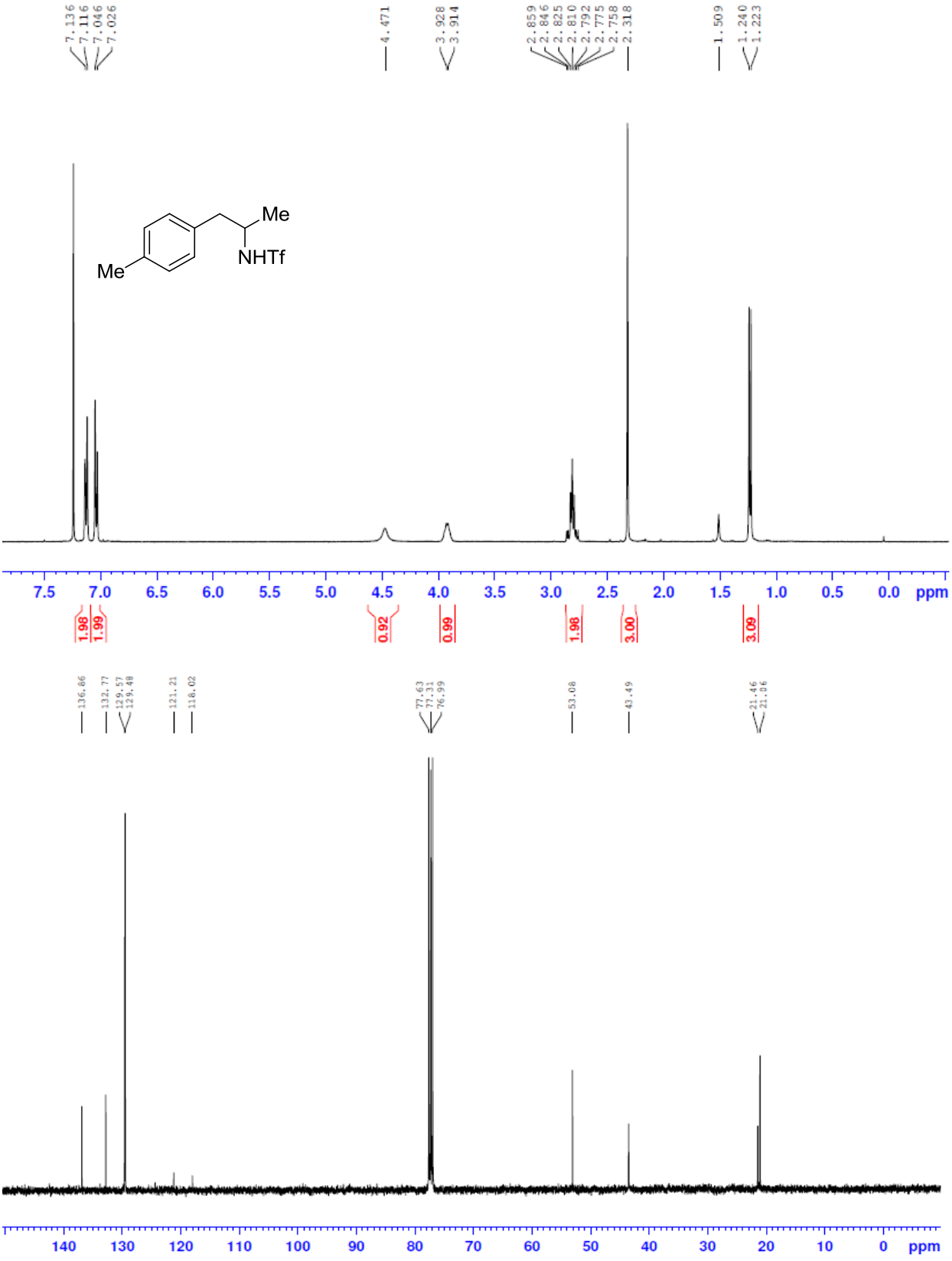

Compound **26b**

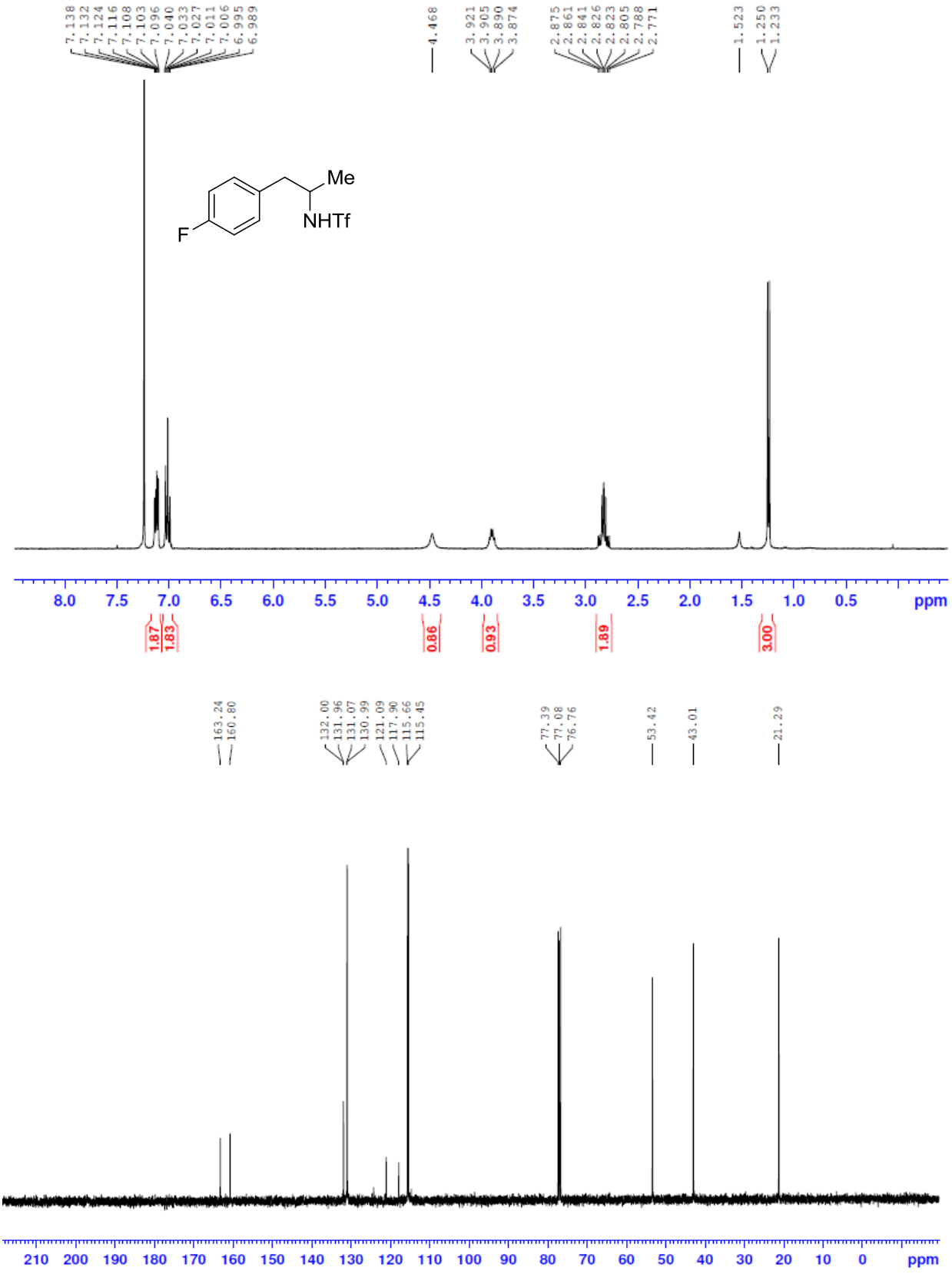

Compound **27b**

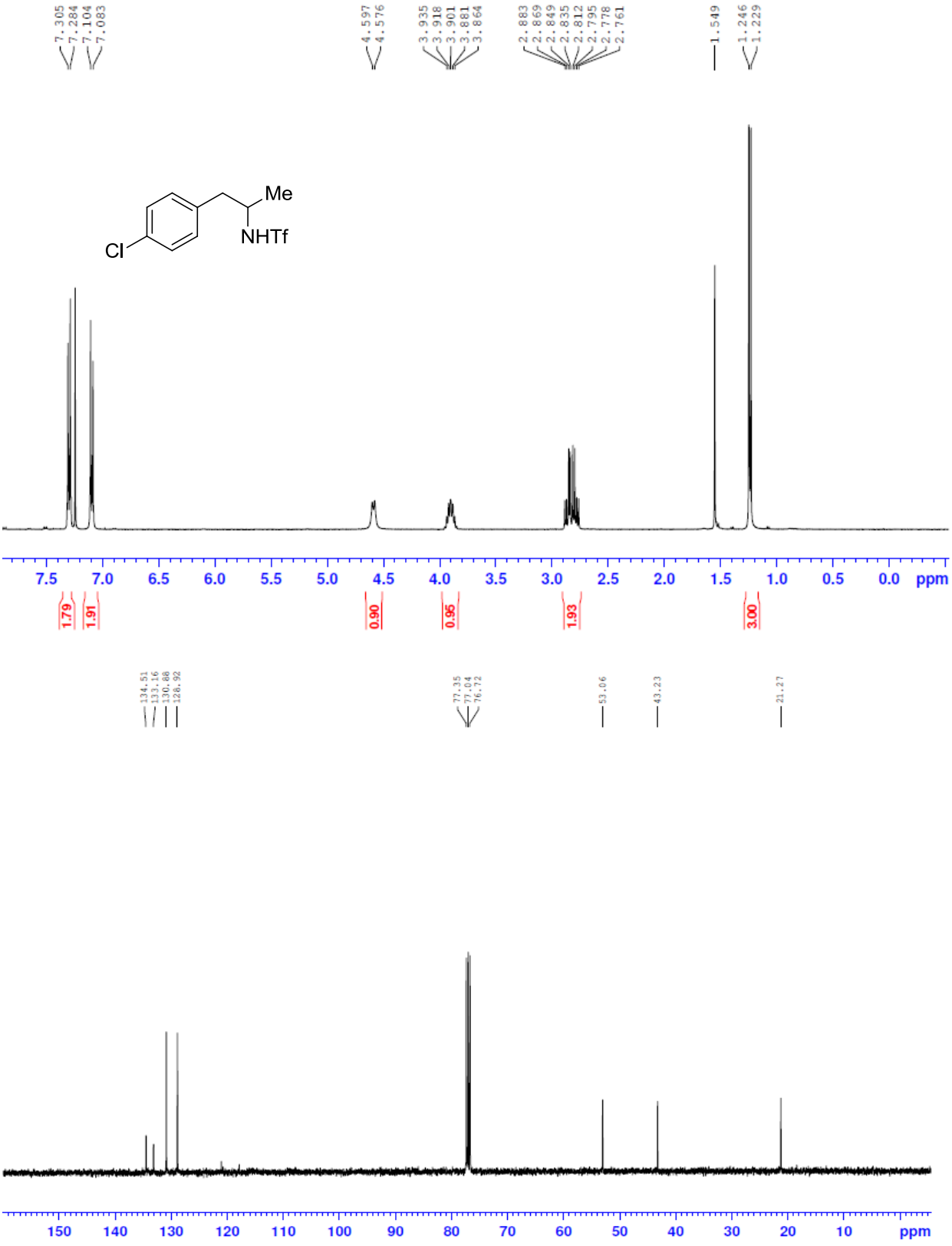

Compound **28b**

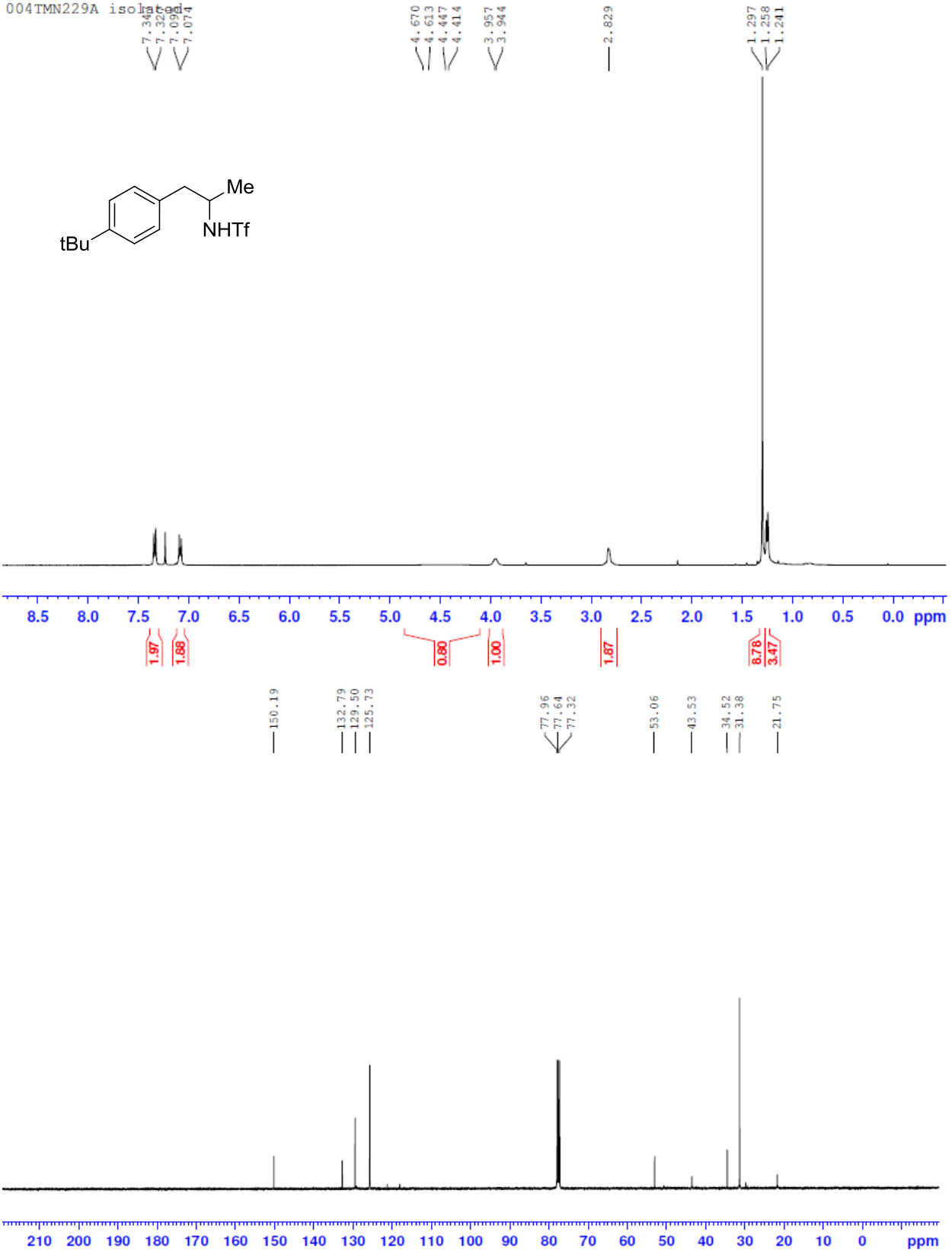

Compound **29b**

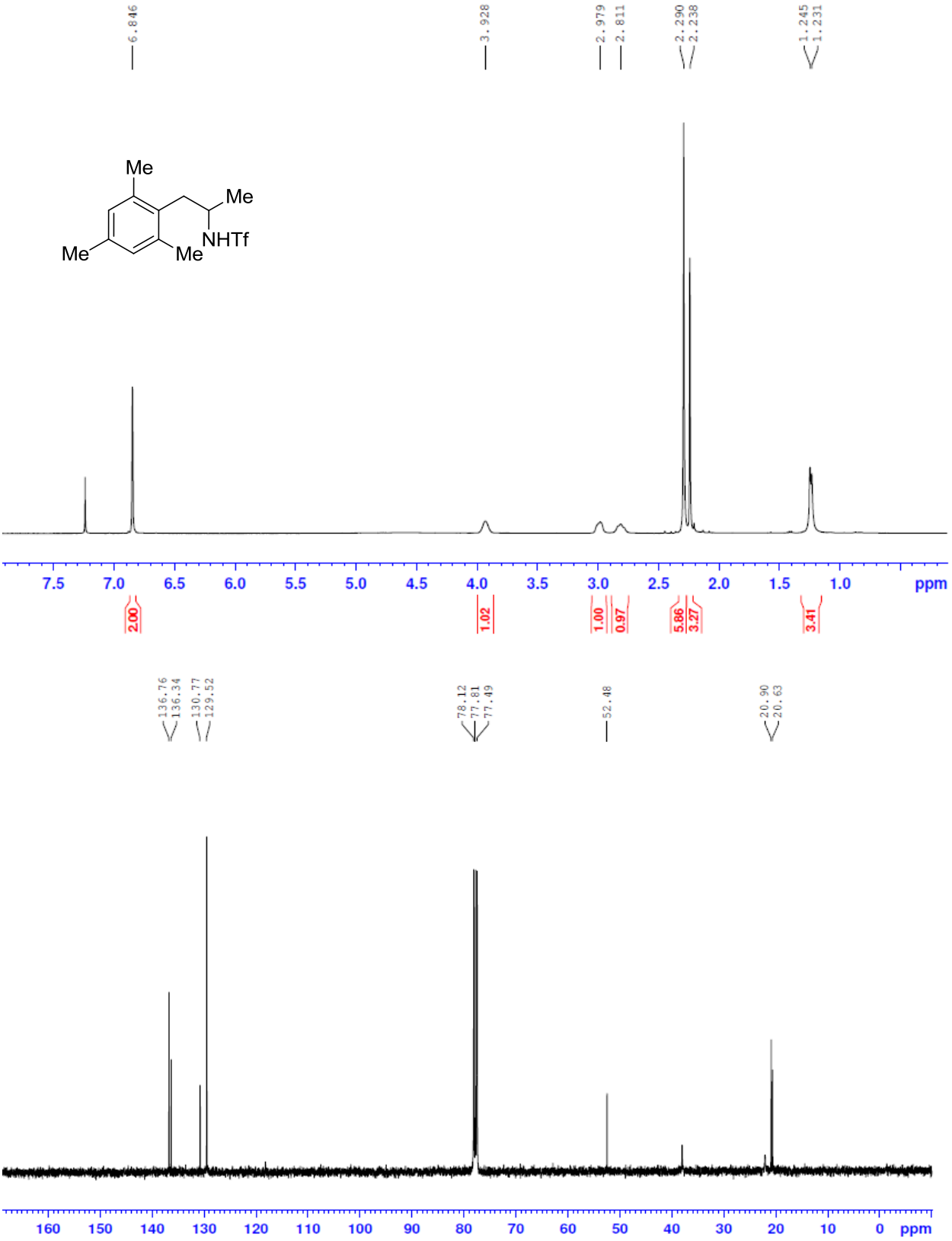

Compound **30b**

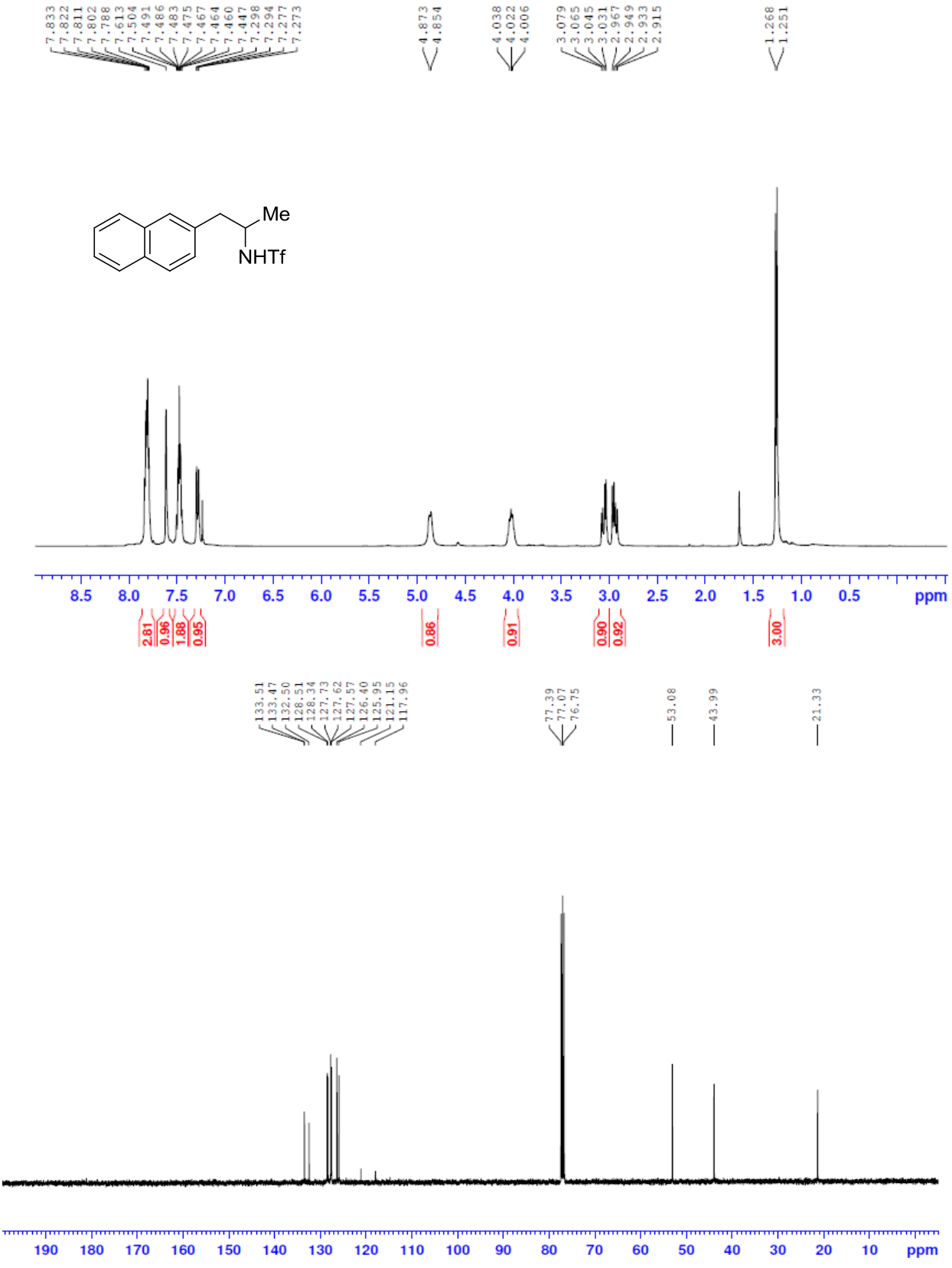

Compound **31b**

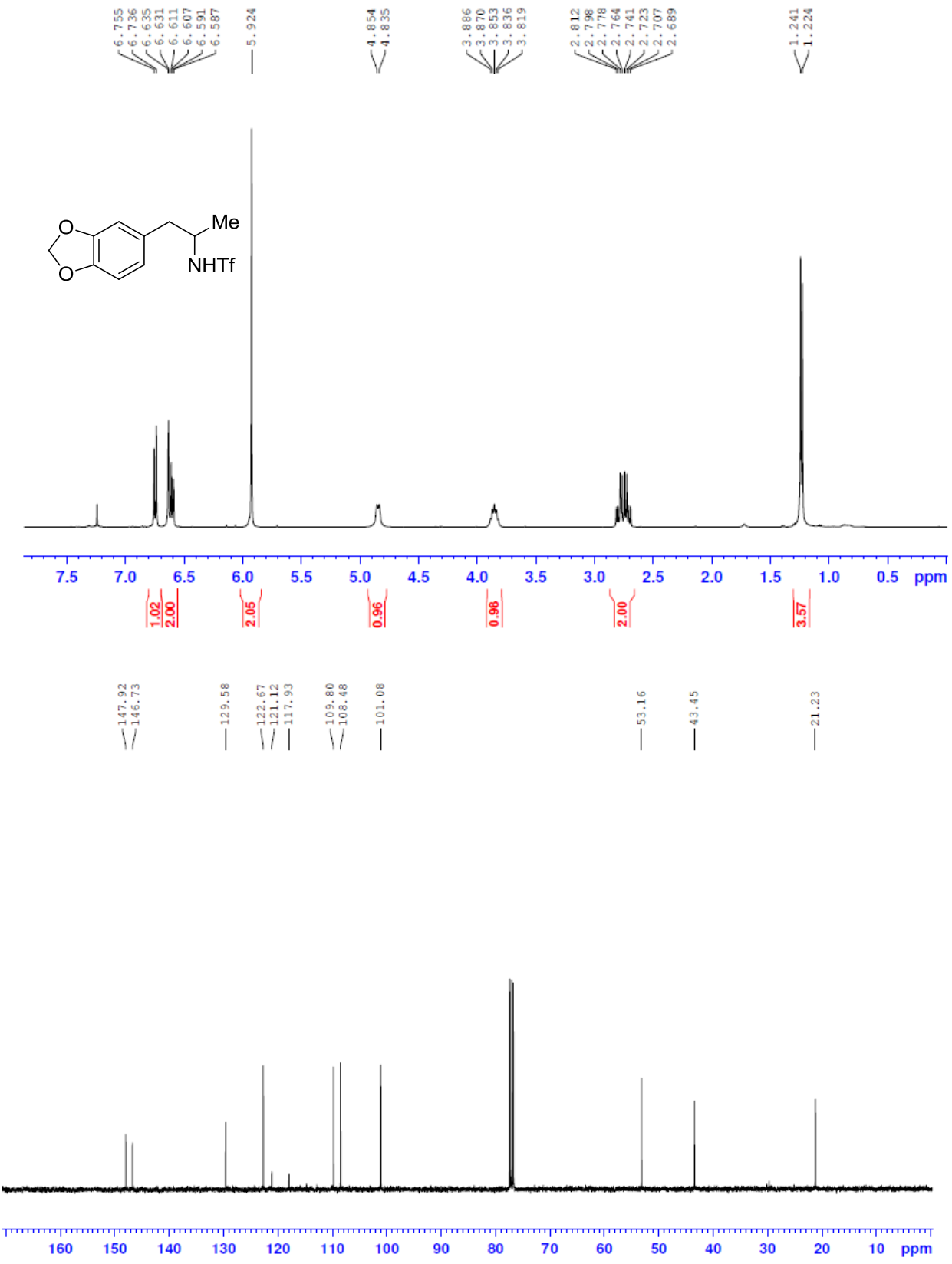

Compound **32b**

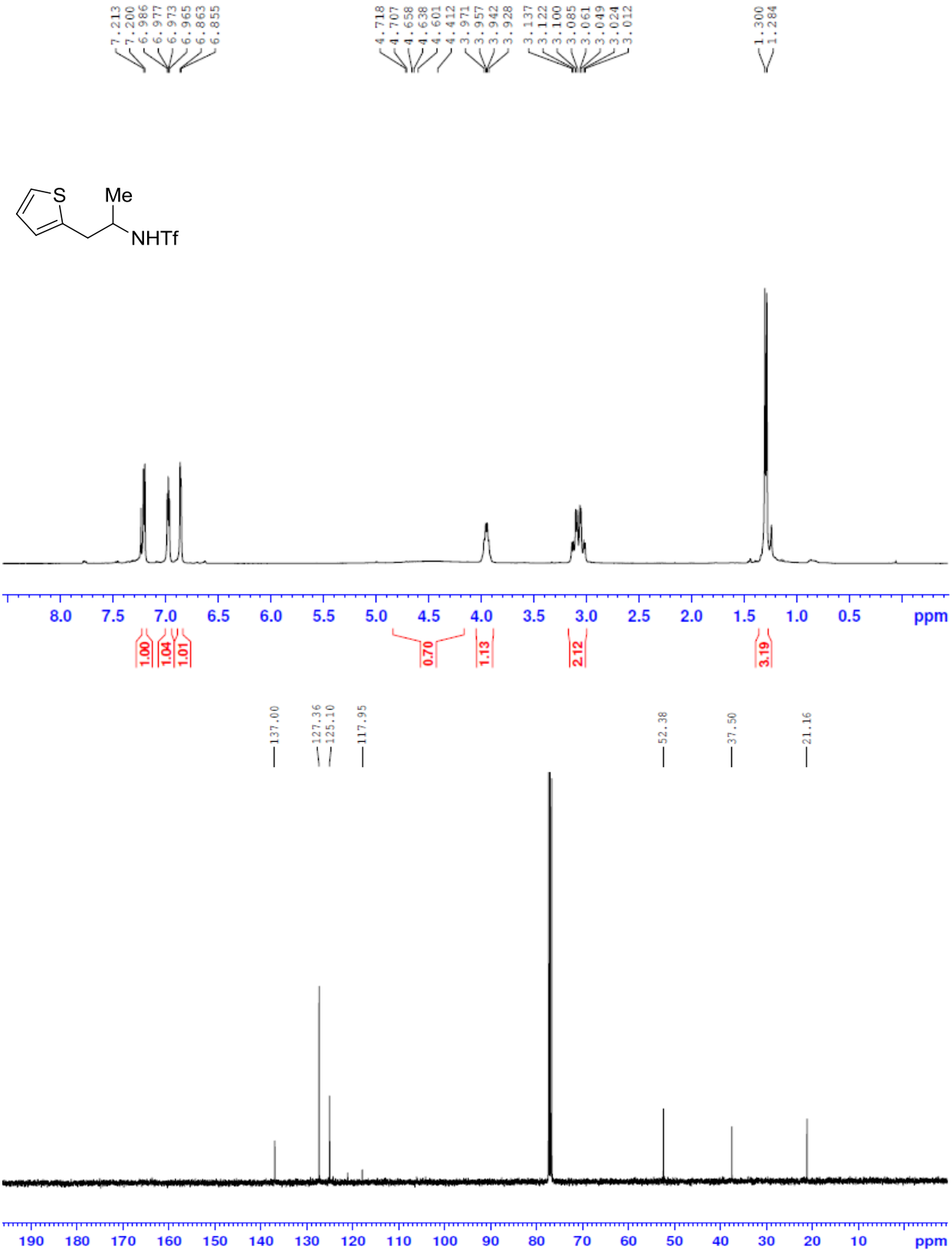

Compound **33b**

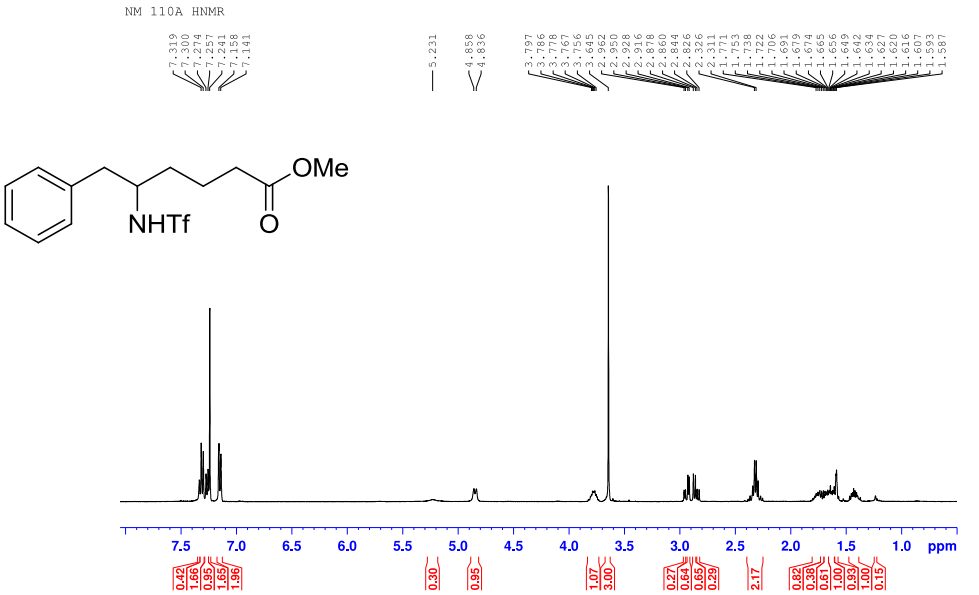

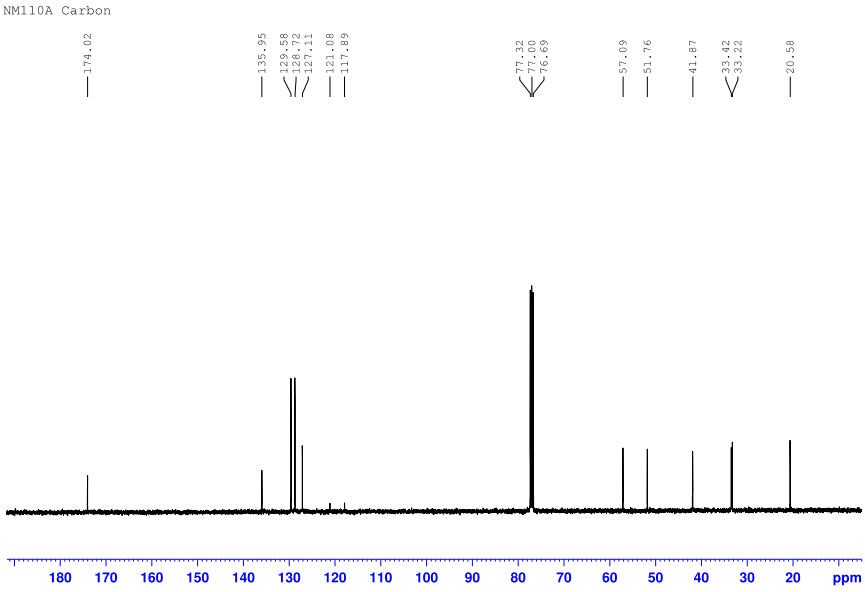

Compound **34b**

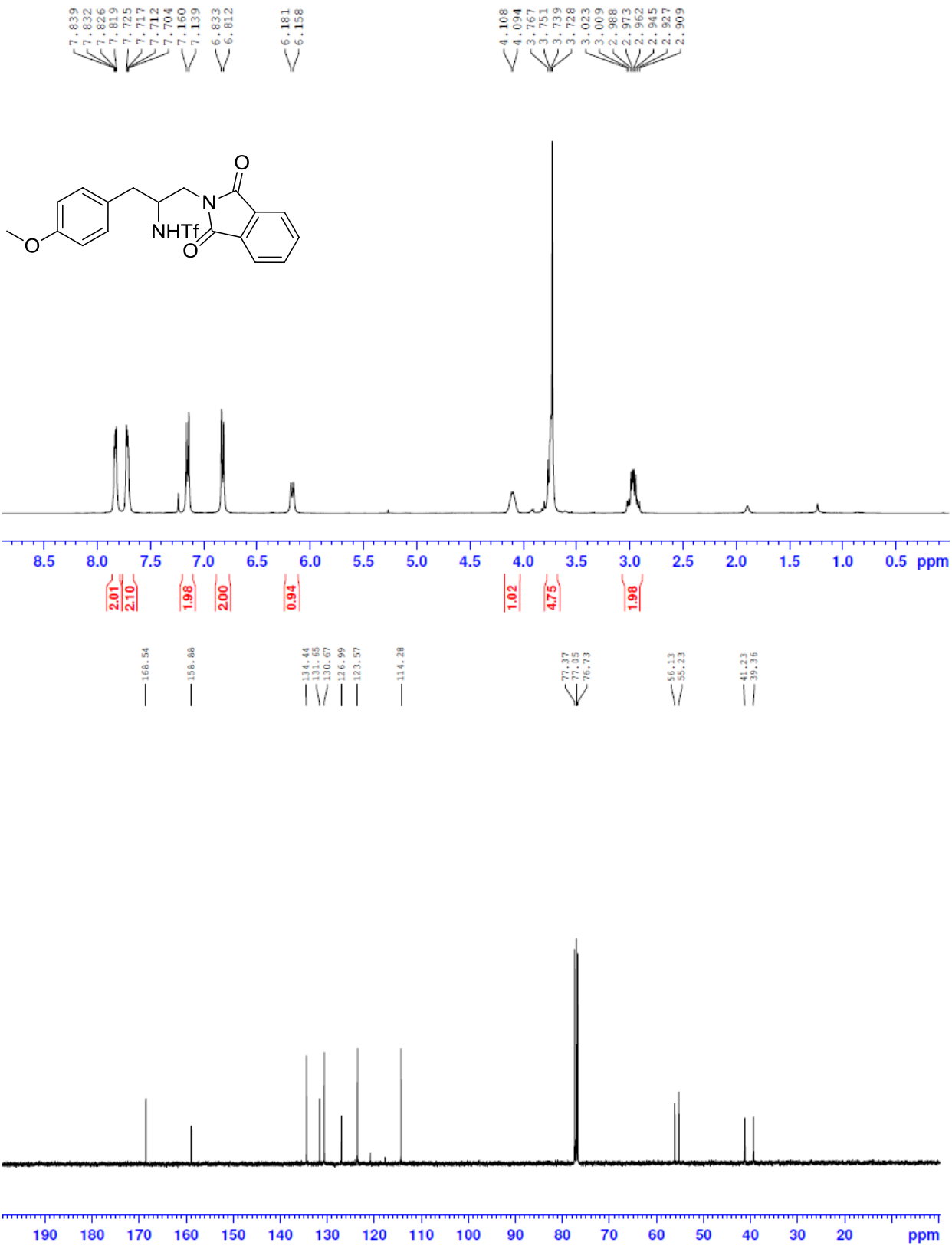

Compound **35b**

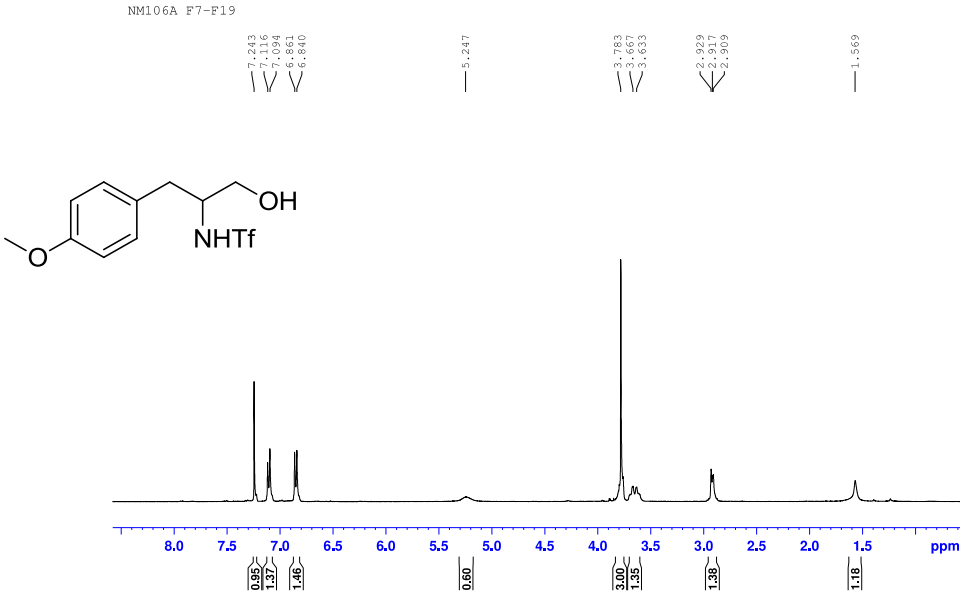

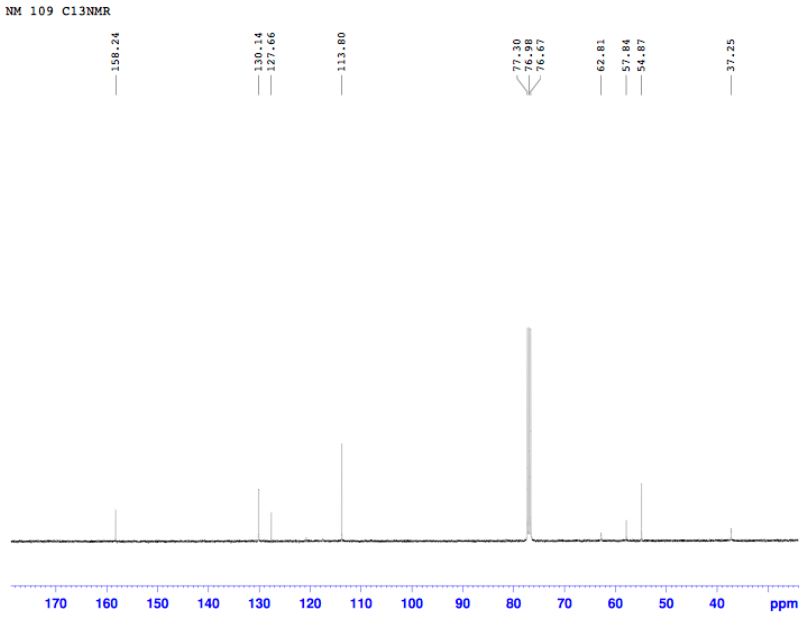

Compound **36b**

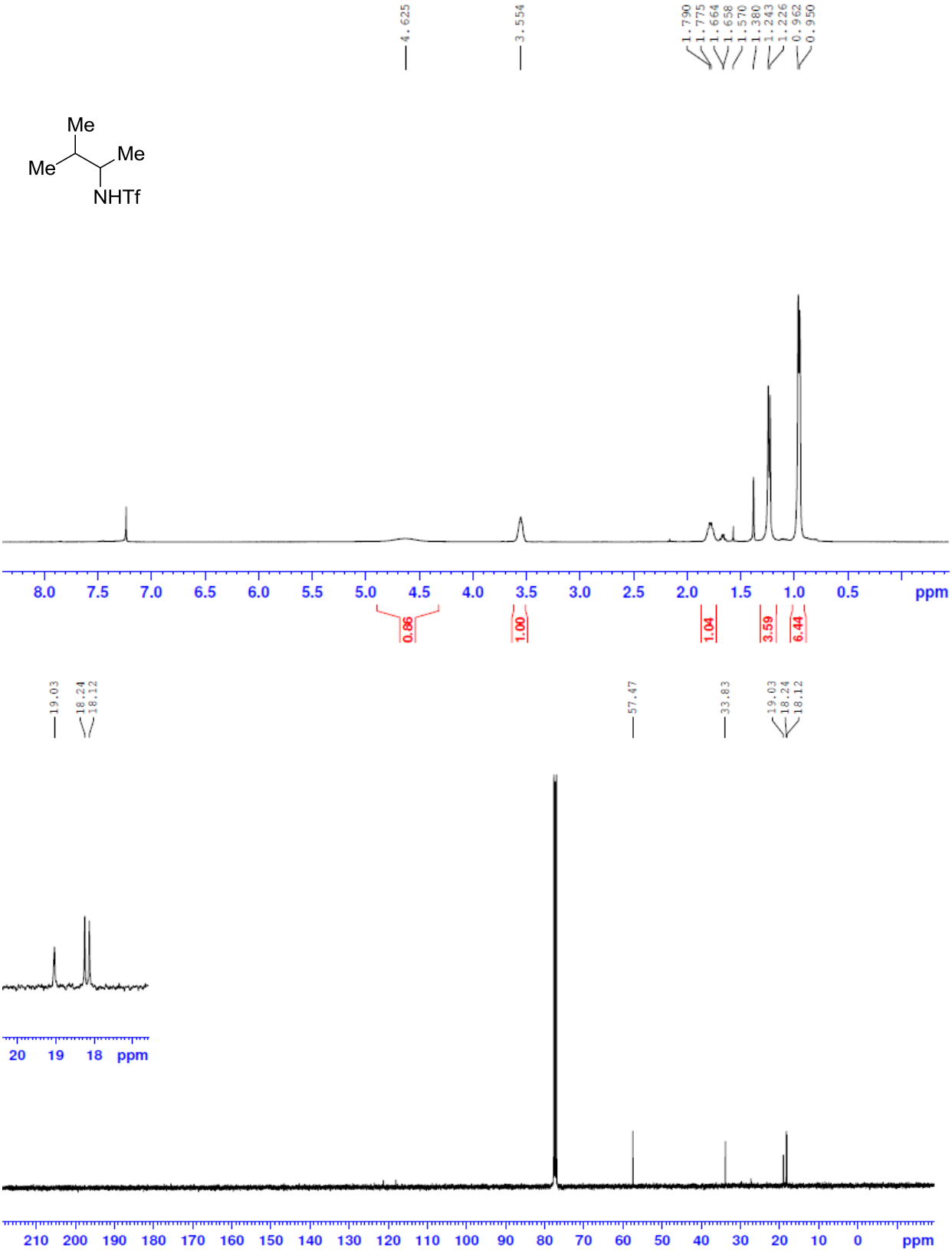

Compound **37**

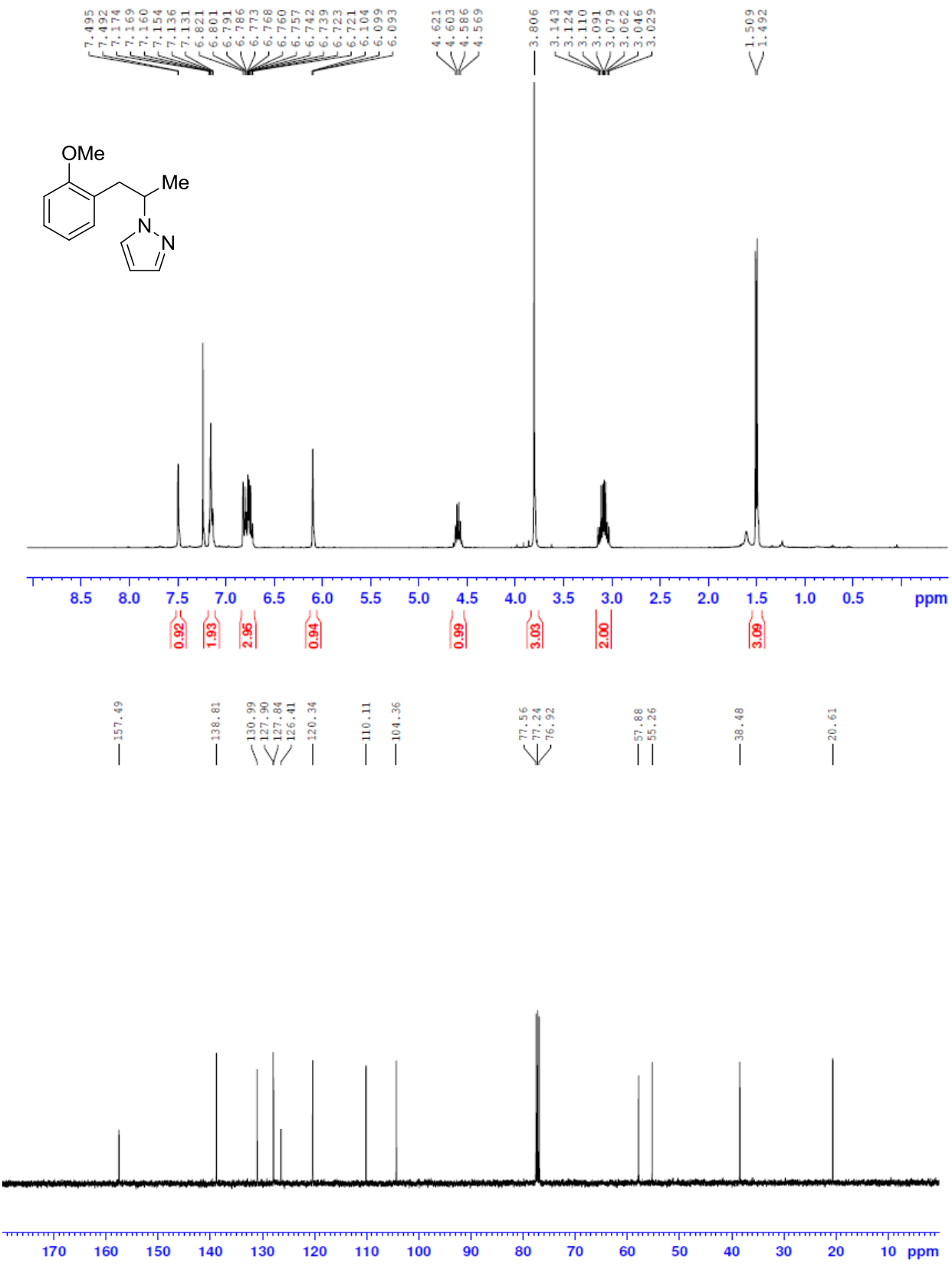
7.495
7.492
7.174
7.169
7.160
7.154
7.136
7.131
6.821
6.801
6.791
6.786
6.773
6.768
6.760
6.757
6.742
6.739
6.723
6.721
6.104
6.099
6.093
4.621
4.603
4.586
4.569
3.806
3.143
3.124
3.110
3.091
3.079
3.062
3.046
3.029
1.509
1.492
OMe
Me
N
N
8.5
8.0
7.5
7.0
6.5
6.0
5.5
5.0
4.5
4.0
3.5
3.0
2.5
2.0
1.5
1.0
0.5
ppm
0.92
1.93
2.95
0.94
0.99
3.03
2.00
3.09
157.49
138.81
130.99
127.90
127.84
126.41
120.34
110.11
104.36
77.56
77.24
76.92
57.88
55.26
38.48
20.61
170
160
150
140
130
120
110
100
90
80
70
60
50
40
30
20
10
ppm

Compound **38**

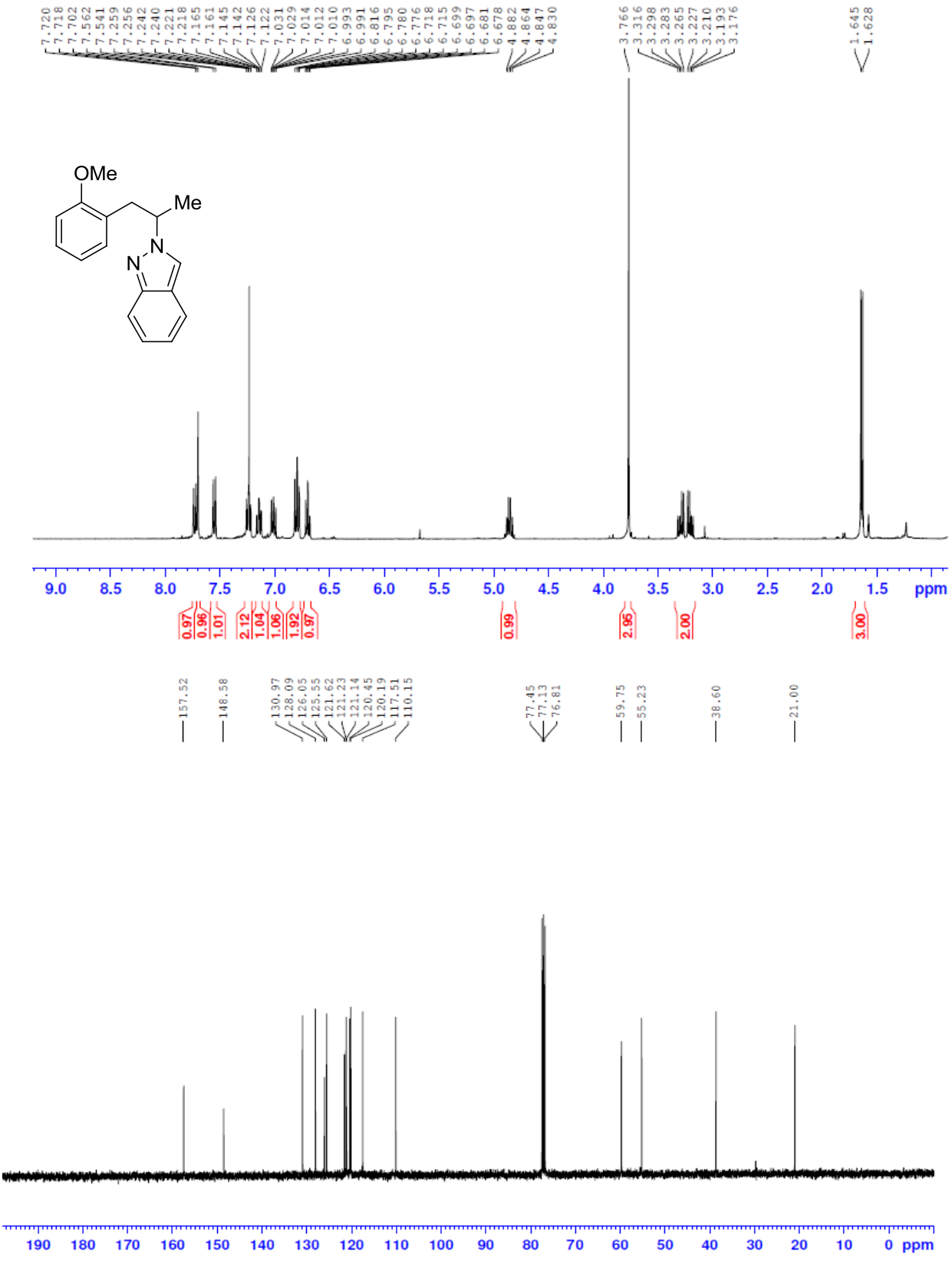
7.720
7.718
7.702
7.562
7.541
7.259
7.256
7.242
7.240
7.221
7.218
7.165
7.161
7.145
7.142
7.126
7.122
7.031
7.029
7.014
7.012
7.010
6.993
6.991
6.816
6.795
6.780
6.776
6.718
6.715
6.699
6.697
6.681
6.678
4.882
4.864
4.847
4.830
3.766
3.316
3.298
3.283
3.265
3.227
3.210
3.193
3.176
1.645
1.628
OMe
Me
N
N
9.0
8.5
8.0
7.5
7.0
6.5
6.0
5.5
5.0
4.5
4.0
3.5
3.0
2.5
2.0
1.5
ppm
0.97
0.96
1.01
2.12
1.04
1.06
1.92
0.97
0.99
2.96
2.00
3.00
157.52
148.58
130.97
128.09
126.05
125.55
121.62
121.23
121.14
120.45
120.19
117.51
110.15
77.45
77.13
76.81
59.75
55.23
38.60
21.00
190
180
170
160
150
140
130
120
110
100
90
80
70
60
50
40
30
20
10
0 ppm

Compound **38**

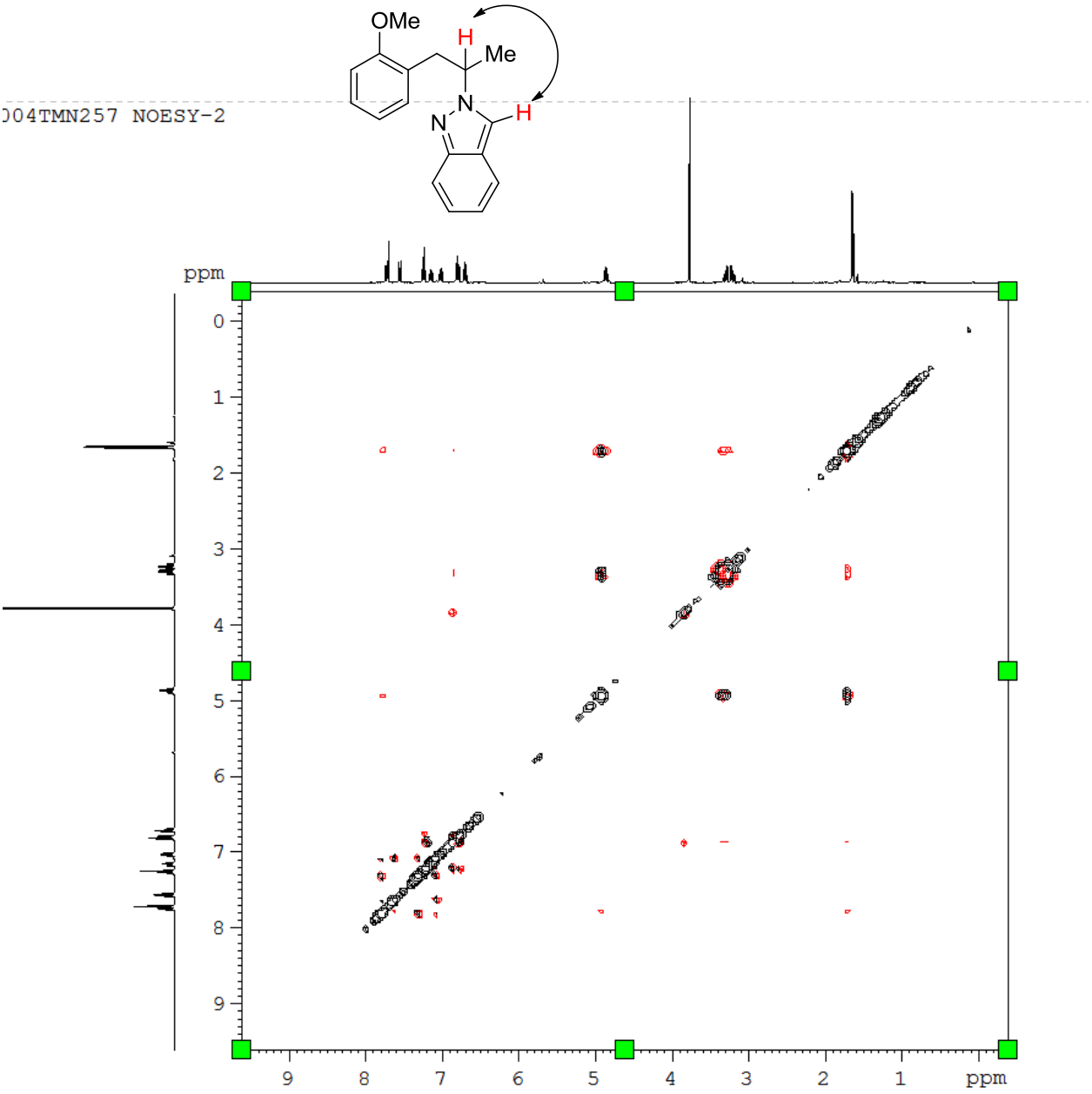

Compound **39**

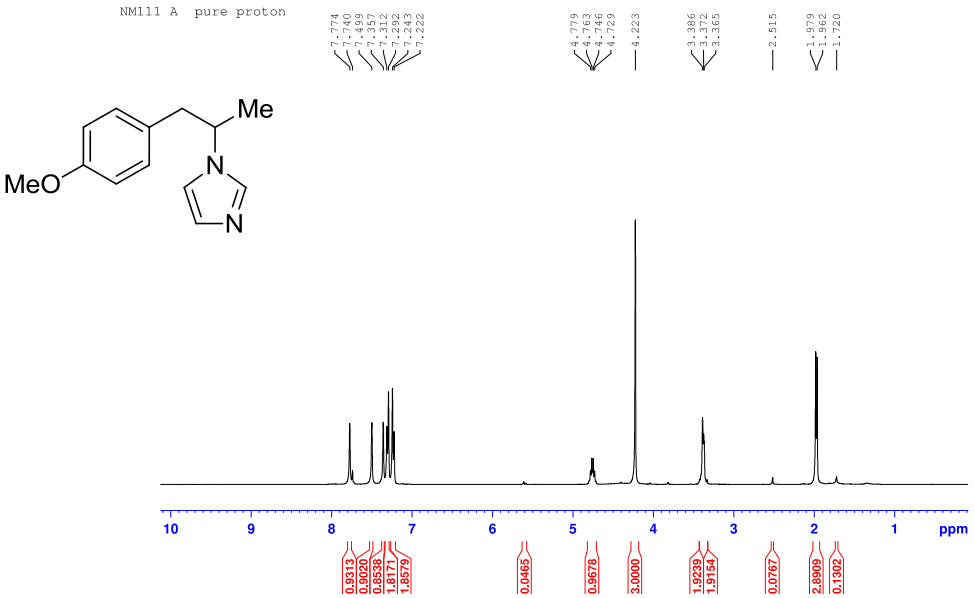
NM111 A pure proton
7.774
7.740
7.499
7.357
7.312
7.292
7.243
7.222
4.779
4.763
4.746
4.729
4.223
3.386
3.372
3.365
2.515
1.979
1.962
1.720
Me
MeO
N
N
10
9
8
7
6
5
4
3
2
1
ppm
0.9313
0.9020
0.8538
1.8171
1.8579
0.0465
0.9678
3.0000
1.9239
1.9154
0.0767
2.8909
0.1302

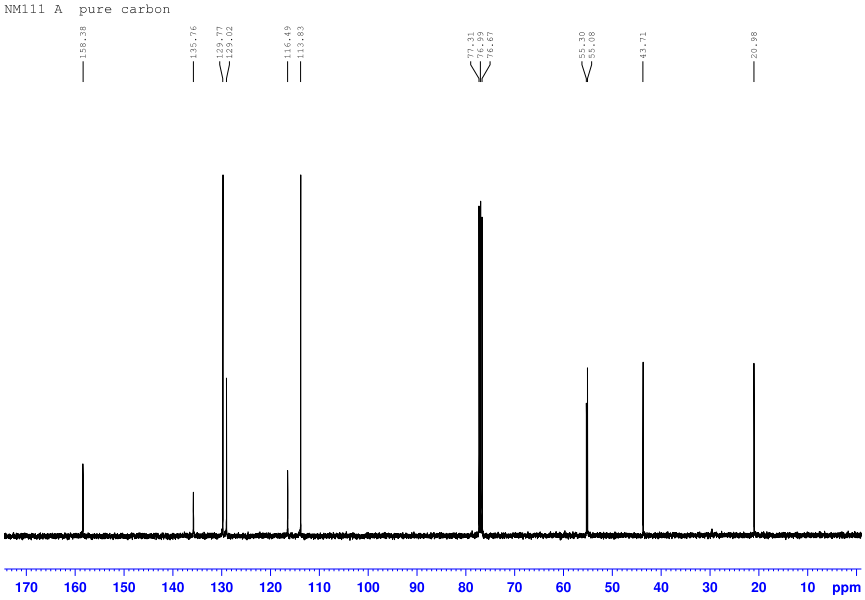
NM111 A pure carbon
158.38
135.76
129.77
129.02
116.49
113.83
77.31
76.89
76.47
55.30
55.08
43.71
20.98
170
160
150
140
130
120
110
100
90
80
70
60
50
40
30
20
10
ppm

Compound **40 (major regioisomer)**

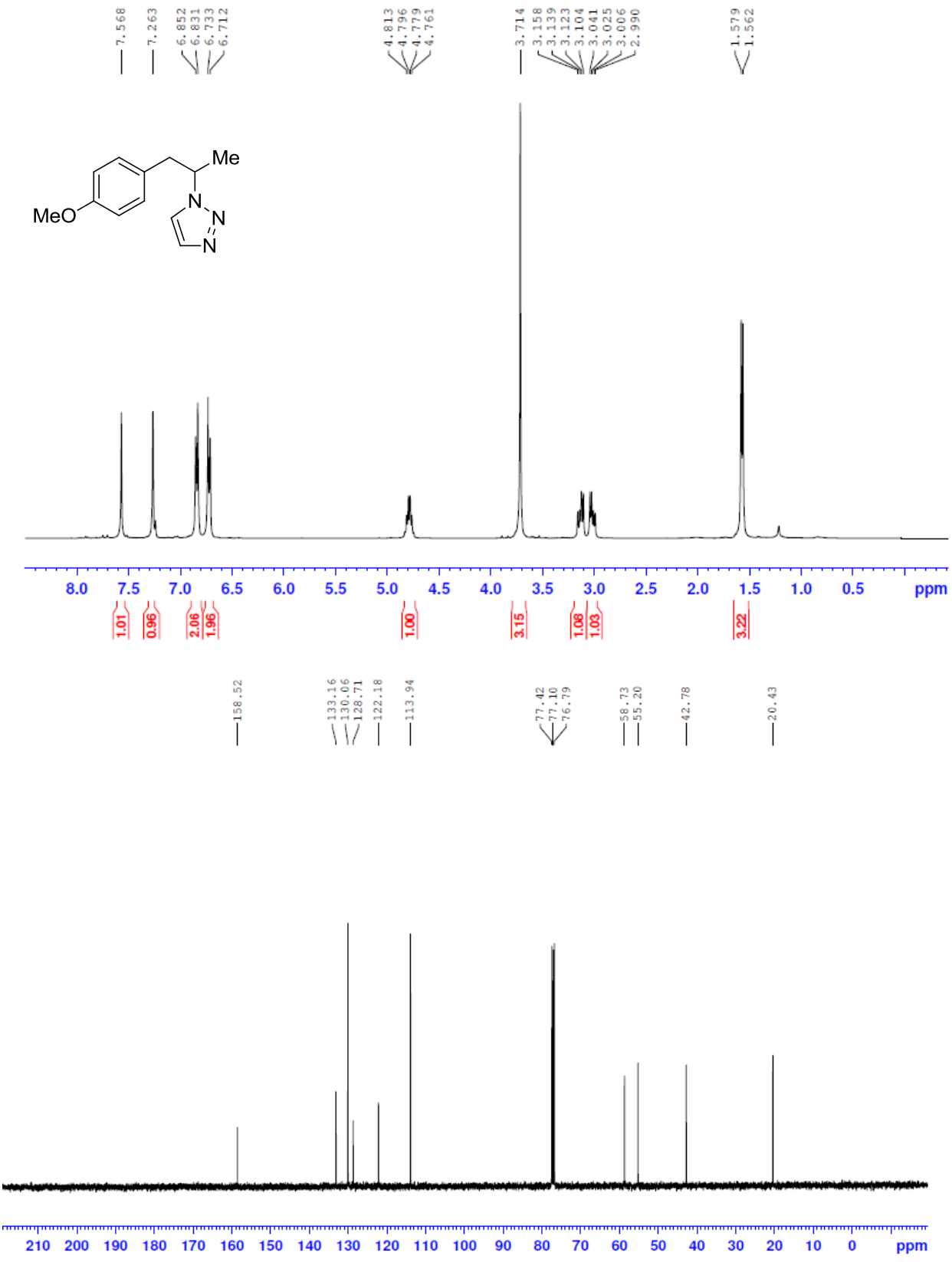

Compound **40 (minor regioisomer)**

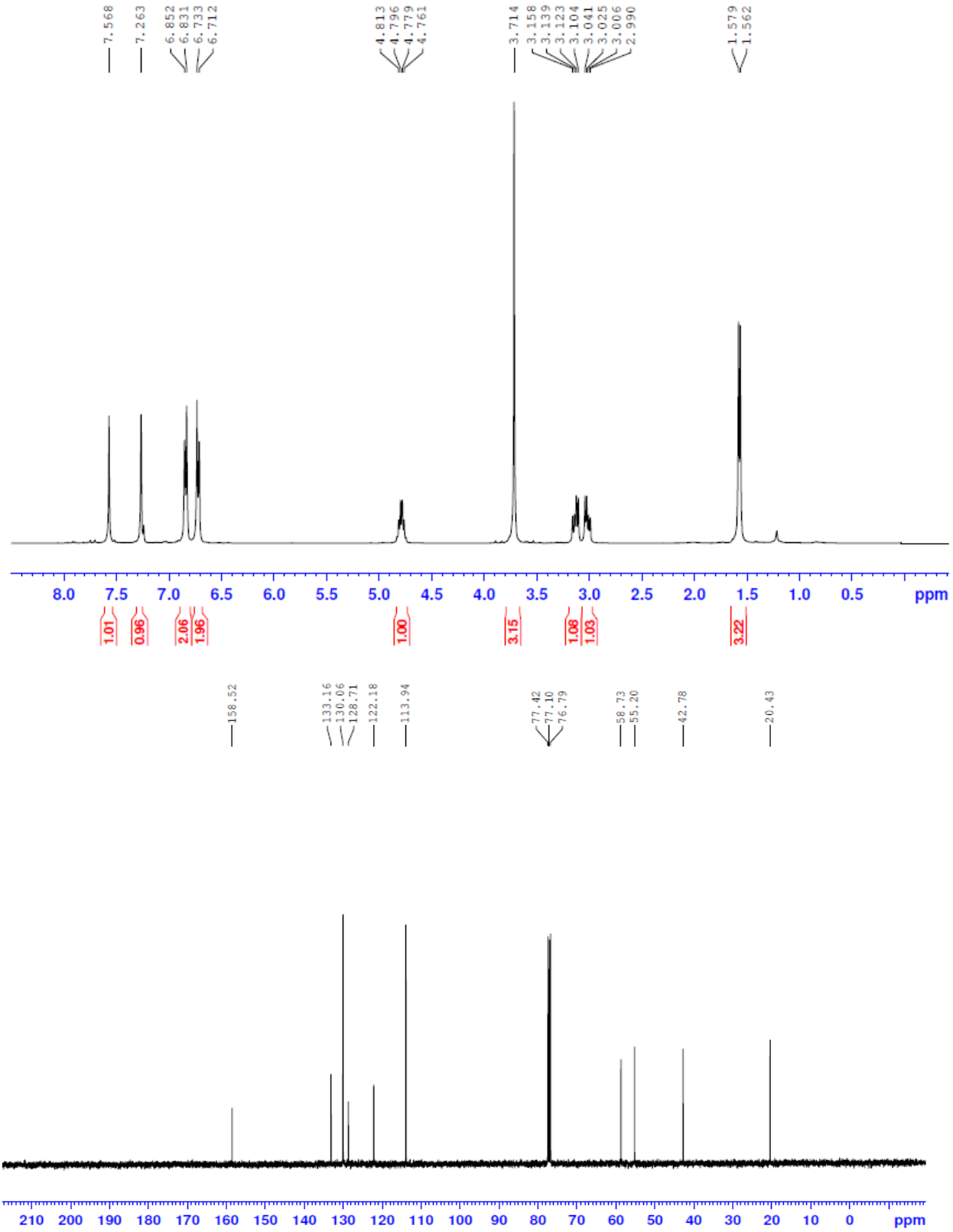

Compound **41 (major regioisomer)**

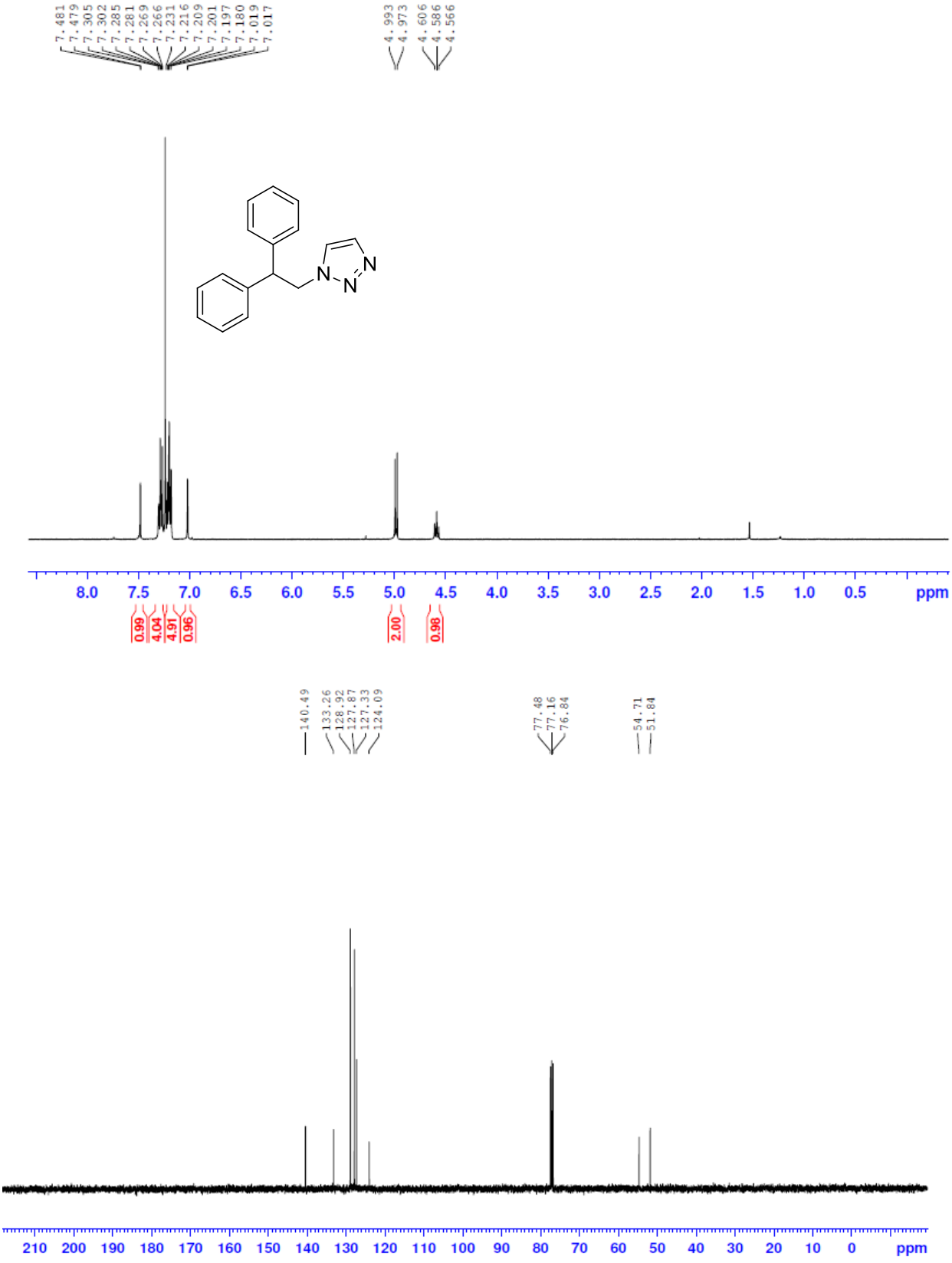

Compound **41 (minor regioisomer)**

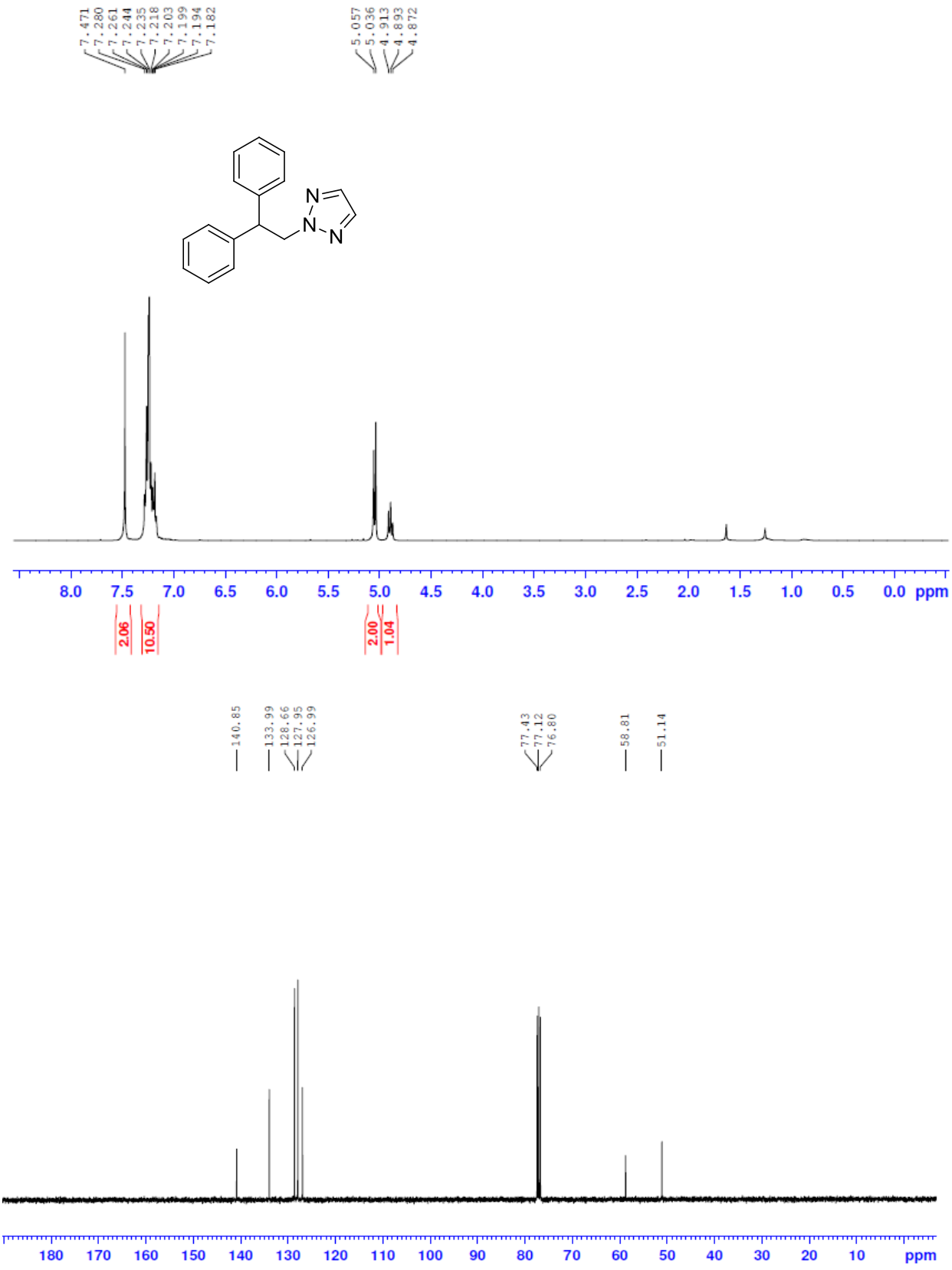

Compound **42 (major regioisomer)**

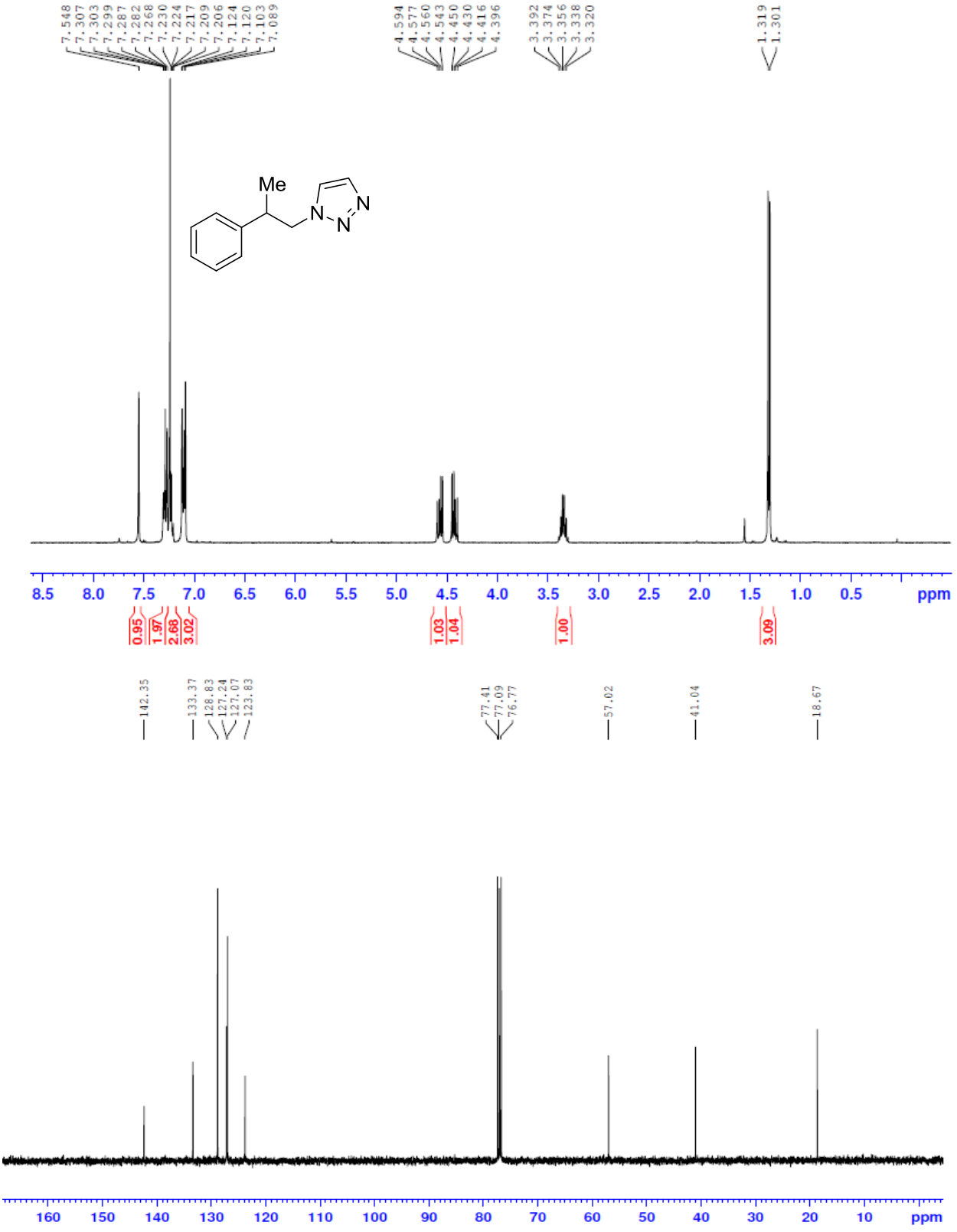

Compound **42 (minor regioisomer)**